

Functional Characterization of an Organ Specific Effector See1 of *Ustilago maydis*



Dissertation

zur

Erlangung des Doktorgrades
der Naturwissenschaften
(Dr. rer. nat.)

Dem Fachbereich Biologie
der Philipps-Universität Marburg
vorgelegt von

Amey Redkar

aus Pune -Indien

Marburg/Lahn, 2014

Functional Characterization of an Organ Specific Effector See1 of *Ustilago maydis*

Dissertation

zur

**Erlangung des Doktorgrades
der Naturwissenschaften
(Dr. rer. nat.)**

Dem Fachbereich Biologie
der Philipps-Universität Marburg
vorgelegt von

Amey Redkar

aus Pune- Indien

Marburg/Lahn, 2014

Die Untersuchungen zur vorliegenden Arbeit wurden von Oktober 2011 bis September 2014 unter der Betreuung von Prof. Dr. Gunther Döhlemann am Max-Planck Institut für terrestrische Mikrobiologie in der Abteilung Organismische Interaktionen in Marburg durchgeführt.

Vom Fachbereich Biologie
der Philipps-Universität Marburg als Dissertation
angenommen am:

Erstgutachter: Prof. Dr. Gunther Döhlemann

Zweitgutachter: Prof. Dr. Alfred Batschauer

Tag der mündlichen Prüfung:

Part of this work was published in the following articles:

Redkar, A., Schilling, L., Hoser, R., Zechmann, B., Krzymowska, M., Walbot, V. and Doehlemann, G. (2014). A secreted *Ustilago maydis* effector guides host cells to form tumors in maize leaves. *The Plant Cell* (under revision).

Schilling, L., Matei, A., Redkar, A., Walbot, V. and Doehlemann, G. (2014). Virulence of the maize smut *Ustilago maydis* is shaped by organ specific effectors. *Mol. Plant Pathol.* **15**: 780-789. doi: 10.1111/mpp.12133.

Other Publications:

van der Linde, K., Mueller, A.N., Redkar, A., Schilling, L. and Doehlemann, G. (2013). Brandpilze mit Pep: *Ustilago maydis* und das pflanzliche Immunsystem. *BIOspektrum* **19**(2): 140. doi:10.1007/s12268-013-0283-3.

Declaration

I hereby declare that the thesis entitled “Functional Characterization of an Organ Specific Effector See1 of *Ustilago maydis*” submitted to the Department of Biology, Philipps Universität Marburg, is the original and independent work carried out by myself under the guidance of my PhD committee and the dissertation is not formed previously on the basis of any award of Degree, Diploma or other similar titles.

(Place / Date)

(Amey Redkar)

“I am thankful to all those who said “NO” to me. Its just because of them I did it myself”

Albert Einstein (1879–1955)

“Science may never come up with a better office communication system than the coffee break”

Earl Wilson (1907–1987)

Zusammenfassung

Ustilago maydis ist der Verursacher des Maisbeulenbrands. Dieser zu den Basidiomyceten gehörende Pilz ist ein biotropher Pflanzenpathogen. Die Etablierung einer biotrophen Interaktion führt zur Ausbildung großer Tumore. Diese Tumorbildung ist Folge der effektiven Unterdrückung des pflanzlichen Immunsystems und des Nährstoffflusses während des Krankheitsverlaufs. Der Pilz sekretiert mehrere hundert Effektorproteine, welche zu unterschiedlichen Zeitpunkten der Besiedelung exprimiert werden und manipuliert auf diese Weise seinen Wirt. Vorhergehende Studien zeigten, dass die Effektorproteine von *U. maydis* organspezifisch wirken und nach Deletion eines organspezifischen Effektors die Ausbildung der Krankheitssymptome in anderen Organen nicht beeinträchtigt wird (Skibbe et al., 2010 und Schilling et al., 2014).

In der vorhergehenden Studie von Schilling et al. 2014 konnten blattspezifische Effektoren identifiziert werden, welche in den jungen Blättern induziert sind. Ein interessanter Kandidat mit ausgeprägter Organspezifität ist *see1* (**S**eedling **e**fficient **e**ffector 1; *um02239*), welcher in infizierten Blättern aktiv ist. Deletionsmutanten von *see1* sind in der Lage den Keimling zu penetrieren und zu besiedeln, können jedoch keine größeren Tumore ausbilden. In der *see1* Deletionsmutante ist die Besiedelung des Mesophylls und des vaskulären Gewebes der Blätter aktiv blockiert. Im Gegensatz dazu wird das infizierte Blütengewebe zu Tumorgewebe transformiert. Dies bestätigt die organspezifische Funktion von See1 im Zell- oder Blattgewebe von Mais.

Ziel dieser Arbeit ist die funktionelle Charakterisierung dieses organspezifischen Effektors See1. Unter dem Einfluss von See1 ist die DNA Synthese in kolonisierten Wirtszellen induziert. Das Hefe-Zwei-Hybrid-System zeigte, dass See1 mit dem Kern/Zellplasma lokalisierten Wirtsprotein SGT1 interagiert, welches den Zellzyklus und die Immunantwort der Wirtspflanze steuert. SGT1 zeigt eine blattspezifische Transkriptionsregulation. Die konstitutive Überexpression des Effektors zeigt eine Anomalie an der Rispenbasis. Die Tumorbildung an der vegetativen Rispenbasis ist ein deutliches Indiz für die spezifische Aktivität des Effektors im vegetativen Gewebe. Wie elektronenmikroskopische Aufnahmen zeigen, transloziert See1 in die Pflanzenzelle wo der Effektor im Zytoplasma und im Zellkern der Wirtszelle lokalisiert. Weiterhin konnte gezeigt werden, dass See1 die Phosphorylierung von SGT1 in Mais an einer für Monokotylen spezifischen Position hemmt, welche für die Aktivierung der Signalkaskade zur Pathogenerkennung verantwortlich ist. Experimente weisen darauf hin, dass *see1* den Zellzyklus des Wirts einleitet, wodurch die besiedelte Wirtszelle mit der Tumorentwicklung beginnt.

Organspezifische Effektoren wie *see1* manipulieren nicht nur die Abwehrmechanismen des Wirts sondern auch seine Stoffwechselaktivität, was zur Tumorbildung führt.

Summary

Ustilago maydis is the causative agent of the corn smut. This basidiomycetous fungus is a biotrophic plant pathogen that succeeds by colonizing living tissue and establishes a biotrophic interaction which results in the formation of enormous tumors. This tumor formation is a result of efficient host immune suppression and nutrient efflux during disease progression. The fungus secretes several hundreds of effector proteins which are expressed at various stages of colonization to modulate the host. Previous studies have revealed that the effector proteins of *U. maydis* are acting in an organ specific manner and deletion of one organ specific effector does not hamper the symptom formation in non-target organ (Skibbe et al., 2010; Schilling et al., 2014).

The previous study of Schilling et al., 2014 identified leaf specific effectors, which are induced in juvenile leaves. An interesting candidate among these that showed a perfect organ specificity was *see1* (**S**eedling **e**fficient **e**ffector 1, *um02239*), which is required in the colonized leaves. Deletion mutants for *see1* are able to penetrate and colonize the seedling but fail to induce expansion of tumors. The deletion mutant is seen to be actively blocked in mesophyll and vascular cell layers of the leaf, which may indicate that the effector function may be confined to a specific cell or tissue type. In contrast, *see1* deletion does not affect tumor formation in the floral parts of the host. Aim of this thesis was the functional characterization of *See1*. Monitoring of the DNA synthesis in host, showed that *See1* is specifically required to induce DNA synthesis in colonized host cells and re-direct them to form tumors. Yeast-two-hybrid analysis showed that *See1* interacts with a nucleo-cytoplasmic host protein SGT1, which is a cell cycle and immune response modulator and which also shows a leaf specific transcriptional regulation. Constitutive overexpression of *see1* caused tassel base abnormality specifically showing tumors in the vegetative base of the tassel pointing towards an active role of *see1* in inducing tumor in vegetative maize tissues. Electron microscopy showed that *See1* is translocated to the plant cell and is localized in the cytoplasm and nucleus of the host cell.

Furthermore, it was demonstrated that *See1* blocks the phosphorylation of maize SGT1 at a monocot specific site which is necessary to activate the signaling cascade upon pathogen perception. Experiments indicate that *see1* specifically activates the host cell cycle release thereby activating the colonized cells to undergo a tumor pathway. Hence organ specific effectors like *see1*, not only manipulate the defense responses, but also the metabolic state of the host cell leading to tumor development.

Abbreviations

AA	Amino acid	H ₂ O _{bid.}	Double distilled water
ABA	Abscisic acid	HA	Haemagglutinin
Amp	Ampicillin	H ₂ O ₂	Hydrogen peroxide
APC	Anaphase promoting complex	hpi	hours post infection
Avr-(Protein)	Avirulence protein	HR	Hypersensitivity response
BIC	Biotrophic interfacial complex	HRP	Hypersensitive response and pathogenicity
bp	Base pairs		
BSA	Bovine serum albumin	HSP90	Heat shock protein 90
Cbx	Carboxin	HSTs	Host-specific toxins
CC9	Maize Cystatin 9 (<i>Corn Cystatin 9</i>)	Hyg	Hygromycin
cDNA	complementary DNA	i.e.	that is
CDC6	Cell division control 6	<i>in planta</i>	inside the plant cell
CFP	Cyan fluorescent protein	<i>ip</i>	iron-sulphur protein
C-terminal	Carboxyterminal	IPTG	isopropyl B D thiogalactopyranoside
Cmu1	Chorismate mutase 1	JA	Jasmonic acid
Δ	Deletion/Delta	Kan	Kanamycin
Da	Dalton	kb	Kilobases
DAMP	Damage-associated molecular pattern	kDa	Kilodalton
dH ₂ O	Doubled distilled water	LRR	leucine rich repeat
DMSO	Dimethylsulfoxid	LysM	lysine motifs
DNA	Deoxyribonucleic acid	M	Molar (g/L)
dpi	days post infection	MAMP	microbe associated molecular pattern
DIC	differential interference contrast	MAPK	mitogen-activated protein Kinase
DTT	Dithiothreitol	min	Minute(s)
eBIFC	enhanced bimolecular fluorescence complementation	ml	Millilitre
EdU	5 ethynyl 2 deoxyuridine	mM	Millimolar (mg/L)
ER	Endoplasmic Reticulum	mm	Millimeter
ET	Ethylene	mRNA	<i>messenger</i> ' RNA
ETI	Effector-Triggered Immunity	N-terminal	aminoterminal
ETS	Effector-Triggered Susceptibility	NADPH	Nicotinamide adenine dinucleotide phosphate
FACS	Fluorescence activated cell sorting	NB-LRR	Nucleotide binding LRR receptors
Fig.	Figure	ng	Nanogramm
fw	forward	nm	Nanometer
gDNA	genomic DNA	nt	Nucleotide
Gent	Gentamycin	OD ₆₀₀	Optical density at 600 nm
GFP	green fluorescent protein	<i>on planta</i>	on the plant surface
h / hrs	Hour	OSD1	Omission of second division 1

PAMP	Pathogen associated molecular pattern	TE	Tris-Cl + Na ₂ -EDTA
PCD	Programmed cell death	TEM	Transmission electron microscopy
PCR	Polymerase chain reaction	TEMED	Tetramethylethylenediamine
PD	Potato dextrose	Tet	Tetracyclin
PEG	Polyethyleneglycol	TPR	Tetratricopeptide
Pep1	protein essential during penetration 1	Tin2	Tumor inducing 2
Phleo	Phleomycin	Tris	Trishydroxymethyl aminomethane
Pit	proteins important for tumor formation	TTSS	Type III secretion system
POX	Peroxidase	U	Unit (Enzyme activity)
Ppi	peptidylprolyl isomerase	UPS	ubiquitin/26S proteasome system
PR	pathogenesis-related	UVI 4	UV-B-Insensitive 4
PRR	pattern recognition receptor	VIGS	virus induced Gene- <i>silencing</i>
PI	propidium iodide	V	volts
PTI	PAMP triggered immunity	WGA	wheat germ agglutinin
PTM	posttranslational modification	YFP	yellow fluorescent protein
qRT-PCR	quantitative ' <i>real-time</i> ' polymerasekettenreaktion	Y2H	yeast two hybrid
R-protein	Resistance protein	e. g.	For example
RAR1	Required for MLA12 resistance	µg	Microgram
rev / rv	reverse	µm	Micrometer
Rif	Rifampicin	µM	Micromolar
RNA	Ribonucleotide		
ROS	reactive oxygen species		
Rpm	rounds per minute		
RT	Room Temperature		
RT-PCR	<i>reverse transcripton</i> ' Polymerase Chain reaction		
s / sec	Seconds		
SA	Salicylic acid		
SAR	systemic aquired resistance		
SCF	skp1-Cullin-F box		
SDS	sodium dodecyl sulfate		
PAGE	polyacrylamide gel electrophoresis		
SE	Standard error		
SGT1	suppressor of G2 allele of skp1		
SIPK	salicylic acid induced protein kinase		
Sp.	species		
Sub. Sp.	Sub. species		
Tab.	Table		
TAE	Tris-Acetate + Na ₂ -EDTA		
TBE	Tris-Borate + Na ₂ -EDTA		

Contents

1 Introduction.....	1
1.1 Infectious and developmental strategies of phytopathogenic micro-organisms.....	1
1.2 Biology of smut fungi.....	2
1.2.1 <i>Ustilago maydis</i> - The causative agent of corn smut.....	4
1.3 The plant immune system.....	6
1.4 Effectors: The key players in manipulating the host.....	9
1.4.1 Translocation of effectors and their characteristics.....	11
1.5 Effectors of <i>U. maydis</i>	12
1.5.1 See1, an organ specific virulence factor.....	16
1.6 Interplay between the cell cycle regulation and defense responses.....	16
1.7 Aims and objectives of this study.....	17
2 Results.....	18
2.1 See1 is an organ specific effector.....	18
2.1.1 See1 is specifically required for expansion of leaf tumors.....	18
2.1.2 See1 is not required for tumor formation in floral parts.....	20
2.2 Phenotype characterization of the $\Delta see1$ mutant.....	21
2.2.1 Saprophytic growth of <i>see1</i> deletion strains.....	21
2.2.2 Microscopic characterization of the infection course in SG200 $\Delta see1$	23
2.2.2.1 SG200 $\Delta see1$ is not impaired in appresoria and filament formation.....	23
2.2.2.2 $\Delta see1$ mutant proliferation is impaired in the mesophyll and vascular layers of leaf.....	25
2.3 Expression analysis of See1 using quantitative real-time PCR.....	26
2.4 Tumor formation in <i>U. maydis</i> - maize interaction: A boost in DNA synthesis of host.....	27
2.4.1 DNA synthesis trigger in maize by wildtype <i>U. maydis</i>	29
2.4.2 <i>U. maydis</i> requires See1 to induce DNA synthesis during leaf tumor formation.....	30
2.4.3 Tumor formation in anthers does not involve <i>U. maydis</i> induced DNA synthesis.....	33

2.5 Constitutive over-expression of <i>see1</i> in infectious hyphae.....	35
2.6 Localization of See1 in infected maize seedlings.....	38
2.6.1 Localization of fluorescent See1 by confocal microscopy.....	39
2.6.2 Transient expression of See1 in <i>Z. mays</i> and <i>N. benthamiana</i>	40
2.6.3 See1 localizes to both cytoplasm and nucleus of maize cell.....	42
2.7 Identification of the host interactors with effector See1	45
2.7.1 See1 interacts with the cell cycle and immune response regulator Zm-SGT1 ..	45
2.7.2 See1 interacts with SGT1 in Co-immunoprecipitation and BiFC	47
2.8 Mechanistic basis of See1 interaction.....	50
2.8.1 See1 inhibits the post-translational modification of Zm-SGT1	50
2.8.2 See1 does not undergo phosphorylation by itself	54
2.9 Conservation of See1 among other smuts.....	54
2.9.1 Complementation of the $\Delta see1$ phenotype by other orthologues	55
2.10 Differential gene expression analysis in SG200 and $\Delta see1$ infected leaves.....	57
3 Discussion.....	63
3.1 <i>U. maydis</i> : A highly specialized biotroph.....	63
3.2 <i>See1</i> : An effector for tumor expansion in maize leaves	64
3.3 Deletion of <i>see1</i> hampers host DNA synthesis in leaf tissues.....	65
3.4 See1 is translocated to host cell cytoplasm and nucleus	67
3.5 Interaction of <i>see1</i> with the nucleo-cytoplasmic protein Zm-SGT1.....	69
3.6 SGT1, a conserved hub acting as effector target.....	71
3.7 Host transcriptional responses to SG200 $\Delta see1$ mutant.....	72
3.8 Significance of See1 in <i>U. maydis</i> induced tumor	73
3.9 Perspectives and Further Outlook	75
4 Materials and Methods	78
4.1 Material and Methods	78
4.1.1 Chemicals	78
4.1.2 Buffers and Solutions.....	78
4.1.3 Enzymes and Antibodies.....	78

4.1.4 Commercial Kits.....	78
4.2 Media	79
4.2.1 Media for cell cultivation and growth	79
4.2.2 Culture conditions for <i>E. coli</i> and <i>A. tumifaciens</i>	80
4.2.3 Culture conditions for <i>U. maydis</i> and <i>S.reilianum</i>	81
4.2.4 Cultivation of <i>S.cerevisiae</i>	81
4.2.5 Determination of cell density of bacterial and fungal cultures	81
4.3 Strains, Oligonucleotides and Vectors	81
4.3.1 <i>E. coli</i> Strains.....	81
4.3.2 <i>A. tumifaciens</i> Strains	82
4.3.3 <i>S. cerevisiae</i> Strains	82
4.3.4 <i>U. maydis</i> Strains.....	82
4.3.5 <i>S. reilianum</i> Strains.....	83
4.3.6 Oligonucleotides	83
4.3.7 Vectors and Plasmids	83
4.3.7.1 Plasmids for generation of stable <i>U. maydis</i> mutants	83
4.3.7.2 Plasmids for the yeast SGT1 complementation and yeast two hybrid analysis	87
4.3.7.3 Plasmids for production of recombinant proteins in <i>E.coli</i>	89
4.3.7.4 Plasmids for transient expression of genes in <i>N. benthamiana</i>	90
4.4 Standard Microbiological Methods.....	94
4.4.1 Rubidium chloride mediated transformation of <i>E. coli</i>	94
4.4.2 Blue White selection of <i>E. coli</i> transformants	95
4.4.3 Transformation of <i>A. tumifaciens</i>	95
4.4.4 Transformation of <i>U. maydis</i>	95
4.4.5 Test for filamentous growth of <i>U. maydis</i>	97
4.4.6 Transformation of <i>S.cereviceae</i>	97
4.5 Molecular Biological Methods	98
4.5.1 Isolation of nucleic acids	98

4.5.1.1 Isolation of plasmid DNA from <i>E.coli</i>	98
4.5.1.2 Isolation of genomic DNA from <i>U. maydis</i>	98
4.5.1.3 Isolation of total RNA from infected maize tissue	99
4.5.1.4 Purification of RNA	99
4.5.1.5 Purification of Plasmid DNA.....	99
4.5.2 <i>In vitro</i> modification of nucleic acids	99
4.5.2.1 Restriction of DNA.....	99
4.5.2.2 Dephosphorylation of linear DNA.....	100
4.5.2.3 Ligation of DNA fragments.....	100
4.5.2.4 Polymerase Chain Reaction (PCR)	100
4.5.2.5 Quantitative real time PCR	101
4.5.2.6 Targeted site directed mutagenesis.....	102
4.5.2.7 Sequencing of nucleic acids	102
4.5.3 Separation and Detection of Nucleic Acids.....	102
4.5.3.1 Agarose gel electrophoresis	102
4.5.3.2 Southern Analysis/Southern Blot	103
4.5.4 Microarray Analysis.....	105
4.6 Biochemical Methods	105
4.6.1 Separation and detection of proteins.....	105
4.6.2 Immunological protein detection by chemiluminescence (Western Blot).....	107
4.6.3 Coomassie staining of proteins	108
4.6.4 Protein determination according to Bradford.....	108
4.6.5 Heterologous production of recombinant proteins in <i>E.coli</i>	108
4.6.6 Purification of GST fusion proteins	109
4.6.7 Purification of HIS tagged proteins	110
4.6.8 Obtaining of denatured proteins from <i>S. cerevisiae</i> for western blot.....	111
4.6.9 Co-Immunoprecipitation	111
4.6.10 Immunoprecipitation of HA tagged proteins from infected maize tissue.....	112
4.6.11 <i>In planta</i> phosphorylation assay	112

4.6.12 Mass spectrometry analysis	113
4.7 Plant Methods	114
4.7.1 Maize Varieties (<i>Zea mays</i> sp.).....	114
4.7.2 Cultivation of <i>Z. mays</i>	114
4.7.3 Infection of <i>Z. mays</i> with <i>U. maydis</i>	114
4.7.4 Quantification of <i>U. maydis</i> infection symptoms	115
4.7.5 Cultivation of <i>N. benthamiana</i>	116
4.7.6 Infiltration of <i>N. benthamiana</i>	117
4.7.7 Transient expression in <i>Z. mays</i> via ballistic transformation	117
4.8 Staining, Microscopy and Image Processing	118
4.8.1 Confocal microscopy.....	118
4.8.2 Staining with Calcofluor white	118
4.8.3 Staining with WGA-AF488 und propidium iodide.....	118
4.8.4 EdU WGA-AF488 based DNA synthesis assay	119
4.8.5 Fluorescence microscopy and image processing	120
4.8.6 Transmission electron microscopy (TEM) with Immunogold labeling.....	120
4.9 Bioinformatic Methods	121
5 Bibliography	123
6 Annexure	142

1 Introduction

Interactions between microbes and plants range over a broad scenario of lifestyles of the pathogen ranging from mutualistic symbioses to parasitism. Primarily, symbiotic relationship describes the benefit of both the interaction partners during interaction. However, very recently this concept is under debate as symbiotic fungal mycorrhiza are also known to secrete several small effector like proteins during colonization (Lahrmann et al., 2013) and hence the symbiotic definition is quoted as “enforced surrender” in modern terms. On the other hand parasitism involves hijacking and manipulation of the host in order to complete the life cycle of the pathogen and hence can be described as an advantage ratio imbalance. Plants are challenged with a large variety of phytopathogenic fungi, bacteria, viruses, oomycetes, nematodes and insects. To cope with these potential dangers they are equipped with a highly efficient multilayered immune system.

In agriculture, worldwide annual yield loss of 16–18 % is due to the attack of plant pathogens (Oerke and Dehne, 1997; Oerke, 2006). The phylum basidiomycota represent an important group of fungi including harmful as well as useful species. On one hand it includes the edible mushrooms from the order *Agaricales* and on the other hand important plant parasites forms such as rust and smut fungi. The *Ustilaginales* represent a highly specialized order of higher basidiomycetes that are special colonizers affecting significant grasses and cereal species (Martínez-Espinoza et al., 2002). Understanding the infection strategies of phytopathogenic fungi, the details of plant defense responses, as well as the interaction of both to establish a compatibility or to prevent it, is therefore of great relevance for economic and biological problems.

1.1 Infectious and developmental strategies of phytopathogenic micro-organisms

To successfully establish themselves within the host, plant pathogens use different infectious and development strategies. This can primarily be divided based on the type of lifestyle of the pathogen, which can be broadly classified into three groups - Necrotrophic, Biotrophic, and Hemibiotrophic.

In the necrotrophic lifestyle, the pathogen kills the colonized host to be saprophytic and feed on the dead material. Necrotrophic fungi such as *Alternaria* sp., *Botrytis* sp., *Fusarium* sp., or *Verticillium* sp., secrete many host-specific toxins (HST's) or reactive oxygen species (ROS) which trigger the cell death. (Friesen et al., 2008; Horbach et al., 2011). Biotrophy refers to a lifestyle in which the pathogen is dependent on the living host cells. These pathogens are more specialized in manipulating a host without causing major cell death. Some parasitic biotrophic pathogens, such as rust fungi are obligate biotrophs,

which gather nutrients exclusively from growing tissues, as they have no access to alternative sources of energy. Biotrophic rust fungi such as *Puccinia* sp., or *Uromyces* sp., must therefore establish a biotrophic interaction with its host over the entire generation time upto which the sporulation is maintained (Mendgen and Hahn, 2002; Horbach et al., 2011). In hemibiotrophic interaction, the biotrophic phase is rather temporary and the pathogen after the initial biotrophic establishment switches on to the necrotrophic mode. Examples for such a lifestyle are *Phytophthora* sp., or *Colletotrichum* sp., (Hahn and Mendgen, 2001; Horbach et al, 2011).

Additionally, pathogens could also be categorized depending on how they penetrate the host; i.e., whether they penetrate through stomata and then grow between the host mesophyll cells, such as *Leptosphaeria maculans* (Stotz et al., 2014) or whether they can penetrate directly by plasma membrane invasion, such as *Blumeria graminis* (Hawes and Smith, 1989; Faulkner and Robatzek, 2012). Filamentous pathogens can also be differentiated according to their growth form within the host plant. For example, a distinction of the intercellular hyphae as in *Cladosporium fulvum*, intracellular growth of the pathogen as in *Magnaporthe oryzae*, or a combination of inter and intracellular growth as in monokaryotic rusts and various smut fungi. However, common to all plant pathogens is the necessity of tackle and work around the plant's immune system to successfully establish and complete their life cycle. Especially for biotrophic pathogens, it is essential to suppress the plant defense and specially to prevent the programmed cell death (PCD) to promote the pathogen cycle.

1.2 Biology of smut fungi

The group of smut fungi (*Ustilaginomycotina*) belongs to the Basidiomycetes and consists mainly of plant pathogens that infect a wide variety of flowering plants (Bauer et al., 2006; Begerow et al., 2006). Characteristic of phytopathogenic smut fungi infection is by formation of a dikaryotic filament which is apparent from the fusion of two haploid sporidia (Bakkeren et al., 2008). The name “smut” itself refers to the black, dusty mass of teliospores resembling soot that is formed as a prominent symptom. Members of *Ustilaginales* are biotrophic pathogens with shorter or longer saprobic phases. According to Vanky (1987) there are about 1200 species of smut fungi in more than 50 genera and they infect approximately 4000 species of angiosperms causing a wide range of symptoms. Smuts also represent pathogens causing severe economic losses to major food crops of the world.

General characteristics of smuts include the dikaryotic phase of the life cycle, which is obligately parasitic on flowering plants. Various organs of the host can be infected including leaves, stem and in a few cases even roots. In most hosts, it is the flowering

parts that are targeted. It is also seen that in some hosts perennial infections are established in which the pathogen survives winter within the host tissue and new growth arising from these tissues in spring, starts the infection cycle again. One example of this behavior is the stripe disease of festucoid grasses caused by *Ustilago striiformis* (Mims et al., 1992). As smuts are highly specialized host colonizers, they hijack the host in such a way that most host cells show little response to the presence of the hyphae and may continue to grow normally. As noted by Luttrell (1981) *Ustilaginales* species are basically growth altering parasites that cause alteration of the host tissues immediately before and during the sporulation process. Apart from stunting, many infected plants are virtually symptomless until the fungus begins to sporulate. An exception is the smut *Ustilago maydis* that infects all the aerial parts of its host plant maize, causing unusual patterns of infection by forming prominent galls, the so called tumors. This tumor induction usually occurs after the initial establishment of the fungus. In most smut diseases the proliferation of the sporogenous hyphae results in chlorosis and/or swelling of the host tissues. However, in case of corn plants infected with *U. maydis*, tumor development resulting from division of the host cells precedes sporulation by some time. Teliospore characteristics such as size, shape, colour and ornamentation are of considerable importance in the taxonomical classification of the *Ustilaginales*. The surface ornamentation of the spores is important at the species level. The teliospores of some smut fungi are capable of surviving in the soil for many years.

The order *Ustilaginales* has been divided into two families, *Ustilaginaceae* and *Tilletiaceae*. They are separated on the basis of mode of teliospore germination (Ingold, 1989). In *Ustilaginaceae* the promycelium is prostrate or transversely septate and the basidiospores develop both laterally and terminally. In case of *Tilletiaceae*, the promycelium is either unicellular or aseptate and the basidiospores are only produced terminally. Classification of species within family *Ustilaginaceae* is based on morphology of teliospores, sori and host range. The family consists of a number of economically important species like *Ustilago avenae* causing loose smut of oats, *U. nuda* causing loose smut of barley, *U. tritici* that causes loose smut of wheat and the corn pathogen *U. maydis*.

Members of the family *Tilletiaceae* differ from *Ustilaginaceae* in teliospore germination. The diploid nucleus in a mature teliospore undergoes meiosis prior to germination and then undergoes mitotic divisions. The haploid nuclei then migrate to promycelium. This promycelium in *Tilletiaceae* does not undergo septation. The major genera in this family include the *Tilletia*, which counters various species that cause cereal diseases. A well known example is the *Urocystis*. Species of this genus produce spore balls composed of an outer layer of sterile cells that surrounds the teliospores. *Urocystis cepulae* is a

pathogen of onion. The small genus *Entorrhiza* in this family infects roots mainly producing gall like sori in host plants of family Cyperaceae. Hence, the smut fungi represent one of the widest range of plant pathogens with different lifestyles.

1.2.1 *Ustilago maydis*: The causative agent of corn smut

The smut fungus *Ustilago maydis* is a facultative biotrophic plant pathogen that belongs within the order of *Ustilaginales* the family of smut fungi *Ustilaginaceae* (Martínez-Espinoza et al., 2002). Most smut fungi have a relatively restricted host range and are common pathogens on plants of Gramineae (Poaceae), which includes important cereal crops such as maize, sorghum, sugarcane, wheat and barley (Brefort et al., 2009). *U. maydis* is specialized to infect maize (*Zea mays* L.) and teosinte (*Zea mays* sub.sp. *mexicana* and sp. *parvigluminis*), which is known to be an ancestral form of cultivated maize (Doebley, 1992). The fungus can infect all the aerial organs of the plant and form massive abnormal smut symptoms in the form of tumors (Kämper et al., 2006). The typical infection pattern of *U. maydis* has been shown in Fig. 1. Within these tumors black pigmented teliospores develop, after profuse proliferation of the fungal hyphae giving the infected plants a sooty appearance.



Fig. 1: *U. maydis* induced tumor formation in maize. *U. maydis* infects all the aerial organs of maize and can infect physiologically varied organs like seedling, tassels (male flowers) and ear (female flowers). The photographs are taken at 10 dpi for seedling and tassel tissue and at 16 dpi for ear tissue.

Unlike many other smut fungi that cause immense world economic damages, *U. maydis* is of comparatively little importance (White, 1999). In many parts of South and Central America, the fungus is not considered as a pathogen but infact the non-toxic plant tumors are considered a delicacy for consumption under the name "huitlacoche" (Valverde et al., 1995). The fungus can be easily cultivated under axenic conditions and the complete life cycle can be completed within a few weeks. This fast completion of the lifecycle under

laboratory conditions makes *U. maydis*, an excellent model to study both cell biological, and phytopathological investigations (Kahmann et al., 2000; Martínez-Espinoza et al., 2002; Steinberg and Perez-Martin, 2008; Djamei and Kahmann, 2012). In addition, *U. maydis* has an efficient homologous recombination system, which allows the usage of dominant selectable markers for stable transformation (Holliday, 2004; Kämper, 2004; Basse and Steinberg, 2004). The deciphered genome sequence (Kämper et al., 2006) allows the identification of interesting candidate genes for reverse genetic approaches and thus offers detailed insights into transcriptome, metabolome, secretome and effectome (Kämper et al., 2006; Doehlemann et al., 2008a; Mueller et al., 2008). *U. maydis* shows a biphasic life cycle, where in the initially formed haploid sporidia grow as saprophytes and are similar to yeast cells. The pathogenic form is formed by dikaryotic filament, which is initiated by the fusion of two haploid sporidia of compatible mating loci (Gillissen et al., 1992; Fig. 2A). The biallelic *a* locus encodes a pheromone / receptor system, which allows the detection and fusion of sporidia with different *a*- loci (Bölker et al., 1992). The formation of a conjugation tube (Fig. 2B) is initiated by pheromone perception and sporidia merge at their apical tips forming a dikaryotic filament (Fig. 2C) (Snetselaar et al., 1996). Development of the resulting dikaryon is determined by the multiallelic *b* locus, which encodes for homeodomain transcription factors, bE and bW. If they originate from different alleles of two hyphae of different mating-type loci, it causes dimerization and finally the formation of the heterodimeric bE / bW complex occurs, which is responsible for both the control of filamentous growth, as well as sexual and pathogenic development (Kämper et al., 1995; Brachmann et al., 2001).

The dikaryotic hyphae are characterized by the actively growing tip. The dikaryon accumulates in the cytoplasm of the hyphal tip, whereas in older areas, increased vacuolation is observed and this is eventually spatially separated by septa (Banuett and Herskowitz, 1994). Due to the hydrophobicity of the plant surface and the presence of fatty acids, the polar growth is finally terminated and leads to the formation of an appressorium (Fig. 2D). After the penetration event the invasive hyphae then grows in close contact with the plant plasma membrane by invaginating it, keeping it completely intact (Doehlemann et al., 2008b). This creates a biotrophic interaction zone, which serves to exchange signals with the plant and is the site where major nutrient exchange occurs (Doehlemann et al., 2008a). Around 5–6 days after infection, a massive proliferation of the fungal tissue can be observed (Fig. 2E) leading to the formation of large fungal aggregates in the apoplastic spaces of the tumorous tissue (Banuett and Herskowitz, 1994; Doehlemann et al., 2008b). This is followed by the sporogenesis, which results in the fragmentation and rounding of hyphae, which eventually become highly melanized and differentiates into diploid teliospores (Fig. 2F). These are then released by bursting of the tumors into the

surrounding environment (Snetselaar and Mims, 1994; Banuett and Herskowitz, 1996). The spores can germinate under suitable conditions followed by meiotic division that leads to the formation of haploid sporidia. These haploid sporidia serve as a primary inoculum for the start of the successive life cycle again (Christensen, 1963).

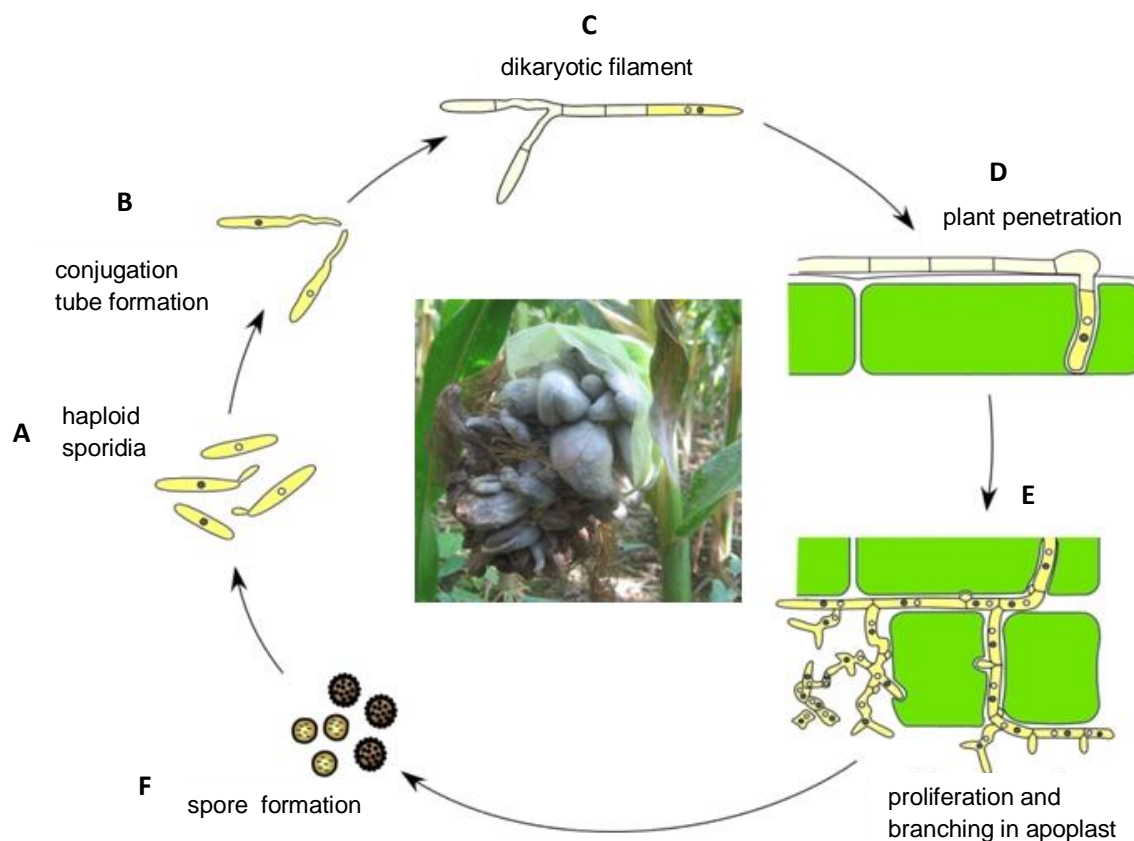


Fig. 2: Schematic representation of the life cycle of *U. maydis*. The diphasic life cycle of *U. maydis* can be divided into a saprophytic (A–C) and a biotrophic phase (D–F). Modified from Doehlemann et al., 2008a.

1.3 The plant immune system

Plants have no mobile immune cells and no well adaptive immune system in comparison to mammals (Ausubel, 2005; Jones and Dangl, 2006). Plant immune responses function in several layers after pathogen attack. The primary defense responses are the physical barriers such as wax, cuticle, epidermal cell wall, and antimicrobial secondary metabolites. This line of defense prevents the pathogen from initial penetration and establishment. In addition, it also protects the plant from dehydration and other environmental influences (Dangl and Jones, 2001; Koeck et al., 2011).

The critical processes of the plant immune system are recognition of a pathogen and induction of suitable defense responses. The defense reaction generated by the plant also has some deleterious effects on itself and these processes need to be tightly controlled. This second line of immunity involves the expression of pathogenicity related (PR) genes,

production of secondary metabolites (eg. alkaloids, phytoalexins) and the deposition of cell walls with callose or lignins. If this line of defense is effective then the plant is considered as non-host and is resistant towards a specific pathogen (Dangl and Jones, 2001; Nuernberger and Brunner, 2002). Activation of this defense signaling is by the detection of conserved microbial signaling molecules so-called MAMP's or PAMP's (**m**icrobe-/**p**athogen-**a**ssociated **m**olecular **p**atterns) (Chisholm et al., 2006; Jones and Dangl, 2006). Such molecules include flagellin or lipopolysaccharide in the case of bacteria, and ergosterol, chitin or β -glucan in the case of fungi and oomycetes (Zipfel, 2009; Boller and Felix, 2009; Dodds and Rathjen, 2010). Recognition of these structures is carried out using specific receptors, known as **p**attern **r**ecogniton **r**eceptors (PRRs). PRRs are modular proteins consisting of an extracellular domain, which is harbouring leucine residues (**l**eucine **r**ich **r**epet, LRR) or lysine motifs (LysM) responsible for the signal perception. These are either plasma membrane spanning receptor like kinases or receptor like proteins without a kinase domain (Zipfel, 2009; Segonzac and Zipfel, 2011). In addition, plants also detect fragments of their own structures (eg. cell wall or cutin fragments), so-called **d**amage-**a**ssociated **m**olecular **p**atterns (DAMP's) (Lotze et al., 2007; Boller and Felix, 2009). These are typically released by injury to the plant tissue, but also by predators or by abiotic factors such as excessive solar irradiation in course of infection by pathogens. Stimulation of PRRs and associated defense mechanisms that allow the host to successfully defeat the pathogens is referred as **P**AMP-**T**riggered **I**mmunity (PTI) (Jones and Dangl, 2006; Dodds and Rathjen, 2010).

Pathogens can manage to overcome the PAMP triggered immunity by evolving virulence factors (effectors) that are enabling them to suppress the plant defense response. In this case, the plant turns susceptible towards a pathogen. Yet, plants develop specialized second stage of defense, the so-called **E**ffector-**T**riggered **I**mmunity (ETI), which is based on the specific recognition of effector proteins that are secreted by the pathogen (Chisholm et al., 2006; Jones and Dangl, 2006). The detection of effectors may activate in turn, specific receptor proteins, called the nucleotide-binding-LRR Receptor (NB-LRRs), (Chisholm et al., 2006). Activation of the NB-LRR receptor generates a defense phenomenon which is generally stronger and faster than PTI, called as hypersensitive response (HR), which is formed due to the production of ROS and PCD in the area of infection and is normally induced to prevent the further spread of the pathogen. In this context, the detected effectors are Avirulence (Avr) proteins and their associated plant proteins are called resistance proteins (R-proteins) (Chisholm et al., 2006; Takken et al., 2006; Dodds and Rathjen, 2010). This recognition does not necessarily have, a gene-for-gene interaction (Flor, 1971), which is a direct physical interaction between R protein and the corresponding Avr protein, as it was in case of the R protein Pi-ta from rice (*Oryza*

sativa) and Avr-Pita described from *M. oryzae* (Jia et al., 2000). In many cases, an indirect recognition seems to occur. Three conceptual models have been proposed to describe the mechanism of indirect recognition. The “guard” model postulates that NB-LRR proteins guard an accessory protein that is targeted and modified by the pathogen effectors (Jones and Dangl, 2006). Target proteins of effectors are subjected to a strong selection pressure, because of which in the course of evolution, duplications of the effector target gene or new proteins with the same function occur, that mimic the actual target protein and serve as prey for effectors. This concept is proposed as “decoy” model (van der Hoorn and Kamoun, 2008). In addition, another model called the bait and switch model, envisages a two step recognition event. First an effector interacts with the accessory ‘bait’ protein associated with the NB-LRR protein and then a subsequent recognition event occurs between the effector and the NB-LRR protein to trigger signaling (Collier and Moffett, 2009).

Plants are also protected by a mechanism called systemic acquired resistance (SAR), which occurs at sites distant from the primary and secondary immune responses and protects plant from subsequent pathogen challenge (de Wit, 2007). SAR is effective against a broad range of pathogens and is dependent on different plant hormones including salicylic acid (SA), jasmonic acid (JA), ethylene (ET), and abscisic acid (ABA). SA regulation is important for resistance to biotrophic pathogens, while JA in association to ethylene regulate resistance to necrotrophic pathogens (Panstruga and Dodds, 2009). The SA and JA defense pathways are mutually antagonistic and many bacterial and fungal pathogens have evolved strategies to exploit the regulation of the hormonal signaling for completion of its life cycle after successful colonization (Kunkel and Brooks, 2000; Kazan and Lyons, 2014). Ultimately, in a molecular “war” between the plant and the pathogen, both the effectors of the pathogen and the host resistance proteins are subjected to a strong selection pressure and thus constantly new strategies for successful infection and immunity arise (Birch et al., 2006; Jones and Dangl, 2006). The basic mechanisms of signal perception and transduction in the context of plant defense are summarized in Fig. 3.

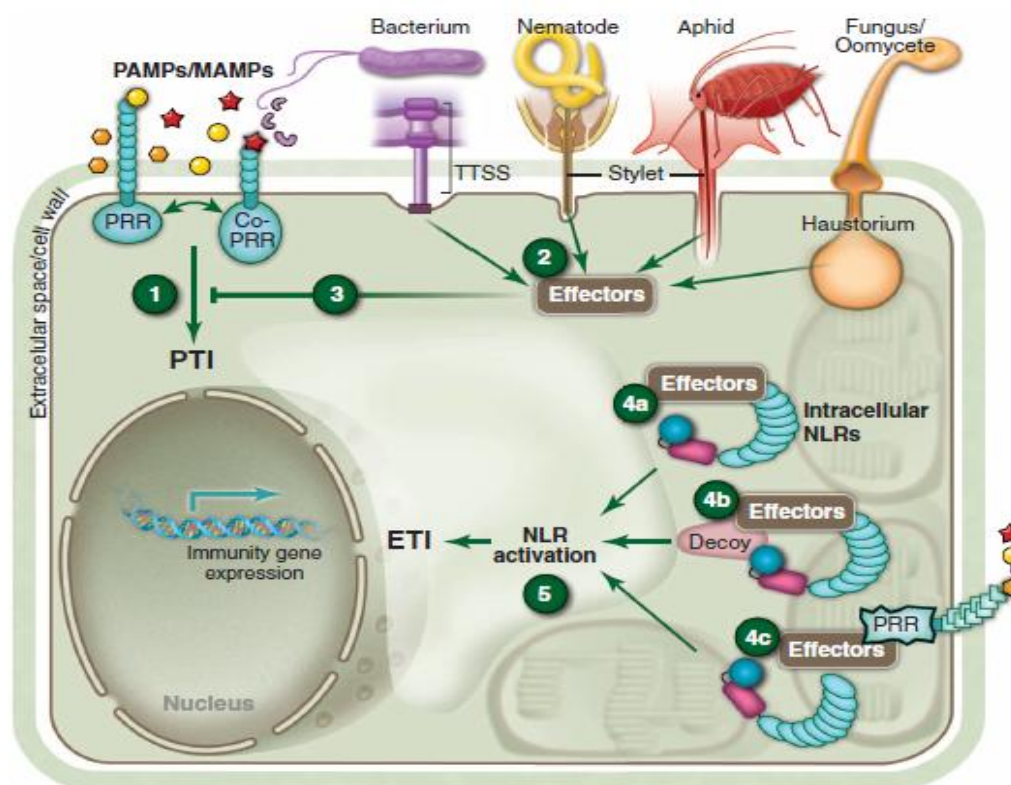


Fig. 3: Schematic figure of the plant immune system. Pathogens of all lifestyle classes (colour coded and labeled) express PAMPs (*pathogen-associated molecular patterns*) and MAMPs (*microbe associated molecular patterns*) as they colonize plants (shapes are colour coded to the pathogens). Plants perceive these via extracellular PRRs (*pattern recognition receptors*) and initiate PRR triggered immunity PTI (*PAMP-triggered immunity*, step 1). Pathogens deliver virulence effectors to both the plant cell apoplast to block PAMP/MAMP perception (not shown) and to the plant cell interior (step 2). These effectors are addressed to specific subcellular locations where they can suppress PTI and facilitate virulence (step 3). Intracellular NLR receptors can sense effectors in three principal ways; first by direct receptor ligand interaction (step 4a); second, by sensing effector mediated alteration in a decoy protein that structurally mimics an effector target, but has no other function in the plant cell (step 4b); and third, by sensing effector mediated alteration of a host virulence target, like the cytosolic domain of the PRR (step 4c). It is not yet clear whether each of these activation modes proceed by the same molecular mechanism, nor it is clear how, or where, each results in NLR dependent ETI (*effector-triggered immunity*). (from Dangl, Horvath and Staskawicz, 2013).

1.4 Effectors: The keys players in manipulating the host

To establish a successful infection and to modulate PAMP triggered plant defense response, plant pathogens secrete proteins and other molecules, collectively termed as effectors, to different compartments of their hosts (Jones and Dangl, 2006). These effectors are the key players in alteration of the structure and function of the host cell during the infection process (Kamoun 2006; Stergiopoulos and De Wit, 2009; Hogenhout et al., 2009). Effectors act either in the intercellular space to handle the primary defense response, or they can act inside the host cell to confer various functions such as re-programming of the host cell to favor infection (Doehlemann et al., 2014). Identification of the function of such virulence proteins has been a major challenge as they lack homologies and sequence similarity to known proteins. The advent of genome sequencing

has enabled large-scale identification of candidate effectors by *in silico* prediction of secreted proteins in pathogen genomes (Kämper et al., 2006; Mueller et al., 2008).

Plant pathogens possess a large variety of secreted effector proteins depending upon their lifestyle. Classically these secreted effectors are generally characterized by the presence of an N-terminal signal peptide for secretion, specific expression during invasion of plant cells and the lack of conserved functional domains which makes the functional tracking of such molecules difficult (Valent and Khang, 2010; Rafiqi et al., 2012). In a compatible interaction, the effectors facilitate suppression of the plant immunity as well as orchestrate re-programming of the infected tissue to make it an active source for nutrient exchange to support pathogen growth and development (Koeck et al., 2011). In bacteria relatively small numbers of effectors are known to exist whereas oomycetes and fungal genomes harbor several hundreds of genes coding for putative effector candidates (Kamoun, 2006; Kämper et al., 2006).

The apoplastic effectors that are secreted and function into the extracellular space during the interaction are seen to have their roles in primary defense suppression. Apoplastic effectors from several pathogens have been shown to be acting as protease inhibitors suppressing the activity of serine/cysteine proteases. The apoplastic avirulence (AVR) effector Avr2 of *C. fulvum* is shown to inhibit the tomato plant-derived cysteine protease RCR3 (Rooney et al., 2005). The *P. infestans* apoplastic effectors EpiC1 and EpiC2 inhibit activity of the tomato protease C14, and the cytoplasmic RXLR effector Avrblb2 focally accumulates near the haustorium and blocks secretion of C14 into the apoplast (Bozkurt et al., 2011). Several fungi are also known to secrete effectors to block chitin induced immunity, which is activated due to the chitin fragments of fungal cell wall that act as PAMP's. Diverse pathogens secrete effectors that contain LysM amino acid domains that either prevent the release of chitin oligosaccharides from fungal cell walls or that sequester these oligosaccharides to prevent recognition. *C. fulvum* secretes the LysM effector Ecp6, which sequesters chitin oligosaccharides released from the fungal cell wall (de Jonge et al., 2010). The *C. fulvum* effector Avr4 contains a different chitin-binding domain and functions to protect the fungal cell wall from degradation by plant chitinases (van den Burg et al., 2004). One of the three LysM effectors in the intercellular wheat pathogen *Mycosphaerella graminicola* has both wall protection and sequestering functions (Marshall et al., 2011). In *M. oryzae*, the LysM effector Slp1 binds chitin oligosaccharides and suppresses chitin-induced immunity mediated by the rice PRR, chitin elicitor binding protein, CEBiP (Mentlak et al., 2011).

1.4.1 Translocation of effectors and their characteristics

During the past decade, it has become apparent that plant pathogenic bacteria, fungi, and oomycetes deliver effector proteins inside the host cell cytoplasm (Dong et al., 2011; Djamei et al., 2011; Park et al., 2012). The concept of effector translocation was first put forward for plant pathogenic bacteria (Gopalan et al., 1996) and the bacterial type III secretion system has been thoroughly studied. Nevertheless, the mechanisms by which effector proteins travel to the plant cell cytoplasm remain poorly understood in fungi and oomycetes. Solving the enigma of how filamentous pathogens deliver their effectors to the inside of plant cells is a fundamental question in plant pathology.

Translocation of bacterial effector proteins has widely been studied by the type III secretion system (TTSS) (Abramovitch and Martin, 2005). This secretory system consists of 15–20 Hrp (hypersensitive response and pathogenecity) proteins building a secretion apparatus (Cornelis and Van Gijsegem, 2000). These effector molecules are shown to specifically modulate the PAMP triggered immunity signaling pathways (Feng and Zhou, 2012). Several of the *P. syringe* type III effectors HopA1 and HopF2 have been shown to interact with the **mitogen activated protein kinase** (MAPK) cascades and are involved in its inactivation. Posttranslational modification of the host proteins is another common strategy employed by the type III effectors (Feng and Zhou, 2012). Type III effectors are able to enter the host nucleus and regulate the transcription mechanism to enhance susceptibility towards the pathogen (Kay and Bonas, 2009).

The effector proteins of various filamentous pathogens that translocate into plant cells are highly diverse in sequence and structure and have most likely evolved a variety of mechanisms to modulate the host cytoplasm. However, the secreted effectors of plant pathogenic oomycetes have evolved a common theme of host-targeting which relies on N-terminal translocation domains that are located after a general secretory signal peptide. Several motifs such as RXLR, LFLAK, and CHXC amino acid sequences, have been shown to be involved in translocation (Jiang et al., 2008). The RXLR leader sequence was shown to be required for translocating the effector into cytosol of host cell (Whisson et al., 2007) but the mechanism required for the translocation is still unclear and under debate (Tyler et al., 2013; Wawra et al., 2013). A study documented by Birch et al., 2008 showed that RXLR motif is also found in 315 *Arabidopsis thaliana* proteins of which 20 % were conserved or members of the endocytosis cycle, suggesting that endocytosis might be involved in the uptake of the RXLR harbouring effector proteins. In the recent years genome sequencing has revealed new effector protein families with conserved amino-terminal motif in other oomycetes, like the YXSL[**RK**] motif for *Pythium ultimum* (Bozkurt et al., 2012).

Identification of motifs involved in cell entry is not as advanced for fungal effectors as it is for oomycetes. Bioinformatic analyses have not yet identified putative translocation motifs for most fungal effectors (Rafiqi et al., 2012). Many powdery mildew effector candidates contain a short Y/F/WXC motif within 30 amino acids of the signal peptide (Spanu et al., 2010; Godfrey et al., 2010) although functional characterization of this motif is lacking. Large families of candidate effectors have been identified from fungal genomes, but except from a common N-terminal signal peptide it is unknown how these fungal effectors target their site of action within the host plant. Nevertheless, the *Uromyces fabae* effector RTP1 was detected in the host cytoplasm suggesting a route for uptake and a function within the host cell (Kemen et al., 2005). Recent studies on fungal effector translocation have indicated that a special structure is involved in translocation of the secreted effectors. In the rice- *M. oryzae* system a highly localized structure, the biotrophic interfacial complex (BIC), was identified as a structure for translocation of the effector proteins into the rice cytoplasm. It was also shown that the effector proteins that reached the rice cytoplasm moved into uninvaded neighbors, presumably preparing host cells for invasion (Khang et al., 2010). In *C. orbiculare* it is also shown that the primary hyphal neck is a specialized structure responsible for the accumulation and translocation of effectors into the host (Irieda et al., 2014). Additionally, sequences that mediate host cell translocation have been detected within host specific toxins of necrotrophic fungi. One well studied example is the C-terminal RGD motif of ToxA from *Pyrenophora tritici-repentis*, which is required for entry into host plant cells (Manning et al., 2008). Also, domains in the N-terminus of the flax rust fungus *Melampsora lini* effectors AvrM and AvrL567 mediate uptake into plant cells, although whether these sequences determine entry into plant cells or other processes is still unclear (Rafiqi et al., 2010; Ve et al., 2013). Moreover, several fungal effectors have been linked to interact with the cognate R gene products (Chauhan et al., 2002). As effectors are directed to the plant cell to overcome disease resistance they might interact with the cognate R gene from plants and are always subjected to a high evolutionary selection causing a high degree of diversity (Win et al., 2007). Hence, the putative functions are really hard to investigate. Although advances in effector identification are numerous, the functional characterization of these novel effector proteins significantly lags behind.

1.5 Effectors of *U. maydis*

U. maydis as biotrophic pathogen is dependent on living plant tissue, which requires the fine suppression of the plant's immune system. To this end, secreted *U. maydis* effectors in the biotrophic interaction zone are crucial for establishing and maintaining biotrophy (Kämper et al., 2006; Doehlemann et al., 2008b). In addition, the fungus causes

comprehensive re-programming of the plant metabolism to initiate tumors. To this end secreted effector proteins that are translocated into the plant cell are of immense importance (Djamei et al., 2011; Tanaka et al., 2014). For *U. maydis* 550 potentially secreted proteins are decoded by *in silico* analysis of the genome sequence (Mueller et al., 2008). Out of these, 168 have a putative enzymatic function, while for the remaining 386 proteins no predictions could be made due to lack of homology to previously known proteins and the majority of these are specific for *U. maydis* (Mueller et al., 2008). Interestingly, the majority of *U. maydis* effectors are organized in gene clusters. Twelve such gene clusters have been identified which code for novel secreted proteins and in several instances these belong to small gene families. Moreover, it was shown that five gene clusters are functionally involved in tumor formation (Kämper et al., 2006).

Overall, very little is known about the function of individual effectors. The subcellular localization of most *U. maydis* effectors is unknown. So far four effectors of *U. maydis* which are found to be involved during the specific stages of the fungal establishment have been functionally characterized. Pep1 (**p**rotein **e**ssential for **p**enetration 1) is known to be essential for the initial establishment of a compatible interaction of *U. maydis*. Deletion mutants for *pep1* are completely non-pathogenic and fail to meet the initial penetration where they are subsequently recognized by the plant. This initiates the accumulation of ROS, papillae, as well as local cell death on the leaf surface (Doehlemann et al., 2009). In further studies, it was shown that this protein is localized in the apoplast and suppresses basal immune response of the plant by targeting and depressing the activity of peroxidases (POX) (Hemetsberger et al., 2012). A novel gene cluster encoding four genes, the so called Pit genes (**p**rotein **i**nvolvement in **t**umor formation) has also been described in *U. maydis*, which consist of two virulence factors that are both required for formation of plant tumors. One of these genes encodes a membrane protein (Pit1) while Pit2 is a small effector that is secreted to the apoplast (Doehlemann et al., 2011). This Pit2 effector has been functionally characterized and is shown to be an inhibitor of a set of apoplastic maize cysteine proteases during the interaction (Mueller et al., 2013).

Translocated effectors in *U. maydis* also seem to have interesting roles. These effectors seems to be acting in monitoring various metabolic processes thereby handling the plant cell machinery to suppress the defense responses on one side and to induce a tumor on the other. The first characterized translocated effector of *U. maydis* is Cmu1 (**C**horismate **m**utase 1). The effector is shown to be taken by the plant cell where it interferes with the synthesis of SA. Cmu1 actively intervenes in the shikimate pathway and catalyzes the conversion of chorismate to prephenate, leaving less chorismate available for the synthesis of SA. This has a negative effect on the SA-dependent plant defense. Cmu1 also spreads via plasmodesmata into adjacent plant cells, which also contributes in these

cells to suppress the plant defense (Djamei et al., 2011). Recently another translocated *U. maydis* effector Tin2 (**T**umor **i**nducing 2), which is a part of the largest fungal effector-cluster identified so far (Brefort et al., 2014) was also functionally elucidated. Tin2 conceals an ubiquitin proteasome degradation motif in Zm-TTK1, a maize protein kinase that regulates anthocyanin biosynthesis pathway, and thus stabilizes the active kinase against degradation thereby inducing the production of anthocyanin in infected tissue by suppressing the lignin pathway (Tanaka et al., 2014).

Since *U. maydis* infects all the aerial parts of corn, there is seen to be an interaction of the pathogen with various developmentally differentiated host tissues. To cope up with these physiologically varied organs, the pathogen has an amazing complexity of effector proteins. A study by Skibbe et al., 2010 revealed that gene expression in *U. maydis* -maize interaction is in an organ specific manner. Interestingly, effector genes are also differentially expressed in different infected maize organs and that some effector mutants affect tumor formation only in specific organs. This suggests that the ability of *U. maydis* to induce tumors in different maize organs relies on its ability to finely tune the host with organ specific effectors. Skibbe and co-workers have suggested a two-step process of colonization in this pathosystem in which a first set of “core” effectors are used to suppress plant defense responses during initial establishment and a second set of specific effectors responds to maize organ that is colonized (organ-specific effectors). This indicates that *U. maydis* is able to sense the different developmental conditions of its host and reacts by secreting a cocktail of specifically tuned effectors for re-programming these specific tissues. To date the functional basis of any organ specific effector remains elusive.

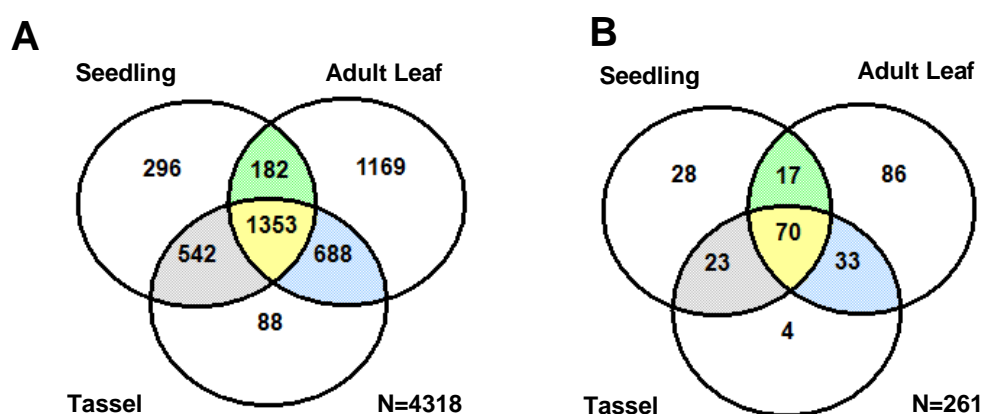


Fig. 4: Organ specific gene expression in *U. maydis*–maize interaction. (A) Organ specific gene expression of the *U. maydis* genes at 3 dpi after infection. More than 36 % of the fungal transcriptome is seen to be organ specific. (B) *U. maydis* genes encoding secretome proteins at 3 dpi that acts in organ specific manner. More than 45 % of the fungal secretome is organ specific at 3 dpi (Modified from Skibbe et al., 2010).

However, a study by Schilling et al., 2014 showed that the organ specific effector deletion mutants in all cases exhibited a quantitative reduction in virulence, measured as both a reduced size and number of tumors. These phenotypes are in clear contrast with the previously described mutants for the *U. maydis* effectors Pep1 and Pit2, which are both blocked before tumors can develop (Doehlemann et al., 2009, 2011). Pep1 and Pit2 both target central components of the plant's immune system. Suppression of the initial host defence by these effectors is essential for the establishment and maintenance of a biotrophic interaction, and effectors with immune-suppressive functions therefore form the first layer of microbial weaponry (Takken and Tameling, 2009). Further progression of disease and in particular, the induction of tumors requires an acclimation to growth in a particular plant organ and possibly, cell type. Therefore, colonization of different cell types by the pathogen would require the suppression of cell-specific defence pathways. Hence, in particular, the induction of plant tumors is from the activities of specialized effectors, which manipulate not only defence responses, but also the host cell metabolic state as well as cell cycle control.

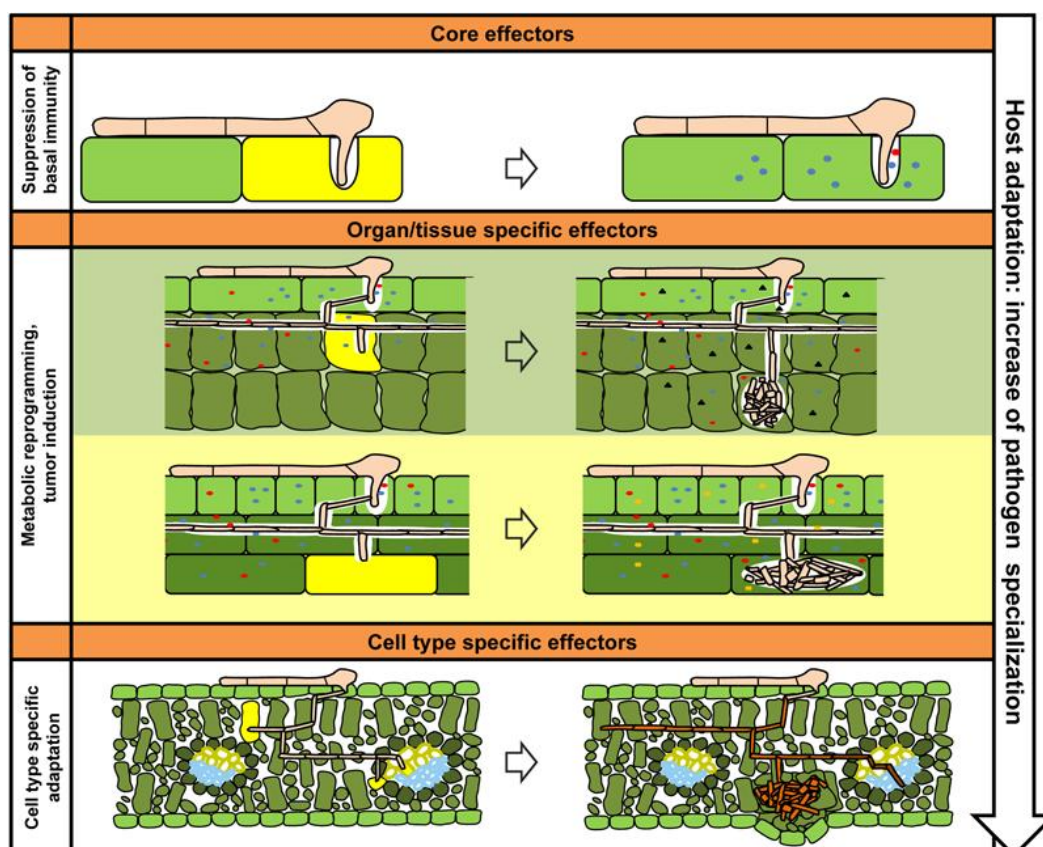


Fig. 5: Model for different classes of effectors acting in the *U. maydis* –maize interaction. Top panel: Establishment of infection during epidermal penetration that requires core effectors (blue, red circles) which suppress basal host immunity. Middle panel: fungal proliferation, metabolic re-programming and tumor induction in different host tissues are supported by the activity of organ specific effectors (triangles, squares). Bottom panel: increasing adaptation to the host plant may coincide with the development of cell type specific effectors, which are tailored to the specific proteome and metabolic conditions of different cell types colonized by *U. maydis*. Yellow plant cells indicate block in fungal development. (from Schilling et al., 2014).

1.5.1 See1, an organ specific virulence factor

On the basis of previous findings from Schilling et al., 2014 that organ specific effectors exist, the next objective was to elucidate the characterization of these effector candidates. An interesting category among these candidates was of the effectors that are specifically induced in leaf as *U. maydis* is the only pathogen in order *Ustilaginales* causing these hallmarking symptoms. An interesting phenotype in this category was shown by the gene *um02239* (now termed *see1*). Hence, this candidate was chosen for further characterization. See1 (**S**eedling **e**fficient **e**ffector 1) effector of *U. maydis* is the 157 amino acid long secreted protein that acts in an organ specific manner. The gene is located on chromosome 5 of *U. maydis* genome, contains no introns and is designated in the MUMDB (MIPS *Ustilago maydis* database) under the designation *um02239*. (<http://mips.helmholtz-muenchen.de/genre/proj/ustilago>). There are no paralogs of *see1* in the *U. maydis* genome analysis using the protein A domain Domain ID SMART program (<http://smart.embl-heidelberg.de/>). The protein shows an N-terminal signal peptide with a length of 21 amino acids. Other functional domains within the protein cannot be predicted. See1 is induced transcriptionally during the leaf tumor formation indicating the role of this effector in shaping the tumors on leaves. Hence, this was a top candidate to investigate the functional and mechanistic basis during the *U. maydis* induced tumor formation.

1.6 Interplay between the cell cycle regulation and defense responses

Many pathogens represent different lifestyles and diverse taxa, alter host cell morphology and/or causes perturbation in the cell cycle progression. Cell division, cell expansion, and cell differentiation are central processes of plant development. They are tightly controlled at various levels to coordinate the development of each organ and to meet challenging physiological conditions. Any misregulation can lead to severe consequences in shape and function as observed in developmental mutants. It was recently found that perturbations of the cell cycle induced signal transduction pathways also involve components of the plant defense response, suggesting a direct link in between cell cycle and plant immunity (Bao et al., 2013). It was shown that the *Arabidopsis* gene OSD1 (**O**mission of the **S**econd **D**ivision 1) and its homolog UVI4 (**U**V-B-**I**nsensitive 4) are negative regulators of the **a**naphase-**p**romoting **c**omplex/**c**yclosome (APC/C), a multisubunit ubiquitin E3 ligase that regulates the progression of cell cycle. Overexpression of OSD1 and UVI4 was seen to enhance immunity to a bacterial pathogen, which is associated with increased expression of disease resistance (R) genes. Enhanced immune response induced by OSD1 overexpression is dependent on Cyclin B CYCB1.1, which is a degradation target of APC/C. These findings suggested that cell

cycle mis-regulation could have an impact on expression of genes, including R genes, in plant immunity. Also DNA repair proteins have been shown to be directly involved in regulation of gene expression during plant defense responses (Song et al., 2011). It is known that the DNA damage response is an intrinsic component of plant immune response and in turn enhances SA-mediated defense gene expression (Yan et al., 2013). On one side of the spectrum, efficient activation of plant defense leads to a hypersensitive response, which can result in programmed cell death. Successful biotrophic pathogens are known to block such defense responses and promote nutrient influx into the infected tissues, which is metabolically highly enriched. Reports on the interplay between the cell cycle and the plant immunity have been started appearing in the recent years; however, the topic is yet to be explored. Hence, a combination of immune suppression and nutrient reallocation can result in uncontrolled host cell proliferation that ultimately results in galls and plant tumors that are caused by different plant pathogens.

1.7 Aims and objectives of this study

The aim of this work was the functional characterization of *See1* (*um02239*), a secreted organ specific effector that is crucial for the initiation of tumors specifically in the leaves during biotrophic interaction between *U. maydis* and its host plant maize. The main objectives of the study were:

- 1) Spatial and temporal expression profile of the effector showing its organ specific nature which was necessary to understand the requirement of such effector in tumor formation.
- 2) To determine the localization of the effector, whether apoplastic or cytoplasmic thereby understanding the host atmosphere for *see1* action.
- 3) Identification and analysis of the maize targets for *see1* which was important in knowing the processes targeted by the effector for symptom development.
- 4) Understanding the mechanistic basis of *See1* action to unravel its function.

2 Results

2.1 See1 is an organ specific effector

2.1.1 See1 is specifically required for expansion of leaf tumors

Three independently generated deletion strains for the effector *see1* (*um02239*) which were previously generated by Ziba Ajami Rashidi were evaluated for their virulence test by infection of the maize seedlings as previously standardized in the maize *U. maydis* patho-system (Kämper et al., 2006). Three independent replicates with 40 seedlings, each for wildtype and mutant infections were performed. The 7 days old maize seedlings were inoculated by syringe inoculation and were scored at 6 and 12 days post infection (dpi) and analyzed for their ability to form virulence symptoms (Fig. 6A and 6B). All three SG200 Δ *see1* strains were reduced in virulence and forming only small tumors in the range of 1–4 mm in diameter at 12 dpi. This tumor category represented about 50 % of the symptoms formed with the SG200 Δ *see1* strains. Tumors at a size of >6–20 mm, which are frequent in SG200 infections were almost absent in SG200 Δ *see1* mutant infections and represented only % of the total symptoms (Fig. 6B). Formation of heavy tumors, which result in altered leaf shape or even stunted growth of infected seedlings, are not observed after infection by the SG200 Δ *see1* mutants.

To verify that the reduced pathogenic phenotype of the deletion mutants SG200 Δ *see1*, is because of the *see1* gene and not due to the side effect or mutations in the flanking regions, the plasmid p123-P*see1*-*see1* in which the *see1* gene is under the control of its endogenous promoter (P*see1*) was amplified from the genomic DNA of solopathogenic wildtype *U. maydis* SG200 and integrated into the *ip* locus (Loubradou et al., 2001) of SG200 Δ *see1* to produce strain SG200 Δ *see1*-*see1*. The generated mutants were confirmed for the presence of the single or multiple integration of the respective candidate by southern blot analysis. Plant infection assays with these strains showed full complementation the Δ *see1* phenotype, i.e., the introduced gene complemented the *see1* deletion phenotype completely and forms large tumors similar to the wildtype strain. This demonstrated that See1 is responsible for the reduced pathogenicity of SG200 Δ *see1*. (Fig. 6A and 6B).

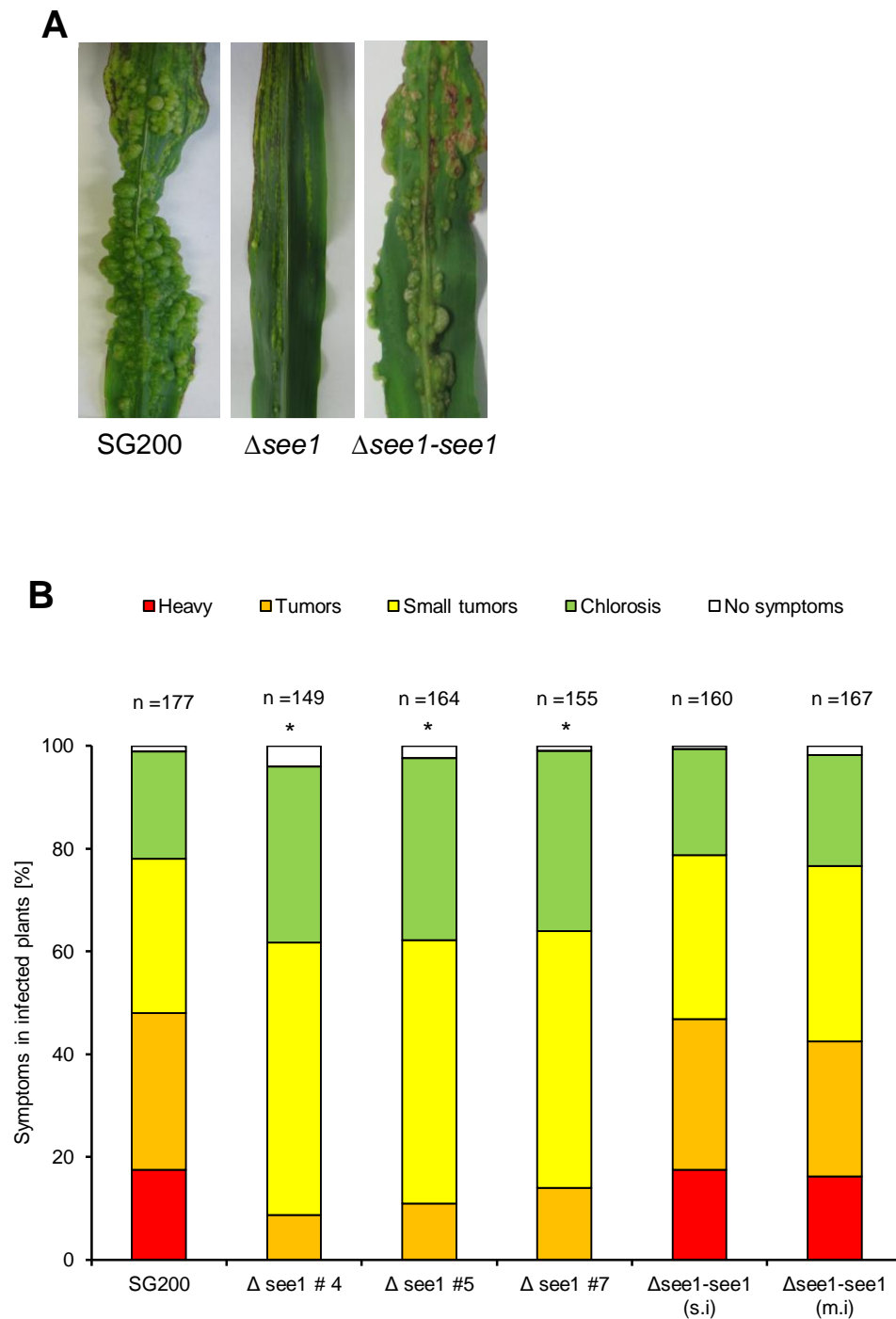


Fig. 6: Disease symptoms caused by the *U. maydis* SG200 $\Delta see1$ and the complementation strain in comparison to the wildtype *U. maydis*. (A) Symptoms caused by *U. maydis* strain SG200 in comparison to the SG200 $\Delta see1$ mutant and the *See1* complemented strain in leaves. The leaf photographs show typical disease symptoms at 12 dpi; The *see1* effector mutant is drastically reduced in virulence and the ability to form tumors were significantly reduced on seedling leaves. (B) Disease rating of the symptoms caused by the three independent SG200 $\Delta see1$ knockout strains and by independent SG200 $\Delta see1-see1$ complemented strains. The disease rating is in comparison to the wildtype progenitor strain SG200 in comparison to the knockout strain SG200 $\Delta see1$ and the complemented strain SG200 $\Delta see1-see1$ in seedling leaves. The mutant shows a significant reduction in virulence on leaves. Disease symptoms were scored at 12 dpi as described in Kämper et al., (2006). SG200, virulent *U. maydis* progenitor strain; $\Delta see1$, deletion mutant for *see1* effector SG200 $\Delta see1-see1$: The complemented strains with single integration (s.i) and multiple integration (m.i). The experiment was performed in three independent biological replicates. n= number of plants infected, *, $P \leq 0.001$.

2.1.2 See1 is not required for tumor formation in floral parts

To test the SG200 Δ see1 mutants on other aerial organs of maize, tassel infections were standardized, as this floral tissue is emerging prior to the cobs in the developmental floral switch of the maize plant. To standardize the tassel infections, two varieties of *Z. mays*, cv. Early Golden Bantam (Olds Seeds, Madison, WI, USA) and cv. Gaspé Flint (University of Giessen, Germany) were used. The dwarf *Zea mays* cultivar ‘Gaspé Flint’ completes its life span in 30–35 days, has an early floral switch (15 days) and suitable for early tassel infections. From the literature it is known that *U. maydis* infects the mitotically active tassel meristem to develop a tumor (Walbot and Skibbe, 2010). In tassel infections the deletion mutants for *see1* develops normal, large tumors that are indistinguishable from the virulent wildtype progenitor strain SG200 (Fig. 7A). Similarly, in maize ears no reduction of tumor formation was observed, supporting a strictly leaf specific role of *see1* for tumor generation (Fig. 7B).

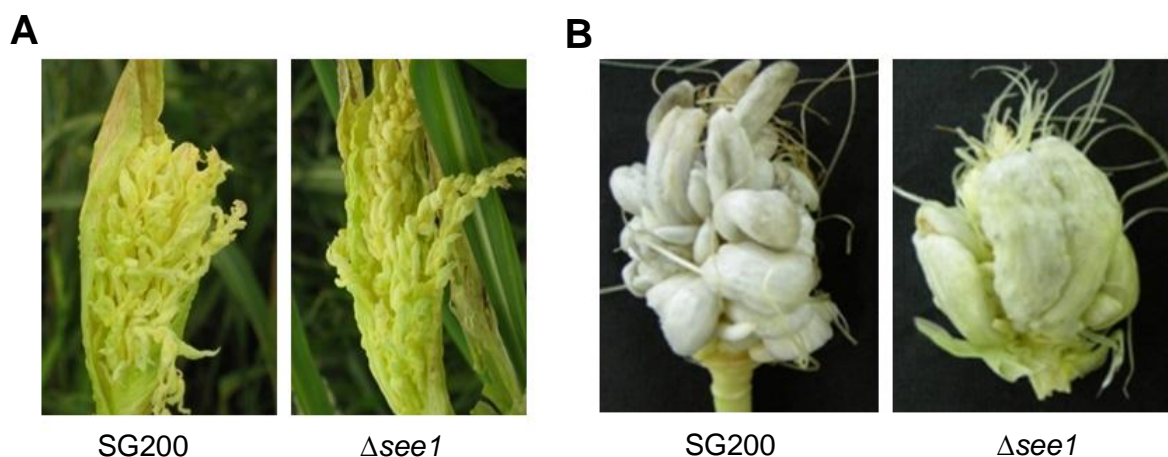


Fig. 7: Disease symptoms caused by the *U. maydis* SG200 Δ see1 mutant in floral parts: Symptoms caused by *U. maydis* strain SG200 in comparison to the SG200 Δ see1 mutant in the male flowers (tassels, A) and the female flowers (ears or cobs, B). The tassel photographs show typical disease symptoms at 14 dpi and ear symptoms at 16 dpi. Similar to SG200, the mutant caused large and numerous tumors in tassel and ear.

To allow the quantitative evaluation of tassel infections comparable with that of the seedling leaves, a new scoring scheme was developed. *U. maydis* developed tassel symptoms were classified into five categories depending on symptom severity (Fig. 8A). The criteria for tassel scoring were based on the area of the tassel converted into tumor as well as the tumor size. In addition developmental changes of the infected tassels were assessed, including a growth arrest at 1–3 cm stage, which was induced by the mutant as well as wildtype SG200 (Figure 8A). For consistency of the observed tassel phenotypes, the previously mentioned two *Z. mays* varieties were tested. Both the tested cultivars showed consistently similar results indicating reproducibility of the symptoms in developing a scoring scheme. The disease rating in the tassels with the observed

symptoms as seen in the two different cultivars of maize have been represented in the Fig. 8B.

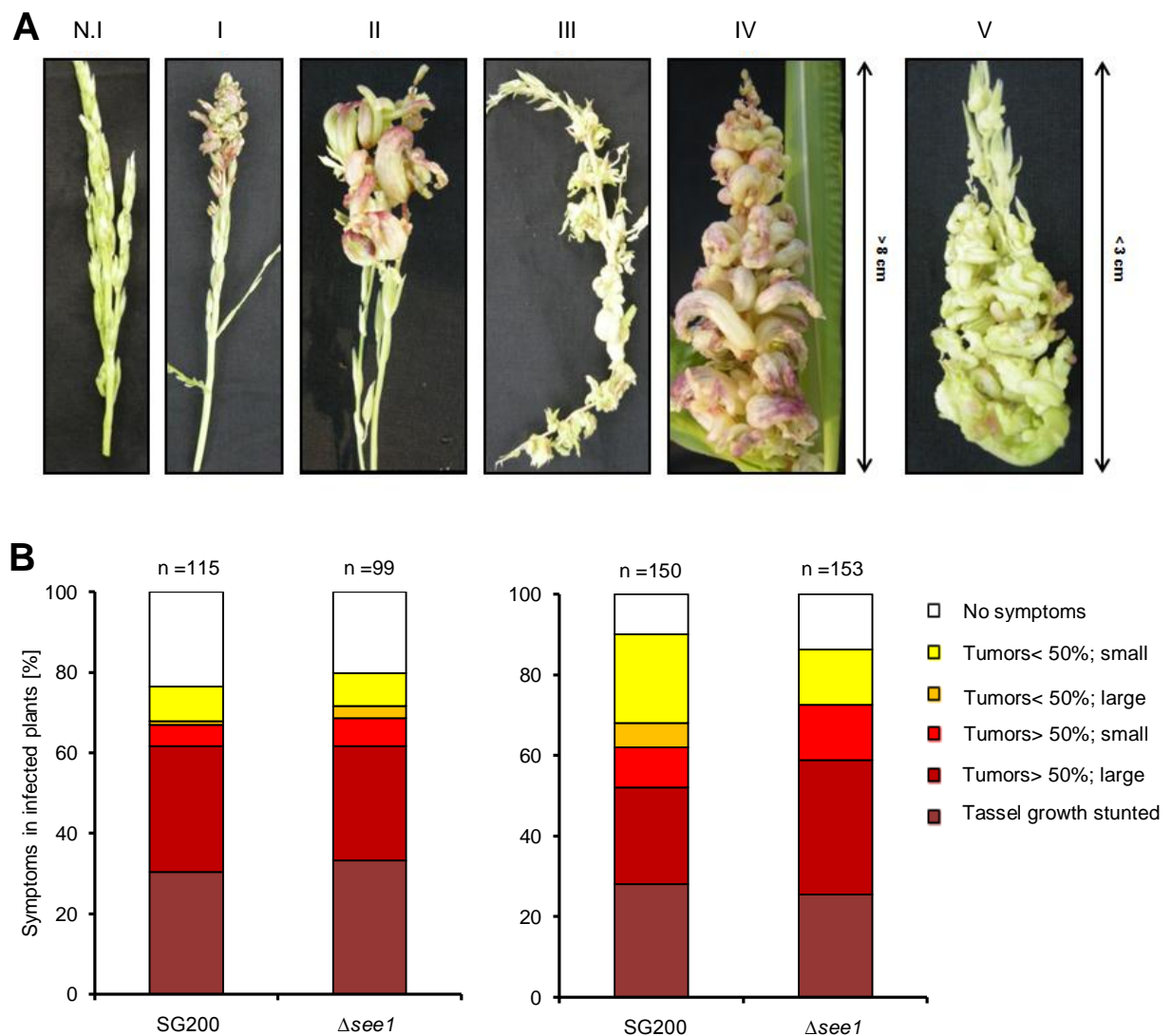


Fig. 8: Disease symptoms caused by the *U. maydis* SG200 $\Delta see1$ mutant in tassels. (A) Scoring scheme for tassel tumors based on the symptoms observed at 14 dpi with *U. maydis*. The details about the scoring classification can be found in section 4.7.4. (B) Disease symptoms caused by SG200 $\Delta see1$ mutant, in comparison to the wildtype progenitor strain SG200 in tassels in Early Golden Bantam (left panel) and Gaspé Flint (right panel). Disease symptoms were classified as described in Schilling et al., (2014). SG200, virulent *U. maydis* progenitor strain; $\Delta see1$, deletion mutant for *see1* effector. The experiment was performed in three independent biological replicates. n = number of plants infected.

2.2 Phenotype characterization of the $\Delta see1$ mutant

2.2.1 Saprophytic growth of *see1* deletion strains

To test whether the deletion of the effector, impaired the vegetative growth of *U. maydis*, all the deletion strains generated were tested for their saprophytic growth in axenic culture as well as different stress media. The axenic cultures of SG200 $\Delta see1$ showed no growth or morphological changes compared to SG200 wildtype strain. The yeast-like growth of

SG200 Δ *see1* sporidial culture in liquid media also corresponded to that of the progenitor strain SG200 (Fig. 9A)

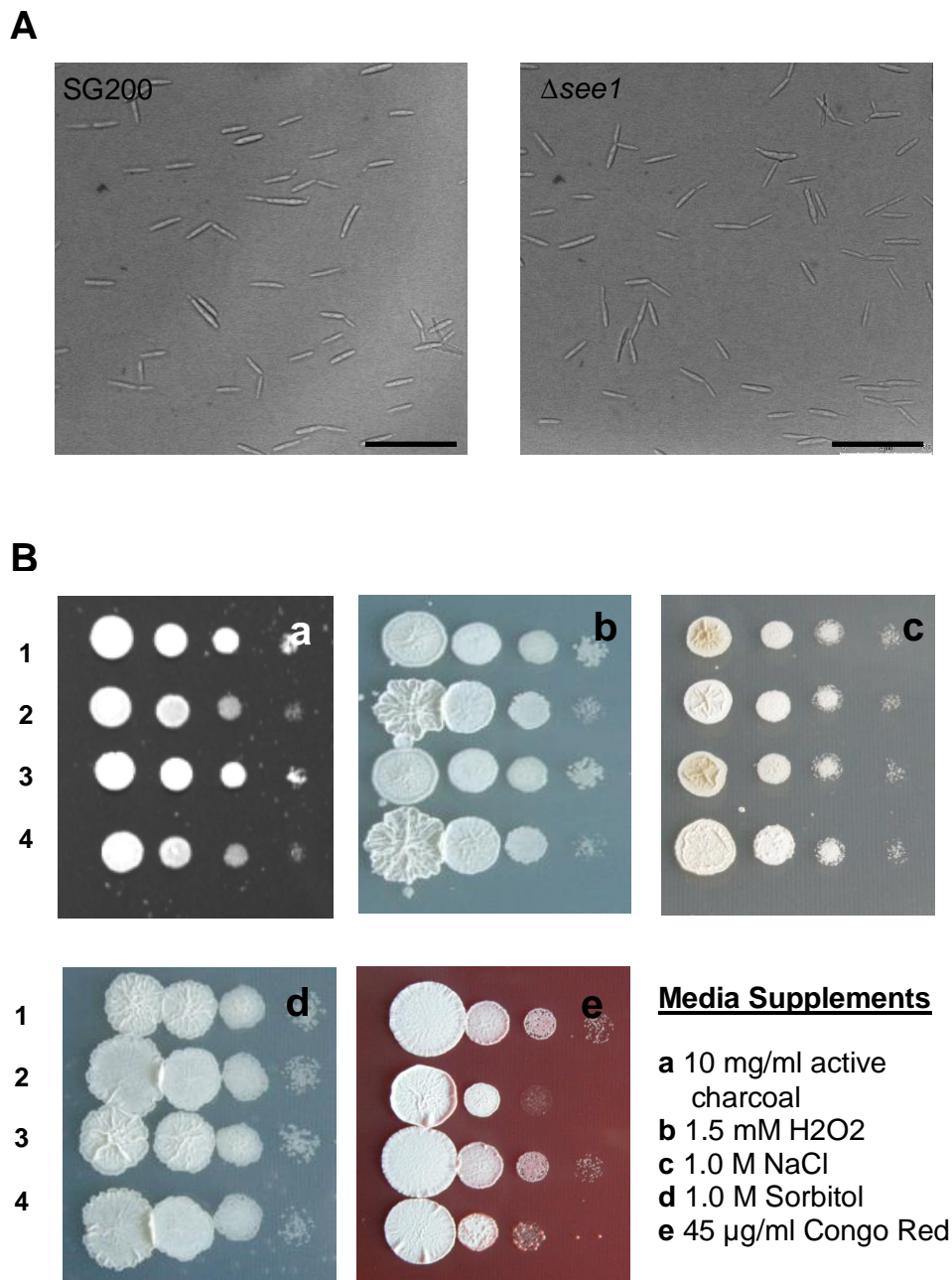


Fig. 9: Stress sensitivity assays and filamentous growth of *see1* deletion strain in comparison to *U. maydis* wildtype. (A) The sporidial culture of the wildtype strain SG200 and mutant SG200 Δ *see1* is similar in appearance showing yeast like cells. Bars = 50 μm (B) Different sensitivity tests for the *see1* deletion strains were used to check for the general fitness. The strains were dropped in 10 dilutions series on the stress substance-containing media as well as PD-charcoal plates dropwise. 1: SG200; 2: SG200 Δ *see1*#4; 3: SG200 Δ *see1*#5; 4: SG200 Δ *see1*#7. a-e reflects the added substance to check for various stress responses.

Also, the growth and colony morphology on minimal and complete media plates showed no differences between SG200 and SG200 Δ *see1*. To check for the fitness of the *See1* mutants the growth of the deletion strains was tested under different stress media and compared to that of SG200 wildtype strain (Fig. 9B). The stress media comprised of the

growth of *U. maydis* with induction of oxidative stress (H₂O₂), Osmotic Stress (Sorbitol, NaCl) and cell wall stress (Congo red). Similarly, the formation of filaments on charcoal containing medium was also not impaired in the mutant strains as compared to the SG200. Since none of the mutant strains showed any significant difference in growth rate or colony morphology relative to the progenitor strain SG200 it could be concluded that deletion of *see1* did not result in general growth defects.

2.2.2 Microscopic characterization of the infection course in SG200Δ*see1*

To investigate in more detail at what stage of biotrophic growth, the SG200Δ*see1* deletion mutant has defects; the different stages of infection were microscopically tracked. In all cases, the analyzed infection area was about 2–3 cms below the infection mark.

2.2.2.1 SG200Δ*see1* is not impaired in appresoria and filament formation

The next step was to check for the ability of the *see1* deletion mutant to form appresoria and filament formation. Calcofluor white was used for recognition of the germinated hyphae on plant surface as well as on parafilm for appresoria development. In filament formation no differences could be observed to that of SG200. Calcofluor white has high affinity for 1–4 β-glucans and visualizes the chitin of *U. maydis*. However, it does not penetrate into the plant tissue and therefore the dye stains only the exposed surface structures of plant and fungal hyphae on the leaf surface.

To test whether the *see1* deletion mutant is able to differentiate appresoria similar to SG200, the ratio of the appresoria formed in between SG200Δ*see1* and SG200 was determined by calculating the total number of hyphae that formed appresoria on the parafilm 16 hours after spraying of the actively growing sporidia. An "Appressorial Marker" (Mendoza-Mendoza et al., 2009) was used for quantification of the appresoria formed. This appressorial marker is based on a fusion of 3X egfp to the promoter of the gene *um01779* (*Pum01779* 3Xegfp) whose expression is specifically during formation of appresoria. Appresoria-forming hyphae can thus be identified due to the accumulation of cytoplasmic GFP and can be traced by fluorescence microscopy. By counter-staining the total number of hyphae growing on the parafilm by Calcofluor white it was possible to identify the ratio of the appresoria-forming hyphae. To investigate the formation of appresoria in the *see1* deletion mutant the plasmid PAM1 (Mendoza-Mendoza et al., 2009) was integrated in the *ip* locus of strain SG200Δ*see1*, to generate a strain SG200Δ*see1*AM1. The corresponding control strain SG200AM1 already existed and previously constructed by Dr. A. Mendoza-Mendoza (Mendoza Mendoza et al., 2009). At

16 hours after incubation, 23.05 % of all germinated hyphae of *see1* deletion mutant formed Appressoria ($23.05\% \pm 2.45$ SD, $n = 308$ hyphae; Fig. 10A and C.). This number did not differ significantly from that for SG200, where 24.92 % of all hyphae formed appressoria ($24.92\% \pm 3.17$ SD, $n = 341$ hyphae; Fig. 10A and C). Therefore, the non-pathogenic phenotype of SG200 Δ *see1* could not be attributed to a reduced formation of appressoria.

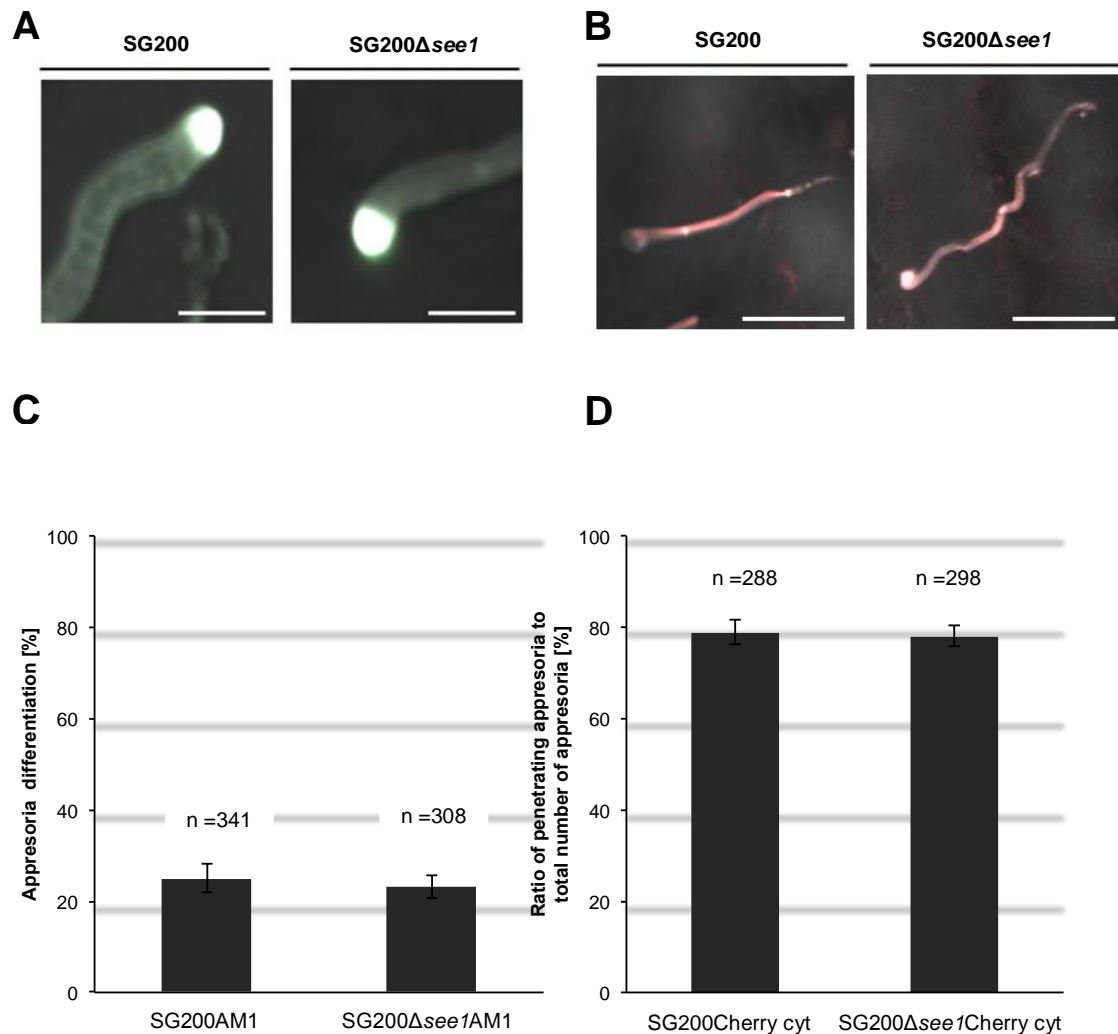
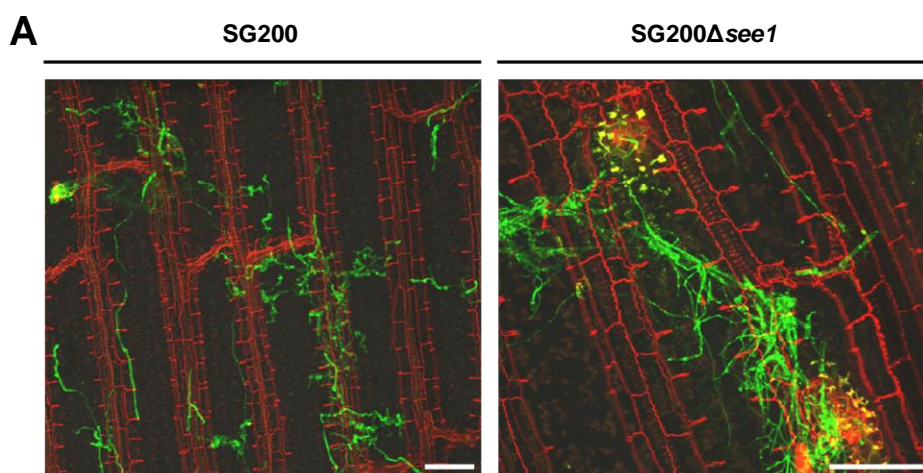


Fig. 10: Microscopic visualization of the early stages of infection in SG200 Δ *see1* in comparison to the wildtype SG200. (A) Differentiation of the *U. maydis* appressoria on the parafilm surface, visualized with calcofluor white (16 hpi) in the wildtype SG200 and mutant SG200 Δ *see1*. Scalebar =5 μ m. (B) The penetration event after appressoria formation in *U. maydis* wildtype strain SG200 in comparison to the SG200 Δ *see1*, visualized on the plant surface by mCherry fluorescence. (C) Quantification of formation of appressoria of SG200 Δ *see1*AM1 compared to SG200AM1 (16 hpi). AM1 denotes the presence of an Appressorial marker in the two strains (Mendoza-Mendoza et al., 2009) that is specifically induced in filaments that differentiate appressoria, a cytoplasmic GFP accumulation is quantified in the hyphae to determine the ratio between the total number of hyphae to appressoria-forming hyphae also counterstained with Calcofluor White. (D) Quantification of penetration efficiency (24 hpi) in wildtype SG200 and *see1* mutant. Here strains expressing constitutive mCherry were used, so that it results into an accumulation of cytoplasmic mCherry. To determine the penetration efficiency ratio of penetrating appressoria to the total number of appressoria were calculated. To visualize the appressoria on planta Calcofluor white was used. Penetrating appressoria were visualized by the cytoplasmic mCherry accumulation as calcofluor white cannot stain the penetrating hyphae.

Next, the ability of $\Delta see1$ to penetrate host epidermis was quantified. For this purpose strains expressing constitutively mCherry were generated under the Potef promoter (SG200-mCherry-cyt and SG200 $\Delta see1$ -mCherry-cyt). By staining the hyphae with Calcofluor white, penetrating and non penetrating appresoria were first identified. mCherry signal was implemented where the penetration hyphae was not detected by the calcofluor white. The ratio of the penetrating appresoria to the total number of appresoria formed in SG200-mCherry cyt and SG200 $\Delta see1$ -mCherry-cyt was about 80 % without any significant difference (Fig. 10B and D). This result shows that the *see1* effector is not required for epidermal penetration.

2.2.2.2 $\Delta see1$ mutant proliferation is impaired in the mesophyll and vascular layers of leaf.

To further investigate the reason for the reduced tumor formation in the SG200 $\Delta see1$ mutants, microscopy implementing WGA-AF488 (wheat germ agglutinin) / propidium iodide (WGA-AF488 which stains fungal hyphae /PI which stains plant cell wall and nuclei) staining of the infected leaf material was performed and samples were analyzed using microscopy. Confocal microscopy of infected leaves with WGA/PI showed that the SG200 $\Delta see1$ mutant initially colonize the maize tissue similar to the progenitor strain SG200 and was not defective in appresoria formation and the penetration events (data shown previously). However at 2 dpi, when the fungal hyphae reach the leaf mesophyll and interspersed vasculature, mutant hyphae were found to cluster at collapsed mesophyll cells, which show increased fluorescence (Fig. 11A). In addition, mutant hyphae failed to traverse from an infected cell into uninfected neighboring cell, which was particularly observed in bundle-sheath cells (Figure 11B). This phenotype was specific to the mesophyll and the vascular cell layers.



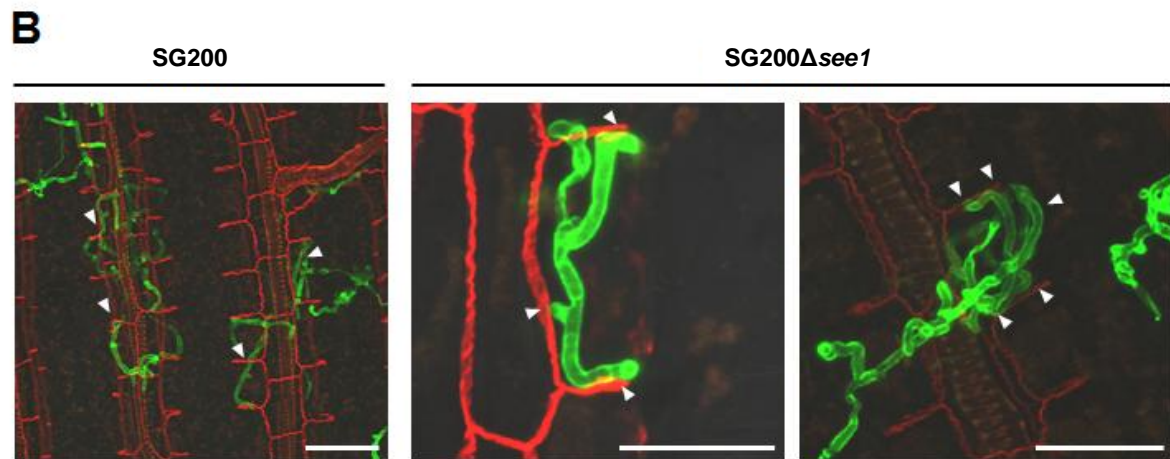


Fig. 11: Confocal laser scanning microscopy of the Δ see1 infected seedling tissues. (A) Successful penetration and initial establishment of the Δ see1 mutant (right panel) in comparison to the wildtype (left panel) at 2 dpi time-point. Bars = 50 μ m. (B) The wildtype strain SG200 proliferates well in the mesophyll and the vascular layers of the leaf. The passing of the hyphae from one cell to another is indicated by white arrowheads. The Δ see1-mutant is often blocked in the mesophyll and surrounding vascular layers of the leaf and is reduced in its ability to pass from cell to cell. The hyphae are frequently trapped in individual cells as indicated by the white arrowheads. Bars = 50 μ m.

2.3 Expression analysis of See1 using quantitative real-time PCR

To get an insight into the expression profile of *see1* during the process of tumor formation, quantitative real time polymerase chain reaction (qRT-PCR) approach was implemented. For this purpose cDNA from different growth phases of *U. maydis* eg. saprophytic growing sporidia in the exponential growth phase and for the temporal and spatial expression profile during serial stages of tumor progression, seedling and tassel tissues with macroscopically recognizable infection symptoms were harvested at successive timepoints from 2 dpi to 14 dpi. As a reference for the internal housekeeping fungal gene *ppi* (*peptidylprolyl isomerase*) was used that comprises of a constitutively expressed transcript (Bohlmann, 1996). In axenic culture no See1 transcript could be detected. The transcription induction of *see1* was found to be specifically induced during biotrophic growth of *U. maydis* representing the effector characteristic (Fig. 12A). The comparison of temporal and spatial expression profile of *see1* during serial stages of tumor progression in both the seedling and tassel tissues showed that the effector is particularly upregulated at the later stages of colonization during the tumor induction and expansion specifically in maize leaves and not required in floral organs (Fig. 12A).

Since only the male flowers (tassels) were used for determination of the spatio-temporal expression analysis over serial disease stages it was interesting to see the expression of the effector in the female flowers (ear) and its correlation with that of the tassels. To confirm this, ear infection was done by numerous inoculations of wounded silk as it was earlier described by Shurtleff, 1980, in the variety “Gaspé Flint” and tumors generated were collected at 12 dpi. The expression level of *see1* when quantified by qRT-PCR, was

similar in both the floral organs as compared to the seedlings which supports the requirement of *See1* only in the vegetative leaf tissues (Fig. 12B).

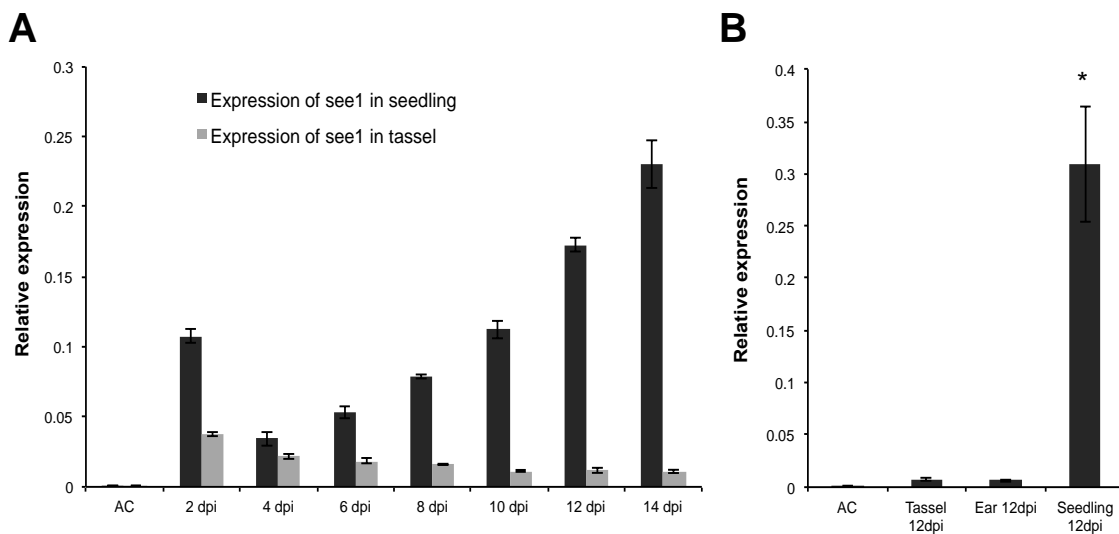


Fig. 12: Expression profile of the *see1* gene during *U. maydis* tumor formation (A) Quantitative real time polymerase chain reaction (qRT-PCR) expression profiling of the *see1* gene during biotrophic phase of *U. maydis* growth in seedling and tassel tissues. Expression levels are shown relative to mean expression of *peptidylprolyl isomerase (ppi)* transcripts. Gene expression was analyzed in axenic culture (AC), seedling, and tassel tissues at consecutive time points from 2 dpi to 14 dpi. Experiment was performed in three independent biological replicates (B) The expression of *See1* was quantified by qRT-PCR to compare leaf, tassel and ear samples, 12 dpi after *U. maydis* SG200 infection (for details see Methods). Error bars show SE. *, $P \leq 0.001$.

2.4 Tumor formation in *U. maydis* –maize interaction: A boost in DNA synthesis of the host

Tumor formation in *U. maydis* interaction is known to be an outcome of the hypertrophy and hyperplasia that is activated by the pathogen in host (De Bary, 1853). Activation of this phenomenon is done by triggering of the host DNA synthesis that activates the plant cell cycle to induce rapid divisions. The approach of monitoring DNA synthesis *in planta*, was used to study how a tumor is developed in this pathosystem. We treated uninfected and infected leaves with 5-ethynyl-2-deoxyuridine (EdU) at several stages of infection in the seedling leaves by immersing the actively colonized leaf area (1–3 cm below the infection mark) and labeled for 5 hours (see details in section 4.8.4). After tissue harvesting EdU incorporation was visualized by attaching a fluorescent tag and maize nuclei were stained with propidium iodide (PI) (Kelliher and Walbot, 2011; Fig. 13A) (see section 4.8.4).

During normal maize leaf development, most cell divisions occur in a narrow zone at the base of the blade, adjacent to the ligule with only sporadic divisions in the differentiating leaves. In a maize seedling, the leaf is growing at a maximum rate just after emergence from the sheath of surrounding older leaves (Fig. 13B). Its growth zone is located at the leaf base, and can be viewed as a linear system with cell division at the base of the leaf

followed by cell expansion and finally resulting in mature tissue (Fig. 13C). Hence the tumor formed in the interaction of *U. maydis* – maize is an outcome of the profuse and rapid cell division events that occurred upon *U. maydis* colonization of the leaf cells. In case of non-infected plants, no DNA synthesis activity was visible in the corresponding leaf area (which is neither part of the apical meristem nor the basal region of the leaf; Fig. 13D), which is in full accordance with prior descriptions of the maize leaf development (Li et al., 2010).

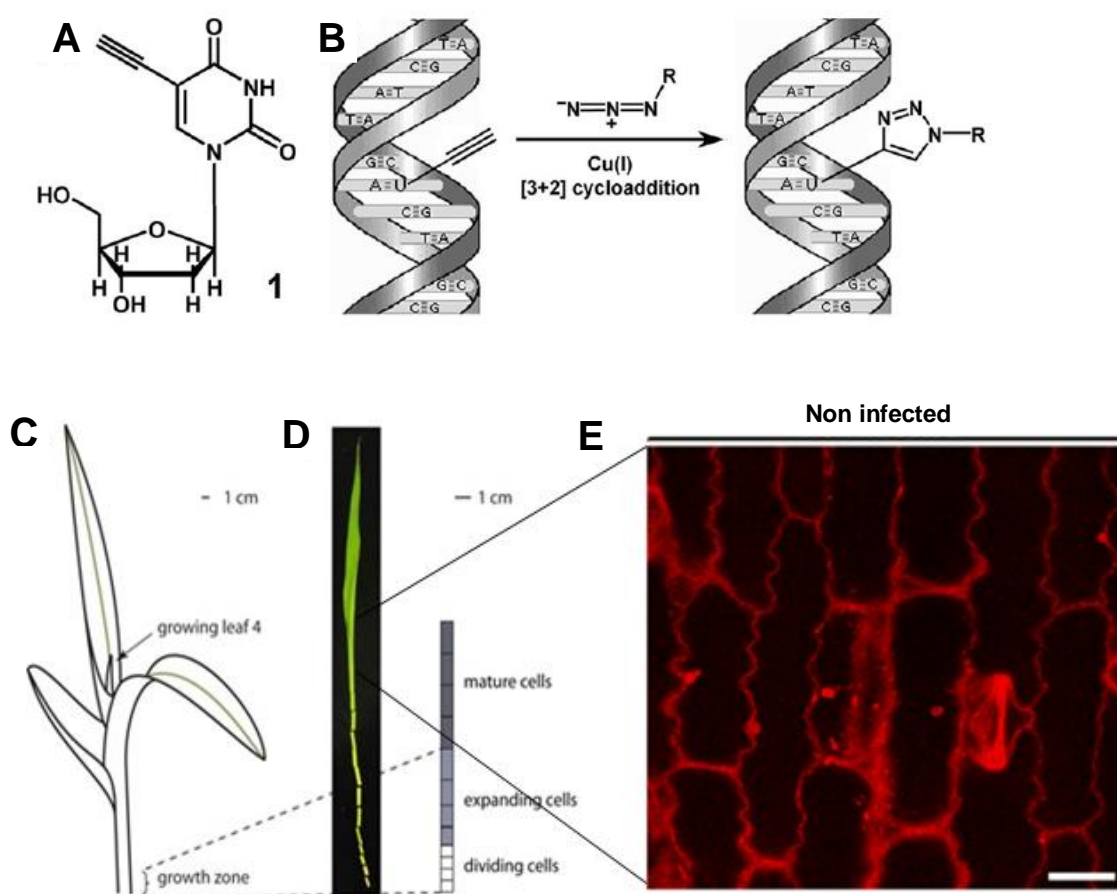
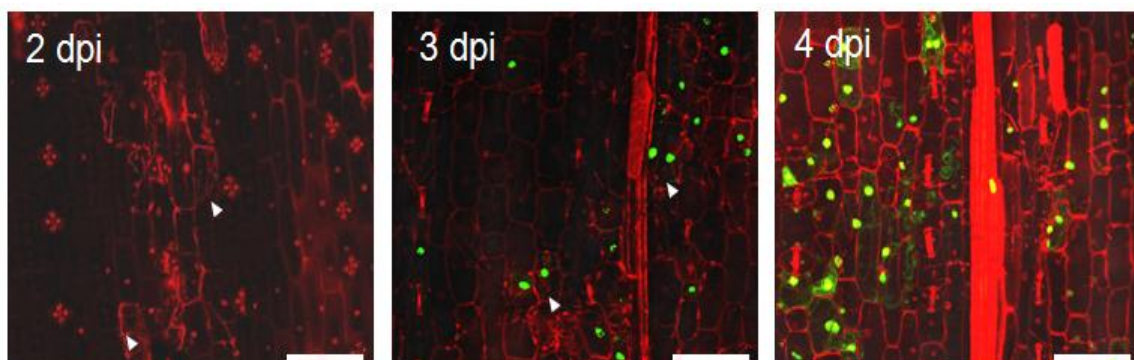


Fig. 13: DNA synthesis in maize leaves by using 5-ethynyl-2-deoxyuridine. (A) Structure of 5-ethynyl-2-deoxyuridine, a thymidine analogue that carries a terminal alkyne group instead of methyl in the 5 position of the pyrimidine ring. (B) Schematic of the click reaction for detecting EdU incorporated into cellular DNA. The terminal alkyne group exposed in the major groove of the DNA helix readily reacts with an organic azide (R, can be any fluorophore) in the presence of catalytic amount of Cu (I) (Taken from Salic and Mitchison, 2008). (C) Schematic overview of maize seedling (C) and leaf (D) growth. The growth rate of the fourth seedling leaf in maize is maximal when it appears from the sheath of the older leaves. At the leaf base all cells are dividing, followed by the cell expansion and differentiation until mature cell size is reached. (Taken from the lab webpage of Dirk Inze, University of Gent, Belgium) (E) Non infected sample did not show any DNA synthesis activity. Plant cell walls were visualized by propidium iodide (PI) staining (red), and the EdU labelled host cell nuclei are visualized by AF488 staining (green) which did not show any signal. Bars = 25 μ m.

2.4.1 DNA synthesis trigger in maize by wildtype *U. maydis*

Since the non-infected maize leaf did not show any DNA synthesis activity, a more thorough confocal microscopic investigation of the host was carried out upon challenge with wildtype *U. maydis* to trace the progression of tumor. The previously described EdU assay to detect the synthesis of DNA was carried out on infected maize leaves at 2 dpi. EdU treatment for 5 hours did not result in any detectable labeling, in colonized maize leaf cells (Fig. 14A). By contrast, minimal number of cells (corresponding to about 25 % of the colonized cells) start to get labelled with the AF488 fluorophore tagged to EdU in the infected samples at 3 dpi. However, the labeling intensity of EdU at this timepoint was at very weak intensity. By contrast, at 4 dpi (the same time point when the first macroscopic symptoms are visible), EdU incorporation into maize DNA was strongly induced (about 70 % of the colonized cells - Fig. 14A). In the further disease progression stages upon invasion of the host cell by fungal hyphae, plant cells synthesized new DNA, which coincided with induction of mitosis, visualized as pairs of labeled cells (Fig. 14B). Such invaded cells conduct multiple division events over several days, which results in the development of tumors (Fig. 14B). Consequently, stained and rapid cell divisions are activated upon *U. maydis* colonization of leaf cells in contrast to the absence of EdU incorporation observed in uninfected plants. Therefore, it can be concluded that the maize DNA synthesis is not required for *U. maydis* to colonize leaves however at 3 dpi when the fungus mainly establishes itself in the deeper layers the onset for hijacking of the host cell begins with the further triggering of DNA synthesis. At 4 dpi timepoint the actual tumor induction in the host is initiated by rapid DNA synthesis activity in the colonized cells.

A

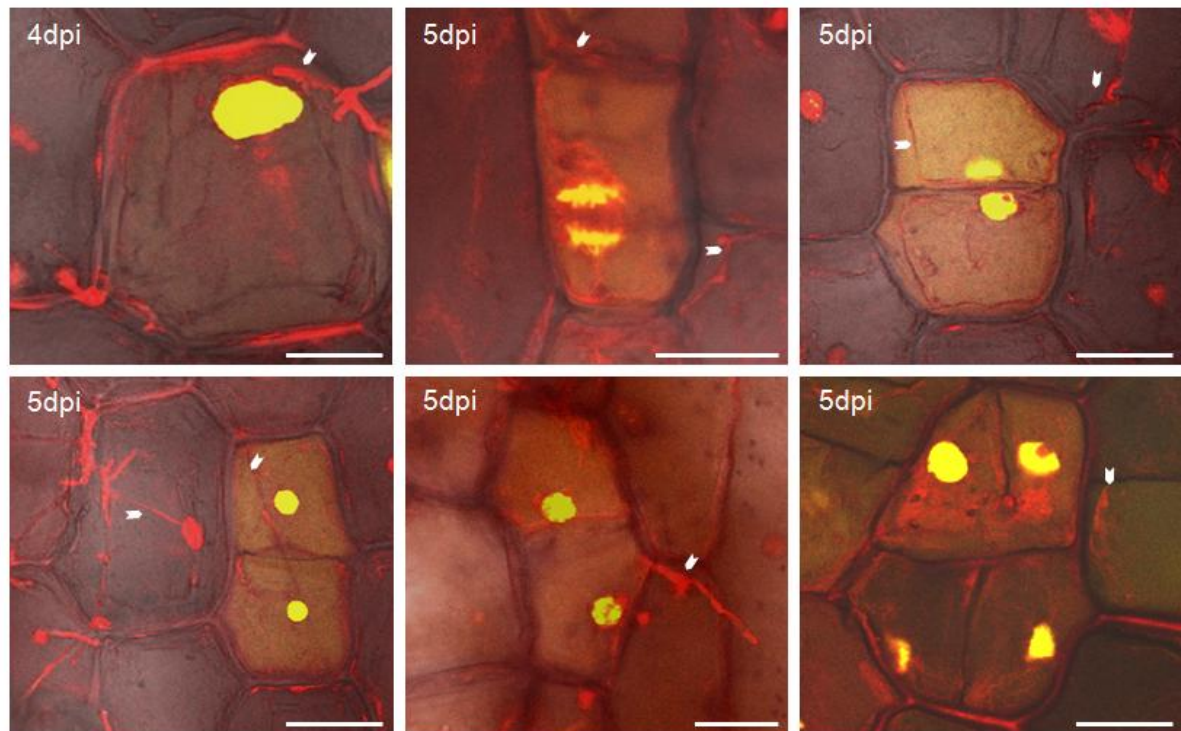
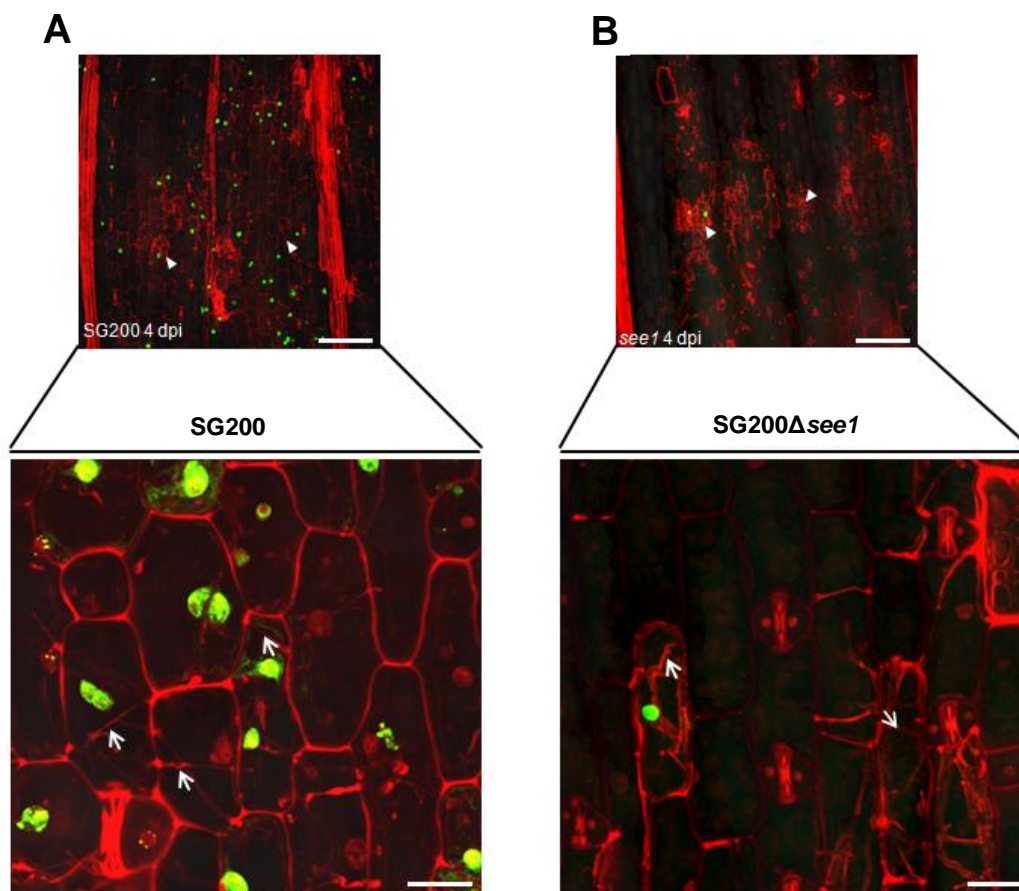
B

Fig. 14: *U. maydis* induces DNA synthesis in maize upon infection (A) Maize seedlings were infected by *U. maydis* wildtype strain SG200 and then tissue was incubated in EdU to visualize *in vivo* DNA synthesis in the host cells. Samples were imaged at 2, 3 and 4 dpi by confocal microscopy. Left Panel: At 2 dpi the fungal proliferation was observed subepidermally; host cells adjacent to fungal hyphae were considered to be colonized cells (white arrows). No EdU incorporation was observed. Middle Panel: At 3 dpi weak EdU labeling was detected in 25 % of the colonized cells. The fungal hyphae are marked with white arrows. Right Panel: At 4 dpi numerous colonized cells showed EdU labeling (green stain) indicating the onset of DNA synthesis in host cells (white arrows). Scale bars = 75 μ m. (B) Cell division events were observed in maize seedling infected by *U. maydis* wildtype strain SG200 at 4 and 5 dpi. EdU incorporation into a cell will result in equally labeled contiguous daughter cells after cell division. Such equally labeled cell pairs were readily observed in SG200-infected seedling leaf tissue. The white arrows point to fungal hyphae associated with maize cells undergoing cell division. It is inferred that re-activation of the cell cycle and rapid divisions are responsible for tumor formation. Bars = 25 μ m.

2.4.2 *U. maydis* requires *See1* to induce plant DNA synthesis during leaf tumor formation

Since the previous experiments showed a link between DNA synthesis and tumor development in *U. maydis* interaction, it was interesting to test maize DNA synthesis during the SG200 Δ *see1* mutant infection. In contrast to SG200, SG200 Δ *see1* infected leaf samples showed a strongly reduced level of DNA synthesis and mitotic activity at the same stage of 4 dpi in the seedling leaves (Fig. 15A). Quantification of EdU labeling revealed that 67.55 ± 4.2 % of the SG200 colonized cells undergoes DNA synthesis 4 days after infection. By contrast, only 7.33 ± 1.7 % of the SG200 Δ *see1* infected cells in maize seedlings showed DNA synthesis (Fig. 15B). In addition to SG200 and the SG200 Δ *see1* mutant, two additional fungal strains were tested for their ability to trigger DNA synthesis in colonized maize seedling. First, seedlings were infected with the maize smut *Sporisorium reilianum*, a close relative of *U. maydis*, which similarly establishes a

biotrophic interaction with maize but forms visible symptoms only in the inflorescences (Schirawski et al., 2010). Interestingly, *S. reilianum* infected leaves did not show any detectable DNA-synthesis at 4 dpi, although dense colonization of the tissue was visible (Fig. 15C). This observation indicates that not colonization of leaves, but specifically the induction of tumors activated the maize cells into S-phase where profuse DNA synthesis is activated. In addition, the *U. maydis* SG200 Δ *tin3* effector mutant was used, which shows a reduction in leaf tumors similar to SG200 Δ *see1* strains (Brefort et al., 2014). This mutant, although not being able to trigger formation of expanded tumors, activated EdU labeling in 44.22 ± 4.0 % of the colonized leaf cells (Fig. 15D). This suggests that the inability of the Δ *see1* mutant to trigger DNA synthesis is not just an indirect consequence of the reduced tumor size, but is specific to the Δ *see1* mutant and therefore functionally linked with the See1 effector. Taken together, this data suggested that the ability of *U. maydis* to initiate a tumor symptom in the leaf among the *Ustilaginales* is by active triggering of the DNA synthesis in the host leaves and the organ specific effectors like *see1* acting in the seedling are responsible for the tuning of this hypertrophoid tissue.



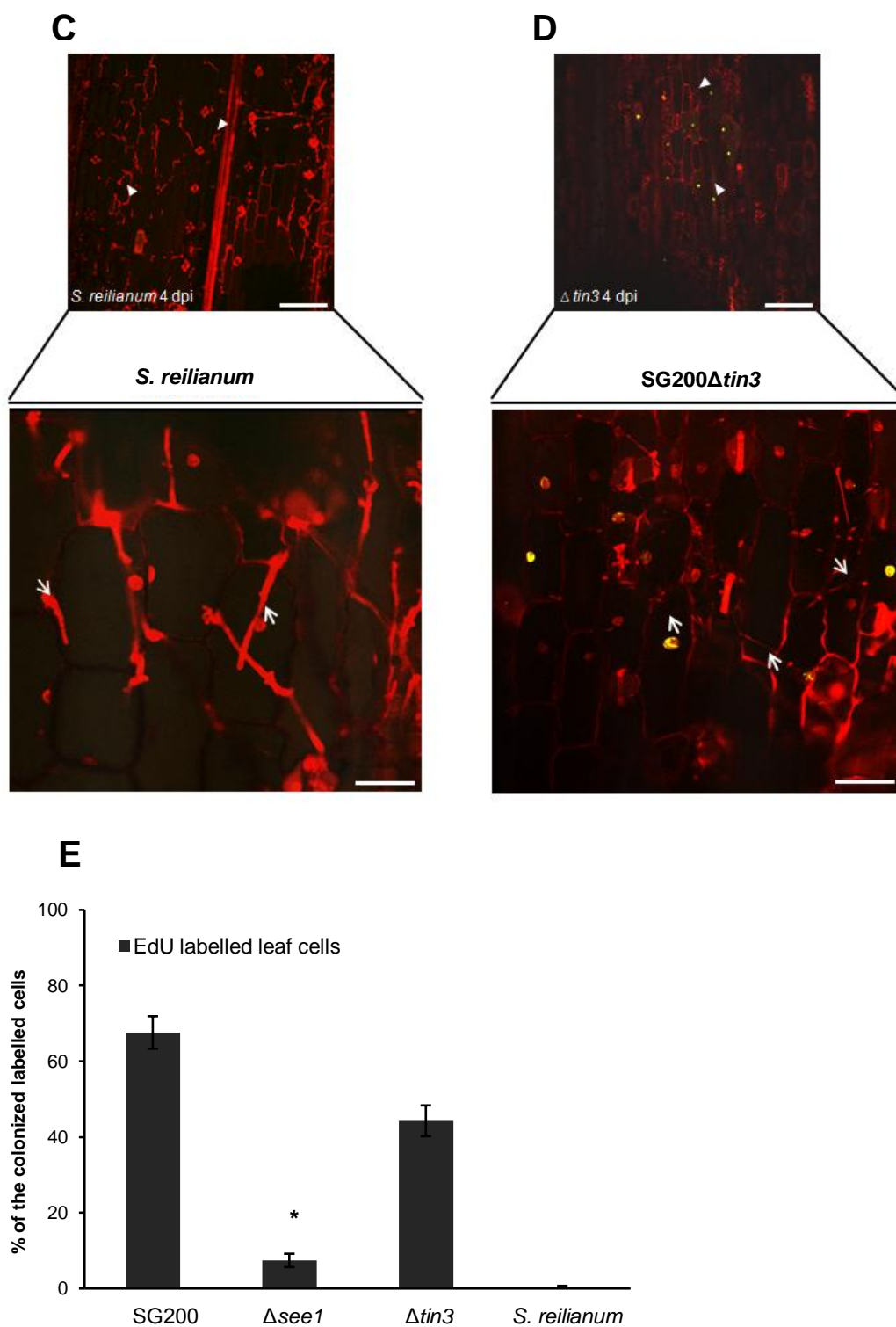
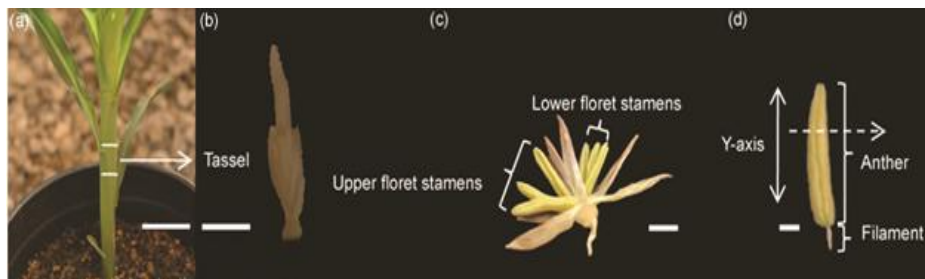


Fig. 15: *See1* requirement for host DNA synthesis in leaf tumor formation. *In vivo* DNA synthesis in seedling tissue infected with (A) *U. maydis* wildtype SG200 (B) SG200 $\Delta see1$ mutant. Samples infected with *Sporisorium reilianum* (C) and SG200 $\Delta tin3$ (D), that has similar phenotype to SG200 $\Delta see1$ in respect to tumor size was used as a control. Fungal hyphae and plant cell walls were visualized by propidium iodide (PI) staining (red) and the EdU labelled host cell nuclei are visualized by AF488 staining (green). Fungal hyphae are shown by the white arrowheads. Bars = 100 μ m for smaller images and 25 μ m for magnified images. (E) Quantification of the EdU-labeled seedling leaf cells in the *in vivo* DNA synthesis assay comparing between infections with wildtype SG200, SG200 $\Delta see1$, SG200 $\Delta tin3$ and *S. reilianum*. Error bars show SE. *, $P \leq 0.001$.

2.4.3 Tumor formation in anthers does not involve *U. maydis* induced DNA synthesis

Since the deletion of the *see1* effector causes a leaf specific phenotype, it was interesting to see the induction of DNA synthesis ability with the mutant in the floral parts primarily the tassels. Within the tassel it is the reproductive anther organs and not the vegetative glumes, palea, lemma and stem that are typically infected and transformed to tumors by *U. maydis* (Fig. 16A). Previous studies by Gao et al., 2013 have shown that *U. maydis* mainly acts passively in generating floral tumors by restructuring the ongoing division.

A



B

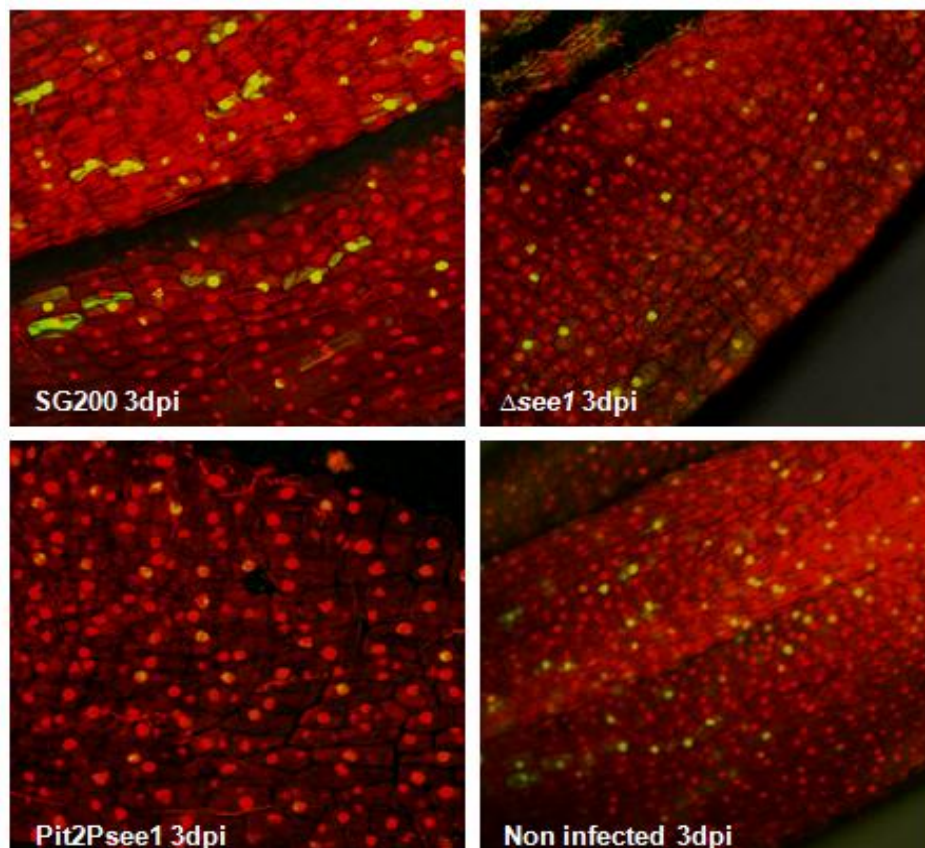


Fig. 16: *U. maydis* does not induce DNA synthesis in anthers: (A) a and b; *U. maydis* infects the actively dividing mitotic tassel in maize to form a tumor. (c) The structure of an individual male flower in maize consisting of the 6 anthers in two pairs of 3 each in the upper and lower floret. The vegetative structures in the flower consist of the stem, vegetative glumes protecting the anthers, the palea and lemma. (d) An individual anther in maize consists of the anther lobe and filament. (Taken from Gao et al., 2013). (B) DNA synthesis in anther tissue infected with SG200 Δ *see1* in comparison to wildtype SG200. Samples infected with strain over-expressing *See1* and uninfected anthers served as controls. (Bottom panel). Nuclei were visualized by propidium iodide staining (red) and EdU-labelled host cell nuclei are visualized by AF488 staining (green). Bars = 100 μ m.

Since *see1* effector is specifically transcribed in the seedling tissue and as $\Delta see1$ mutant failed to induce DNA synthesis in the colonized seedling the study of monitoring DNA synthesis upon *U. maydis* colonization was also extended to anthers within the tassels with comparison to the wildtype SG200 and the SG200 $\Delta see1$ mutant along with the noninfected tissue. The EdU was injected in the tassel and the labeling was done for a 5 hour period as that for seedling (for details see section 4.8.4). Actively dividing anthers prior to the meiotic switch which were in the range of 0.1–0.2 mm after 3 dpi were harvested in 100 % ethanol and then processed for the labeling reaction (see section 4.8.4). In line with the previous reports of reprogramming of *U. maydis* in anthers, we observed no significant differences in EdU labeled cells in noninfected tissue compared to *U. maydis* infected tissue. Both non-infected anthers, SG200 and $\Delta see1$ infected anthers contained about 60 % cells in S-phase over a 5 hour labeling period (Fig. 17), consistent with previous reports that majority of anther cells during the rapid proliferation period will label with a 4 hour labeling treatment (Kelliher and Walbot, 2011). It appears that *U. maydis* infection does not alter DNA-synthesis activity in anthers, which is in contrast to the situation in leaves. About 42 % of the EdU-positive anther cells were colonized by the fungus at 4 dpi, with no significant difference between SG200 and the $\Delta see1$ mutant. From this data it can be concluded that See1 is not involved in modulating host DNA synthesis and cell division during anther colonization and hence there is no role of seedling specific effector like *see1* in the non-target organ which results in the normal symptom formation with the $\Delta see1$ mutant in the anther cells.

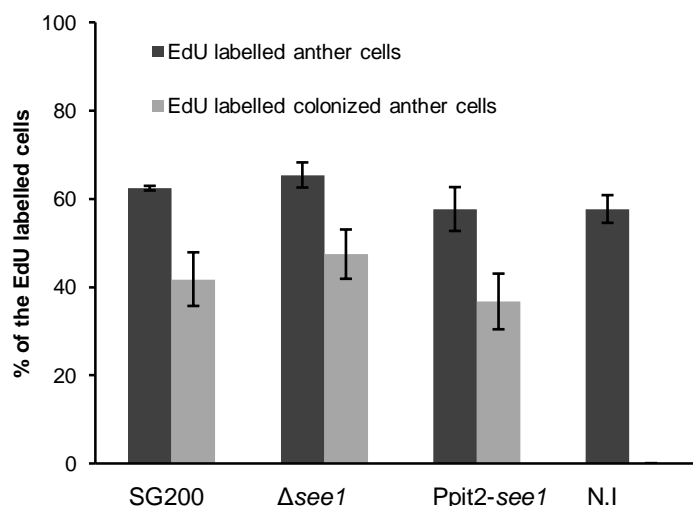


Fig. 17: *U. maydis* does not induce DNA synthesis in anthers. Quantification of the EdU labeled nuclei relative to total anther nuclei per image examined, after infection with wildtype SG200, SG200 $\Delta see1$, See1 over-expressing strain (Ppit2-*see1*) and non infected (N.I) tissue. Within the population of EdU positive cells, the number colonized by fungal hyphae was also quantified in the infected samples. Error bars show SE.

2.5 Constitutive over-expression of *see1* in infectious hyphae

To further explore the role of *see1* in tumor induction, a *U. maydis* strain constitutively expressing *see1* during the entire infection process was generated. To this end *see1* was expressed under control of the *pit2*-promoter; (Doehlemann et al., 2011) which is active throughout the infection process. The over-expression of *see1* in leaves and the individual parts of the tassels particularly in anthers as well as in vegetative tassel base upon infection with this strain was confirmed by qPCR (Fig. 18). Seedling leaves were infected with the resulted over-expression strain Ppit2-*see1*. Scoring of disease symptoms showed that the Ppit2 driven *see1* expression did not result in a phenotype significantly different from the wildtype strain demonstrating that over expression of *see1* did not further increase *U. maydis* virulence in leaves (Fig. 19A).

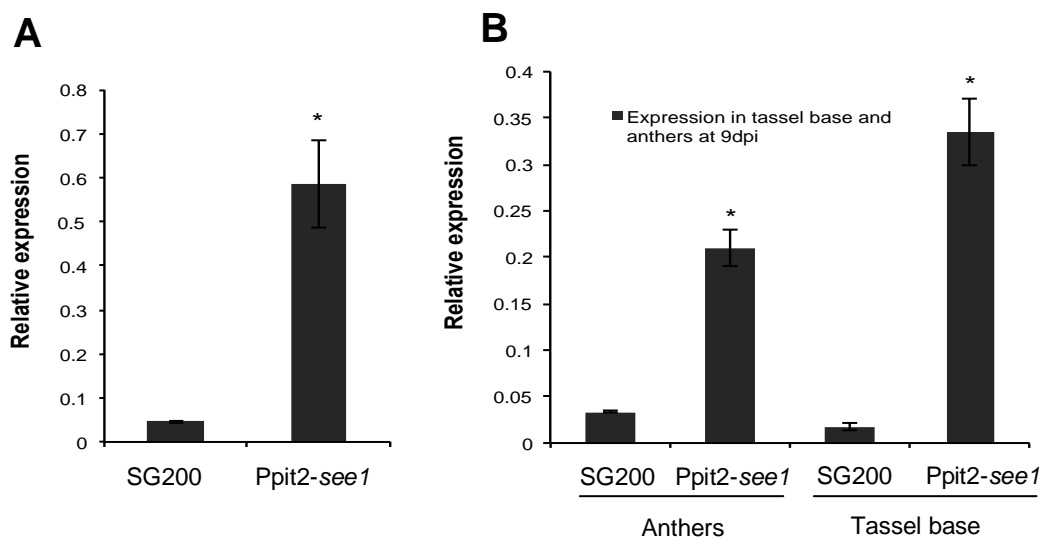


Fig. 18: Constitutive over-expression of *see1* in seedling and floral tissues. (A) qRT-PCR confirmation of overexpression of Ppit2-*see1* in seedlings. (B) Quantification of the *see1* gene expression in the individual tassel parts of plants infected with the over-expression strain (Ppit2-*see1*) in comparison to plants infected with the wild type SG200 strain. Error bars show SE. *, $P \leq 0.001$.

To see if this generated strain could act and show its role in a non-target organ, like the tassels where it is not expressed in a native situation, tassel infections were also conducted. Surprisingly, this *See1* overexpression strain caused an unexpected tassel phenotype: While wildtype *U. maydis* almost exclusively triggers tumors in anthers, over-expression of *see1* caused extensive tumor formation in the vegetative tassel base (the terminal node and internode) and the entire tassel including spikelets became green in some cases (Fig. 19B). During the maize tassel development, after the floral switch when tassel emerge from the whorl of immature leaves, the glumes (outer leaf-like spikelet organs) do become green, but the *See1* mediated greening occurred precociously when the still immature tassel was within the whorl of enveloping leaves.

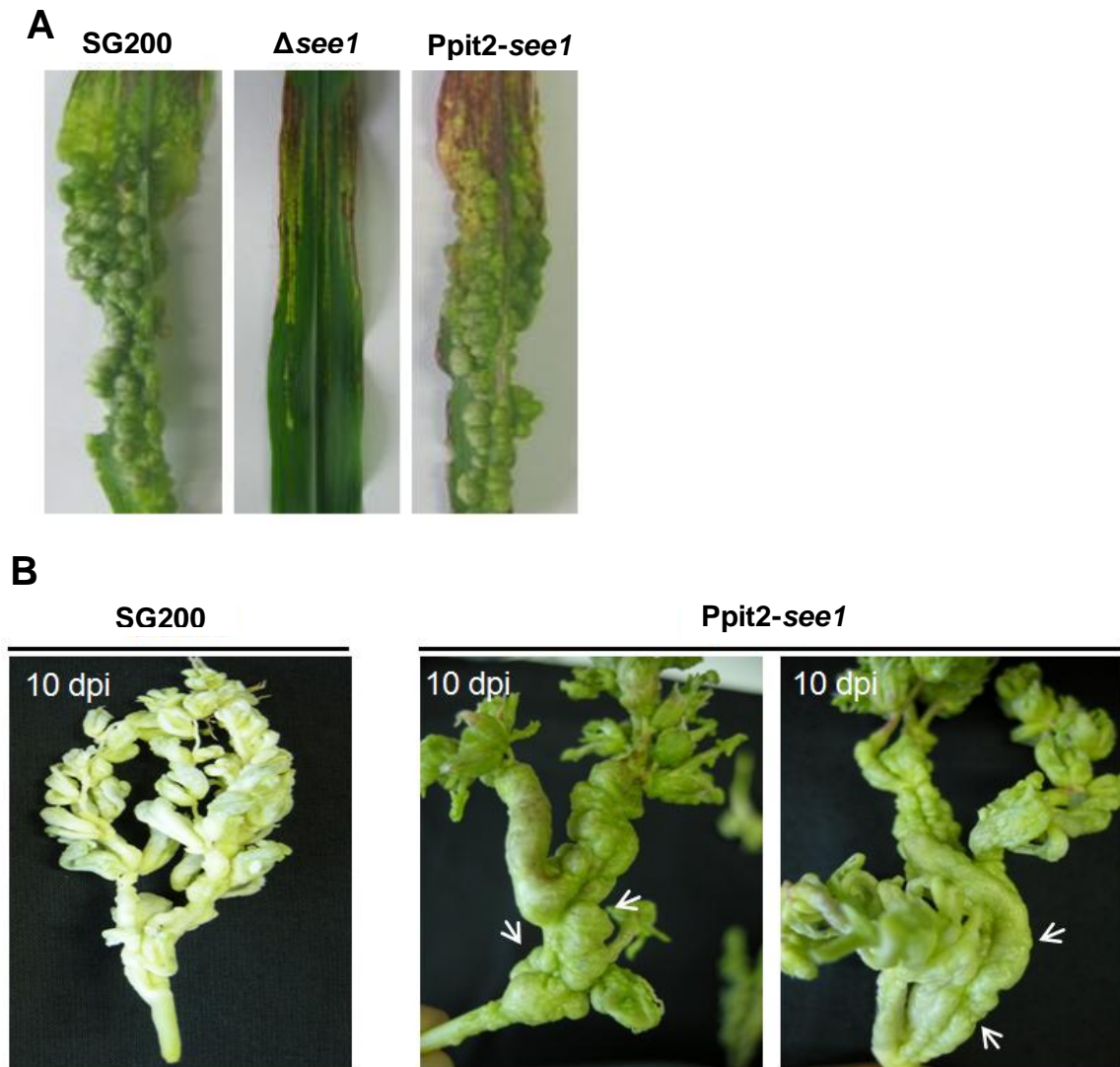


Fig. 19: Constitutive overexpression of *see1* results in tumors in vegetative tassel parts. (A) Overexpression of *See1* in leaf tissues leads to a wildtype phenotype with no further increase in tumor size as compared to the wildtype SG200. (B) Tassel base abnormality occurs much more frequently with constitutive overexpression of *see1* in comparison to the wildtype strain SG200. Tumor formation in the tassel base is indicated by the white arrows.

The *see1* over-expressing strain showed a tassel base abnormality in about 38 % of the infected plants where SG200 wildtype strain caused only 8 %. The appearance of the greenish tassels was also significantly higher in comparison to the wildtype strain, corresponding to 20 % of the infected plants (Fig. 20B and C). Previously, precocious anther emergence and anther greening was reported in SG200 infected tassels, in the spikelet near the tumors (Walbot and Skibbe, 2010). These results suggest that *U. maydis* causes physiological and developmental changes within tassels that result in abnormal phenotypes of infected organs.

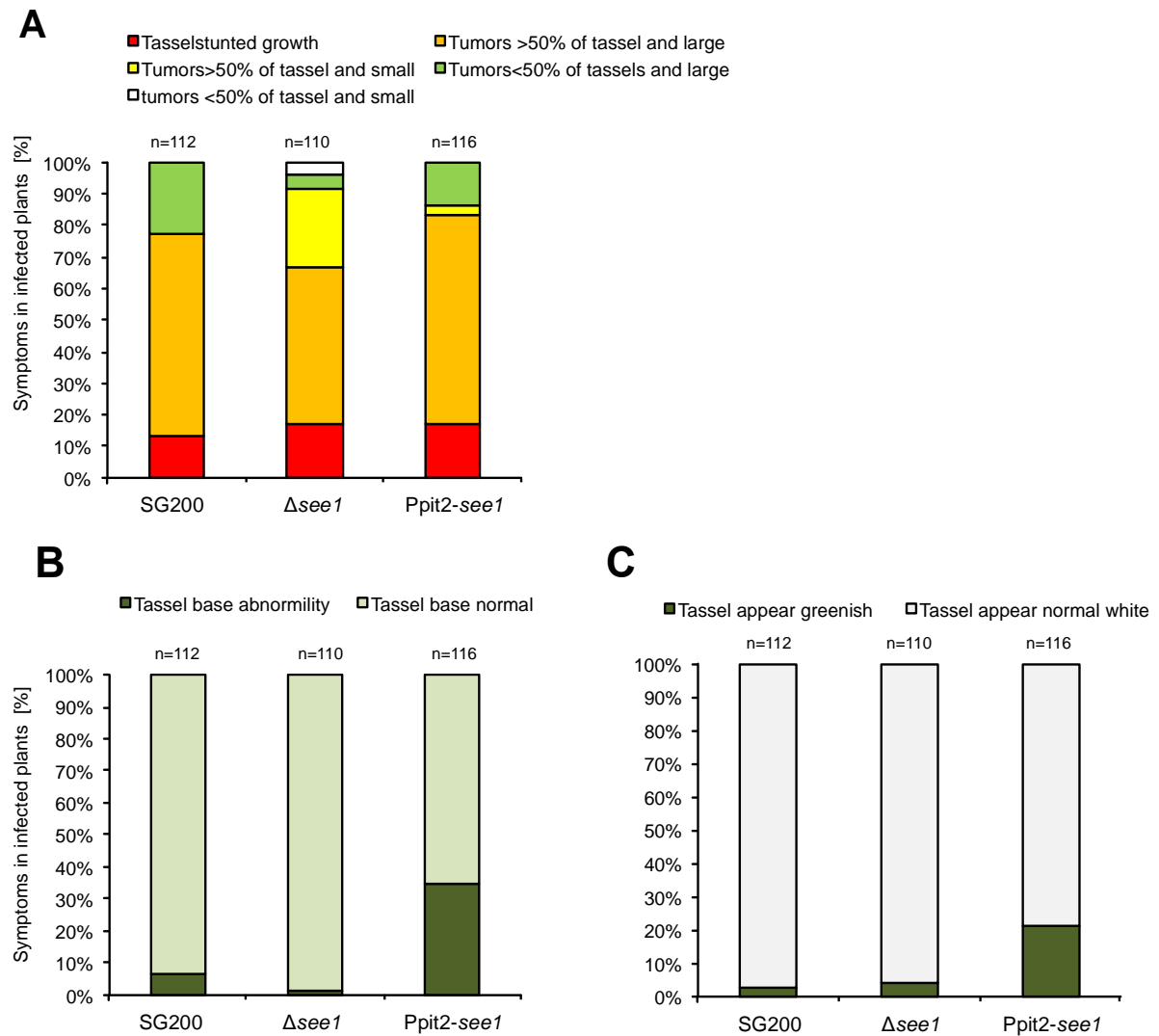


Fig. 20: Overexpression of *See1* results in two abnormalities in tassels: Tumors at the tassel base and greenish tassels. (A) Disease symptoms of tassels infected with *See1* over-expressing strain (Ppit2-*see1*) in comparison to the wildtype progenitor strain SG200 and SG200 Δ *see1*. (B) The tassel base abnormalities in plants infected with the strain over-expressing *see1* in comparison to wildtype and the SG200 Δ *see1* strain. (C) The greenish appearance of the tassel infected by *See1* over-expressing strain was quantified as the number of greenish tassels to the total number of tassels infected. All the symptoms were scored at 14 dpi. The experiment was performed in three independent biological replicates. SG200, virulent *U. maydis* progenitor strain; Δ *see1*, deletion mutant for *see1* effector; Ppit2-*see1*, The *see1* over-expressing strain with *pit2* promoter. n = number of plants infected.

This over-expressing strain was also used for monitoring the DNA synthesis by quantification of the EdU labeled cells in anthers upon *U. maydis* colonization in addition to SG200 and Δ *see1*. Anthers from the infections with the constitutively over-expressing strain did not show any significant differences in the EdU labeling compared to the earlier described observations with SG200 (Section 2.4.3). The over-expression terminal node/internode phenotype was also correlated to the *in planta* DNA synthesis approach by calculating the number of EdU labeled cells in the tumorous tassel base of the ectopically over-expressing strain (Fig. 21A and B). The percentage of EdU labeled cells in the tassel base of the *see1* over-expressing strain was significantly higher in a t- test as

compared to the wildtype SG200 indicating that the abnormal phenotype is a direct outcome of the excessive cell division resulting from *see1* over-expression. In summary, from these data it can be concluded that See1 is required to stimulate *U. maydis* induced tumor formation by promoting host DNA synthesis in vegetative tissue, but not in maize anthers.

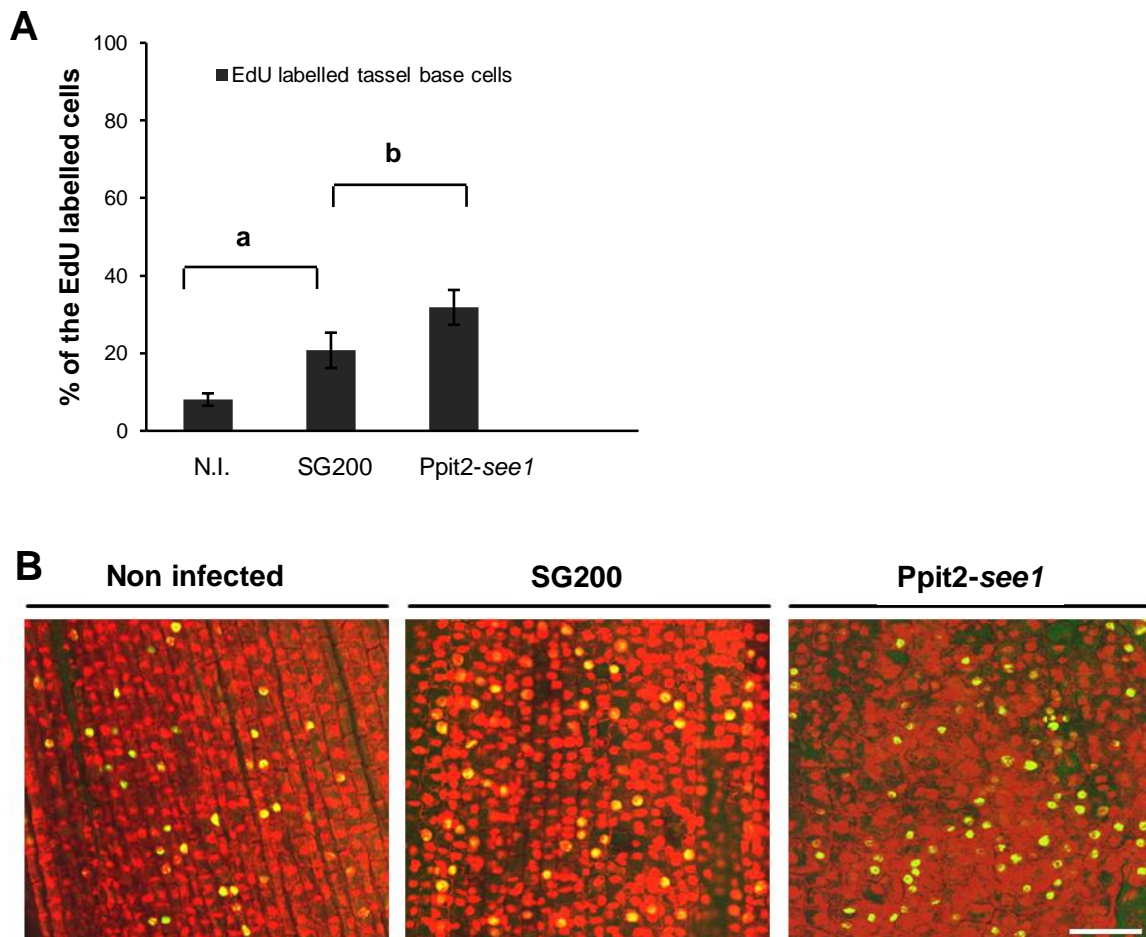


Fig. 21: Over-expression of *see1* results in tumor proliferation in vegetative tassel parts. (A) Quantification of the EdU labelled cells in the *in vivo* DNA synthesis assay in tassel base infected with the *See1* over-expressing strain (Ppit2-*see1*) in comparison to either the wildtype SG200 infected or noninfected (N.I) tassels. There was a significant difference in the number of EdU labelled nuclei in the abnormal tassel base region as compared to the wildtype SG200 infected or noninfected. Error bars show SE. a and b, $P \leq 0.05$. (B) Detection of *in vivo* DNA synthesis in the tassel base colonized by *See1* over-expressing strain (Ppit2-*see1*) in comparison to tissue colonized by wildtype strain SG200 and noninfected tissue. The total nuclei were visualized by PI staining (red) and the EdU labeled cell nuclei were visualized by AF488 staining (green). Bars = 50 μm .

2.6 Localization of *See1* in infected maize seedlings

The next objective of the study was to understand the localization of *See1* during the biotrophic growth in *U. maydis* infection. Different methods were implemented for this like the live cell imaging by fusion of the fluorescence tag to effector *see1*, transient expression of the fluorescent protein in *Z. mays* and *N. benthamiana*. Additionally, immunogold labeling detection of the *See1* tagged to 3X HA was also applied using transmission electron microscopy (TEM) to localize the protein in the native situation

during the tumor development. This same approach was also implemented for the previous translocated effector Cmu1 of *U. maydis* which turned out to be extremely fruitful (Djamei et al., 2011).

2.6.1 Localization of fluorescent See1 by confocal microscopy

To visualize See1 *in planta*, the strain SG200 Δ see1-see1-mCherry was generated, which in the endogenous locus has a 3'-terminal fusion of mCherry with the open reading frame of see1 and the fusion gene was expressed under the control of See1 promoter. The functionality of the fusion protein was verified in plant infection which resulted in heavy tumors similar to the wildtype strain SG200. The localization of the fusion protein was done by using confocal laser scanning microscopy. The Fig. 22A and B, shows a Confocal "Z-stacks" of the intracellularly growing hyphae in the plant cell from 4 days after infection. In this case, the protein accumulated at the hyphal tip and also at the cell to cell penetration, where the fungal hyphae from one plant cell enter into a neighboring cell.

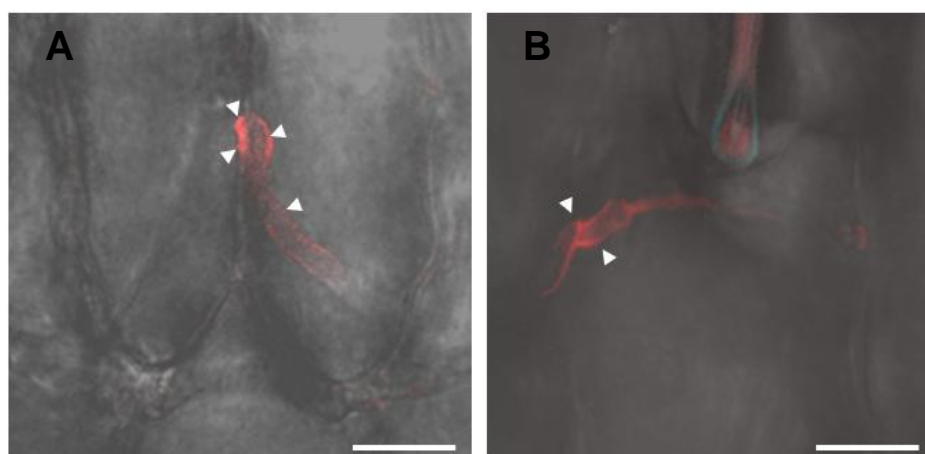


Fig. 22: Localization of the See1-mCherry in the intracellularly growing *U. maydis* hyphae at 4 dpi. (A-B) Infection with the See1-mCherry which is shown in red fluorescence in the hyphae. White arrows indicate sites of enhanced See1 secretion. Both the images are confocal Z stacks. Bars = 50 μ m.

Since the See1 effector has a prominent expression during the later stages of tumor development, it was not possible to localize this protein in the initial stages of fungal establishment. Moreover, the confocal approach at the later stages where a tumor is actually initiated was difficult to take the sample for live cell imaging. Hence a possible diffusion of See1 in cell spaces or a potential transfer to the cytoplasm of maize cells could not be visualized by the fusion of See1 to mCherry. Since some fluorescence signal was detected during the early colonization stages of plant by the fungal hyphae, it could be concluded that the fusion protein was secreted from the hyphae. However, by this methodology it could not be differentiated whether the fusion protein was in the apoplast, in the fungal cell wall or cytoplasm of plant cell.

2.6.2 Transient expression of See1 in *Z. mays* and *N. benthamiana*

Transient expression was implemented for localization of See1 in *Z. mays* which was done by using particle bombardment approach. See1₂₂₋₁₅₇-mCherry encoding fusion protein lacking the N-terminal secretion signal was transiently expressed in maize leaves under the 35S promoter. As a transformation control, PIP₄₂₆₋₅₉₃-yellow fluorescent protein (YFP) was co-expressed, also under the control of 35S promoter. The encoded protein of PIP-YFP localizes exclusively to the plant nucleus which helps in identification of transformed cells. This transformation control was co-bombarded along with the See1₂₂₋₁₅₇-mCherry. See1₂₂₋₁₅₇-mCherry was found to localize to the cytoplasm and nucleus of transformed maize cells (Fig. 23A). Additionally, the See1₂₂₋₁₅₇-mCherry signal spread to the nuclei of neighbouring cells, from the transformed cell (Fig. 23A) as is shown by the white arrowheads. As controls for this experiment and for the confirmation of the translocation to the neighboring cells, mCherry expressed alone as well as the apoplastic effector Pit2 construct (Mueller et al., 2013) that was tagged with mCherry (designated as Pit2₂₆₋₁₁₈-mCherry), localized to the cytoplasm and nucleus of transiently expressed epidermal cells (Fig. 23B and C). However, the movement of the fluorescence signal from the transformed to the neighboring cells was lacking for both mCherry and Pit2-mCherry. The specific translocation of See1-mCherry between neighboring maize cells is consistent with previous reports on *U. maydis* effectors Cmu1 and Tin2, both of which were found to be translocated from biotrophic hyphae into the host cell. (Djamei et al., 2011; Tanaka et al., 2014).

An alternative approach for the localization of See1 by live cell imaging was the transient expression in *N. benthamiana* by using the *Agrobacterium* mediated transformation. Similar to the bombardment 35S-See1₂₂₋₁₅₇-mCherry was transformed to the *Agrobacterium* strain GV3101 wherein, the transformation was performed as described by (Flowers and Vaillancourt, 2005). The transformants were infiltrated into *N. benthamiana* leaves (3–4 week old) according to (Sparkes et al., 2006). (For details see the section 4.7.6). Microscopy of the infiltrated samples after 3 days showed See1-mCherry fluorescence in the transformed cells in the nucleus and cytoplasm. Additionally the cytoplasmic strands were clearly seen indicating the cytoplasmic localization of See1 (Fig. 24). Collectively, these results demonstrate that See1 might be functioning within the plant cytosol and is probably translocated into the plant cell.

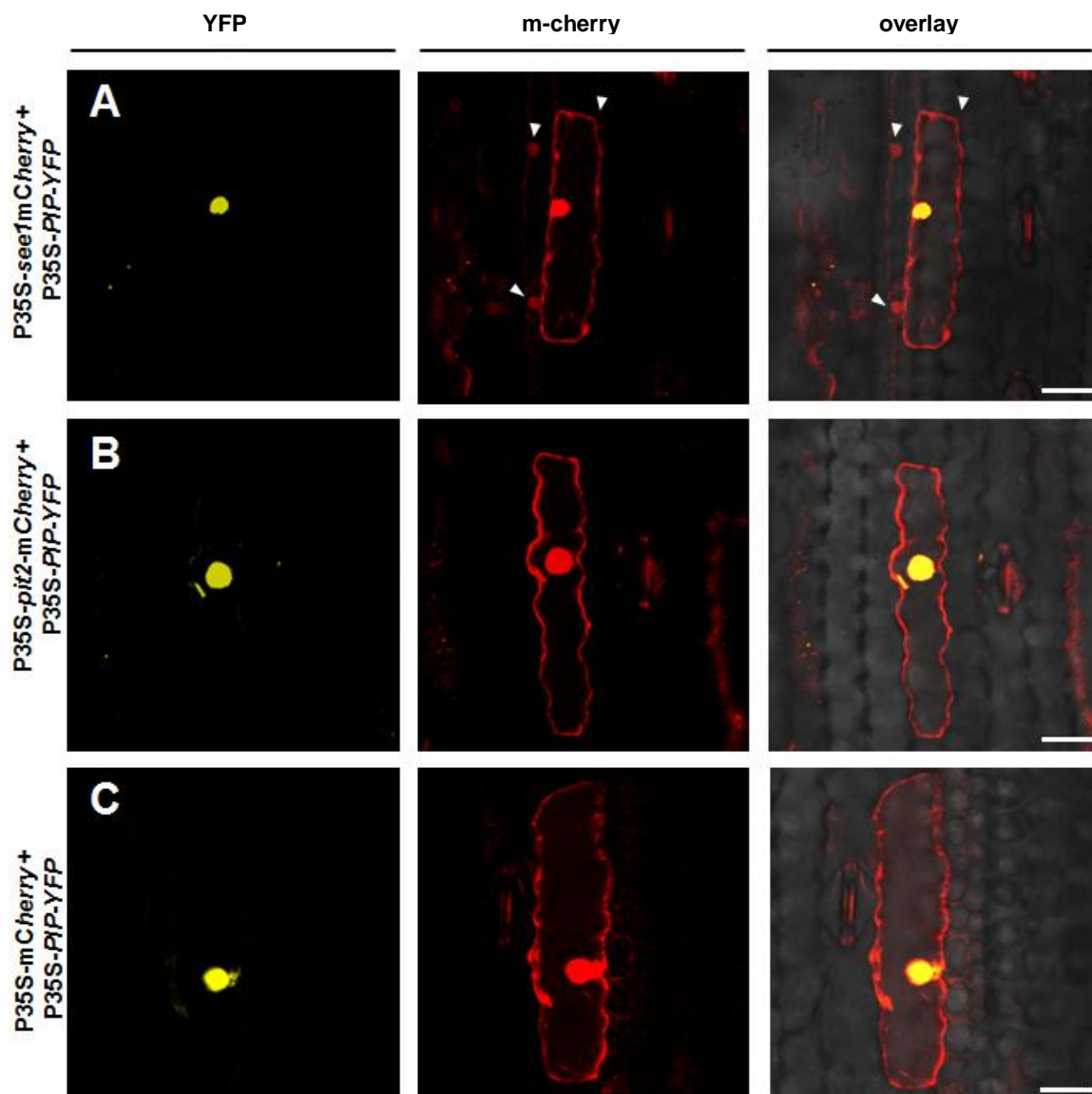


Fig. 23: See1 is transferred to cells neighboring to transformed cell. (A) Transient expression of 35S-*see1*₂₂₋₁₅₇-*mCherry* in maize epidermal cells with nuclear PIP-YFP control. See1-mCherry is localized to the cytoplasm and nucleus and is transferred to the adjacent neighboring cells as shown by white arrowheads. Scale bar = 25 μ m. (B) Confocal microscopy of 35S-*pit2*₂₆₋₁₁₈-*mCherry* transiently expressed in maize epidermal cells. The transformed cell (left panel) expresses a PIP-YFP control that is specifically localized to the nucleus. Pit2-mCherry is localized to the cytoplasm and nucleus. Scale bar = 25 μ m. (C) Confocal microscopy of 35S-*mCherry* transiently expressed with 35S-PIP-YFP in maize epidermal cells. The PIP-YFP control is specifically localized to the nucleus. mCherry is localized to the cytoplasm and nucleus. Scale bar = 25 μ m.

Additionally, in the transient expression of the *N. benthamiana*, it was seen that the group neighboring cells are frequently transformed showing cytoplasmic and nuclear fluorescence (Fig. 24). The expression level was high for 3 days after infiltration by the *Agrobacterium* mediated transformation. Hence, the confocal microscopy on *N. benthamiana* infiltrated samples was done after 3 dpi.

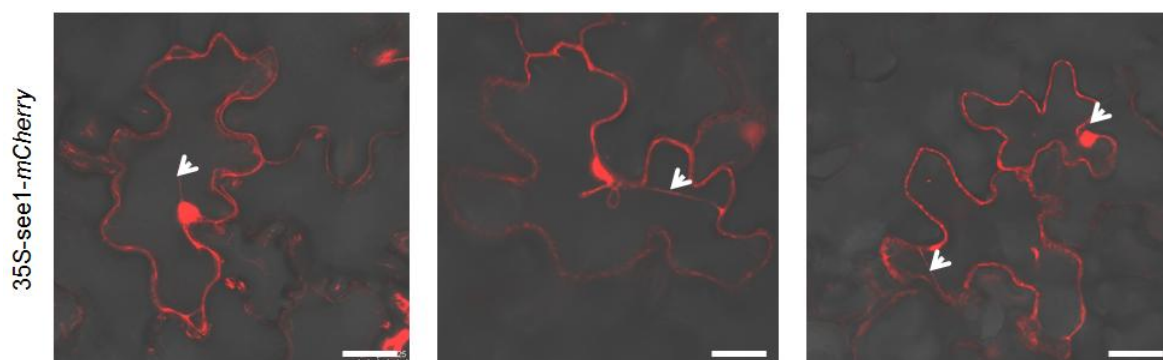


Fig. 24: See1 shows nuclear and cytoplasmic localization upon transient expression in *N. benthamiana*. Transient expression of 35S-*see1*₁₂₂₋₁₅₇-mCherry in *N. benthamiana* via *Agrobacterium* mediated transformation shows nuclear and cytoplasmic localization and in some cases a signal in the neighboring cells which are also transformed. Scale bar = 25 μ m.

2.6.3 See1 localizes to both cytoplasm and nucleus of maize cell

In addition to the previously described assays, a transmission electron microscopy (TEM) approach in combination with immunogold labeling was implemented. For this a C-terminal 3X HA-tagged versions of the effector were expressed under the native promoter in the SG200 Δ *see1* deletion strain. The 8 days old maize seedlings were infected by a standard method with sporidial suspension of the respective strains and the infected leaf areas were collected at 2 and 6 dpi for TEM preparation for immunogold detection of the HA tag. To verify expression and stability of the 3X HA-tagged See1 proteins (Psee1-SPsee1-See1-3X HA), western blot analysis after immunoprecipitation from infected plant tissue was performed at 2 and 6 dpi (the same timepoints at which samples were collected for TEM) (Fig. 25A). The signal at a desired size of 20.98 kDa indicated that the protein is stably expressed. For the immunolocalization, plants infected with SG200 served as negative controls. Two additional controls for immunolabeling were also employed. First, strain SG200 Psee1-SPsee1-mCherry-3X HA, which expresses secreted mCherry under control of the *see1* promoter and the second, strain SG200 Psee1-GFP-3X HA, which expresses cytoplasmic green fluorescent protein (GFP) driven by the *see1* promoter. The sample preparation was done by a modified method of Heyneke et al., 2013. For details see section 4.8.6. The subsequent TEM investigations were carried out in co-operation with Dr. Bernd Zechmann (Karl-Franzens University of Graz, Austria, currently at Baylor University, Center for Microscopy and Imaging, Texas, USA). The initial concentration of the antibody was standardized to reduce the intensity of the background labeling. In the TEM images, no gold labeling was seen in plant tissue infected with the parental strain SG200, indicating absence of unspecific background labeling (Fig. 25B). The non-secreted GFP-3X HA control, showed absence of labeling in the biotrophic interphase and signal was detected exclusively inside the fungal hyphae (Fig. 25C). The

sample with secreted mCherry-3xHA control showed labeling mainly in the biotrophic interphase, as well as in the fungal hyphae, indicating that mCherry is secreted by the fungus but not taken up in the plant cell (Fig. 25D).

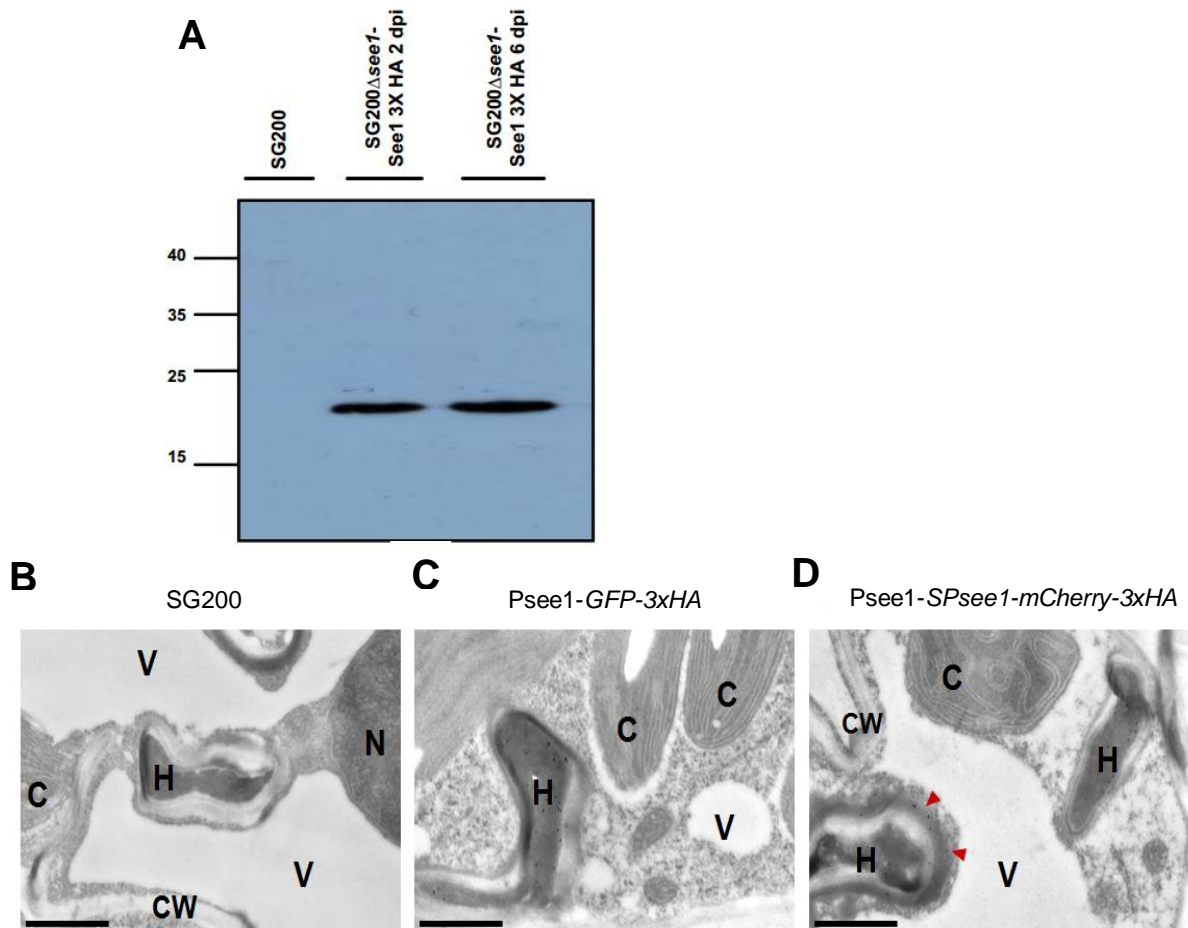


Fig. 25: Localization of See1 via immunogold labeling (A) See1-3X HA immuno-precipitated from infected plant tissue displays the expected size of 20.98 kDa. Plants infected with SG200 and SG200 Δ see1-see1-3X HA were subjected to anti-HA immunoprecipitation 2 and 6 dpi. The western blot was developed with anti-HA mouse antibodies and demonstrates that full length See1-3X HA is present in SG200 Δ see1-see1-3X HA infected tissue whereas no signal can be detected in SG200-infected plants. Controls for the TEM-micrographs showing immunogold labeling of 3X HA in leaves of *U. maydis* infected maize. (B) No gold particles were bound to wild-type infected tissue specimens (left panel). (C) Gold labeling was restricted to fungal hyphae (H) in GFP-3xHA samples as GFP was not secreted by the fungus (middle panel). (D) Gold particles bound to the secreted mCherry control could be found in hyphae (H) and at the biotrophic interface (red arrowheads) but not inside the plant cells despite proximity to hyphae. Psee1-SPsee1-mCherry-3xHA expression demonstrates that mCherry is secreted by the fungus but not taken up by the plant (right panel). Bars=1 μ m.

In contrast, See1-3X HA was detected in the fungal hyphae, the biotrophic interface but also inside the plant cytoplasm and predominantly inside the plant cell nucleus (Fig. 26A). The distribution of gold particles was quantified for all constructs, verifying the specific localization of See1-3X HA in the host cytoplasm and nucleus (Fig. 26B). In summary, it can be concluded that the See1 effector is secreted from biotrophic hyphae into the host cell, where it accumulates within the cytoplasm and nucleus.

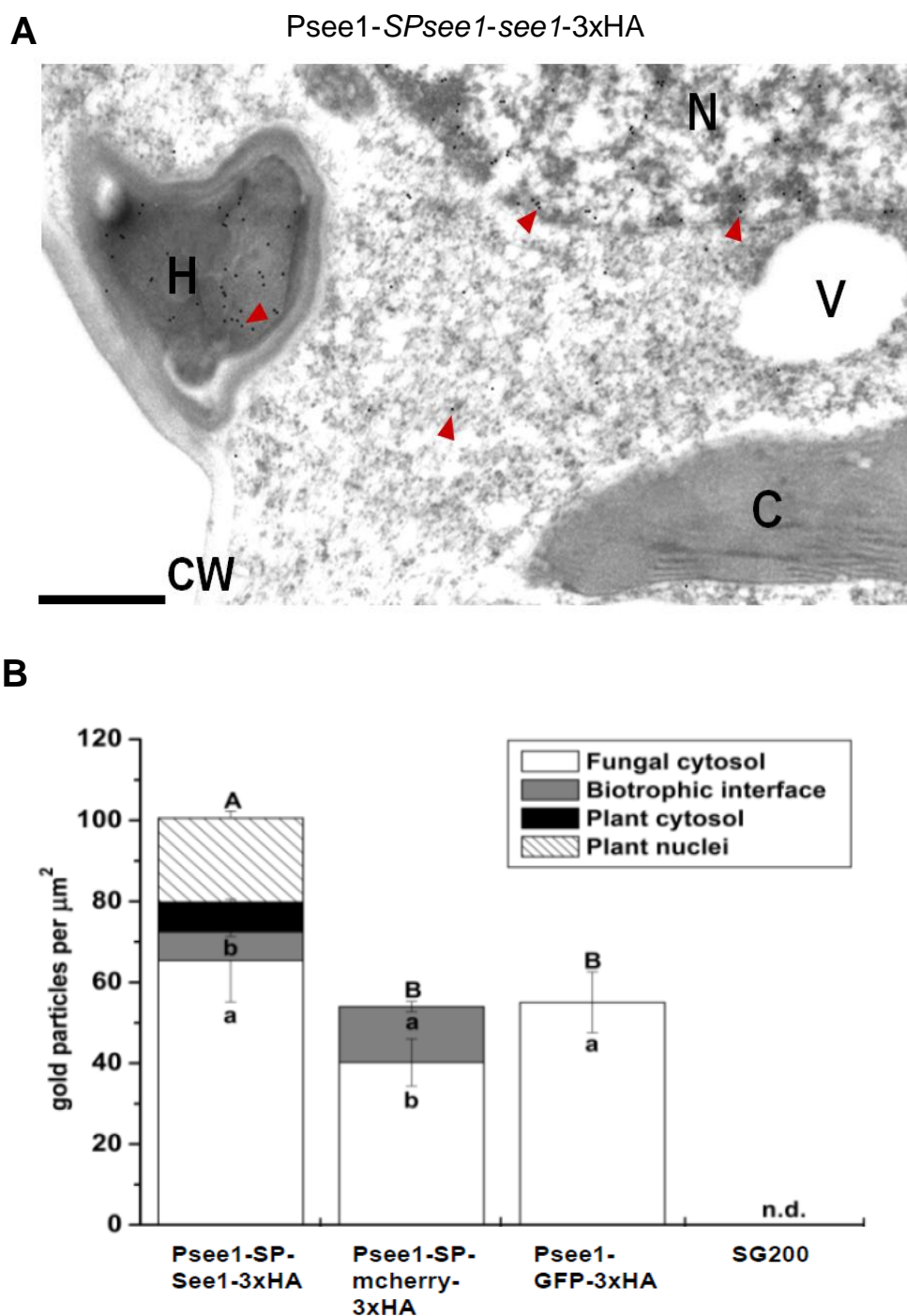


Fig. 26: See1 is translocated to the plant cell cytoplasm and nucleus. (A) Immunogold labeling of See1 could be found in hyphae (H), the cytosol and nuclei (N) as shown by the red arrowheads but not in chloroplasts (C), vacuoles (V), or the cell wall (CW) when the See1 effector was tagged with 3X HA in the strain Psee1-SPsee1-See1- 3X HA. Bars=1 μ m. (B) Graph shows the spatial distribution of gold particles bound to See1-3X HA in different cell compartments of leaves from Psee1- See1-3X-HA along with the secretory (mCherry-3X HA), nonsecreted (GFP-3X HA) and SG200 wildtype controls. Graph show means with standard errors and documents the amount of gold particles per μ m² in the individual cell compartments of three independent cross-sections. Different lowercase letters indicate significant differences ($P < 0.05$) between the individual cell compartments whereas uppercase letters indicate significant differences between the total amounts of labeling signal for all analyzed cell compartments taken together. Data were analyzed with the Kruskal-Wallis test followed by post-hoc comparison according to Conover (1999). n.d.= not detected.

2.7 Identification of the host interactors with effector See1

To identify the host proteins that are targeted by *see1* a yeast two hybrid screening (Y2H) was performed using a normalized cDNA library from the infected tissues. Among the several methods that are used for the interactor screening, the widely utilized and the accepted method is the yeast two hybrid system (Munkvold and Martin, 2009).

2.7.1 See1 interacts with the cell cycle and immune response regulator Zm-SGT1

To identify proteins interacting with See1, full length See1₂₂₋₁₅₇, without its secretion signal was used against a normalized cDNA library of *U. maydis* infected maize leaves and tassels. The expression of this bait fusion protein Myc-See1 was confirmed by a western blot (Fig. 27A). In screening, two putative interaction partners were identified from this screen, corresponding to a maize homolog of SGT1 (suppressor of G2 allele of *skp1*) and a zinc finger like transcription factor. From 60 clones that were isolated from high stringency selection medium, sequences encoding a maize homolog of SGT1 were frequently identified in a maximum number of clones. Maize genome encodes for two SGT1 of which only one form could be predominantly found in our Y2H screen.

To verify the interaction between See1 and SGT1, the SGT1 gene was amplified from cDNA synthesized from maize (cv. Early Golden Bantam) and re-tested in the yeast two-hybrid system. On plating the yeast transformants on selection medium of high stringency, no growth of yeast colonies was seen that contained a corresponding sequence for the full length protein of SGT1 (SGT1_{full}). In contrast, under these conditions for yeast expressing a SGT1 version without a tetratricopeptide (TPR) domain can be observed up to a dilution level of up to 10⁻³ growth (Fig. 27B and C). This suggests that the SGT1 protein interacts with See1 after it has been post-translationally modified. Moreover, See1 might interact with the entire resistance signaling complex, which is composed of SGT1 (suppressor of the G2 allele of *skp1*), RAR1 (required for Mla12 resistance) and HSP90 (heat shock protein 90) (Shirasu, 2009) making a conformational change responsible for disturbance in plant immunity. SGT1 was originally found in yeast as a cell cycle regulator necessary for the kinetochore formation (Kitagawa et al., 1999). This well-known regulator of cell cycle progression in yeast and an important factor in host and non-host resistance in plants, which has three functional domains, the TPR domain, the CHORD containing domain (CS) and the SGT1 specific domain (SGS) (Kitagawa et al., 1999; Peart et al., 2002). There are also two variable regions in the protein that are species-specific (Fig. 27B).

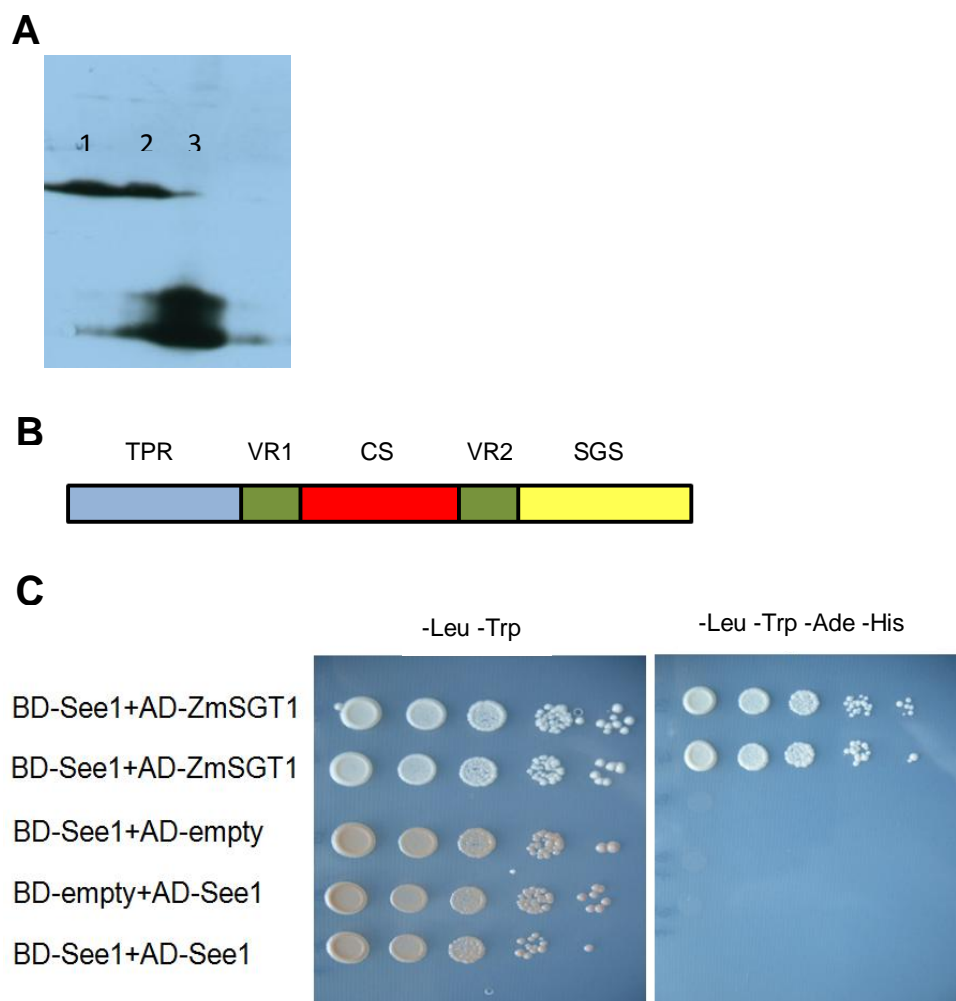


Fig. 27: See1 interacts with the cell cycle and the immune response modulator Zm-SGT1 (A) Myc-See1 immuno-precipitated from the transformed yeasts displays the expected size of 35.52 kDa as seen in lane 1 and 2. The transformed yeasts with the empty vector served as a negative control which is in lane 3 displaying a desired size of 21.7 kDa of the GAL4 BD alone. The western blot was developed with anti-Myc mouse antibodies and demonstrates that stable expression of the fusion bait protein. (B) Domain structure of maize SGT1 depicting three important domains: TPR, CS and the SGS. The two variable regions in the protein are species specific. (C) Yeast-Two-Hybrid experiment to test for the interaction of See1 and maize SGT1. The drop assay was done by serial dilutions (see Material and Methods), and strains were tested on low and high stringency plates to check for the specificity of the interaction. Results were documented 4 days after the drop assay.

To test whether, the identified maize protein is a functional SGT1 protein, temperature sensitive mutants of *Saccharomyces cerevisiae*, YKK 57 (*sgt1-5*) and YKK 65 (*sgt1-3*) (Kitagawa et al., 1999), which are restricted in cell cycle phases at G1 and G2 respectively, under 37 °C heat stress, were transformed with full length Zm-SGT1 identified in the Y2H screen under GAL4 yeast promoter. Under permissive and restrictive temperatures, Zm-SGT1 complemented growth defect of *S. cerevisiae* strain YKK57 (*sgt1-5*), indicating functionality of the identified maize homolog. Expression of Zm-SGT1 in *S. cerevisiae* strain YKK 65 (*sgt1-3*), which is defective at G2 showed normal growth at permissive temperature, while complementation at 37°C was only partial (Fig. 28).

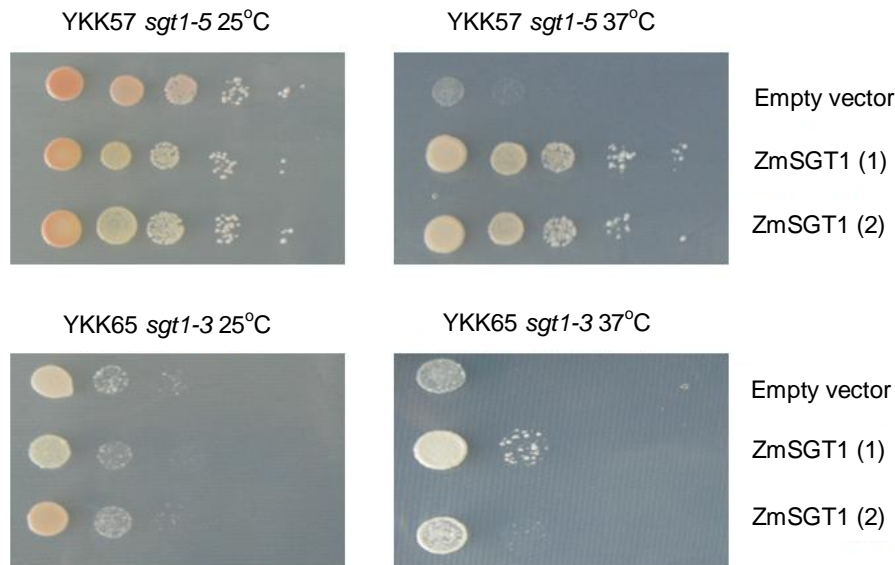


Fig. 28: See1 interacts with the ZmSGT1 which is functional in yeast cell cycle mutants (A) Dilution series of yeast strains YKK57 (*sgt1-5*) and YKK65 (*sgt1-3*) complemented with Zm-SGT1 or empty vector (EV) after growth at the permissive (25°C) and restrictive (37°C) temperatures. Yeast strains were transformed with Zm-SGT1, (cloned into pGREG GAL), or by same backbone empty vector. The transformants were selected on Sc-Ura 2% glucose plates. The strains were spread on Sc-Ura 2% galactose plates and incubated for 4 days to test the ability of Zm-SGT1 to complement the temperature-sensitive *sgt1-5* and *sgt1-3* growth defects. The ZmSGT1 (1) and (2) are two independent clones dropped in the assay.

2.7.2 See1 interacts with SGT1 in Co-immunoprecipitation and BiFC.

In addition to the yeast two hybrid, the See1-SGT1 interaction was also verified by the *in planta* Co-Immunoprecipitation (Co-IP) experiments (in co-operation with Lena Schilling). This was done by expressing both the proteins heterologously in *Nicotiana benthamiana*. As expression controls, P35S-See1-Myc and P35S-SGT1-HA were separately expressed in *N. benthamiana* leaves. This allowed a Co-IP of See1-c Myc and SGT1-HA from the plant protein extract using an anti-HA affinity matrix and subsequent detection of See1 c-Myc using anti-c-Myc antibodies by Western Blot (Fig. 29A). In contrast, no signal could be detected when the protein extracts from the infiltrated plants samples containing either See1 or SGT1, together with the corresponding empty vector were used (Fig. 29A). Thus, the direct interaction of the See1 and SGT1 was confirmed.

To investigate the interaction of See1 with Zm-SGT1 *in vivo*, a microscopic approach was followed, implementing the technique of bimolecular fluorescence complementation (BiFC). This experiment was also done by Lena Schilling. Here, the nucleotide sequences of two potential interaction partners can be fused with one half of a nucleotide sequence encoding a YFP chromophore. These constructs can be expressed using ballistic transformation via particle bombardment in epidermal cells of *Z. mays* (Section 4.7.7) and the transformed leaf areas were examined microscopically. In this assay, it is assumed that only direct interaction of the two proteins in the spatial proximity of interaction partners for each other leads to the adhesion of the two YFP fragments and form a

functional chromophore. Microscopic observation therefore proves YFP fluorescence in a specific compartment of the plant cells. Since this approach has some limitations, such as the lack of expression as appropriate, and a negative control some steps were modified as per Hemetsberger et al., 2012. (Fig. 30)

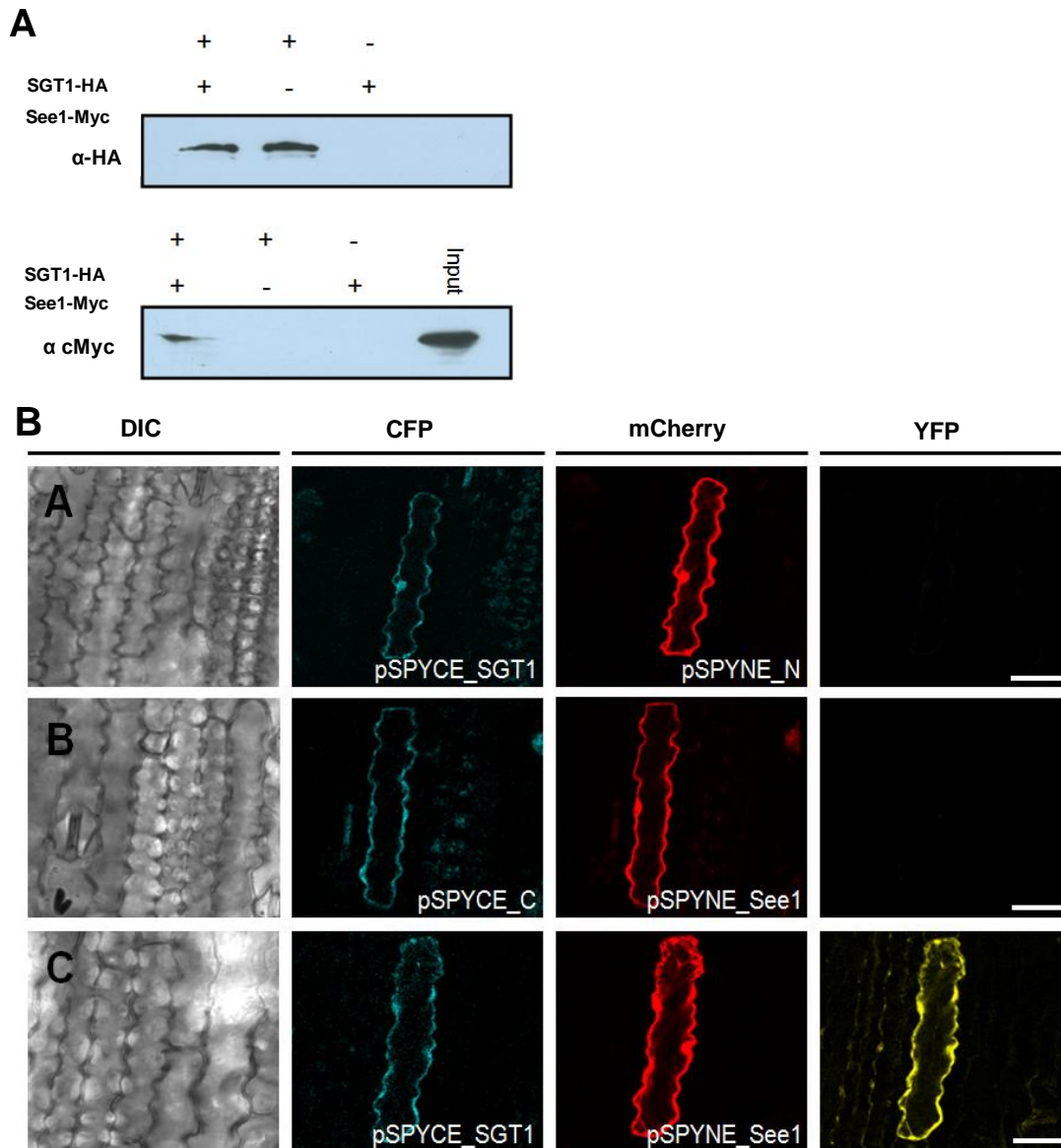


Fig. 29: See1 interacts with Zm-SGT1 in Co-immunoprecipitation and BiFC. (A) Co-immunoprecipitation shows interaction of See1 and SGT1 fusion-proteins isolated from transiently expressing *N. benthamiana* cells. The SGT1 was tag purified and See1 was pulled down. In the absence of SGT1, no See1 signal was detected. (B) Confocal images showing *Z. mays* epidermal cells expressing BiFC constructs. (A) A plant cell co-expressing pSPYCE-SGT1 and pSPYNE-mCherry. Blue and red channels show cytoplasmic co-localization of the respective signals. No complementation of fluorescence is observed in the YFP channel. (B) Co-expression of pSPYCE-CFP and pSPYNE-See1. Blue and red channels show cytoplasmic co-localization of the respective signals. No complementation of fluorescence is observed in the YFP channel. (C) A cell co-expressing pSPYCE-SGT1 and pSPYNE-See1. Both signals co-localize in the nucleus and cytoplasm. The YFP channel exhibits YFP fluorescence reflecting the direct interaction of See1 and SGT1. Bars = 25 μm. This figure has been generated from the work of Lena Schilling.

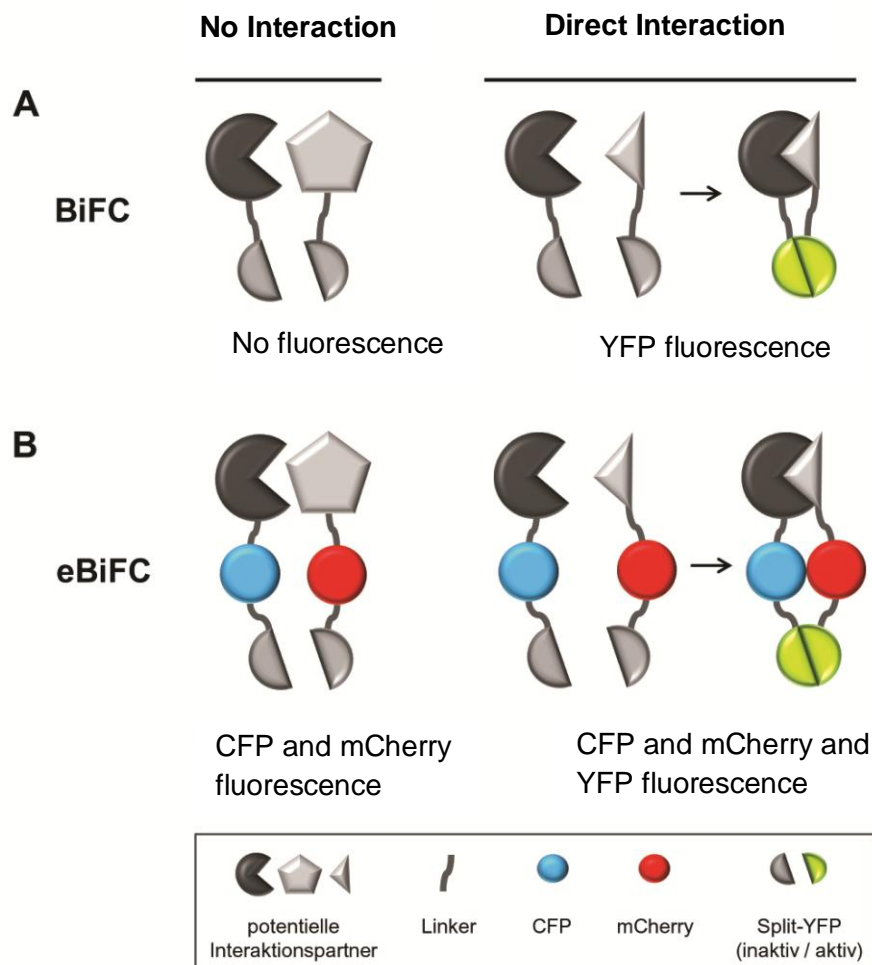


Fig. 30: Schematic representation of BiFC and eBiFC . (A) BiFC, based on a shared YFP chromophore (split-YFP). In the case of a direct interaction of two proteins, the YFP-parts come together in close proximity and there is a fluorescence complementation, i.e. upon successful interaction of two labeled proteins, the result is a YFP fluorescence (right side). If there is no interaction, no fluorescence signal is visible (left side). B: In contrast to the simple BiFC in eBiFC even in the absence of direct interaction of the labeled proteins, the fluorescence signals of CFP and mCherry allow the control of expression and localization of individual proteins (left side). In an interaction additionally a YFP fluorescence is observed (right side). Taken from the doctoral thesis of Christoph Hemetsberger.

A mCherry-tag was fused to the C-terminus of the N-terminal part of YFP (pSPYNE_N). Similarly, a CFP-tag was added to the C-terminal part of YFP (pSPYCE_C). Via ballistic transformation of maize epidermal cells, both constructs were transiently expressed under the control of the 35S promoter. Cells expressing both pSPYCE_C and pSPYNE_N fused to Zm-SGT1 and See1 were designated as pSPYNE-P35S-See1-mCherry-N_YFP-Myc and pSPYCE-SGT1-CFP-CYFP-HA. The cells exhibited cytoplasmic and nuclear fluorescence signals for both mCherry and CFP, indicating expression of the fusion proteins. Expressions of pSPYNE_N-mCherry with pSPYCE_SGT1 did not result in any detectable YFP signal, demonstrating that no unspecific protein dimerization occurred (Fig. 29A). Similarly, no YFP fluorescence was detected when pSPYCE-CFP was co-expressed with pSPYNE-mCherry fused to see1 (pSPYNE_See1) (Fig. 29B). In contrast, cells that co-expressed pSPYNE_See1 and pSPYCE_Zm-SGT1 showed a

complementation of YFP fluorescence (Fig. 29C), indicating interaction of See1 and Zm-SGT1 in the cytoplasm and nucleus of maize cells. Considering all of these results, it can be concluded that See1 interacts with Zm-SGT1 in the cytoplasm and nucleus of maize cells.

2.8 Mechanistic basis of the See1 interaction

Recently, it has been shown that SGT1 undergoes specific phosphorylation by Salicylic acid induced protein kinase (SIPK), a MAPK activated in response to pathogen assault in *N. benthamiana* (Hoser et al., 2013). This phosphorylation of SGT1 finely tunes the nucleocytoplasmic distribution of the N-receptor of tobacco. So, it was tempting to understand if similar mechanistic basis of phosphorylation dependent exists in See1-SGT1 interaction during *U. maydis* infection.

2.8.1 See1 inhibits the post-translational modification of Zm-SGT1

A major question arising from the See1 interaction with Zm-SGT1 is how the effector interferes with SGT1 at the molecular level. From the previous available literature, we tested whether See1 interferes with the phosphorylation of SGT1 after *U. maydis* infection. The *in planta* phosphorylation of SGT1 in the presence of See1 was analyzed by a transient expression assay as the See1 - SGT1 interaction could be transferred to *N. benthamiana*. The schematic representation of the *in planta* phosphorylation assay is shown in the Fig. 31.

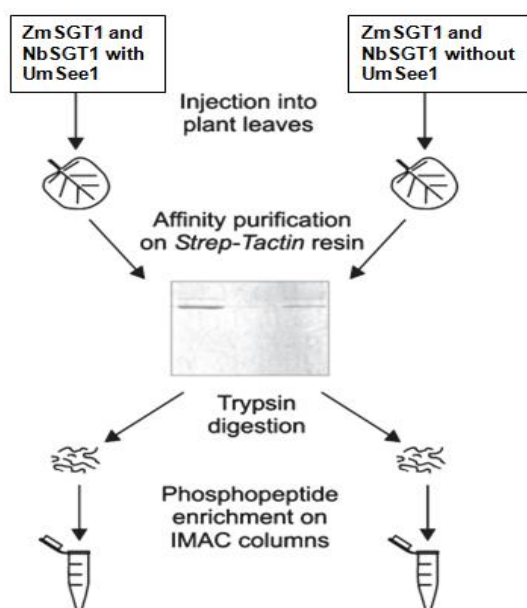


Fig. 31: Schematic representation of *in planta* phosphorylation assay. NbSGT1 or ZmSGT1 protein carrying a C terminal Strep tag II epitope was transiently coexpressed with MEK2^{DD}, SIPK and Umsee1 or the empty vector in *N. benthamiana* leaves. SGT1 (Suppressor of G2 allele of SKP1) was then affinity-purified, separated by SDS-PAGE and stained with Coomassie Blue. The excised bands corresponding to SGT1 were subjected to mass spectrometric analysis. Figure modified from Hoser et al., 2013.

A. tumefaciens strains carrying *P35S-Zm-SGT1-StrepII* were infiltrated along with the *P35S-SIPK*. The *pTA7001-see1-HA* was activated under the control of Dexamethasone (DEX) promoter. The SIPK was triggered with the upstream MAPK of *N. benthamiana* (*NtMEK2^{DD}*), which was also under DEX promoter. As a control for this experiment the *P35S-Nb-SGT1-StrepII*, was used replacing the *Zm-SGT1* as the phosphorylation site in this interaction is well-characterized in the previous literature (Hoser et al., 2013). As an additional control for the experiment the above construct combination of *Zm-SGT1* and *Nb-SGT1* were co-infiltrated along with the *pTA7001* empty constructs. The co-infiltrated *N. benthamiana* leaves were kept for 2 days incubation to ensure expression of the constitutive promoter constructs. Subsequently, *NtMEK2^{DD}* and *See1* expression was induced by treatment of the infiltrated leaves with Dex. Proteins were extracted from leaf samples collected 5 hours after induction and SGT1 was affinity-purified via its Strep tag II. The *NbSGT1* showed a phosphorylation at the previously identified MAPK phosphorylation site of *S₃₅₈* (Hoser et al., 2013). This phosphorylation was independent of *See1* as we could not detect a difference in the presence or absence of the *See1* effector. The various combination including controls that were used for the *in planta* phosphorylation assay have been summarized in Tab. 1.

Tab. 1: Combination of strains infiltrated in *N. benthamiana* for *in planta* phosphorylation assay.

Sr. No	Combination infiltrated	Interesting peptides identified	Interesting peptides identified + Phospho (ST)
1	MEK2 ^{LD} + SIPK + ZmSGT1 + UmSee1	NVEAPVAATVEDKEDVA NMDNTPPVVEPPSKPK TVEASPPDGMEK	None
2	MEK2 ^{LD} + SIPK + NbSGT1 + UmSee1	KVEGSPPDGMEK	KVEGSPPDGMEK + Phospho (ST)
3	MEK2 ^{LD} + SIPK + ZmSGT1 + pTA	NVEAPVAATVEDKEDVA NMDNTPPVVEPPSKPK TVEASPPDGMEK	NVEAPVAATVEDKE DVANMDNTPPVVEP PSKPK + Phospho (ST) phosphorylation by MAPK, T in TP motif is phosphorylated
4	MEK2 ^{DD} + SIPK + NbSGT1 + pTA	KVEGSPPDGMEK	KVEGSPPDGMEK + Phospho (ST)
5	MEK2 ^{KR} + pROK + ZmSGT1 + pTA	NVEAPVAATVEDKEDVA NMDNTPPVVEPPSKPK TVEASPPDGMEK	None
6	MEK2 ^{KR} + pROK + NbSGT1 + pTA	KVEGSPPDGMEK	None

Surprisingly, frequent occurrence of only one phosphopeptide derived from Zm-SGT1 (Mascot score of 126), comprising phosphorylated T₁₅₀ residue was detected by mass spectrometry (Fig. 32A and B) only in the absence of See1. The phosphorylated position also represents the putative MAPK target site which is conserved only in some monocot species including *Z. mays*, *Oryza sativa* and *Sorghum bicolor*. Moreover, the site is situated in the variable region of Zm-SGT1 (Fig. 33A). Strikingly, in See1 co-infiltrated samples, no phosphorylation could be detected at T₁₅₀, indicating the interference of See1 with phosphorylation of SGT1. As a negative control, we co-expressed inactive kinase *NtMEK2^{KR}* with SGT1. In this case, SIPK was not included because its transient expression results in slightly increased SIPK activity and associated activation of defense responses (Zhang and Liu, 2001). Under these conditions, SGT1 phosphorylation was not detected. Hence from the above data it can be concluded that See1 is blocking the Zm-SGT1 phosphorylation.

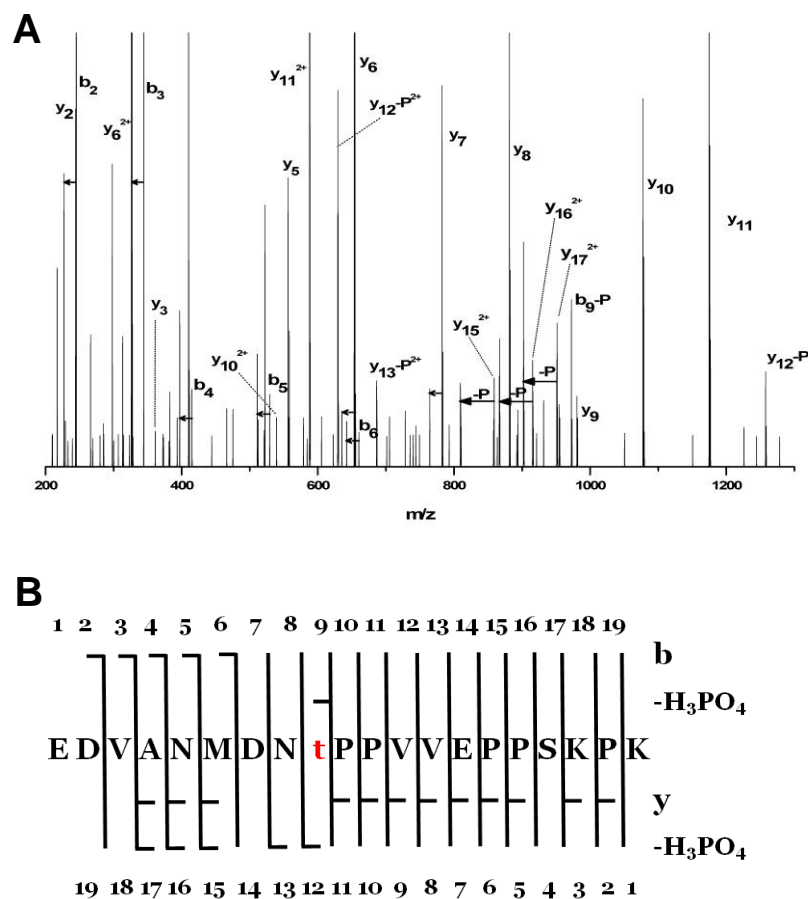


Fig. 32: In planta phosphorylation of Zm-SGT1. (A) Fragmentation spectrum assigned to the phosphorylated form of the peptide EDVANMDNTPPVVEPPSKPK (MASCOT score 126). (B) Peptide sequence with assigned y, b, y-H₂O, b-H₂O, y-H₃PO₄ and b-H₃PO₄ ions present. In (A) loss of H₃PO₄ is denoted by -P, loss of H₂O is marked by short horizontal arrows, whereas a longer arrow symbolizes pairs of detected signals corresponding to y_n and y_n-H₃PO₄. The majority of signals of the MS/MS spectra are assigned to the above species. The presence of several y_{n>11}-H₃PO₄ and b₉-H₃PO₄ accompanied by y_{15,16,17} pinpoints threonine at position 9 as the unequivocal phosphorylation site within the peptide.

The peptides identified by the Mass Spectrometry in the presence and absence of See1 are highlighted below. The peptides frequently detected in the MS spectra correspond to the peptide in the variable region of the maize SGT1 protein. (Fig. 33B and C).

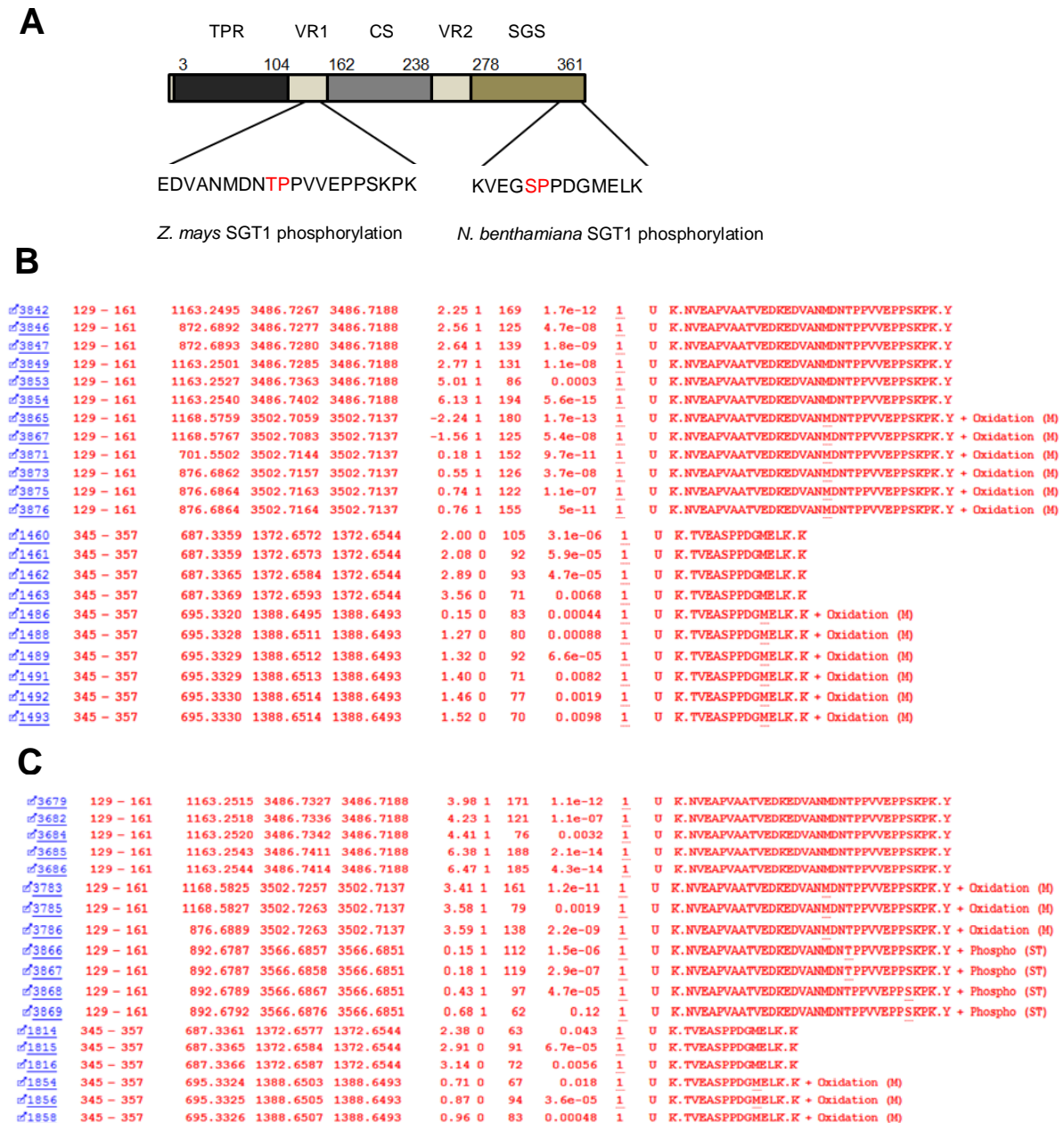


Fig. 33: *In planta* phosphorylation of Zm-SGT1. (A) The examined phosphorylation site of *Z. mays* SGT1 falls within the variable region of the protein, and the phosphorylation site of *N. benthamiana* SGT1 within the SGS domain. The prominent phosphopeptide detected in the *in planta* phosphorylation of Zm-SGT1 is shown. The phosphopeptide of Nb-SGT1 detected previously by Hoser et al., (2013) is also indicated. (B) Peptide sequences of Zm-SGT1 detected in the Mass spectrometry in the presence of See1 with no phosphorylation detected for any of the peptide observed. (C) Peptide sequences of Zm-SGT1 detected in the Mass spectrometry in the absence of See1 where phosphorylation is detected at T150 for the peptide corresponding in the variable region of the protein.

2.8.2 See1 does not undergo phosphorylation by itself

The previous results about the *in planta* phosphorylation assays demonstrated that See1 is interfering with the post-translational modification of SGT1. Thus, the next hypothesis was if See1 would be undergoing phosphorylation by itself when bound to Zm-SGT1. To confirm this *in planta* phosphorylation assay was implemented by infiltration of See1 fused to a HIS-Strep tag. The 35S-See1 was infiltrated along with Zm-SGT1 and activated by MEK2^{DD} and SIPK. Protein was extracted from the leaf samples and the leaf extract was subjected to Mass Spectrometry analysis. None of the peptides detected from See1 showed any phosphorylation under these tested conditions (see Annexure) indicating that it might be undergoing the post-translational modification that could not be detected by the Mass Spectrometry Approach. This question will be addressed in the next perspectives of the project to understand the mechanism involved in the See1-SGT1 interaction.

2.9 Conservation of See1 among other smuts

The genome of two smut fungi related to *U. maydis*, the maize anther smut *S. reilianum* and the barley covered smut *U. hordei*, have recently been sequenced (Schirawski et al., 2010; Laurie et al., 2012). Both genomes contain each one coding sequence with a significant similarity to the *U. maydis see1* gene. An amino acid alignment of See1 orthologues, however, show only weak conservation with the encoded protein sharing only 40 % (*S.reilianum*) and 34 % (*U.hordei*) sequence identity to the *U. maydis* See1, respectively. The amino acid alignment of the See1 protein from *U. maydis* along with its orthologues from the closely related smuts has been represented in the Fig. 34.

```

Um 02239      1 MLFTTFVSELLLVILCLVHVS-AHPLQSFRRSSAIGKKHKIKSRQFEELI
Sr 13434      1 MRASTLVSLLLTL-LALTT-ARPTNTPRRSS----KHKIKSRQFEELI
Uh 03678      1 --MKRVLTLILVFLLFALTLA-PPRHAR----LHKKHK---RQLEELI

Um 02239      50 AQGAEDSIELFEPPRVHDSSEQIHERTEQQNITTKNIILAINKNSRKHGG
Sr 13434      45 AARADETLELYDAPRVHDSSEKIHEGTQNNVTTTRILAAIRESRARQSR
Uh 03678      42 LVGAEDSVELFDHPRIHDTSEKIHEAAEQNIT----VQHLEEIKRKK--

Um 02239      100 --LHRLPAQVQGEGEFTYDRQRNAVGSYRYGDSHGNSREAEYSVADHQSA
Sr 13434      95 QRTQRLPLATTSQGEYSYDLQRSGVGLYSQQDGTGNSRMDGYAEESRQSG
Uh 03678      86 --LRKLQILMLDRKKFEQE-----NVSERRRLKVERGGE

Um 02239      148 SGEYKFGPTT-
Sr 13434      145 FERYRVGDSYT
Uh 03678      118 GG-----

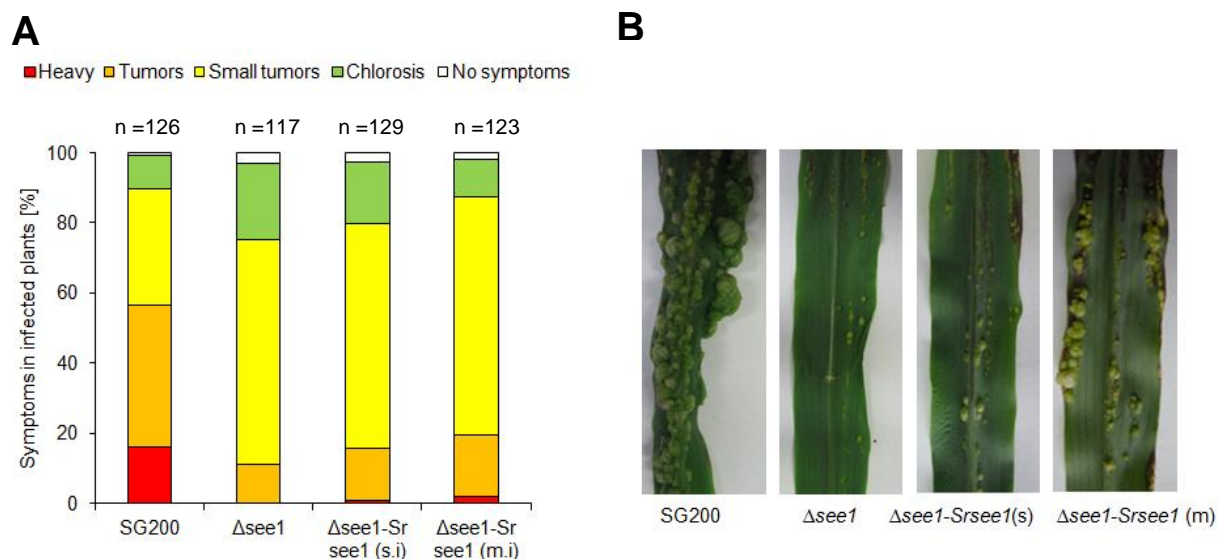
```

Fig. 34: Conservation of See1 in related smut fungi. Comparison of the amino acid sequences of *U. maydis* See1 (*Um02239*) with orthologues from *S. reilianum* (*Sr13434*) and *U. hordei* (*Uh03678*). Red boxes represent the signal peptide as predicted by SignalP 4.0. The green framed area features two conserved region blocks that may act as functional virulence domains.

Since this organ specific effector is also conserved in smuts causing only floral symptoms, it indicates that *U. maydis* seedling specific proteins have gained novel functions by accelerated divergence. The protein alignment shows that the protein is overall highly diversified and there are two conserved blocks which are present in the central region of the protein which might contribute to the virulence function.

2.9.1 Complementation of the $\Delta see1$ phenotype by *See1* orthologues

To see if the *See1* orthologues in the closely related smuts that cause only floral symptoms, could functionally complement the SG200 $\Delta see1$ mutant phenotype in leaves the orthologues along with their respective promoters were cloned to generate a plasmid p123-P_{Srsee1}-Srsee1 and p123-P_{Uhsee1}-Uhsee1. The template was amplified from wild type *S. reilianum* SRZ2 or the *U. hordei* solopathogenic strain DS200 (Doehlemann et al., 2014) and integrated into the *ip* locus (Loubradou et al., 2001) of SG200 $\Delta see1$ to produce SG200 $\Delta see1$ -Srsee1 or SG200 $\Delta see1$ -Uhsee1. These generated constructs were confirmed for the presence of the single or multiple integration of the respective candidate by southern blot analysis. Plant infection assays with generated strains did not show the ability to complement the $\Delta see1$ phenotype. The strains were not comparable in pathogenicity symptoms with wildtype SG200 strain, i.e. the introduced gene did not complement the *see1* deletion phenotype completely. Hence it can be concluded from these results that the *S. reilianum* or *U. hordei* *see1* cannot complement the $\Delta see1$ phenotype along with their respective promoters. The results of these disease ratings have been shown in Fig. 35.



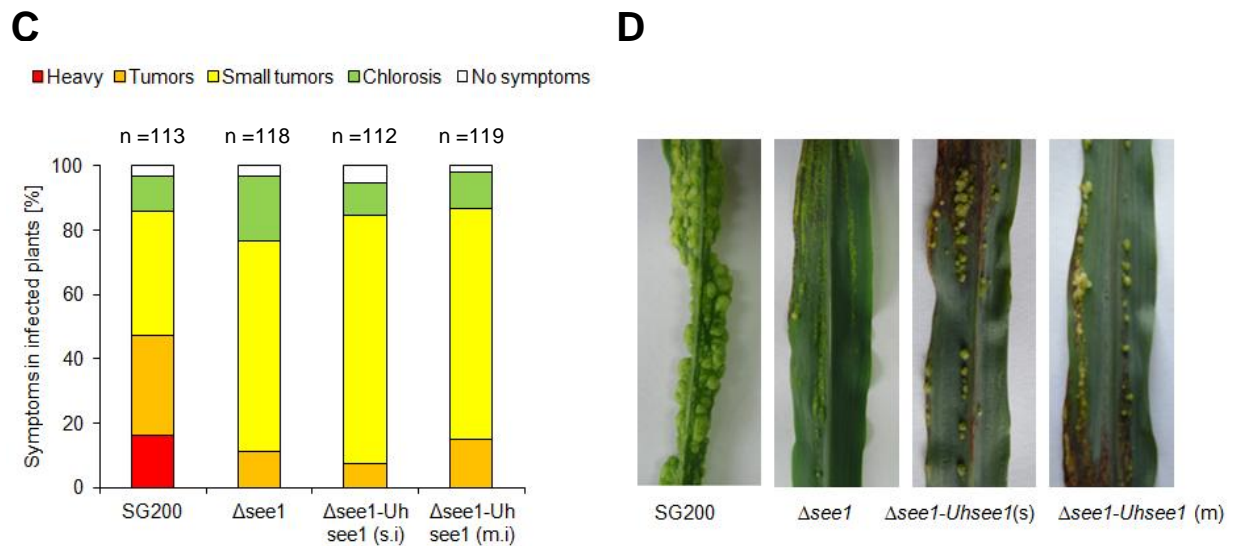
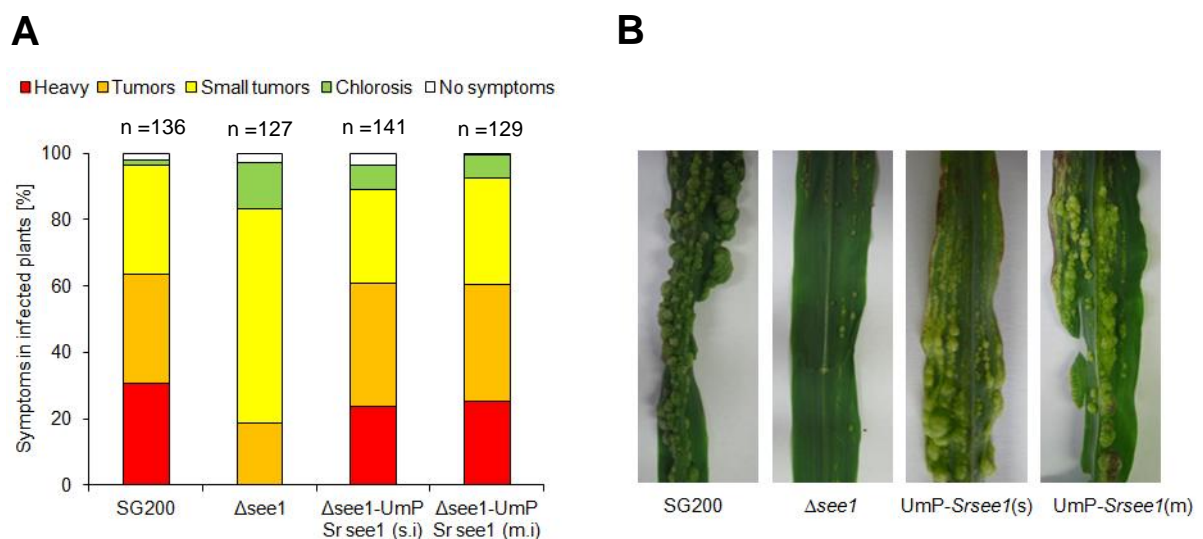


Fig. 35: Complementation of the SG200 $\Delta see1$ by orthologue from *S. reilianum* and *U. hordei*. (A) Quantification of infection symptoms on maize seedlings at 12 dpi. SG200: Virulent *U. maydis* strain that causes wildtype symptoms. $\Delta see1$: *see1* deletion mutant. $\Delta see1$ -Srsee1: SG200 $\Delta see1$ complemented with a construct containing the *see1* from *S. reilianum*. (B) Representation of typical symptoms of infection caused by the strains described in (A) at 12dpi. (C) Quantification of infection symptoms on maize seedlings at 12 dpi by *U. hordei* orthologue. SG200: Virulent *U. maydis* strain that causes wildtype symptoms. $\Delta see1$: *see1* deletion mutant. $\Delta see1$ -Uhsee1: SG200 $\Delta see1$ complemented with a construct containing the *see1* from *U. hordei*. (B) Example of typical symptoms of infection caused by the strains described in (A) at 12dpi. s.i: single integration and m.i: multiple integration, n= number of plants infected.

Next, the two orthologues were expressed under the promoter of *U. maydis see1*. The resulting constructs p123- P_{Umsee1} -Srsee1 and p123- P_{Umsee1} -Uhsee1 were integrated into the *ip* locus (Loubradou et al., 2001) of SG200 $\Delta see1$. The generated strains SG200 $\Delta see1$ - P_{Umsee1} -Srsee1/Uhsee1 were then used for plant infections as described previously. *S. reilianum see1* could fully complement the SG200 $\Delta see1$ phenotype indicating that the orthologue from *S. reilianum* is functional (Fig. 36A and B). On the other hand the *U. hordei see1* could not complement the SG200 $\Delta see1$ phenotype (Fig. 36C and D). These results also indicate that *U. maydis* sense the colonized organ and the expression of organ specific effector might be regulated by specific transcription factors.



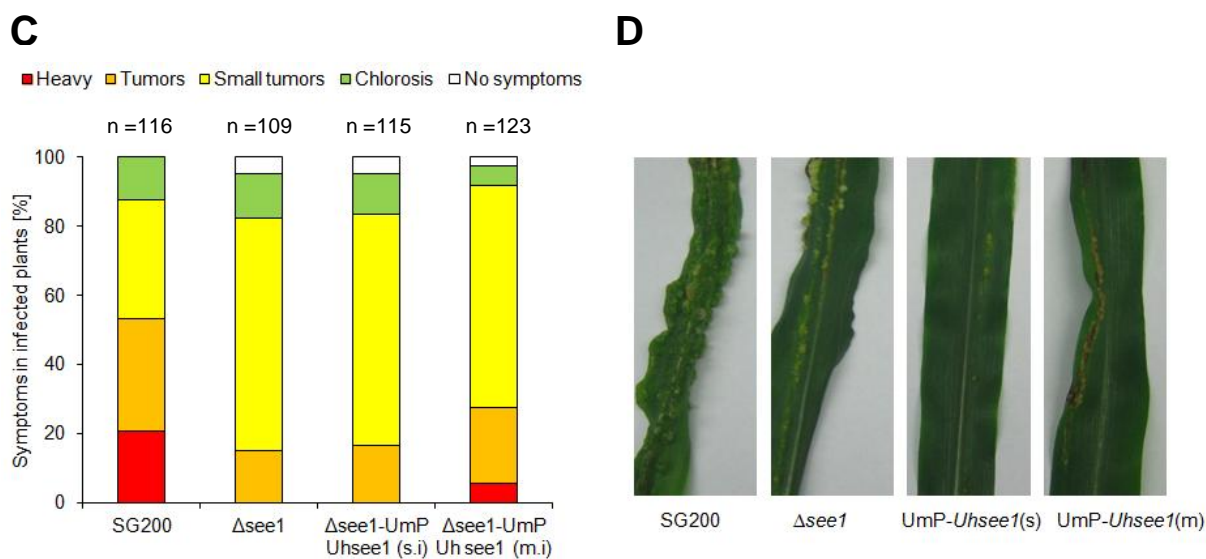


Fig. 36: Complementation of the SG200 $\Delta see1$ by orthologue from *S. reilianum* and *U. hordei* in the presence of native *U. maydis* promoter. (A) Quantification of infection symptoms on maize seedlings at 12 dpi with the Srsee1 under Umsee1 promoter in comparison to the wildtype and *see1* deletion mutant. (B) Example of typical symptoms of infection caused by the strains described in (A) at 12dpi. (C) Quantification of infection symptoms on maize seedlings at 12 dpi with the Uhsee1 under Umsee1 promoter in comparison to the wildtype and *see1* deletion mutant. (D) Representation of typical symptoms of infection caused by the strains described in (A) at 12 dpi. SG200: Virulent *U. maydis* strain that causes wildtype symptoms. $\Delta see1$: *see1* deletion mutant. $\Delta see1$ -UmP Srsee1: SG200 $\Delta see1$ complemented with a construct containing the *see1* from *S. reilianum* under *U. maydis see1* promoter. $\Delta see1$ -UmP Uhsee1: SG200 $\Delta see1$ complemented with a construct containing *see1* from *U. hordei* under *U. maydis see1* promoter. s.i: single integration and m.i: multiple integration. n= number of plants infected.

2.10 Differential gene expression analysis in SG200 and SG200 $\Delta see1$ infected leaves

To investigate the impact of *see1* on the host at molecular level transcriptome profiling of the infected was done by using Agilent microarrays. Leaf samples infected with *U. maydis* (SG200, SG200 $\Delta see1$ and mock control) were collected at 6 dpi from three independent biological replicates. This timepoint was selected in order to capture the differences in the host upon tumor elicitation and development. RNA from the infected tissue was prepared from the independently collected samples and hybridized to 4x44k custom-designed Agilent microarray chips for maize (array platform designed by the Walbot Lab). The microarray data obtained in this study were analyzed using the Partek Genomics Suite version 6.12. Expression values were normalized using the RMA method. Criteria for significance were a corrected p-value (per sample) with an FDR of 0.05 and a fold-change of >2. Differentially expressed genes were calculated by a 1-way ANOVA.

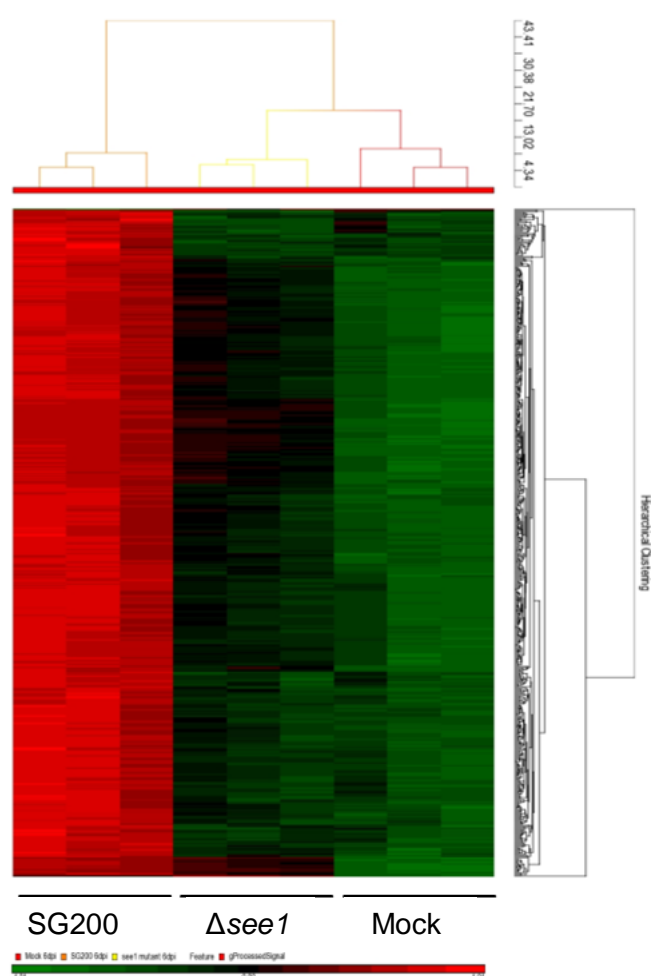


Fig. 37: Plant transcriptome analysis of SG200 (wildtype) and SG200 Δ see1 (mutant) infected tissue using microarray hybridization. Hierarchical clustering was performed by the Partek Genomics Suite version 6.12 to visualize expression of maize genes transcriptionally regulated 6 dpi by *U. maydis* strain SG200 (left), infection by SG200 Δ see1 (middle), and mock inoculation (right). The X-axis depicts clustering of the microarray samples for each of the three biological replicates per inoculation. The Y-axis shows clustering of the regulated maize transcripts based on similarity of their expression patterns. red: upregulated genes; green: downregulated genes; black: not significantly altered.

The microarray analysis indicated that in response to *U. maydis* wild type infection, 10,952 maize transcript abundances were altered, while SG200 Δ see1 infection resulted in significant regulation of only 773 maize genes (Supplemental Dataset 1: CD attached). Hierarchical clustering of the SG200-induced maize genes visualized the reduced transcriptional response of maize leaves to the *see1* deletion mutant (Fig. 37). When directly comparing SG200 to SG200 Δ see1 expression profiles, 549 genes were significantly induced (>two-fold) in SG200 compared to the SG200 Δ see1 at 6 dpi, while only two genes were repressed (Supplemental Dataset 2: CD attached). Among the wild type induced transcripts, particularly genes involved in DNA modification (i.e. histones), DNA replication and DNA damage repair, as well as cell cycle associated genes were enriched. 71 of the 549 SG200-induced genes classify in GO-terms associated to DNA metabolism and cell cycle regulation (Tab. 2). For example, DNA replicase delta, which is involved in S-phase DNA replication (TC280511), is 690-fold induced in wildtype

infections compared to SG200 Δ see1. DNA histone H3, which is involved in the cell proliferation (TC298222), is 862-fold induced in wildtype infections. Maize Skp1 (TC293032) is 426-fold induced in SG200 infections versus SG200 Δ see1. As another example, a LRR receptor like protein from maize, which is responsible for protein phosphorylation and regulation of cell division (TC307447) is also upregulated by 230-fold in the SG200 infected samples. Together, these data suggest that SG200 Δ see1 fails to induce tumor growth in leaves at the level of host cell DNA synthesis and cell proliferation. On the transcriptome level, this is reflected by absence of the induction of maize genes associated with DNA metabolism, DNA damage repair and cell cycle regulation, all of which are hallmarks of maize responses to wildtype *U. maydis* during tumor development (Doehlemann et al., 2008).

Tab. 2: Differentially expressed Top GO terms related to the DNA synthesis and cell differentiation

Gene ID	GO No.	GO Description	Sequence Description	Fold change SG200 vs SG200 Δ see1
CF919894	41	P:cortical microtubule organization; F:hydrolase activity; P:negative regulation of MAP	dual specificity protein phosphatase pbs1	677
TC301470	20	P:translational initiation; P:methylation-dependent chromatin silencing; P:cell-cell signaling	protein argonaute 10-like	578
TC282828	20	P:cellular response to phosphate starvation; F:phosphatidate phosphatase activity; C:pl	phytochrome-associated protein 1	367
TC294593	19	P:myo-inositol transport; F:glucose transmembrane transporter activity; P:mannitol tran	polyol transporter 5-like	327.425
TC307652	17	P:transmembrane transport; P:positive gravitropism; P:leaf formation; C:basal plasma me	auxin efflux carrier	895.397
TC299855	17	P:response to oxidative stress; P:negative regulation of growth; P:oxidation-reduction	peroxidase 15-like	821.735
TC301172	17	P:mitotic cell cycle; P:gene silencing by RNA; F:DNA-dependent ATPase activity; P:respo	dna repair protein rad51 homolog	67.738
TC294810	15	F:DNA-directed DNA polymerase activity; F:metal ion binding; P:double-strand break repa	dna polymerase alpha catalytic subunit	403.239
TC279595	14	C:cytosol; C:nucleosome; P:response to water deprivation; C:mitochondrion; C:nucleolus;	histone h4	749.097
TC279279	14	C:cytosol; C:nucleosome; P:response to water deprivation; C:mitochondrion; C:nucleolus;	histone h4	691.187
TC279246	14	C:cytosol; C:nucleosome; P:response to water deprivation; C:mitochondrion; C:nucleolus;	histone h4	541.567

TC306450	14	F:glucan exo-1,3-beta-glucosidase activity; F:beta-L-arabinosidase activity; F:cellobio	beta-glucosidase 44	506.238
TC310738	13	P:translation; P:endonucleolytic cleavage to generate mature 3'-end of SSU-rRNA from (S	40s ribosomal protein sa	417.245
TC307447	13	P:regulation of cell adhesion; P:regulation of cell division; P:protein phosphorylation	leucine-rich repeat receptor-like protein kinase family protein	230.113
TC306407	13	C:membrane coat; P:methylation-dependent chromatin silencing; P:chromatin silencing by	microtubule-associated protein tortifolia1-like	155.289
TC311056	13	P:regulation of G2/M transition of mitotic cell cycle; F:RNA polymerase II carboxy-term	cyclin-dependent kinase b2-1-like	118.332
TC283433	12	P:microtubule-based process; P:gene silencing; P:histone modification; C:cytoskeletal p	atp binding	747.103
TC287119	12	C:Cajal body; P:histone H3-K9 methylation; P:defense response to bacterium, incompatibl	Argonaute family protein	251.56
TC279950	11	P:response to glucose stimulus; P:response to sucrose stimulus; P:response to fructose	pyrophosphate--fructose 6-phosphate 1-phosphotransferase subunit alpha-like	674.109
TC294404	11	C:cytoplasm; P:response to nematode; C:plant-type cell wall; P:cell wall modification;	probable pectinesterase pectinesterase inhibitor 40-like	641.189
TC281806	11	C:plant-type cell wall; F:xylan 1,4-beta-xylosidase activity; P:xyloglucan metabolic pr	alpha-xylosidase 1-like	568.093
TC300114	10	F:molecular_function; P:biological_process; P:regulation of transcription, DNA-dependen	ap2-like ethylene-responsive transcription factor at2g41710-like	836.606
TC292250	10	P:mitotic cell cycle; P:stomatal lineage progression; P:negative regulation of cyclin-d	cyclin-dependent kinases regulatory subunit	729.831
TC300266	10	P:mitotic cell cycle; C:cell wall; F:microtubule binding; C:nucleolus; P:thigmotropism;	microtubule-associated protein rp eb family member 3	144.046
TC286934	10	P:meiosis II; P:regulation of cyclin-dependent protein serine/threonine kinase activity	type a-like cyclin	120.597
TC298222	9	C:nucleosome; P:cell proliferation; F:DNA binding; P:nucleosome assembly; C:nucleus; F:	histone h3	862.773
TC298215	9	C:nucleosome; P:cell proliferation; F:DNA binding; P:nucleosome assembly; C:nucleus; F:	histone h3	794.373

TC301787	7	P:regulation of transcription, DNA-dependent; F:core promoter binding; P:transcription,	transcription factor pcf3-like	586.847
TC287426	7	P:regulation of cell cycle; F:identical protein binding; P:histone H3-K9 methylation; P	tetratricopeptide repeat-like superfamily protein isoform 1	152.837
TC298187	7	C:nucleosome; P:cell proliferation; F:DNA binding; P:nucleosome assembly; C:nucleus; F:	histone h3	150.782

As it was earlier seen from the microarray that many genes corresponding to histones and DNA synthesis are not induced in the SG200 Δ *see1* to that of wildtype infected tissues, the next follow-up experiment was the verification of the expression profile of some of these cell cycle markers. In this regard a Histone H3 (TC298222), a cell division regulatory protein 2 (TC314811), the putative LRR receptor (TC307447) and the cyclin dependent kinase regulatory subunit (TC292250) were selected for the confirmation of expression profile in between SG200 wildtype and the Δ *see1* infected leaves which were showing an interesting regulation in the array data. Each of the above selected candidates showed a high up-regulation in the wildtype infected tissue, which was totally negligible in the mutant infected leaves (Fig. 38). This showed a direct involvement of *See1* in the regulation of these cell cycle markers that were prominent in forming a tumor.

On the other hand, to investigate whether a particular phase of the cell cycle or cellular process is targeted in the *See1* interaction, we particularly focused on the late G1 and S phase as the Edu Labelling experiments strongly suggested the defect around synthesis. qRT-PCR was used to monitor the expression of CDC6 gene which is a key marker in the formation of pre-replication complex. Literature shows that CDC6 is mainly required to form the pre-replication complex but has no role in its activation to progress the cell cycle. Over-expression of CDC6 leads to activation of CDC28 that suppresses nuclear division. In the Δ *see1* infected tissue, the CDC6 seems to be induced throughout the disease progression. Hence, because of its constant over-activation the pre-replication complex may not be activated to progress the cell cycle transitions thereby leading to arrest in the cell cycle at G1 by which any EdU labeling is not observed (Fig. 38).

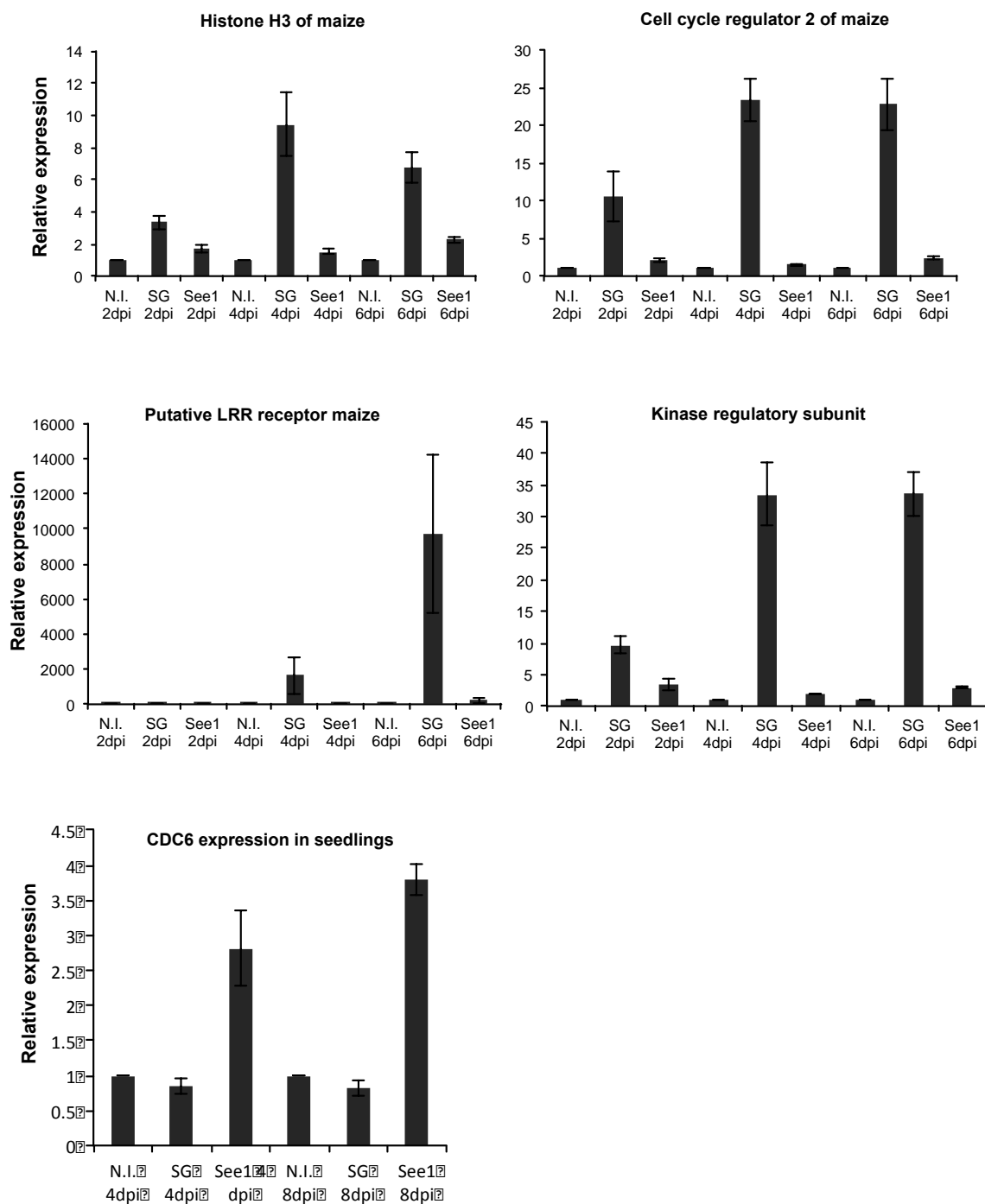


Fig. 38: Expression profile of the cell cycle marker genes during *U. maydis* wildtype infection in comparison to the mock and *see1* effector mutant. Quantitative real time polymerase chain reaction (qRT-PCR) expression profiling of the indicated marker gene during biotrophic phase of *U. maydis* growth in seedling tissues. Expression levels are shown relative to mean expression of *glyceraldehyde 3 phosphate dehydrogenase (gapdh)* transcripts. Gene expression was analyzed in noninfected (N.I), wildtype SG200 (SG) and the *see1* effector mutant (See1) at consecutive time intervals from 2 dpi to 6dpi. In CDC6 the gene expression was analyzed in noninfected (N.I), wildtype SG200 (SG) and the *see1* effector mutant (See1) at 4 dpi and 8dpi. Error bars show SE.

3 Discussion

For a better understanding of the organ specific effector role, in tumor formation as well as for understanding of the plant immune factors that are targeted by such effectors during infection, the present work has contributed to the understanding of relation between the tumor formation and role of organ specific effectors in *U. maydis* /maize pathosystem. The focus of the work was not only the functional characterization of organ specific effector *see1*, but also aiming to the elucidation of the mechanistic basis of this interaction with the host immune network. It was shown that *See1*, which is hypothesized to be involved in shaping of tumors in *U. maydis*, disease is targeting the immune assembly of the plant by hijacking the central immune components of a host cell leading to the induction of a tumor by the elicitation of host DNA synthesis to an excited state. These organ specific effectors in general might be targeting the modulation of plants native metabolic state as well as the cell cycle control to raise a tumorous symptom.

3.1 *Ustilago maydis*: A highly specialized biotroph

U. maydis is seen to have a broad molecular repertoire of effectors for active compatibility (Boller and He, 2009). This specialized feature to the fungus is gained by evolution of pathogen effectors tailored to individual host organs. It is shown that nearly 45 % of the secretory proteins show an organ specific expression pattern (Skibbe et al., 2010). It is well known that intrinsic mutations in maize can disrupt normal development in the host and can enhance or suppress tumor growth (Walbot and Skibbe, 2010). So, it is of immense importance for the pathogen to evolve the virulence proteins to tailor the specific host tissues.

To cope up with these physiologically varied host environments, *U. maydis*, might have evolved a large set of effectors for tumor formation in vegetative tissues than in the floral parts. Floral tumors may result from the general pathogenicity factors that are conserved within other smuts. Hence a discrete complex tumor model exists for *U. maydis* in which establishment of compatibility and suppression of general plant defense is done by core effectors and disease progression occurs by the activity of organ specific effectors by re-directing the physiology and development of a specific organ primordium (Skibbe et al., 2010). This makes *U. maydis* a specialized model biotroph that helps to understand biotrophy and ultimately tumor formation in plants.

3.2 See1: An effector for tumor expansion in maize leaves

The secreted effector protein See1 is an organ specific virulence factor of *U. maydis* that promotes tumor formation in vegetative maize tissues. The expression profile of *see1* show perfect organ specificity, supporting the specific requirement of this effector in tuning formation of tumors in maize leaves but not in floral tissues. The effector is mainly seen to be induced during tumor progression when there is division and expansion of the host cells. However, there was an initial induction of expression at 2 dpi which might be because of the initial triggering of the defense reaction in plant due to the sensing of the fungus. On the other hand, the expression of *see1* in tassel was minimal as compared to the seedling and did not show an increase over the serial stages of tumor expansion indicating that it has no role in non-target organ.

The mutants deleted for this effector exhibited a quantitative reduction in virulence, measured as both a reduced size and number of tumors only in the seedling leaves. The observed phenotype was in clear contrast with the previously described mutants for the *U. maydis* effectors Pep1 and Pit2, both of which are blocked before tumors can develop (Doehlemann *et al.*, 2009, 2011). The deletion mutants for these “core effectors” *pep1* and *pit2* cause host cell death responses, which appear macroscopically as necrotic lesions at the sites of infection. Pep1 and Pit2 both target central components of the plant’s immune system. Suppression of the initial host defense by these effectors is essential for the establishment and maintenance of a biotrophic interaction, and therefore these effectors form the primary virulence factors in colonization (Doehlemann *et al.*, 2008a; Takken and Tameling, 2009). The progression of disease and in particular, the tumor induction is carried out by specialized effectors like See1 evolved for targeting of the host depending upon the specific physiological conditions existing in the target organ. Recent literature has also shown that plant defense response also acts cell specifically. For example, independent guard cell signalling elements function in stomatal defense in *Arabidopsis thaliana* (Montillet and Hirt, 2013). So, it is hypothesized that in a specialized pathogen like *U. maydis* more complex phenomenon of cell specificity could also exist. Yet till date the existence of cell type specific effectors is still unknown.

As *see1* is specific to leaf tissues, deletion mutants for this effector does not exhibit any defect in ability of tumor formation in the floral parts demonstrating, no role in this organ. Confocal microscopy of SG200 Δ *see1* mutant infected leaves showed that the mutant successfully penetrated the host and established itself in the initial stages of colonization. However, during the later stages when the fungal hyphae reached the leaf mesophyll cell layer, the mutant displayed defects in passing from cell to cell and entrapment of the fungal hyphae in the mesophyll cells or the adjacent vascular cells was observed. This may point towards the ability or an organ specific effector also being specific to the

mesophyll cell layer which is characteristic to the leaf tissue. However, the cell type specific nature of this effector remains to be elucidated and hence is an open question to understand if the organ specific effectors like *see1* can also act cell specifically in the target organ.

3.3 Deletion of *see1* hampers host DNA synthesis in leaf tissues

Plant biotrophs often establish highly specialized and localized interaction sites where primarily nutrient exchange occurs. The ultimate aim of such interaction is to disturb and activate the high energy metabolic state of the host cell ultimately targeting the DNA synthesis and the host cell proliferation. For acquisition of nutrients, biotrophic fungi have to divert metabolism of host which is done via extracellular and invasive hyphae. As nutrient exchange is a central feature of such biotrophic- plant interaction, transporters are seen to play an important role. Many nutrient transporters are seen to be highly upregulated during the interaction. For example, the phosphate transporter MtPT4 is expressed specifically in arbuscule containing cells (Gomez et al., 2009). In addition, sucrose transporters and some aquaporins are expressed in parasitic nematodes during the formation of galls (Hofmann et al., 2007). *U. maydis* is also shown to express a novel, plant membrane localized saccharose transporter (Srt1) during the biotrophic phase whose deletion affects virulence. Srt1 is an H⁺ symporter specific for sucrose that guarantees efficient carbon supply by transporting disaccharide saccharose without producing apoplastic plant defenses (Wahl et al., 2010). Its functional role as a saccharose transporter was confirmed by demonstrating the functional complementation of the *srt1* mutant of *U. maydis* by *A. thaliana* saccharose transporter AtSuc9. Recent evidences have shown that modulation of the host nuclear ploidy is a common plant biotrophic mechanism for specialized lifestyle utilizing all nutrients of host with minimum harm. Host endoreduplication at the adjacent sites of nutrient exchange has been reported for a diverse set of plant biotrophic interaction. Reduced host endoreduplication results in decreased biotrophic growth and/or development (Chandran et al., 2010; Mounoury et al., 2010). Hence, it is not surprising that *U. maydis* tailors the host cell state and cell number in tumor formation.

In monocots, the leaf development proceeds basipetally (from tip to base) in a regular and continuous manner (Evert et al., 1996). The initial divisions in maize leaf are initiated from a population of around 40 meristematic cells (Poething and Szymkowiak, 1995). As these cells divide to produce the leaf blade and sheath, cell divisions are mainly restricted to the leaf base (Sylvester et al., 1990). Hence, during maize leaf development, most cell divisions occur at the base of the leaf blade and the other cells are already differentiated (Li et al., 2010). This study by Li and co-workers, 2010 via transcriptome analysis showed

that the basal region of maize leaf is enriched in cellular functions such as DNA synthesis, cell wall synthesis and hormone signaling. Tumors formed in *U. maydis* infections are due to events that occurred after fungal colonization in the subepidermal leaf cells at around 4 dpi in the central region of the leaf blade which is a transition zone from sink to source tissue. Transcripts associated with the photosynthetic machinery are enriched in this zone (Li et al., 2010). The DNA synthesis activity seen in this region is solely due to the pathogen trigger to induce tumor. In the case of non-infected plants, no such activity was seen in the corresponding leaf area supporting the prior descriptions of the maize leaf development (Li et al., 2010). This stage of infection at 4 dpi coincides with the normal appearance of EdU labeling indicative of DNA synthesis activation trigger in leaves infected with wildtype fungus. Labeling of *U. maydis* colonized seedling tissue showed several division events at 4-5 dpi, indicating that open-ended active induction of cell division in the host occurs after initial fungal establishment and is followed by sustained proliferation of maize cells. However, in the SG200 Δ *see1* mutant no such DNA synthesis activity was seen in the leaves demonstrating a lack of the host cell trigger for division. This indicates that in maize leaves in zones with post-mitotic differentiated cells, *U. maydis* requires *See1* to re-activate host cell DNA synthesis, which is a pre-requisite for tumor formation. This phenomenon is seen to be unique for the vegetative tissues.

In the floral tissues, the situation is seen to be entirely contradictory to that of leaves as *U. maydis* only re-programs cell fate but does not act as an oncogenic agent (Gao et al., 2013). As reported previously by (Gao et al., 2013) during the initial 2 days of anther colonization *U. maydis* is shown to be present on the epidermis. At later time points subsequent establishment of the fungus alters cell fate specification events, ongoing cell division patterns and cell expansion depending upon the developmental stage and type of the invaded cell. The fungus mainly induces ectopic periclinal divisions in the somatic cell types in the anther that add an extra cell layer resulting in disrupted anther lobe architecture. Frequent anticlinal and periclinal divisions are also observed in the middle layers of infected anther which otherwise undergo only a few anticlinal divisions after their birth. Hence, in the floral tissues *U. maydis* acts only as a passive agent and does not require *de-novo* activation of plant cell proliferation, because in this highly proliferating tissue the tumors are a result of re-directing cell division and cell expansion parameters from normal development into a tumor pathway (Gao et al., 2013). Hence in the detection of the EdU labeled cells we did not observe and significant difference in either *see1* deletion or *see1* over-expression strain as compared to the wildtype SG200. In case of non-infected anthers equal number of cells showed EdU labeling indicating the presence of native ongoing synthesis during development.

As the initial experiments indicated need of See1 for triggering the tumor, the further interest was to check if the overexpression of See1 could result in enlarged tumors in comparison to the wildtype. Constitutive over-expression of See1 did not show any hypervirulence phenotype in the leaf tissues, indicating that the overexpression of this effector beyond the native expression level had no effect as several other factors might be essential to co-ordinate the tumor growth. However, over-expression of See1 led to tumor formation in the vegetative parts of the tassel base, which in wildtype infections were not tumorous under the tested conditions. This suggests that See1 is specifically acting in vegetative tissues in alien parts. The phenomenon might be of significance to the fungus in nature, where floral tumors are more frequent in occurrence. See1 and other leaf-specific effectors might be of importance for host adaptation and evolution of *U. maydis*, as they promote the formation of tumors in vegetative parts which is an important factor in colonizing perennial grasses or exploiting seedlings. Seedling and immature plant infections allows completion of the fungal life cycle in a short duration of 2 weeks multiple times during a vegetation period, because this infections style is independent from development of plant inflorescences. All these experiments illustrate that effectors like See1 are particularly used for triggering symptoms in vegetative parts independent to the floral tissue symptom development, which is a characteristic feature of several smut fungi.

3.4 See1 is translocated to host cell cytoplasm and nucleus

An important aspect in the functional characterization of an effector is to follow its localization inside the host during infection after it is secreted. Monitoring effector trafficking from pathogen to the host cell is technically challenging as many filamentous fungal pathogens are not suitable for genetic manipulations. There are several methods employed to describe the localization of the secreted effectors. Many of the effector translocation assays to date are based on the proxy experiments conducted independently of the pathogen in a transient assay. Although translocation motifs such as the RxLxE/Q/D motif in *Plasmodium falciparum* or RXLR-dEER motif in oomycete plant pathogens (Dou et al., 2008; Bhattacharjee et al., 2012) have been suggested, fungal effectors in general do not have highly conserved uptake amino acid motifs described till date (Ellis et al., 2007; Kamoun, 2007). *In situ* translocation assay systems have been established by Transmission electron microscopy in combination with immunogold labeling and nuclear targeting assays using live cell imaging of fluorescent reporter proteins (with fused NLS signals) Kemen et al., 2005; Djamei et al., 2011 and Khang et al., 2010.

Transient expression of See1 following both methods of *A. tumifaciens* mediated transformation in *N. benthamiana* and ballistic bombardment of fluorescent tagged effector

in maize showed the *see1* effector to be localized in the cytoplasm and nucleus of maize cells. Interestingly, the effector protein was also seen to be transferred to cells neighboring to a transformed cell in both the approaches. The specific translocation of See1-mCherry between neighboring maize cells is consistent with the previous reports from *U. maydis* and *M. oryzae* showing characteristic for translocation. The *U. maydis* effectors Cmu1 and Tin2, are both translocated from biotrophic hyphae into the host cell and shows subsequent movement in between neighboring cells (Djamei et al., 2011; Tanaka et al., 2014). It can be speculated that subsequent cell-to-cell movement may reflect a general feature of effectors taken up by plant cells or their chemical property. These proteins could act to stimulate the surrounding cells not yet in contact with fungal hyphae to promote fungal proliferation. For See1, the independent approach of immunolabeling clearly confirmed that the effector is translocated to the plant cell cytoplasm and nucleus. However, movement of See1 to the neighboring cells was not observed in the TEM approach. This discrepancy might result from different expression levels in the two approaches. While in the immunolabeling See1 was expressed by fungal hyphae from its native promoter, plant derived expression in the transient assays was driven by the 35S promoter. Nevertheless, based on the present data we cannot exclude that the cell-to-cell movement observed in the transient assay is an experimental artifact of the exogenous expression of the effector, rather than a feature of normal infections. On the other hand, the phenomenon of cell to cell movement for translocated effectors has also been established for *M. oryzae* effectors in rice cells (Khang et al., 2010). It is clearly seen that the translocated effectors spread to three to four cells away from the invaded cell which is mainly to prepare the host cells before pathogen entry. This movement between cells was proposed to occur via the plasmodesmata, which is also opted by the infectious hyphae for cell-to-cell movement in case of *M. oryzae* (Kankanala et al., 2007; Djamei et al., 2011). Proteins in the plant cytoplasm have been seen to move freely through the cytoplasmic sleeve in plasmodesmata through targeted or non-targeted mechanisms (Oparka et al., 1997; Zambryski et al., 2004). In *M. oryzae* pathosystem, there is known to be a size exclusion limit on proteins that move through plasmodesmata (Khang et al., 2010). As indicated in this study for rice blast, the effector fusion proteins larger than 45 kDa are translocated into rice cells, but fail to show a cell to cell movement. *M. oryzae* is so far the only filamentous pathogen that has been shown to deliver fluorescent effector fusion proteins into host cells using fluorescence microscopy of the natural infected tissues. Translocation attempts of the same assay has not been successful in *P. infestans*, *U. maydis* or *C. higginsianum* (Whisson et al., 2007; Djamei et al., 2011; Kleemann et al., 2012). This suggests that these pathogens might translocate lower effector quantities too dilute for detection of a fluorescence signal. It is also possible

that *M. oryzae* uses a different translocation system that translocates large fusion proteins.

In the recent years, it is also shown that the translocated effectors may follow a different secretory pathway than the endoplasmic reticulum (ER)/Golgi. A recent study in *M. oryzae* has identified two distinct effector secretion pathways (Giraldo et al., 2013). Apoplastic effectors are seen to follow the conventional ER/Golgi secretory pathway and the host translocated or cytoplasmic effectors are secreted via a different pathway involving the exocyst complex. However, the extent to which effectors from other pathogens may follow the phenomenon of distinct secretory routes remains still unknown. Functionally, translocated effectors are seen to target the general immune system of the plant by responding to several cytoplasmic proteins including the 'R' genes. Host ubiquitylation system is frequently seen to be an effector target of translocated effectors. The *P. infestans* Avr effector Avr3a was shown to bind and stabilize a potato U box E3 ubiquitin ligase CMPG1 and block cell death (Bos et al., 2010). The *M. oryzae* effector AvrPiz-t binds to the rice RING E3 ubiquitinating ligase and destabilizes it to suppress the PAMP immunity (Park et al., 2012). Translocated effectors of *U. maydis* are seen to target several defense related pathways. All these reports indicate that translocated effectors have more complex functions. Hence, it was exciting to see the host targets of effector See1 being organ specific confined to the vegetative parts.

3.5 Interaction of see1 with the nucleo-cytoplasmic protein Zm-SGT1

See1 was found to interact with *Z. mays* SGT1 in a yeast two hybrid screen. SGT1 is present in both the cytoplasm and the nucleus of plant cells and localization in the transient assays and TEM approach is consistent with the host interactor. The interaction of See1 and Zm-SGT1 in the yeast two hybrid assays was confirmed independently by Lena Schilling who performed *in planta* co-immunoprecipitation. In addition, the BiFC data showed that this interaction takes place in both the cytoplasm and nuclei of maize cells. SGT1 functions as co-chaperone and forms a part of a chaperone complex together with RAR1 and HSP90 (Shirasu, 2009) functioning as immune sensor in modulating NLR receptor proteins. Upstream of the SGT1/RAR1/HSP90 complex is the EDS1 (enhanced disease susceptibility 1) protein. In *A. thaliana*, EDS1 is required for the function of several R proteins (Aarts et al., 1998), basal resistance to virulent isolates of several pathogens (Parker et al., 1996; Xiao et al., 2005) and non-host resistance to two biotrophic pathogens of *Brassica oleracea* (Parker et al., 1996). SGT1 functions as a key component of the signal transduction pathway that leads to disease resistance in plants (Austin et al., 2002; Azevedo et al., 2002). This cellular regulation is ongoing by the post-translational modification (PTM) of the SGT1 protein by phosphorylation. This mechanism is shown to

be widely functioning in activation of SGT1 in the signaling cascade and controlling dynamic cellular mechanisms controlling its nucleo-cytoplasmic partitioning based on the phosphorylated or non-phosphorylated state (Hoser et al., 2013). In yeast, SGT1 phosphorylation negatively regulates its dimerization, thereby facilitating its localization to the nucleus (Bansal et al., 2009). Additionally, the subsidiary chaperons like HSP70 have been demonstrated to promote nuclear localization of SGT1 via its close interaction (Nöel et al., 2007). The mass spectrometry analysis showed the interference of *see1* with the phosphorylation status of Zm-SGT1. The interaction of Zm-SGT1 with See1 results in inhibition of its MAPK-triggered phosphorylation at T₁₅₀. This phosphorylation site is conserved only in some monocots. The consequences of this detected inhibition of phosphorylation site might be to block the activation of downstream signaling.

In the last years, it has been shown that ubiquitin/26S proteasome system (UPS) plays a central role in the plant pathogen interaction via protein degradation (Dielen et al., 2010). All cellular processes from division to cell death are controlled by the UPS system (Dreher and Callis, 2010). A regulatory change in the UPS system has a broad effect on cell re-programming during plant defense. As a regulatory system it is involved in mechanisms such as cell cycle control, programmed cell death and also plant development (Jurado et al., 2008; Stone and Callis, 2007; Brukhin et al., 2005). SCF (Skp1, CDC53p/Cul1 F box) ubiquitin ligases which are active components of the UPS system are shown to be essential components of the R gene mediated resistance. SGT1 also corresponds to a E3 ubiquitin ligase mediating plant defense signaling. The literature provides a large body of data on mechanism of *A. thaliana* SGT1. AtSGT1 protein has a regulatory role in early R-gene mediated plant defenses (Austin et al., 2002). Among the three domains of SGT1 the CS domain resembles the crystalline domain of the co-chaperone HSP20 (Dubacq et al., 2002; Garcia-Ranea et al., 2002). The other components of the immune regulatory co-chaperone complex RAR1 and HSP90 have been shown to interact with the CS domain of SGT1 (Azevedo et al., 2002; Takahashi et al., 2003). RAR1 has provided a possible link between ubiquitination and R gene mediated resistance against a range of pathogens in monocot and dicot species (Muskett et al., 2002; Tornero et al., 2002). From all the available literature concerning plant SGT1, this protein is seen to be required for responses that are mediated by a diverse range of R gene structural types, which induce resistance against a variety of pathogens (Azevedo et al., 2002; Liu et al., 2002; Tor et al., 2002). The conserved function of SGT1 in regulating SCF activity in plants is supported by complementation of yeast *sgt1* mutations by the two highly related *A. thaliana* SGT1 genes (*SGT1a* and *SGT1b*), and by the observation that SGT1 co-immunoprecipitates with core SCF subunits in *Hordeum vulgare* (barley) and in *N. benthamiana* extracts (Azevedo et al., 2002; Liu et al., 2002). Strong evidence to confirm this function has come

from the recent discovery that in *A. thaliana* the SGT1b isoform was found to be required for SCF-mediated auxin response in seedling roots (Gray et al., 2003). SGT1 is widely seen to be active in vegetative leaf tissues (Noël et al., 2007), however, its expression and regulation in plant floral organs has not been investigated till date to the best of our knowledge.

In maize—*U. maydis* pathosystem where cell cycle regulation and suppression of the defense responses are of equal importance, SGT1 might seem to have a crucial role. The complementation of the *sgt1* cell cycle mutants of yeasts by all plant SGT1 indicates the conservation of the cell cycle function and possibility of utilization of this protein in unusual infection pattern. The hijacking of SGT1 in *U. maydis* interaction might also have a dual role in disturbing the host immunity and in triggering of the plant DNA synthesis. The role of SGT1 in promoting fungal disease has been shown in the recent years. *B. cinerea* has been shown to exploit the SGT1-mediated HR cell death pathway to initiate its necrotrophic life style (El Oirdi and Bouarab, 2007). A study by Cuzick et al., (2009) reported *F. culmorum* utilizing *sgt1b* in disease development in buds and flowers of *A. thaliana*. Due to all this literature, it is extremely interesting to elucidate the exact role of SGT1 and significance of its interaction with *see1* to form a tumor.

3.6 SGT1, a conserved hub acting as effector target

In the last years, the host SGT1/RAR1/HSP90 complex has been shown to be a target of several effector proteins from bacteria. *Pseudomonas syringae* effector AvrB was shown to interact weakly with *A. thaliana* SGT1b (Cui et al., 2010). Another *P. syringae* effector, AvrPtoB, showed a genetic interaction with SGT1 and RAR1, requiring these co-chaperones to suppress plant immunity (Hann and Rathjen, 2007). Additionally, the *P. syringae* effector HopI1 was shown to interact with HSP70 (Jelenska et al., 2010), which is an active component initiating signaling by interaction with the SGT1/RAR1 complex. Recently, effector proteins from *Salmonella enterica* and *Xanthomonas campestris* have been shown also to interact with SGT1 (Bhavsar et al., 2013; Kim et al., 2014). Consistent with the previously mentioned importance of CS domain of SGT1, these effectors were shown to bind to SGT1 at the CS domain signifying this domain to be important for SGT1 regulation during immune responses. It was shown that *Salmonella* type III effector SspH2 enhances the SGT1 dependent innate immune responses in both animals and plants. Interaction of SspH2 with SGT1 is mediated by CS and SGS domain where the CS domain mediates the interaction with Hsp90 and SGS domain mediates substrate specificity by binding to LRR receptors (Bhavsar et al., 2013). *X. campestris* effector AvrBsT was shown to interact with SGT1 and an upstream kinase PIK1 promoting the hypersensitive cell death response in a phosphorylation dependent manner (Kim et al.,

2014). It is known that the SGT1 mediated pathways may vary in different plants and are also specific to a particular pathogen (Wang et al., 2010). SGT1 is known to be used by some fungal pathogens in promoting disease symptoms. Like *X.campestris* the necrotrophic fungus *B. cinerea* uses SGT1 to initiate cell death (Cuzick et al., 2009). As shown previously, *F. culmorum* is known to utilize SGT1b to cause full disease symptoms in buds and flowers of *A. thaliana*. This is the only report that described SGT1 in floral tissues; however this study did not include gene expression of whole flowers because of the complexity of floral tissues. This points towards a tissue specific role of SGT1 protein in *A. thaliana*.

In light of all these findings, SGT1 likely represents a conserved hub targeted by several effectors from bacterial as well as fungal pathogens, utilizing it according to the need of the pathogen lifestyle. This supports the early study of evolutionary different effectors targeting a common host defense protein (Song et al., 2009) and is also consistent with the model of evolutionary different virulence effectors targeting conserved hubs in a plant immune system network (Mukhtar et al., 2011). The role of SGT1 in biotrophic interactions till date is only shown to be involved in resistance. However, *U. maydis* is seen to implement the SGT1 function for symptom development as shown for fungal pathogens with different lifestyles. The precise steps following the interference of See1 with post-translational modification of Zm-SGT1 resulting in re-activation of the maize cell cycle and ultimately in tumor formation remain to be elucidated biochemically. It is hypothesized from the available literature, that effectors from several pathogens that are interacting with SGT1 may induce a conformational change of the chaperone complex in the cytoplasm (Boter et al., 2007; Shirasu, 2009) leading to the disturbance of innate immunity in the host cell. Therefore, it will be of prime interest to work out the detailed molecular mechanism of the See1 Zm-SGT1 interaction.

3.7 Host transcriptional responses to SG200 Δ see1 mutant

Prominent biological processes that are altered in plants infected with SG200 Δ see1 comprise of the cell cycle related genes and the genes involved in DNA modification (i.e. histones). For Eg. DNA histone H3, which is involved in the cell proliferation and nucleosome assembly maintenance are seen to be 700–900-fold induced in wildtype infections (TC298222, TC298173, TC298172, TC298215) and are altered upon deletion of the see1 effector. Histone H3 proteins are seen to be specifically enriched among the GO terms associated with DNA damage response and cell cycle regulation. Histones are among the important DNA binding proteins that control the level of DNA transcription and proper cell cycle progression. In several eukaryotes it has been shown that the level of H3 phosphorylation, which is minimal in interphase, increases during mitosis for proper

execution of cell division (Gurtley et al., 1975). This phosphorylation of H3 histone is shown to be involved in two structurally opposed processes: transcriptional activation (Mahadevan et al., 1991; Clayton et al., 2000) and chromosome compaction during cell division (van Hooser et al., 1998; Kansas and Cande, 2000). Phosphorylation of H3 histone is initiated in late G2 and then spreads throughout upon chromatin condensation upto the end of mitosis (Houben et al., 1999). This phosphorylation event is mainly to identify the different domains of the chromosomes and to mark their progress through the cell cycle (Pigent and Dimitrov, 2003). Since the SG200 Δ see1 mutant is defective in inducing DNA synthesis, there is a significant alteration in the histones thereby not promoting cell division which results only in small tumors.

Another important protein, SKP1 (S phase kinase associated protein 1) which is a small protein of approximately 160 amino acids also seen to have an interesting differential regulation in the wild-type *U. maydis* infection. As a core protein component of the SCF type E3 ubiquitin ligase that mediate protein degradation by the 26S proteome skp1 plays a key role in cell cycle regulation and the signal transduction in eukaryotes. The SKP1 from maize (TC293032) is also seen to be 426 times upregulated in the wild-type infection as compared to the Δ see1 mutant. Protein degradation is a particularly effective method for promoting unidirectional progression in the cell cycle because of its irreversibility. Currently, three major cell cycle transitions, entry into S phase, separation of the sister chromatids and exit from mitosis are known to require the degradation of specific proteins. Skp1 from yeast and humans has been shown to connect the cell cycle regulators to the ubiquitin proteolysis machinery through a novel motif, the F box (Bai et al., 1996). Skp1 is clearly important for several cell cycle events. Each skp1 mutant phenotype of cell cycle arrest in G1 and G2, and chromosome instability, suggests a connection between regulation of proteolysis in different stages of the cell cycle (Bai et al., 1996). Together, this data suggests that SG200 Δ see1 fails to induce tumor growth in leaves at the level of host cell DNA synthesis and cell proliferation.

3.8 Significance of See1 in *U. maydis* induced tumor

The formation of tumorous tissues by *U. maydis* is still not well understood. It is unclear why this unique smut causes these unusual symptoms among the *Ustilaginales*. Two hypotheses can be speculated behind the tumor induction in *U. maydis* infection. Firstly, colonization of the vegetative tissues forming this unique mode of infection makes the infection pattern independent of the development of floral tissues which are normally colonized by this class of pathogens. To achieve successful flourishment in vegetative parts, the fungus creates a tassel like environment for its proliferation. So, the seedling specific effectors might have evolved to accommodate the pathogen in the vegetative

tissues making it enable to colonize all aerial parts. Secondly, *U. maydis* has developed multiple layers of defense suppression adapting it to colonize physiologically varied tissues. In the course of this multiple defense suppression, the pathogen of course triggers cell cycle release thereby causing a tumor symptom. The effector *see1* which interacts with SGT1 might suggest the interplay between the defense regulation and cell cycle control. Some studies on this aspect have already been shown in *A. thaliana* (Bai et al., 1996)

Secondly, phytohormones are known to regulate the plant growth from cell division to organ development. Recently more evidence has emerged for a role for JA mediated responses in cell cycle progression. Jasmonates are known to control the leaf growth by repressing the cell division and progression of endoreduplication in *A. thaliana* (Noir et al., 2013). It is known that up-regulation of methyl jasmonates (MeJA) delays the switch from the mitotic cell cycle to the endoreduplication cycle, which accompanies cell expansion and inhibits mitosis arresting the cells at 'G1' before the 'S' phase. Considering this literature available a preliminary experiment of the metabolic responses of wildtype strain SG200 and SG200 Δ *see1* infected seedlings were measured (in collaboration with Eric Schmelz, USDA, Florida, USA) which showed a strong induction of the methyl jasmonates in the mutant infected tissues at an early timepoint of 2 dpi (data not shown). This suggests that the jasmonate induction in the early stages of SG200 Δ *see1* infection might be responsible for delaying or preventing the cells to pass the checkpoint of DNA synthesis in the *see1* deletion mutant. Since the *see1* mutant did not show any 'S' phase labeled cells, expression of the cell cycle marker corresponding to late G1 was examined. Cell division control 6 (CDC6) is essential factor for DNA replication acting in recruiting DNA helicases that open the replication fork (De Pamphilis, 2003). Overexpression of CDC6 does not affect the overall development but stimulates endoreduplication. Upon deletion of the *see1* effector the *U. maydis* Δ *see1* is seen to be regulating the CDC6 by its over-expression aiming to complete the DNA synthesis. However, other factors of hormonal balancing also seem to be disturbed leading *U. maydis see1* mutant on a wrong track. MeJA that are seen to be upregulated in the mutant might be involved in the pause of the mitotic cycle thereby arresting the cells in G1 phase prior to the S transition.

Plant organ development is the result of strict spatial and temporal genetic control and the co-ordination of cell division, growth and differentiation (Tsukaya, 2005; Gonzalez et al., 2012). Cell division, endoreduplication and expansion are alternative strategies contributing to plant organ growth and size (Massonnet et al., 2010). However the role of cell cycle regulation and cell division in plant growth and organ development is controversial. *U. maydis* seems to be activating cell re-differentiation leading to the tumorous growth for rapid completion of the sexual phase. *U. maydis* attempts to actively

modulate plant division for its pattern of infection with seedling specific effectors like *see1*. Hence the deletion of *see1* leads to a wrong co-ordination of the DNA synthesis trigger which results only in small tumors. So, the organ specific effector See1 guides the host cells to form tumors in maize leaves.

3.9 Perspectives and Further Outlook

Considering the available literature from *A. thaliana* it would be of prime interest to dissect the downstream signaling network, i.e. to identify and characterize proteins that interact and/or are affected by Zm-SGT1. The recent key advances in structural biology have made a great contribution in understanding plant- pathogen interactions. Structural biology provides an elegant way to resolve the protein functions that were not apparent from sequences alone. Eg. NLP's and E3 ligase domain of AvrPtoB. Understanding of the plant immunity has also been quite successful. Eg. The interaction of Pto with AvrPto and AvrPtoB₁₂₁₋₂₀₅, and the oligomerization of CC and TIR domains of NB-LRRs. The availability of protein structures has provided a direct insight into molecular function. It would be interesting to get the crystal structure of effector See1 to predict its molecular function. Furthermore, knowledge on the three dimensional structure of the See1-Zm-SGT1 complex may identify See1 residues being required to interfere with SGT1. This could aid in generating mutant proteins with specific alterations regarding the interference with Zm-SGT1. This would require, the heterologous production of these proteins, which has not yet succeeded in *E. coli* for See1 (see Annexure) but Zm-SGT1 has been successfully produced (shown in Annexure). The use of a eukaryotic expression system such as *Pichia pastoris* might be of interest which also led to success in the case of *C. fulvum* effector ECP6 (de Jonge et al., 2010) and for another effector *um01829* of *U. maydis* (personal communication with Lena Schilling).

The next objective of the work would be to screen the virulence motifs in See1 and the interacting domain of SGT1. Preliminary experiments on these lines have confirmed by the yeast drop assay that the Chord domain (CS) of SGT1 is important in the interaction. However, further confirmation by immunological tests are lacking which could be the *in planta* co-immunoprecipitation in *N. benthamiana*. It would be of interest to map the interacting domains of the See1-SGT1 interaction to understand the molecular mechanism in detail. Furthermore, the molecular mechanism and the co-relation of phosphorylation and virulence of See1 is to be investigated and is an essential part of future work. Key experiments that contribute to the elucidation of this question include the testing of the inactive *see1* versions or orthologue of *see1* from *U. hordei* that does not complement the knockout phenotype, in the phosphorylation assay. These are expected not to inhibit the phosphorylation of Zm-SGT1 being inactive in function. At the same time

this would allow to directly test the consequences of Zm-SGT1 phosphorylation and may also show whether See1 holds additional functions in the host cells that are not linked to the interaction with Zm-SGT1. Also, the investigation of the upstream signaling components involved in the interaction and activation of Zm-SGT1 should be identified. Of particular interest, is the upstream MAPK which is responsible for activation of the phosphorylation cascade in maize. This can be investigated by the yeast two hybrid approach by using SGT1 as a bait protein which would allow the identification of the individual components of the SGT1 complex in maize as probable interactors. Some initial attempts to trace the kinase involved in phosphorylation activation were made by using ZmCDPK10 and ZmCDPK11 which did not result in the activation of the phosphorylation cascade. Hence Y2H would be a choice of system to trace the actual kinase involved. Identification and expression of the individual interactors of SGT1 complex in *E. coli* could allow the *in vitro* phosphorylation assay to see the inhibitory role of *see1 in vitro*. Investigating the role of SGT1 for *U. maydis* induced tumor formation is important. This could be done by virus induced gene silencing (VIGS) of SGT1 in maize and assessing the symptom formation. VIGS in maize in response to *U. maydis* has already been established in the lab before by van der Linde et al., 2011. Alternative to this would be to generate the transgenic maize lines with phosphonull and phosphomimic SGT1 and to test the phenotype of *U. maydis*. Previous attempts in this direction have shown that transgenic lines for overexpression of CC9 in maize have been successfully produced (van der Linde et al., 2012).

Additionally, from the fungal side it would be interesting to see what controls the regulation of expression of the organ specific effectors? The next important step lies in identifying the precise sequence motifs that regulate the expression of organ specific effectors. The regulation of organ specific effectors might be epigenetically regulated upon the cell type specific conditions via a transcription factor. This indication is due to the *S. reilianum see1* orthologue that complements the *see1* knockout is only under the *U. maydis* promoter. Moreover, expression profiling of this orthologue from *S. reilianum* in leaves is completely different than that of *U. maydis see1*. This suggests that *U. maydis* is able to sense the cell types to secrete these organ specific effectors. What signal tells *U. maydis* about the colonized organ and the secretion of particular organ specific effectors is an interesting point. In this regard, the promoter analysis of the See1 effector could be done to identify transcription factor involved if any. Hence, it would be of prime interest to get the motifs residing in the promoter region that are responsible for the regulation of expression of See1 to vegetative organs and yeast one hybrid analysis to investigate its interacting partners. Further, it would be of outstanding interest to analyze if the observed DNA synthesis and cell cycle inactivation defect is a direct consequence of See1 effector

deletion. Some initial experiments on this aspect have been mentioned in the current study involving the microarray analysis and the expression of some of the cell cycle marker genes involved at specific checkpoints. This points out towards a major role of See1 in tumor elicitation. Confirmation of this aspect can be done by transformation of See1 and SGT1 together in the cell cycle defective yeast strains to check for their impact on activation of cell cycle and measured by Fluorescence activated cell sorting (FACS). Additionally, to trace the function of *see1* a different approach could be the generation of the transgenic lines of *A. thaliana* that are expressing See1 under the DEX inducible promoter. Since *Arabidopsis thaliana* SGT1a shows an interaction with See1 (data not shown) it would be interesting to see the EdU Labelling in plants constitutively expressing *see1* to that of the empty vector control. This could also shed light into the probable role of See1 and its mechanistic basis.

4. Materials and Methods

4.1 Materials and Methods

4.1.1 Chemicals

All chemicals used in the study were obtained from Difco (Augsburg), GE Healthcare (München), Invitrogen (Darmstadt), Merck (Darmstadt), Roche (Mannheim), Roth (Karlsruhe), IBA (Goettingen), Fluka (Buchs) and Sigma-Aldrich (Deisenhofen). The specific chemicals for electron microscopy were procured from London Resin Company, Berkshire, UK.

4.1.2 Buffers and Solutions

Standard buffers and solutions are prepared according to Ausubel *et al.* (2002) and Sambrook *et al.* (1989). Special buffers and solutions are listed with the corresponding methods. All buffers, media and solutions were autoclaved for 5 min at 121 °C. Heat sensitive solutions were filter sterilized (Pore size 0.2 µm; Merck, Darmstadt).

4.1.3 Enzymes and Antibodies

All the restriction enzymes were purchased from New England Biolabs (NEB, Frankfurt / Main). DNA polymerases particularly the Phusion® Hot Start High-Fidelity DNA polymerase was procured from Thermo Scientific (Bonn) or the RedMix containing the Taq polymerase was obtained from Bionline, Luckenwalde. Ligation of DNA molecules was performed with T4 DNA ligase (Thermo Scientific, Bonn). For the enzymatic degradation of RNA RNase A (Serva, Heidelberg, Germany) was used. Enzymatic degradation of fungal cell walls was carried out by using Novozyme 234 (Novo Nordisk, Copenhagen, Denmark). Antibodies were purchased from Sigma-Aldrich (Deisenhofen) and Cell Signaling Technology (Danver, USA). A detailed list of antibodies used is given in section 4.6.2 (Table 7).

4.1.4 Commercial kits

For purification of PCR products, plasmids as well as for the elution of DNA fragments from agarose gels, the Wizard® SV Gel and PCR Clean-Up System from Promega (Mannheim, Germany) was used. The isolation of plasmid DNA from bacterial cultures was carried out with QIAprep® Mini Plasmid Kit from Qiagen (Hilden, Germany). The TOPO® TA Cloning Kit was procured from Invitrogen (Karlsruhe, Germany) and was used for the direct cloning of PCR products. The insertion of point mutations in plasmids was

performed using the QuikChange Multi Site-Directed Mutagenesis Kit (Stratagene, LaJolla / USA). For digoxigenin labeling of PCR products, the DIG High Prime kit (Roche, Mannheim, Germany) was used. ECL Plus Western blot detection reagent (GE Healthcare, Munich) was used for chemiluminescence detection. Special kits used for specific experiment, are listed under the respective method.

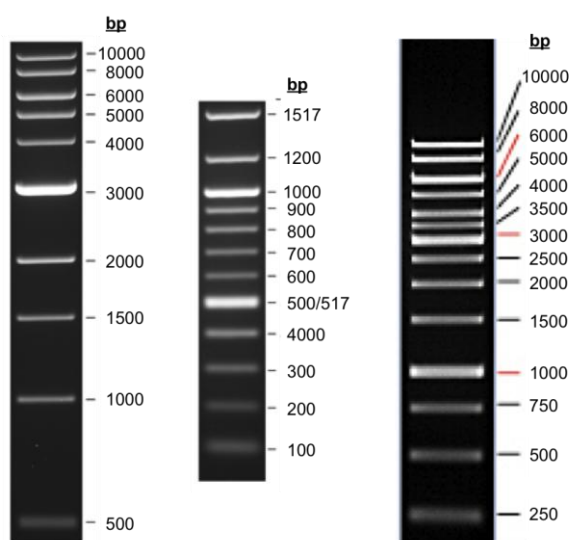


Fig. 39: DNA- markers. In this work the following DNA markers were used. '1 kb ladder' (left; NEB), '100 bp ladder' (middle; NEB) and *GeneRuler 1 kb DNA ladder* (right; Fermentas).

As size standards for electrophoretic separation of DNA fragments the marker of 1 kb ladder and 100 bp ladder from NEB (Frankfurt /Main) and *GeneRuler 1 kb DNA ladder* from Fermentas/Thermo Scientific (Bonn) was used throughout for all experiments (Fig. 39). All other ladders used have been described in the individual methods section.

4.2 Media

4.2.1 Media for cell cultivation and growth

For the cultivation of microorganisms, the media listed in Table 3 were used. All media unless otherwise indicated, were autoclaved before use at 121 °C for 5 min.

Tab. 3: Media used for cultivation of micro organisms

Name	Composition	Notes
dYT (-Agar) (Sambrook et al., 1989)	1.6% (w/v) Tryptone 1.0% (w/v) Yeast extract 0.5% (w/v) NaCl 1.5% (w/v) Bacto Agar	in H2Obid.
dYT Glycerol medium	1.6% (w/v) Tryptone 1.0% (w/v) Yeast extract 0.5% (w/v) NaCl 87% glycerol	in H2Obid.
YEPS _{light} (modified from Tsukada et al., 1988)	1% (w/v) Yeast extract 1% (w/v) Peptone 1% (w/v) Saccharose	in H2Obid.
Potato-Dextrose-Agar (PD)	2.4% (w/v) Potato-Dextrose Broth	in H2Obid.

	2% (w/v) Bacto Agar	
PD-Charcoal-Agar	Same as PD, with addition of 1.0% (w/v) activated charcoal	in H2Obid.
Regeneration Agar (Schulz et al., 1990)	1 % (w/v) Agar 1M Sorbitol In YEPS light (described above)	in H2Obid.
NSY-Glycerin	0.8% (w/v) Nutrient Broth 0.1% (w/v) Yeast extract 0.5% (w/v) Saccharose 69.6% (v/v) Glycerol	in H2Obid.
YPDA (-Agar)	2% (w/v) Peptone 1 % (w/v) Yeast extract 0.003% (w/v) Adenine-Hemisulfate 2% (w/v) Bacto Agar	in H2Obid., adjust pH 6.5, Addition of 2% (w/v) filtered Glucose after autoclaving
YPDS-Agar	2% (w/v) Peptone 1 % (w/v) Yeast extract 2% Glucose 1M Sorbitol 2% (w/v) Bacto Agar	in H2Obid.
SD (-Agar)	0.67% (w/v) Yeast nitrogen base Without amino acids 0.06% (w/v) Dropout Solution [(-Ade, -His, -Leu, -Trp) or (-His, -Leu, -Trp, - Ura)] 2% (w/v) Bacto Agar	in H2Obid., adjust pH 5.8 Addition of 2% (w/v) filtered Glucose after autoclaving

4.2.2 Culture conditions for *E.coli* and *A.tumefaciens*

E. coli and *A. tumefaciens* bacteria were grown in dYT liquid medium (Sambrook et al., 1989) at 37 °C (*E. coli*) or 28 °C (*A. tumefaciens*) with shaking at 200 rpm. All different antibiotics used for culturing different strains have been listed in Table 4. Glycerol stocks of the cultures were prepared by adding 25 % (v/v) glycerol and stored at -80 °C.

Tab. 4: Antibiotics used for the cultivation of *E.coli* and *A. tumefaciens*

Antibiotic	End concentration [µg/ml]
Ampicillin (Amp)	100
Kanamycin (Kan)	40
Chloramphenicol (CIm)	44
Rifampicin (Rif)	40
Streptomycin (Strp)	100
Gentamicin (Gent)	50
Tetracyclin (Tet)	25

4.2.3 Cultivation of *U. maydis* and *S. reilianum*

YEPS_{light} liquid medium (modified according to Tsukuda et al., 1988) was a standard culturing medium for the liquid cultures of *U. maydis* and *S. reilianum* used in this work. The cultivation of the cultures was carried out at 28 °C and 200 rpm. Potato dextrose agar, solid medium was used for the cultivation of all *U. maydis* or *S. reilianum* clones which may have been added to the selection medium with 2 µg/ml carboxin (Cbx) as the selection marker. For the production of glycerol stocks a densely grown overnight culture was added to 50 % NSY-glycerol and then stored at – 80 °C.

4.2.4 Cultivation of *Saccharomyces cerevisiae*

For the cultivation of *S. cerevisiae* strains (AH109, wildtype) or the *sgt1* temperature sensitive mutants of yeasts (YKK57 and YKK65) were grown in the YPD medium. For selection of transformed *S. cerevisiae* strains SD medium was used which was supplemented with adenine, histidine, leucine and/or lacking tryptophan/uracil, was used depending upon the selection marker on the plasmid. Stock cultures were prepared by adding glycerol to 25 % (v/v) and stored at – 80 °C.

4.2.5 Determination of cell density of bacterial and fungal cultures

The cell density of liquid cultures was determined in a Novaspec II photometer (Pharmacia Biotech / GE Life Sciences, Munich, Germany) at 600 nm (OD₆₀₀ nm). To ensure a linear dependence, cultures were diluted by appropriate dilutions to values below 0.8. As a reference value, the OD₆₀₀ nm of the corresponding culture medium was used. In *U. maydis* and *S. cerevisiae* an OD₆₀₀ nm of one corresponds to a cell count of 1.5 x 10⁷ cells. In *E. coli* and *A. tumefaciens*, this value corresponds to about 1 x 10⁹ bacterial cells.

4.3 Strains, Oligonucleotides and Vectors

4.3.1 *E. coli* Strains

The following enlisted *E.coli* strains were used for all the cloning work and generating various constructs throughout the study. Special strains if used in the study have been mentioned in the respective section.

Tab. 5: In this work the following *E. coli* Strains were used.

Strain [Genotype]	Implication	Reference
K-12 Top10 [F- <i>mcrA</i> Δ (<i>mrr-hsd</i> RMS- <i>mcrBC</i>) Φ 80 <i>lacZ</i> Δ M15 Δ <i>lacO</i> 74 <i>recA1</i> <i>ara</i> Δ 139 Δ (<i>ara-leu</i>)7697 <i>galU</i> <i>galK</i> <i>rpsL</i> (StrR) <i>endA1</i> <i>nupG</i>]	Plasmid amplification/ Cloning	Grant <i>et al.</i> , (1990)/ Invitrogen (Karlsruhe)
K-12 DH5 α [F- Φ 80d <i>lacZ</i> Δ M15 Δ (<i>lacZYA-argF</i>) U169 <i>deoR</i> <i>recA1</i> <i>endA1</i> <i>hsdR</i> 17 (rK ⁻ , mK ⁺) <i>phoA</i> <i>supE</i> 44 λ - <i>thi</i> 1 <i>gyr</i> A96 <i>relA</i> 1]	Plasmid amplification/ Cloning	Hanahan (1983)/ Gibco/BRL (Eggenstein)
BL21(DE3)pLys [F ⁻ <i>ompT</i> <i>gal</i> <i>dcm</i> <i>lon</i> <i>hsdSB</i> (rB -mB -) A(DE3) pLysS(cm ^R)]	Heterologous Expression of protein	Novagen/Merck (Darmstadt)

4.3.2 *A. tumefaciens* Strains

For transient expression of proteins in *N. benthamiana*, *A. tumefaciens* mediated transformation technique was used with strain GV3101 (Koncz and Schell, 1986), which has a chromosomal Rifampicin (Rif) resistance. In addition, this strain contains the Ti plasmid pMP90 which the necessary for DNA transfer *vir* genes, but contains an otherwise non-functional T-DNA region and mediates Gentamycin (Gent) resistance. In addition, the strain used comprises a localized Ti helper plasmid Tetracyclin (Tet) resistance. By this, the replication of plasmids in *A. tumefaciens* is mediated.

4.3.3 *S. cerevisiae* strains

As a starting strain for all yeast two-hybrid experiment listed in this work the yeast strain AH109 (Clontech, Saint-Germain-en-Laye, France) was used. This strain has auxotrophy for tryptophan, alanine, histidine and leucine. For the SGT1 complementation assays, the temperature sensitive yeast strains *sgt1-3* and *sgt1-5* were used, which harbours auxotrophy for histidine, leucine, tryptophan and uracil.

4.3.4 *U. maydis* strains

All the *U. maydis* strains produced in the course of this work and their descriptions are listed in Table 12 of the Annexure to this work. For the integration of genes into the *ip* - Locus (*sdh2*) plasmids were used, which carry a carboxin-resistant allele *ip* (*ipR*) (Broomfield and Hargreaves, 1992). These plasmids were first linerized with SspI or AgeI and inserted via homologous recombination with the endogenous, carboxin-sensitive, *ip* allele (*ipS*) into the genome of *U. maydis* (see section 4.4.4). Resulting strains were verified (see section 4.5.3.2) by Southern blot analysis. The transformed strains carrying an insertion in the *ip* locus were determined and constructs, unless otherwise stated, in a

single copy insertion were used for further experimentation. The plasmids used for the generation of the *E.coli* strains are described in Section 4.3.7.

4.3.5 *S. reilianum* strains

The *S. reilianum* used in this study were the two mating types SRZ1 and SRZ2 of the maize *S. reilianum* isolates (Schirawski et al., 2010). These strains were used as a control for some DNA synthesis experiment carried out in this work.

Tab. 6: *S. reilianum* –Strains used in this study

Name	Genotype	Reference
SRZ1	<i>a1 b1</i>	Schirawski et al., (2010)
SRZ2	<i>a2 b2</i>	Schirawski et al., (2010)

4.3.6 Oligonucleotides

All the oligonucleotides that are used in this work were purchased from MWG (Martinsried, Germany) or Sigma-Aldrich (Deisenhofen) and are listed in Table 13 of the Annexure to this work.

4.3.7 Vectors and Plasmids

4.3.7.1 Plasmids for generation of stable *U. maydis* mutants

The starting plasmids used in this work as well as the other plasmids that are generated over the work are described for the preparation of stable *U. maydis* mutants. The fusion of gene for the purpose of *see1* complementation in *U. maydis* always occurred with the sequence encoding the signal peptide region of the protein (AA 1-21)

p123 (Aichinger et al., 2003)

This plasmid contains the GFP gene under the control of the *otef* promoter and the *nos* terminator. This is the starting plasmid for the cloning of complementation construct. For all processes, based on this plasmid constructs generated are linearized for transformation of *U. maydis* by restriction digestion with *SspI* or *AgeI* in the *cbx* locus and can then be inserted by homologous recombination into the *ip* locus. It harbors Amp resistance and complements Cbx resistance.

p123-mCherry (obtained from G. Doehlemann)

This plasmid contains the mCherry gene under the control of the constitutive *otef* promoter and of the *nos* terminator. For the transformation of *U. maydis*, the plasmid can be inserted by a digestion (eg. with *SspI*) in the *cbx* gene into the *ip* locus.

PCRII-TOPO (Invitrogen, Karlsruhe)

Vector for cloning PCR products by means of topoisomerase activity. The DNA segments cloned can be confirmed and checked with EcoRI. The plasmid can be used for blue-white selection. The sequencing of the inserts is possible by using primers M13 uni (-43) and M13 rev (-49).

pBS hhn (Kämper et al., 2004)

This plasmid contains an 1884 bp hygromycin resistance cassette flanked by the restriction site of SfiI interfaces. The hph gene is controlled by the hsp70 promoter and the nos terminator. The resistance cassette derived from pBS-hhn was used for Deletion constructs to make the knockout strain.

pCRII-TOPO_ ΔUm02239 (Ajami-Rashidi, 2011)

Plasmid containing the deletion of Um02239 consisting of the 5' and 3' flank, which included the Hygromycin resistance cassette. The resistance cassette derived from the vector pBS-hhn. The introduction of the construct was performed by topoisomerase activity.

p123-Psee1-UmSee1 (Schilling et al., 2014)

Contains *um02239* (*see1*) under control of the native promoter and the nos terminator. For the transformation of *U. maydis*, the plasmid can be inserted by digestion with the enzyme (SspI) in the *cbx* gene into the *ip* locus. The PCR fragment was inserted into the vector by SbfI and NotI sites.

p123-Psee1-UmSee1-mCherry

This plasmid was generated for localization of *see1* during the biotrophic invasion. Here, the sequence of *um02239* was fused to the mCherry, so that when expressed under control of the native promoter a fusion protein containing *see1-mCherry* is generated which is secreted by the fungus and which could be localized using confocal microscope. Primers OAR03 and OAR04 were used for generation of this PCR fragment and insertion was done by enzymes HindIII and BamHI.

p123-Ppit2 (Mueller et al., unpublished)

Contains promoter of *um01375* (*pit2*). Behind it there is a multiple cloning site with restriction sites of several enzymes for cloning purposes. Construction of this plasmid was done by inverse PCR using primers Oma104 and Oma105, restriction digestion with XmaI and subsequent ligation.

p123-Ppit2-UmSee1

Contains *um02239* (*see1*) under control of the *pit2* promoter and the nos terminator. This plasmid was generated for the constitutive overexpression of See1 throughout the tumor development. The plasmid was constructed by amplification of the *see1* gene and cloning it into p123-Ppit2 by using enzymes SacII and XbaI. The primers OAR07 and OAR11 were used for amplification.

p123-Ppit2-UmSee1-mCherry

Plasmid which was generated for microscopic localization of UmSee1 upon overexpression under the Pit2 promoter. Here, the sequence of *um02239* (*see1*) was fused to the mCherry and expressed under control of the Pit2 promoter. A fusion protein containing *see1-mCherry* is generated which could be localized after secretion with confocal microscope. Primers used for this gene amplification were OAR07 and OAR08 with restriction sites SacII and XbaI.

p123-Ppit2-SrSee1

Contains *sr13434* (*Srsee1*) under control of the *pit2* promoter and the nos terminator. This plasmid was generated for the constitutive overexpression of Srsee1 throughout the tumor development. The plasmid was constructed by amplification of the *see1* gene from *S. reilianum* and cloning it into p123-Ppit2 by using enzymes SacII and XbaI. The primers OAR42 and OAR43 were used for amplification.

p123-Psee1

Contains promoter of *um02239* (*see1*). Behind it there is a site for the restriction enzyme site NcoI for cloning purposes. Construction of this plasmid was done by just the amplification of the See1 promoter (667 bp) with the primers OAR26 and OAR27 harboring the restriction sites SbfI and NcoI and cloned into p123 vector.

p123-Psee1-Srsee1

The *S. reilianum see1* orthologue (*Sr-see1*, *Sr13434*) was amplified by using the primers OAR28 and OAR29 on the genomic DNA of *S. reilianum* as a template. The amplified fragment was digested by the restriction enzymes NcoI and NotI and integrated into the vector p123-Psee1 to generate the construct p123-Psee1-Srsee1 to investigate if the orthologue can complement under the native Um promoter.

p123-Psee1-Uhsee1

The *U. hordei see1* orthologue (Uh-see1, *Uh03678*) was amplified by using the primers OAR116 and OAR117 on the genomic DNA of *U. hordei* solopathogenic strain DS200 as a template. The amplified fragment was digested by the restriction enzymes NcoI and NotI and integrated into the vector p123-Psee1 to generate the construct p123-Psee1-Uhsee1 to investigate if the orthologue can complement under the native Um promoter.

p123-Psrsee1-Srsee1

The *S. reilianum see1* orthologue (Sr-see1, *Sr13434*) was amplified along with its promoter on the genomic DNA of *S. reilianum* as a template, by using the primers OAR36 and OAR37. The amplified fragment was digested by the restriction enzymes SbfI and NotI integrated into the vector p123 via same restriction sites to generate the construct p123-Psrsee1-Srsee1. This construct was to see if the orthologue of *see1* can complement the knockout with its native promoter.

p123-Puhsee1-Uhsee1

The *U. hordei see1* orthologue (Uh-see1, *Uh03678*) was amplified along with its promoter on the genomic DNA of *U. hordei* (DS200- solopathogenic strain) as a template, by using the primers OAR38 and OAR39. The amplified fragment was digested by the restriction enzymes SbfI and NotI, integrated into the vector p123 to generate the construct p123-Puhsee1-Uhsee1 to see the complementation of knockout.

p123-Psee1-GFP- 3X HA

This construct was generated to use as a non-secretory control in the TEM immunogold experiment. The GFP was amplified from the template vector p123 with the primers OAR98 and OAR99. Reverse primer was integrated with the 3X HA tag for creating a fusion of GFP 3X HA. The amplified fragment was digested by the restriction enzymes NcoI and NotI and integrated into the vector p123-Psee1 to generate the construct p123-Psee1-GFP-3X HA which was used as a non-secretory control.

p123-Psee1-SPsee1-mCherry- 3X HA

This construct was generated to use as a secretory control in the TEM immunogold experiment. This cloning was done by a two step ligation in which the *See1* secretion signal was amplified with a mCherry overhang. The mCherry was amplified as a fusion protein fused to 3X HA. The two amplified fragments were mixed together and then a third fragment amplifying the signal peptide of *see1* along with the mCherry 3XHA was generated. Primers used for this PCR were OAR231 and OAR101. The amplified

fragment was digested by the restriction enzymes NcoI and NotI and integrated into the vector p123-Psee1 to generate the construct p123-Psee1-SPsee1-mCherry-3XHA which was used as a secretory control.

p123-Psee1-See1- 3X HA

This construct was generated for the localization of the See1 effector via its natural secretion. The *um02239* (*see1*) was amplified along with its promoter and secretion signal as a fusion protein fused to 3X HA with the primers OAR95 and OAR96. The amplified fragment was digested by the restriction enzymes SbfI and NotI and integrated into the vector p123 to generate the construct p123-Psee1-SPsee1-See1-3XHA which was used for immunogold labeling.

4.3.7.2 Plasmids for the yeast *sgt1* complementation and Yeast two hybrid Analysis

pGBKT7 (Clontech, Mountain View, USA)

Plasmid was used for yeast two-hybrid analysis (bait vector). This is both as a control plasmid (empty vector), as well as a template for starting of gene fusions of different variants with the integrated See1 Gal4 DNA binding domain and a cMyc tag fusion. It conveys Kan resistance and contains the tryptophan (TRP) auxotrophy.

pGBKT7- UmSee1

Plasmid for the performance of the yeast two-hybrid analysis for gene *um02239* (*see1*) without its secretion signal which was amplified by the primers OAR40/41 and cloned via NdeI and BamHI in pGBKT7. This bait plasmid was used for screening the normalized cDNA library.

pGBKT7- ZmSGT1

Plasmid for the yeast two-hybrid interaction study with Umsee1 and Zm-SGT1. The ZmSGT1 was amplified by the primers OLS130/131 and cloned via NdeI and BamHI in pGBKT7. This bait plasmid was used for screening the one to one interaction of Umsee1 with Zm-SGT1

pGBKT7- Uhsee1

Plasmid for the yeast two-hybrid interaction study with Uhsee1 and Zm-SGT1. The UhSee1 was amplified by the primers OAR60/61 and cloned via NdeI and BamHI in

pGBKT7. This bait plasmid was used for screening the one to one interaction of Uhsee1 with Zm-SGT1

pGBKT7- Srsee1

Plasmid for the yeast two-hybrid interaction study with Srsee1 and ZmSGT1. The SrSee1 was amplified by the primers OAR63/64 and cloned via NdeI and BamHI in pGBKT7. This bait plasmid was used for screening the one to one interaction of Srsee1 with ZmSGT1

pGADT7 (Clontech, Mountain View, USA)

Plasmid was used for yeast two-hybrid analysis (prey vector). This is both as a control plasmid (empty vector), used as a template for starting gene fusions for various See1/SGT1 variants with the integrated Gal4 activation domain and an HA tag. It conveys Amp resistance and contains the Leucine (LEU) auxotrophic marker.

pGADT7- ZmSGT1

Plasmid for the yeast two-hybrid interaction study with Umsee1 and Zm-SGT1. The ZmSGT1 was amplified by the primers OLS130/131 and cloned via NdeI and BamHI in pGADT7. This prey plasmid was used for screening the one to one interaction of Umsee1 with ZmSGT1.

pGADT7- UmSee1

Plasmid for the performance of the yeast two-hybrid analysis for gene *um02239* (*see1*) without its secretion signal. The gene was amplified by using the primers OAR40/41 and cloned via NdeI and BamHI in pGADT7.

pGADT7- Uhsee1

Plasmid for the yeast two-hybrid interaction study with Uhsee1 and ZmSGT1. The UhSee1 was amplified by the primers OAR60/61 and cloned via NdeI and BamHI in pGADT7. This bait plasmid was used for screening the one to one interaction of Uhsee1 with ZmSGT1

pGADT7- Srsee1

Plasmid for the yeast two-hybrid interaction study with Srsee1 and ZmSGT1. The SrSee1 was amplified by the primers OAR63/64 and cloned via NdeI and BamHI in pGADT7. This bait plasmid was used for screening the one to one interaction of Uhsee1 with ZmSGT1

pEZY45 –UmSee1

This is a gateway destination vector used for yeast transformation and has a GAL4 inducing promoter. It has a C terminal HA epitope. The Umsee1 gene without its secretion signal was cloned from the entry clone pENTR-D-TOPO via homologous recombination and used for the yeast complementation assay in the *sgt1* mutants along with ZmSGT1. The plasmid has a tryptophan (TRP) auxotrophy marker for selection.

pGREG 536-7XHA (obtained from AG Mösch)

This plasmid is a yeast expression vector with the GAL inducible promoter and a 7X HA tag at the N-terminal. There is a multiple cloning site present at the downstream of the GAL4 promoter. The plasmid has a uracil auxotrophic selection marker.

pGREG 536-7XHA-ZmSGT1

This plasmid is a yeast expression vector and was used for the cloning of the Zm-SGT1 by using the primers OAR105 and OAR107 with the restriction sites EcoRI and XhoI under the GAL inducible promoter. The plasmid was used to see the functional complementation of the ZmSGT1 in the yeast *sgt1* mutants.

pB42AD (Ura3) GAL1-7XHA (obtained from AG Mösch)

This plasmid is a yeast expression vector with the GAL inducible promoter and a 7X HA tag at the N-terminal. There is a multiple cloning site present at the downstream of the GAL4 promoter and has a uracil auxotrophic marker.

pB42AD (Ura3) GAL1-7XHA –ZmSGT1

This plasmid was used for the yeast complementation assay in the *sgt1* mutants with the ZmSGT1. The ZmSGT1 was amplified using the primers OAR65 and OAR66 from the cDNA of noninfected maize cv. Early Golden Bantam. The amplified product was cloned with the restriction sites EcoRI and PstI to generate a SGT1 fusion protein with 7X HA tag.

4.3.7.3 Plasmids for production of recombinant proteins in *E.coli***pET15b (Novagen, Madison / USA)**

The vector contains a T7 promoter, which is regulated by a lac operator. The expression of gene is under control of the T7 lac promoter which can be carried out only in strains that contain the bacteriophage T7 gene 1, which encodes the T7 RNA polymerase. Under the control of the promoter the expression of introduced gene can be regulated and induced by isopropyl- β -D-thiogalactopyranoside (IPTG). The 5'-end is fused to a

sequence coding for a hexahistidine-tag (6XHis tag). It is possible to purify the expressed proteins on Ni-NTA system.

pET15b-His- Umsee1

This plasmid was generated to produce Umsee1 in *E. coli*. It was the *see1* gene (*um02239*) which was amplified without its secretion signal using the primers OAR40/41 with the restriction sites NdeI and BamHI. The amplified product when cloned is fused at the 5'-end to a sequence encoding a His tag which is used in the purification of the protein after expression in *E.coli*.

pET15b-His- ZmSGT1

This plasmid was generated to produce ZmSGT1 in *E. coli*. It was ZmSGT1 gene which was amplified using the primers OAR110/111 with the restriction sites NdeI and BamHI. The amplified product when cloned is fused at the 5'-end to a sequence encoding a His tag which is used in the purification of the protein after expression in *E.coli*.

pRSET-GST-PP (Schreiner et al., 2008)

This plasmid is based on one from Invitrogen (Karlsruhe) under the name pRSET plasmid. This was modified by replacement of a Hexa-histidine tag by a GST (glutathione-S-transferase) tag at the 3' end. At the end of GST gene is a region which encodes a PreScission protease recognition sequence, which enables to remove the GST-tag after the protein purification. This plasmid is mediated by Amp resistance and served as the starting plasmid for preparing the See1 pRSET expression vector.

pRSET-GST-PP- UmSee1

The plasmid was generated to produce UmSee1 in *E. coli*. It contains the *um02239* gene without signal peptide. The gene was amplified with primers OAR108 and OAR109 and cloned via SacI and HindIII in pRSET-GST-PP.

4.3.7.4 Plasmids for transient expression of genes in *N.benthamiana*

pGreenII 0029 (Hellens et al., 2000)

Starting plasmid for transient expression of genes in *N. benthamiana*. This plasmid is based on pGreen0000 (Hellens et al., 2000) and conveys Kan resistance.

pGreen- See1 (w/o SP)

Plasmid was used for the transient expression of See1 in *N. benthamiana*. See1 (*um02239*) was amplified without its secretion signal by using the primers OAR45 /46 and cloned via restriction sites XbaI and SacI in pGreen-CP1A (Mueller et al.2013) by taking out CP1A with the same restriction sites.

pGreen- See1 -mCherry

Plasmid was used for the transient expression of See1 in *N. benthamiana*. It contains See1 (*um02239*), with and without its secretion signal which was fused to mCherry to obtain a fusion protein. This PCR product was amplified by the primers OAR48 and OAR49 for with signal peptide construct and OAR50/49 for without signal peptide construct. Both the PCR products were cloned via XbaI and SacI in pGreen-CP1A (Mueller et al.2013) by excising out CP1A with the same restriction site. The plasmid was used for the localization of See1 upon transient expression in *N. benthamiana* via *Agrobacterium* transformation.

pGreen- See1 –Myc (Schilling, 2014)

This plasmid was used for the transient expression of See1 in *N. benthamiana* for the *in planta* co-immunoprecipitation. It contains See1 (*um02239*), without its secretion signal and was fused to Myc epitope to obtain a fusion protein. This PCR product was amplified by the primers OLS147 and OLS148 and cloned via XbaI and SacI in pGreen vector.

pGreen- SGT1 –HA (Schilling, 2014)

Plasmid was used for the transient expression of ZmSGT1 in *N. benthamiana* for the *in planta* co-immunoprecipitation. It contains ZmSGT1 which was fused to HA epitope to obtain a fusion protein. This PCR product was amplified by the primers OLS149 and OLS152 and cloned via XbaI and BamHI in pGreen vector.

pGreen- SPYNE-mCherry (Hemetsberger et al., 2012; Schilling, 2014)

eBiFC expression vector for expression of candidate genes *N. benthamiana* under the control of the 35S promoter. For the amplification of mCherry from p123-mCherry the primer pair OCFH11 / OCFH10 was used so that an N-terminal RSIATA linker sequence was inserted. The PCR product was cloned via the restriction sites XhoI and XmaI in pUC-SPYCE-35S. The open reading frame was then ligated with HindIII and EcoRI restriction digests in the vector pGreen0029. To remove unnecessary restriction sites in two multiple cloning sites two inverse PCR reactions with the primer pairs OCFH48 / OCFH49 and OCFH50 / OCFH51 were performed.

pGreen- SPYCE-CFP (Hemetsberger et al., 2012; Schilling, 2014)

eBiFC expression vector for expression of candidate genes *N. benthamiana* under the control of the 35S promoter. For the amplification of p123-CFP, CFP from the primer pair OCFH9 / OCFH10 was used so that an N-terminal RSIATA linker sequence was inserted. The PCR product was cloned via the restriction sites XhoI and XmaI in pUC-SPYCE-35S. The open reading frame was then ligated to a restriction digestion with HindIII and EcoRI in the vector pGreen0029. To remove unnecessary restriction sites in two multiple cloning sites two inverse PCR reactions with the primer pairs OCFH48 / OCFH49 and OCFH50 / OCFH51 were performed.

pGreen- SPYCE-CFP _ZmSGT1 (Schilling, 2014)

eBiFC expression vector for expression of candidate genes ZmSGT1 in *N. benthamiana* under the control of the 35S promoter. For the amplification of ZmSGT1 the primer pair OLS120 and OLS121 was used and the product was cloned with the restriction sites BamHI and XhoI in the already generated SPYCE-CFP vector by Hemetsberger et al., 2012.

pGreen- SPYNE-mCherry _Umsee1 (Schilling, 2014)

eBiFC expression vector for expression of candidate genes Umsee1 in *N. benthamiana* under the control of the 35S promoter. For the amplification of Umsee1 without its secretion signal the primer pair OLS119 and OLS120 was used and the product was cloned with the restriction sites BamHI and XhoI in the already generated SPYNE-mCherry vector by Hemetsberger et al., 2012.

pGreen- PIP –YFP (obtained from Armin Djamei)

This plasmid was used as the control for the transient expression assay of See1 in *Z. mays* via ballistic bombardment. The fusion protein PIP-YFP specifically localizes to the plant nucleus and hence easily distinguishes the transformed cell along with the See1-mCherry vector which has a nucleo-cytoplasmic localization

pENTR-D-TOPO (Invitrogen, Karlsruhe)

This is a directional entry TOPO vector for the Gateway technology which does not use any restriction enzymes and is dependent on principle of homologous recombination. The intergration of the gene depends on the recognition sequence CACC at the N terminal of the of the entry site.

pENTR- D-TOPO-Umsee1

Entry clone for the generation of the destination vectors for transient plant expression of See1 under an inducible promoter destination vector. The Umsee1 was amplified by using the primers OAR86/88 for fragment with secretion signal and with the primers OAR89/88 for product without the secretion signal. Both the products generated were cloned as per the manufacturer's instructions.

pENTR -D-TOPO-ZmSGT1

Entry clone for the generation of the destination vector for transient plant expression of ZmSGT1. The gene was amplified by using the primers OAR133/134 for amplification without stop codon for a C terminal fusion and by OAR133/135 with stop codon for a N terminal fusion destination vector. Product generated was cloned as per the manufacturer's instructions.

pTA7001 (Procured from Prof. Nam Hai Chua, USA)

A DEX inducible plant expression vector which is used for the stable expression in *A. thaliana* or transient expression in *N. benthamiana* for *in planta* assays.

pTA7001- See1-HA

The vector was used for the induction of Umsee1 under DEX promoter for the *in planta* phosphorylation assay. The Umsee1 without its secretion signal was amplified along with the primers OAR92 and OAR93 which was integrated with a HA tag to formed the fusion protein with See1-HA and cloned with the restriction sites SpeI and XhoI.

pGWBSH- HA-ccDB-Nos (procured from IBB, Poland)

This plasmid is Gateway destination empty vector with an N terminal HA tag for the purification of the protein.

pGWBSH -ccDB-Strep-His-Nos (procured from IBB, Poland)

This plasmid is Gateway destination empty vector with a C terminal Strep and His tag for the purification of the protein.

pGWBSH -ZmSGT1-Strep-His (generated from IBB, Poland)

This plasmid is Gateway destination empty vector with a C terminal Strep and His tag for the purification of the protein. This vector was used for the cloning and expression of ZmSGT1 *in planta* phosphorylation assay. The ZmSGT1 was cloned via recombination from the pENTR-D-TOPO-ZmSGT1 without the stop codon.

pROK2-NbSGT1-6X HIS.Ala-Ala-Strep II (Hoser et al., 2013)

This is a destination vector with the SGT1 from *N. benthamiana* and fused to a 6X HIS Strep II tag. The construct was used as a control in the *in planta* phosphorylation assay and was previously generated by Rafal Hoser from IBB, Poland.

pROK2-SIPK (Hoser et al., 2013)

This is a destination vector with the SIPK from *N. benthamiana*. The construct was used for the transient *in planta* phosphorylation assay and was previously generated by Rafal Hoser from IBB, Poland.

pTA7002-NtMEK2^{DD}/NtMEK2^{KR} (Hoser et al., 2013)

The vector was used for the induction of the constitutive active kinase MEK2^{DD} and the inactive kinase MEK2^{KR} from *N. benthamiana* which are under DEX promoter and used for the *in planta* phosphorylation assay. These constructs were previously generated by Rafal Hoser from IBB, Poland.

4.4 Standard Microbiological Methods

4.4.1 Rubidium chloride mediated transformation of *E. coli*

E. coli transformation was carried out using the modification of the protocol from Cohen et al. (1972). To produce competent bacterial cells for transformation, 100 ml dYT medium supplemented with 10 mM of MgCl₂ and MgSO₄ was used. The medium was inoculated with 1 ml of a fresh overnight culture and incubated to an OD₆₀₀ nm ≈ 0.5 at 37 °C and 200 rpm. The cells were pelleted by centrifugation for 15 min at 3,000 rpm and 4 °C and resuspended in 33 ml ice-cold RF1 solution. After 30 to 60 min incubation on ice, the cells were again centrifuged (15 min, 3,000 rpm, 4 °C) and the supernatant was removed. Cell pellet was resuspended in 5 ml ice-cold solution of RF2 and incubated for 15 min. The cell suspension was aliquoted into 1.5 ml eppendorf tubes in volume of 50 µl, freezed in liquid nitrogen and stored at -80 °C. For transformation, an aliquot of cells was thawed on ice, each 50 µl and 1-5 µl plasmid (1-5 ng plasmid DNA) or 1-5 µl ligation mixture (see section 4.5.2.3) and incubated for 30 min on ice. After a heat shock of 60 seconds at 42 °C, the transformation mixture was incubated for 2 min on ice, mixed with 200 µl dYT medium, and incubated for 1 hour at 37 °C and 650 rpm in an eppendorf thermal block. The 100 µl of this mixture was plated on a selective dYT plate with the appropriate selection marker and incubated overnight at 37 °C.

RF1-Solution	100 mM RbCl 50 mM MnCl ₂ x 4 H ₂ O 30 mM K-Acetate 10 mM CaCl ₂ x 2 H ₂ O 15% (v/v) Glycerin in H ₂ O _{bid.} , pH 5.8 (Acetate), sterile filtered
RF2-Solution	10 mM MOPS 10 mM RbCl 75 mM CaCl ₂ x 2 H ₂ O 15% (v/v) Glycerin in H ₂ O _{bid.} , pH 5.8 (NaOH), sterile filtered

4.4.2 Blue-White-selection of *E. coli* transformants

For the cloning of the PCR products into PCRII-TOPO a blue white selection screen is used to select the transformants. The correct insertion of the construct into the pCRII-TOPO results in disruption of the lacZ gene, so that no functional beta-galactosidase is expressed, which cleaves X-Gal into a blue dye indigo. Colonies in which plasmids contain inserts, thus remain on X-Gal-containing plates are white and thus easily distinguishable from the blue colonies, vectors without insertion of the desired construct. For this, 100 µl of a 2 % X-gal solution was added one hour before to the selective YT plate before plating out the transformation batch.

4.4.3 Transformation of *A. tumefaciens*

The preparation and transformation of *A. tumefaciens* was carried out according to a protocol by Höfgen and Willmitzer (1988), with minor modification where in place of the YEB liquid medium dYT liquid medium was used.

4.4.4 Transformation of *U. maydis*

Protoplasts preparation and transformation of *U. maydis* was performed following a modification of the protocol according to Schulz et al., (1990) and Gillissen et al., (1992). The mentioned protocols were modified as follows. Preculture of *U. maydis* cells were grown in 4 ml YEPS_{light} medium and incubated for 8–10 hours at 28 °C and 200 rpm. This pre-culture was then diluted 1:300 in 50 ml of fresh YEPS_{light} medium and incubated at 28 °C and 200 rpm to an OD₆₀₀ nm of about 0.8 maximum. After achieving the optimal cell

density, the cells were harvested by centrifugation (10 min at 2800 g and 4 °C), washed once with 25 ml ice cold SCS buffer, centrifuged again (10 min at 2800 g and 4 °C) in 2 ml of SCS buffer containing 2.5 mg/ml Novozyme. Cells were incubated for 5–10 min at room temperature until 50 % of the cells begin to protoplast, which was monitored using a microscope. The cigar-shaped *Ustilago* sporidial cells turn into a spherical shape after lysis of the cell wall. After complete protoplast formation, 10 ml SCS buffer was added and the protoplasts were centrifuged for 10 min at 4 °C and 1500 g. This step was repeated twice to remove the Novozyme. The supernatant was discarded and the resulting pellet was washed three times with ice-cold 10 ml STC buffer to completely remove Novozyme residues. Thereafter, the pellet was resuspended in 0.5 ml ice cold STC buffer and aliquots were made with 50 µl protoplasts in pre-chilled 1.5 ml microcentrifuge tubes for immediate use or stored at -80 °C for later use.

The transformation of *U. maydis* protoplasts were carried out as follows; 30 min before transformation, bottom layer of the petri plate was prepared by pouring 10 ml Regeneration Agar medium containing 2X appropriate antibiotic, mainly the carboxin (Cbx). Then a second layer of Regeneration agar (10 ml, no antibiotics) was poured as a top layer on the transformation plate. An aliquot of protoplasts was thawed on ice and upto 5 µg of linearized plasmid DNA (up to 10 µl) and 1µl heparin solution (1mg/ml) was added to the propoplasts and the mixture was incubated on ice for 10 min. This was followed by addition of 0.5 ml STC /PEG solution and a further incubation was done for 10 min on ice. The entire transformation mixture was then spreaded on the regeneration agar plate and incubated for 4–7 days at 28 °C. Small colonies that appeared on plate were singled out and grown on antibiotic-containing PD Agar plates. Resulting single colonies were used for DNA preparation (see section 4.5.1.2) and verified by Southern blot analysis (see section 4.5.3.2).

SCS-Solution	20 mM Na-Citrate, pH 5.8 1M Sorbitol in H ₂ O _{bid.} , sterile filtered
STC-Solution	10 mM Tris-Cl, pH 7.5 100 mM CaCl ₂ 1 M Sorbitol in H ₂ O _{bid.} , sterile filtered
STC/PEG-Solution	15 ml STC 10 g PEG4000

Regenerations-Agar (Schulz et al., 1990) Top: 1.5% (w/v) Bacto-Agar
 1M Sorbitol in YEPS_{light}

Bottom: LikeTop, in addition twice-concentrated antibiotic

4.4.5 Test for filamentous growth of *U. maydis*

U. maydis strains were grown in liquid medium YEPS_{light} until the OD₆₀₀ nm of approximately 0.8 and incubated at 28 °C. The cells were harvested (3500 rpm, RT, 5 min; Thermo Scientific) and the pellet was then resuspended in sterile water and OD₆₀₀ nm of the culture was adjusted to 1.0. About 5 µl of each suspension was dropped on PD plates containing activated charcoal. After drying of the dropped inoculum, the plate was sealed with parafilm and incubated at 28 °C for 24 hours. Filamentous growth was evident by the formation of a white mycelium showing the fussy growth.

4.4.6 Transformation of *S.cereviceae*

Transformation of *S. cerevisiae* was performed as described in the DUAL membrane starter kit manual. For this purpose, 5 ml YPD liquid medium were inoculated with a single colony of AH109 or the respective yeast strain and incubated overnight at 28 °C and 200 rpm. The overnight pre-culture was diluted in 50 ml of YPD medium, at a ratio 1:50 and grew until OD₆₀₀ nm of 0.6 -0.8. Subsequently, the cells were harvested by centrifugation at 2,500 g for 5 min at RT and the resulting pellet was resuspended in 2.5 ml sterile water. Thereafter, 100 µl of cell suspension was added to each 300 µl PEG-Li-acetate Mix, including 1.5 µg of the DNA to be transformed. This was followed by a heat shock which was performed for 45 min at 42 °C. Cells were then centrifuged at 700 g for 10 min and the pellet was resuspended in 100 µl of 0.9 % NaCl solution. The full transformation mixture was then plated on the appropriate selective medium and incubated for 3–5 days at 28 °C. Small yeast colonies that are seen on the plates are then transferred to single out on the plates with same selection marker and further used for the assay.

PEG / LiOAc Master Mix 240 µl 50 % (w/v) PEG 4000
 36 µl 1M lithium acetate
 25 µl single-stranded carrier DNA

4.5 Molecular Biological Methods

4.5.1 Isolation of nucleic acids

4.5.1.1 Isolation of plasmid-DNA from *E. coli*

Plasmid DNA was isolated using the QIAprep Mini Plasmid Prep Kit, which works on the principle of alkaline lysis. 2 ml of an *E. coli* overnight culture was centrifuged at 17,000 g for 2 min and the media supernatant was discarded. The cell pellet was resuspended in 250 µl buffer P1 mainly functioning for cell lysis. Then 250 µl of buffer P2 was added to the samples and mixed by inverting the tube several times. This was followed by addition of 300 µl buffer P3 which is to neutralize the pH of the mixture and to precipitate the proteins, which were pelleted together with the cell debris by centrifugation at 17,000 g for 10 min. The clear supernatant was then transferred in a new microcentrifuge tube and 600 µl of ice-cold isopropanol was added, resulting in the precipitation of plasmid DNA. The precipitation reaction was centrifuged to get the plasmid DNA pellet (10 min at 17,000 g). The supernatant was discarded and the resulting pellet was washed with 800 µl 80 % ethanol and again centrifuged for 10 min at 17,000 g. Thereafter, the supernatant was discarded and the pellet was briefly dried to remove the residual ethanol. The plasmid was resuspended in 50 µl sterile water.

4.5.1.2 Isolation of genomic DNA from *U. maydis*

For the isolation of genomic DNA from *U. maydis* a modified protocol from Hoffman and Winston (1987) was used. First, 2 ml of *U. maydis* overnight culture was pelleted by centrifugation for 2 min at 17,000 g and supernatant was discarded. The cell pellet was re-suspended by addition of 400 µl *Ustilago* lysis buffer, 500 µl phenol/chloroform and 0.3 g of glass beads (0.4–0.6 mm; Sartorius, Göttingen, Germany). The samples were lysed on a Vibrax VXR shaker (IKA, Staufen) with shaking at 2500 rpm for 20 min and then centrifuged for 15 min at 17,000 g. Thereafter, the upper layer of approximately 400 µl was removed into a new microcentrifuge tube and DNA was precipitated by addition of 1 ml of 100 % ethanol and centrifuged for 2 min at 17,000 g. The supernatant was discarded and the resulting pellet was briefly dried, resuspended in 50 µl TE buffer containing 20 µg/ml RNase A and incubated for 15 min at 55 °C and 1,200 rpm in a Thermomixer (Eppendorf). The DNA was stored until use at -20 °C.

<i>Ustilago</i> lysis buffer	50 mM Tris-HCl, pH 7.5
	50 mM Na ₂ -EDTA
	1% (w/v) SDS in H ₂ O bid.

Phenol /chloroform, 50 % (v/v) of phenol (equilibrated with TE-buffer)
 50 % (v/v) chloroform

4.5.1.3 Isolation of total RNA from infected maize tissue

For the extraction of RNA from infected maize seedling or tassel tissue each infected sample was harvested at the desired timepoint and immediately frozen in liquid nitrogen. The sample was then homogenized using a mortar and pestle under constant nitrogen cooling. The RNA was extracted from the resulting powder using the TRIzol® extraction method (Invitrogen, Karlsruhe, Germany) according to manufacturer's instructions. A quality and quantity inspection was carried out by photometric measurement on the NanoDrop ND_1000 spectrophotometer (Thermo Scientific, USA). The RNA quality was also assessed on the 1 % TBE gel.

4.5.1.4 Purification of RNA

The cleaning of extracted RNA was performed with the RNeasy® Mini Kit from Qiagen (Hilden, Germany) according to manufacturer's instructions. A quality and quantity inspection was carried out subsequently by photometric measurement at the NanoDrop ND_1000 spectro-photometer (Thermo Scientific, USA).

4.5.1.5 Purification of plasmid DNA

Nucleic acids (eg PCR or restriction mixtures) were purified and cleaned up with the Wizard SV Gel and PCR purification System (Promega, Mannheim, Germany) from Agarose gel fragment, eluted and purified according to manufacturer's instructions.

4.5.2 *In vitro* modification of nucleic acids

4.5.2.1 Restriction of DNA

For the restriction of DNA fragments, type I restriction endonucleases I (NEB, Frankfurt / Main) were used. The procedure was followed, depending on the purpose for 2–16 hours incubation time in enzyme specific temperature. The amount of DNA used for digestion was in between 0.5 and 5 µg. A typical reaction mixture was composed as follows:

0.5 – 2 µg plasmid DNA
2 µl enzyme specific 10X NEB-Puffer 1–4
2 µl 10X BSA
0.5 U Restriction endonuclease
20 µl vol with H₂O_{bid.}

4.5.2.2 Dephosphorylation of linear DNA

Dephosphorylation was done whenever necessary in the cloning procedure, for example when a blunt-end ligation has been desired. Here, each of the 5'-phosphate group at the end nucleotides was removed. Alkaline phosphatase (Roche, Mannheim, Germany) or the Antarctic phosphatase (NEB, Frankfurt, Main) was used for this purpose. The duration and temperature of incubation of the enzyme being used is mentioned below. A typical approach consisted of the following reaction mixture:

20 µl Restriction reaction
10 µl Dephosphorylation buffer
25 U alkaline / antartic Phosphatase
add 100 µl with H₂O_{bid.}

4.5.2.3 Ligation of DNA fragments

For ligation of DNA fragments the T4 DNA ligase (Roche, Mannheim, Germany) was used. In ligation reaction in which, a linearized vector should be ligated with an insert, the corresponding DNA was used in a molar ratio of 1:3 to 1:10. Ligation was performed for at least two hours (RT) or overnight (16 °C) in a circulating waterbath. A typical ligation mixture with a volume of 20 µl was composed of the following components:

n mol Vector DNA
5 x n mol bzw 2 x n mol Insert
2 µl 10x T4-DNA-Ligase-buffer
400 U T4 DNA-Ligase
add 20 µl with H₂O_{bid.}

4.5.2.4 Polymerase Chain Reaction (PCR)

To amplify DNA fragments for cloning or for analytical purposes, the polymerase chain reaction (PCR) was used (Mullis et al., 1986). Depending on the application, different polymerases were used. For amplification of DNA for cloning purposes, Phusion® Hot Start High-Fidelity DNA polymerase was used (Finnzymes / Thermo Scientific, Bonn). For analytical purposes, RedMix (Bioline, Luckenwalde) was used which contained Taq polymerase. The following are typical approaches for the individual polymerases which have been described, according to the purpose, with a volume of 20 or 50 µl. Here, the respective PCR program used is represented by the following scheme: initial denaturation - [denaturation - annealing- elongation] x number of cycles - final elongation. The elongation time was chosen based on the expected fragment size and rate of synthesis by the polymerase used. The annealing temperature used was based on the melting

temperature of the oligonucleotides which was calculated previously by the Clone Manager 9.0 (Sci-Ed Software, Cary / USA) *in silico*. All PCR reactions were performed in a Thermocycler (T personnel, Biometra, Jena).

PCR Approach with Phusion-Polymerase (Standard polymerase to approx. 6 kb; Finnzymes-Thermo Scientific / NEB, Frankfurt am Main):

Approach approx. 100 ng template DNA
 200 μ M dNTPS (1:1:1:1 ratio)
 1 μ M Primer 1 (binds on 5' Strand)
 1 μ M Primer 2 (binds on 3' Strand)
 1 x concentrated HF- or GC-Puffer (Finnzymes-Thermo Scientific)
 0.5 U Phusion-Polymerase

Program: 98 °C/30 s – [98 °C/30 s – 55-74 °C/15 s – 72 °C/10 s/kb] x 30-40
 cycles – 72 °C/10 min- Final hold

PCR Approach with RedMix (Colony-PCR/Screens on a large scale; Biotin, Luckenwalde):

Approach 1 x concentrated RedMix
 1.25 μ M Primer 1 (binds on 5' Strand)
 1.25 μ M Primer 2 (binds on 3' Strand)
 1 μ l cell culture or 1 colony (fungi or bacteria or yeast)

Program: 94 °C/2 min – [94 °C/30 s – 50-65 °C/20 s – 72 °C/30 s/kb] x 30-40
 cycles– 72 °C/10 min – Final hold

4.5.2.5 Quantitative *real-time* PCR

For quantitative real-time PCR (qRT-PCR) clean cDNA was synthesized before and possible DNA residues in the RNA samples were removed using the 'Turbo DNA-free' kit (Ambion / Applied Biosystems, Darmstadt). The isolated RNA was then transcribed with the 'First strand cDNA Synthesis Kit (Fermentas) according to manufacturer's instructions in cDNA reverse transcription protocol. The cDNA generated was therefore used for the qRT-PCR reactions, which was performed with the help of, IQ SYBR® Green Supermix' kit from Bio-Rad (Dreieich, Germany) following the manufacturer's instructions. For the PCR reactions 1–5 μ l cDNA were used in the control. As a reference dye fluorescein (20 nM; Bio-Rad, Munich, Germany) was used. The reactions were performed in a Bio-Rad iCycler system using the program 95 °C / 2 min - [95 °C/30 s - 62 °C/30 s - 72 °C/30 s] x

45 cycles. The specificity of the reaction was checked after completion of the PCR based on the calculated melting curve of the run. The Threshold Cycle Software version 3.0 was determined using the Bio-Rad. The relative expression values were calculated using the program Gene Expression Macro (Bio-Rad, Munich, Germany) or with the REST[®] Relative expression software tool (Qiagen, Hilden) (Pfaffl et al., 2002). The calculations for the relative expression were curated manually using the Microsoft Excel program.

4.5.2.6 Targeted site directed mutagenesis of nucleic acids

The targeted exchange of one or more bases in the plasmids was performed by PCR using the QuikChange Multi Site-Directed Muta genesis kit (Stratagene, LaJolla / USA) which uses a Quick change Multi Enzyme Blend. The protocol used for this mutation and base substitution was according to the manufacturer's instructions. Upto three oligonucleotides were designed for the amplification of the entire plasmid with one oligonucleotide containing the corresponding mutation/s in the primer sequence.

4.5.2.7 Sequencing of nucleic acids

All constructs generated, were checked by sequencing for any of the unwanted point mutations in the desired gene. All sequencing was carried out at MWG (Martinsried, Germany) according to the principle of the chain termination method (Sanger et al., 1977). Corresponding plasmids containing fragments to be sequenced were first isolated by using the QiaPrep Plasmid Prep Kit (Qiagen, Hilden) as described in the section 4.5.1.1 and the concentration of present was determined spectrophotometrically before the samples were sent for sequencing. The concentration of the samples for sequencing was adjusted according to the instructions provided by the MWG Sequencing.

4.5.3 Separation and Detection of Nucleic acids

4.5.3.1 Agarose gel electrophoresis

For size-specific separation of nucleic acids, an agarose gel electrophoresis was performed with the DNA migrating toward the anode, due to its negative charge. For this purpose, agarose gels of concentration between 0.8 and 2 % were prepared, depending on the size of the fragments to be separated. The agarose was dissolved by boiling in the microwave in 1X TAE buffer or 0.5 X TBE buffer depending upon the need. After cooling to about 60 °C, ethidium bromide (final concentration: 0.25 g / ml) was added to the cooled agarose mixture. The gel was poured in a liquid state into an assembled gel casting tray. Upon solidification the gel was transferred to the desired gel running compartment and covered with 1X of the same buffer in which the gel was prepared. The samples to be loaded were mixed with the loading buffer and separated at a constant voltage of 80 to 120 volts (V). DNA was then visualized by UV irradiation at 365 nm as

ethidium bromide intercalates with the nucleic acid. The documentation was done with a Gel documentation unit (BioDoc IT system; EIA).

5x TBE-buffer	440 mM Tris-Base 440 mM Boric acid 10 mM EDTA, pH 8.0
50x TAE-buffer	2 M Tris-Base 2 M Acetic acid 50 mM EDTA pH 8.0
6x Gel loading dye (non denaturing)	50% (v/v) Sucrose 0.1% (v/v) Bromphenol blue Adjust with TE-buffer/water and filter sterilize.

4.5.3.2 Southern Analysis/ Southern Blot

Firstly, by the method described in Section 4.5.1.2 genomic DNA from the *U. maydis* transformants to be analyzed was isolated and about 5 µg of DNA was subjected to digestion with restriction endonucleases. The enzymes were selected taking the Cbx locus into consideration so that the number and / or size of the resulting fragments were altered at this locus due to the integration of the transformed construct. The digested DNA was precipitated by adding 1/10 final volume of 3 M potassium acetate and 3 volumes of 100 % ethanol and incubated for 30 min at -20 °C. This was followed by a centrifugation for 5 min at 17,000 g. The supernatant was discarded and the resulting pellet was first washed with 750 µl 80 % ethanol and then re-centrifuged for 5 min at 17,000 g. Subsequently, the supernatant was completely removed and the pellet was briefly dried and resuspended in 20 µl of 1X DNA loading buffer. Thereafter, the DNA fragments were separated by means of gel electrophoresis for about 4 hrs (1X TAE buffer, 0.8 % agarose, 90 V). Prior to the transfer of the DNA onto the membrane, depurination was performed, wherein the transfer of large DNA fragments is facilitated. For this purpose, the agarose gel was first incubated with slow shaking for 15 min in 0.25 N HCl on a roller and then neutralized for 15 min in 0.4 N NaOH till the bromophenol dye front turns blue again. Subsequently, DNA was transferred from the gel to a nylon membrane (Hybond-N+, GE Healthcare, Munich, Germany) by method following the modification of a protocol by Southern (1975). The transfer was carried out finally by the transfer solution (0.4 N NaOH) that was sucked into a stack of paper towels by capillary forces of a buffer reservoir through the gel and the DNA fragments are eluted by the flow of liquid from the gel, and

are bound to the nylon membrane. The transfer was done usually overnight, but at least for 6 hours, in which case the paper towels were replaced at regular intervals.

The DNA transferred to the membrane was immediately fixed by cross-linking (Ultraviolet crosslinker, Amersham Life Science) and the membrane was transferred to a hybridization tube and pre-hybridized with 20 ml Southern hybridization buffer for 15 min at 65 °C in a hybridization oven (UVP HB-1000 Hybridizer Cambridge, UK). The specific detection of immobilized DNA was performed using digoxigenin (DIG). The labeled DNA fragments were generated by PCR using the PCR DIG and Labeling mix kit (Roche, Mannheim, Germany) which were amplified according to the manufacturer's instructions. The pre-hybridization was followed by hybridization step wherein the prepared DNA probe was denatured before use for 10 min at 100 °C and then mixed with 40 ml of pre-warmed southern hybridization buffer at 65 °C. The hybridization step is done for overnight at 65 °C in the hybridization oven. The next morning, the membrane was washed twice for 15 min with southern wash buffer at 65 °C. All the further steps for developing the membrane were performed following the protocol for Southern blot development from Sambrook et al., 1989. Development of the blot was done by exposure of a light-sensitive film (Kodak XAR-5 X-Omaz) depending on the intensity of the signal for about 1–30 min and developmen was carried with an X-ray film developer machine (QX-60, Konica).

1 M sodium phosphate buffer	Solution 1: 1 M Na ₂ HPO ₄ Solution 2: 1M NaH ₂ PO ₄ * H ₂ O Solution 1 to be taken in SD bottle and addition of Solution 2, as long as the close pH reaches to 7.0
Southern hybridization buffer	500 mM sodium phosphate buffer, pH 7.0 7 % (w /v) SDS
Southern wash buffer	0.1 M sodium phosphate buffer, pH 7.0 1 % (w /v) SDS
DIG buffer 1	0.1 M Maleic acid, pH 7.5 0.15 M NaCl
DIG buffer 2	0.1 M Maleic acid, pH 7.5 0.15 M NaCl 1 % (w /v) milk powder (to be prepared fresh)
DIG buffer 3	0.1 M Maleic acid, pH 9.5 0.1 M NaCl 0.05 M MgCl ₂
DIG wash buffer	0.1 M Maleic acid, pH 7.5 0.15 M NaCl 0.3 % (v /v) Tween-20

CDP-Star solution	100 µl CDP-Star (Roche, Mannheim, Germany) in 10 ml DIG buffer 3
-------------------	---

4.5.4 Microarray Analysis

For the microarray experiments, maize plants (Early Golden Bantam) were grown in a phytochamber in a 15 hr/9 hour light/dark cycle; light period started/ended with 1 hour ramping of light intensity. Temperature was 28 °C and 20 °C, relative humidity 40 % and 60 % during light and dark periods, respectively, with 1 hour ramping for both values. Plants were inoculated with H₂O (mock), SG200, and SG200Δ*see1* as described previously in virulence assays for seedling infections. Infected or water-inoculated tissue from 15 plants per experiment was harvested at 2 dpi and 6 dpi timepoint by excising a section of the third leaf between 1 and 3 cm below the injection holes. For RNA extraction, material was pooled; ground to powder under liquid nitrogen and RNA was extracted with Trizol reagent (Invitrogen, Karlsruhe, Germany). RNA was purified applying the RNeasy kit (Qiagen, Hilden, Germany). Microarray analyses were performed with 200 ng total RNA extracted from *U. maydis* infected samples and the mock control. For the selected time points, samples from three independent biological replicates were labeled and hybridized according to Agilent's One-Color Microarray-Based Gene Expression Analysis Low Input Quick Amp Labeling protocol (version 6.5). Cy5-labeled probes were hybridized to 4x 44k custom-designed Agilent microarray chips for maize based on a previous 4x 44k custom-designed Agilent microarray described in Skibbe et al., 2010. The preparation of the one color spike mix labeling, hybridization, microarray washing and scanning was done by following the one color microarray based protocol from Agilent. Microarray image files were analyzed using Agilent's Feature Extraction software v. 10.5 which calculates for each spot a background corrected signal intensity value (gProcessedSignal) that was used for further analysis. The microarray data obtained in this study were analyzed using the Partek Genomics Suite version 6.6. Expression values were normalized using the RMA method. Criteria for significance were a corrected p-value (per sample) with an FDR of 0.05 and a fold-change of ≥ 2 . Differentially expressed genes were calculated by a 1-way ANOVA.

4.6 Biochemical Methods

4.6.1 Separation and detection of proteins

The separation of proteins was performed by Sodium dodecyl sulfate polyacrylamide gel electrophoresis (SDS-PAGE) according to Laemmli (1970). In this method, it is possible to

separate denatured proteins according to their molecular size, in an electric field. A complete denaturation of the analyzed protein samples was followed with 1X SDS gel loading buffer in the presence of 100 mM dithiothreitol (DTT) for 5 min at 99 °C. This binds the negatively charged SDS molecules to the proteins and due to a negative charge migrates them proportional to the molecular size of the protein. The vertical PAGE gels (10.5 x 11.5 x 0.1 cm) were used (Mini Protean System, BioRad, Munich, Germany), which were composed of stacking and separating gel. By using appropriate combs (BioRad, Munich, Germany) in the stacking gel, wells were formed into which the prepared protein samples can be loaded. The stacking gel is relatively of coarse porosity and is used to concentrate the sample before it enters the separation gel. In the separating gel, the proteins are separated in the polyacrylamide according to their molecular size, with smaller proteins migrating faster through the gel than larger ones. The higher the proportion of acrylamide, the higher is the meshed molecular network. Thus higher percentage gels are used for separation of the small proteins and low percentage gels are used for the separation of large proteins. The 1X SDS running buffer is used in the gel chamber. The molecular mass of proteins could be estimated using a prestained protein ladder (prestained protein marker 10-170 kDa, Fermentas, St. Leon-Roth). A typical gel run was performed at a voltage of 120-160V for about 1 hour.

6x SDS-gel loading buffer	4M Tris-HCl, pH 6.8 6 % (w /v) SDS 0.15 % (w /v) bromophenol blue 60 % (v /v) glycerol
SDS running buffer	25 mM Tris-HCl, pH 8.3 192 mM Glycine 4 mM SDS
Stacking gel	5 % (v/v) acrylamide 0.1 % (w/v) SDS in 125 mM Tris-HCl, pH 6.8 to initiate the polymerization: 0.1 % (w/v) ammonium persulfate 0.05 % (v/v) of tetramethylethylene diamine (TEMED)
Separating gel	12-17 % (v/v) acrylamide 0.1 % (w/v) SDS in 375 mM Tris-HCl, pH 8.8 to start the polymerization, 0.1 % (w/v) ammonium persulphate 0.05 % (v/v) TEMED

4.6.2 Immunological protein detection by chemiluminescence (western blot)

The proteins were separated by SDS PAGE and were then transferred by semi-dry transfer system (BioRad, Munich, Germany) to a nitrocellulose membrane. For transferring procedure a layer of 3 mm whatman paper was wetted in transfer buffer and then covered with the nitrocellulose membrane. This was then followed by the SDS gel by removing all the generated air bubbles. Another layer of the whatmann paper which was previously equilibrated for about 5 min in transfer buffer is added upon the gel. The transfer was performed for 1 hour at 100 mA and 25 V per Gel for 1 hour. Subsequently, protein amounts transferred to the membrane can be specifically detected. The membrane was then incubated for 1 hour at RT with blocking solution, which was then replaced with antibody solution containing the primary antibody and incubated for around 16 hour at 4 °C. Thereafter, the membrane was washed three times for 10 min with TBS-T buffer and then incubated in TBS-T buffer containing the secondary antibody for 1 hour at RT. The antibodies used in this study are listed in Table 7. After three more washes with TBS-T buffer for 10 min each, the membrane was then incubated for 5 min with ECL Plus western blotting detection reagent (GE Healthcare, Munich, Germany) and then sealed in a plastic bag. Following this the membrane was placed in a cassette with intensifying screen set. This was followed by exposure of a film (Kodak X-Omaz XAR-5) for 1–60 min, depending on the intensity of the signal observed. Films were developed in an X-ray film developer machine (QX-60, Konica, Munich, Germany).

Western transfer buffer	25 mM Tris-HCl, pH 10.4 192 mM glycine 15 % (v/v) methanol
TBS-T buffer,	50 mM Tris-HCl, pH 7.5 150 mM NaCl 0.1 % (v/v) Tween 20
Blocking solution	5 % (w/v) milk powder in TBS-T buffer
Antibody solution	antibody diluted in 0.5 % (w /v) milk powder in TBS-T buffer

Note: The primary antibody solution was prepared in blocking buffer. However for the secondary antibody solution and the subsequent washing procedures the TBS-T buffer without any milk powder was used.

Tab. 7: Antibodies used and HRP conjugates

Antibody	Use concentration	Reference Source
anti-HA (from mouse)	Monoclonal primary antibodies from Mouse, which was used for the detection of HA fusion proteins (dilution 1:10,000).	Sigma-Aldrich (Deisenhofen)
anti-c-Myc	Monoclonal primary antibodies from Mouse, which was used for the detection of c-Myc fusion protein (dilution 1:5,000)	Sigma-Aldrich (Deisenhofen)
anti-mouse-HRP (from Horse)	secondary antibody for the detection primary antibodies obtained from mice immunized were obtained (dilution 1:2,500)	From Cell signalling technology (Danver, USA)
Streptavidin-peroxidase	conjugate covalently bonded Streptavidin and horseradish peroxidase for the detection of biotin (dilution 1:3,000).	Sigma-Aldrich (Deisenhofen)

4.6.3 Coomassie staining of proteins

To make proteins visible after SDS-PAGE Page Blue Protein colour solution (Fermentas, St. Leon-Roth) was used according to manufacturer's instructions. This solution is based on the coomassie brilliant blue R250 colloid Coomassie solution that allows detection of proteins in the SDS gel to a detection limit of about 5 ng. The decolorization of the gels was performed by washing in sterile H₂O. Staining with the dye was usually done for overnight.

4.6.4 Protein determination according to Bradford

Quantitation of protein levels in protein extracts or by purification of proteins was carried out using the method of Bradford (1976). To create a calibration curve bovine serum albumin (BSA) was used as standard.

4.6.5 Heterologous production of recombinant proteins in *E.coli*

For the production of proteins in *E. coli*, the protein expression strains Tuner (DE3) pLysS cells or BL21 (DE3) pLysS cells were used. Information with respect to the transformed plasmids of the resulting strains and the corresponding induction conditions can be found in Table 8. The desired gene was cloned before in the appropriate protein expression vector for *E. coli* as mentioned in the table below.

Tab. 8: Conditions for the heterologous production of recombinant proteins

Plasmid	Strain	IPTG [mM]	Incubation time [h]	Incubation temperature [°C]
pRSET-GST-PP-UmSee1	Tuner(DE3)pLysS-GST- See1	1	8	28
pET15b-His-ZmSGT1	BL21(DE3)pLysS-CP2-His	1	4	28

From the respective *E. coli* strains a preculture was first inoculated in dYT liquid medium, supplemented with the required antibiotics. This was incubated overnight at 37 °C and 200 rpm. The following day, the pre-culture was diluted 1:100 in 2000 ml dYT liquid medium with the addition of appropriate antibiotics and was distributed in amounts of 200 ml in fifteen 1 liter Erlenmeyer flasks. The cells were then incubated to an OD₆₀₀ nm of 0.6–0.8 at 37 °C and 200 rpm before the induction of genome-encoded T7 RNA polymerase by adding an appropriate amount of IPTG (see Table 8). After the required OD₆₀₀ is reached the cells were induced with appropriate amounts of IPTG for protein production. Following the incubation period specified for each individual construct in Table 7, each culture was centrifuged at 4 °C for 30 min and 6,000g and cells were harvested and stored at -20 °C. A pellet in this case corresponds to the amount of 400 ml culture.

4.6.6 Purification of GST fusion proteins

The N-terminal fusion of a glutathione-S-transferase (GST) tag allows affinity purification using glutathione coupled to Sepharose and simultaneously increases the solubility of the fused protein. To obtain proteins without GST-tag, a PreScission protease cleavage site is present which is located between GST and the target protein. This is a commercial for the PreScission® protease (GE Healthcare, Uppsala, Sweden) specific recognition sequence consisting of amino acids LeuGluValLeuPheGln / GlyPro, being cut between Gln and Gly. Further receiving the PreScission® protease itself contains also a GST-tag, so that they also binds to glutathione Sepharose and only the cut from the GST-tag protein is located at the end of the flow.

The cell pellets stored at -20 °C was thawed on ice for cell lysis, resuspended in 20 ml lysis buffer GST and incubated 20 min at RT. Thereafter, the suspension was sonicated five times for 30 sec on ice. The insoluble mass was then removed by centrifugation (30 min at 4 °C and 45,000g). In parallel, a gravity flow column with 1 ml of glutathione sepharose 4B (GE Healthcare, Uppsala, Sweden) was loaded and equilibrated with 10 ml of PBS buffer. The supernatant of the centrifuged lysate was applied to the column and incubated for 1h at 4 °C on a rotary shaker (Kisker Biotech, Steinfurt, Germany). The column was then opened and the flow rate, which contained unbound proteins, was

discarded. This was followed by three washes each with 10 ml PBS buffer and a washing step with 10 ml PreScission®-cleavage buffer. This was followed by the specific removal of the GST tags using the PreScission® protease (GE Healthcare, Uppsala, Sweden). For this purpose 160 U PreScission® protease was added to 2 ml of PreScission®-cleavage buffer, which together was added to the column and incubated for 16 hours at 4 °C. The next day, the column was opened and the flow rate, of the protein without the GST tag was absorbed. Remaining proteins were removed by washing twice with 2 ml per PreScission®—rinsed cleavage buffer. All flow-through fractions of four columns were pooled and concentrated using Amicon Ultra-4 columns (Millipore/Merck, Darmstadt, Germany) with an exclusion size of 3 kDa to a final volume of about 6 ml according to the manufacturer's specification. The resulting protein solution was sterile filtered by a gel filtration column (HiLoad Superdex 200, GE Healthcare, Uppsala, Sweden), previously equilibrated with 50 mM Tris storage buffer, and eluted with the same buffer. The obtained fractions were analyzed by SDS-PAGE and those that were contained pure protein were pooled together by using Amicon Ultra-4 columns (Millipore / Merck, Darmstadt, Germany) focused with a cutoff threshold of 3 kDa up to a volume of about 500 µl. The corresponding protein concentration was then determined by Bradford assay (Bradford, 1976). Corresponding protein solutions were stored at 4 °C for short term storage. For the long term storage, glycerol was added to a final concentration of 10 % (v/v) and stored at -80 °C.

4.6.7 Purification of HIS tagged proteins

The production of bacterial pellets was same as that described for the GST protein purification. The bacterial pellets were produced from two liters of culture and then resuspended as described previously.

Bacterial pellets stored at -20°C were thawed in HIS lysis buffer: 300 mM NaCl; 50 mM NaH₂PO₄; 10 mM imidazol; 1mM PMSF; 0,1% (w/v) lysozyme; pH 8.0 After thawing the cell suspension was sonicated in the Dr. Hielscher Sonicator UP 200H sonicator (5 cycles of 20 seconds, amplitude 60 %) and then centrifuged: 15000 g, 30 min, 4 °C. The supernatant was loaded onto HisTrap HP column (GE Healthcare Bio-Sciences) in AKTA FPLC system equilibrated with the HIS-tag lysis buffer. The column was washed with 50 ml of HIS wash buffer: 300 mM NaCl; 50 mM NaH₂PO₄; 20 mM imidazol; pH 8,0. For elution of the protein bound to the resin, HIS elution buffer was used: 300 mM NaCl; 50 mM NaH₂PO₄; 250 mM imidazol; pH 8.0. Eluted fractions containing protein were identified at 280 nm light. Collected protein was then concentrated on the Ultracel-3K Centrifugal Filters (Millipore) to a concentration of about 10mg/ml.

4.6.8 Obtaining of denatured proteins from *S. cereviceae* for western blot

The *S. cerevisiae* strains used for the yeast two hybrid assays were checked for the expression of the desired protein of interest by western blot analysis. In general, *S. cerevisiae* was grown as an overnight culture in liquid medium and the cells in the initial culture of 2 ml were harvested by centrifugation (5 min at 17,000 g). This was followed by the addition of about 0.3 g of glass beads and 50 μ l SDS-gel loading buffer with 100 mM DTT. Subsequently, the samples were first heated for 5 min at 99 °C and then shaken for 15 min on a Vibrax-VXR shaker (IKA, Staufen, Germany), before the samples were re-incubated for 5 min at 99 °C. The samples were then centrifuged at 17,000 g for 2 min and finally 15 μ l of each supernatant was used for SDS-PAGE protein resolution.

4.6.9 Co-Immunoprecipitation

The *in planta* Co-immunoprecipitation experiment was done to confirm the interaction of See1 and SGT1 when transiently expressed in *N. benthamiana*. To this end the appropriate constructs with See -Myc and SGT1-HA were heterologously expressed in *N. benthamiana*. As expression controls these constructs were separately expressed along with the appropriate empty vector. For all experiments, the *A. tumefaciens* strain GV3101 was used. The transformation of *A. tumefaciens* was performed as described by Flowers and Vaillancourt, 2005). The transformants were infiltrated into 3–4 weeks old *N. benthamiana* leaves according to the protocol described by (Sparkes et al., 2006). The leaves were harvested and ground in liquid nitrogen, 4 days postinfiltration. The ground powder was mixed with buffer (50 mM Tris-HCl, 150 mM NaCl, pH 7.0). The resulting leaf extract was centrifuged at 3,500 rpm at 4 °C and subsequently sterile filtered through a 0.2 μ m filter. The protein concentration of the extract was determined with Roti [®]-Quant protein quantitation assay (Carl Roth, Karslsruhe, Germany). To 1 ml leaf extract containing 2 mg/ml protein, 50 μ l of anti-HA Affinity Matrix (Roche Diagnostics, Mannheim, Germany) was added and samples were incubated over night at 4 °C on a rotation wheel. The samples were then centrifuged through Pierce SpinColumns (Thermo Scientific, Rockford, USA), washed once with buffer (50 mM Tris-HCl, 150 mM NaCl, pH 7.0) and protein was finally eluted by boiling samples in 2X SDS loading buffer for 5 min. Appropriate amounts of the eluted proteins were separated by SDS-PAGE, followed by transfer to a nitrocellulose membrane. After electro-blotting, the membrane was saturated with 5 % (w/v) non-fat dry milk in TBS-T (50 mM Tris-HCl, 150 mM NaCl, pH 7.6, 0.1 (v/v) % Tween-20 for 1 hour at RT. After blocking, the membrane was washed three times with TBS-T followed by incubation with the primary antibody (anti-HA antibody: 1:10,000, anti-c-Myc antibody: 1:5,000; Sigma-Aldrich, St Louis, USA) over night at 4 °C. Membranes were washed three times prior to incubation for 1 hour with HRP-conjugated secondary

antibody (anti-mouse, 1:5,000; Cell Signalling, Danvers, USA). Signals were detected by using SuperSignal West Pico Chemiluminescent Substrate (Thermo Scientific, Rockford, USA).

4.6.10 Immunoprecipitation of HA-tagged proteins from infected maize tissue

To ensure and demonstrate the stability of various HA-fused proteins after infection with *U.maydis*, the maize plants of the cv Gaspé Flint were initially infected with the corresponding strain (see section 4.7.3). The infected leaves along with the appropriate dpi were harvested by marking of the infected leaf areas below the infection mark, frozen in liquid nitrogen and ground to a fine powder. Mortar and pestle prechilled in liquid nitrogen was used for this purpose. Round about 1 ml of frozen plant powder was then added into 15 ml Falcon tubes and homogenized with TBS buffer with protease inhibitor cocktail (Roche, Mannheim, Germany 1 tablet per 20 ml of TBS buffer was used). The homogenate was made up to a volume of about 10 ml by adding the desired amount of buffer if necessary. Subsequently, the extract was filtered through a Whatmann filter paper to remove the crude plant debris and centrifuged for 10 min, at 4 °C and 10,000 g. Next, the supernatant was transferred into a new 15 ml Falcon tube and 20 µl anti-HA affinity matrix (Roche, Mannheim, Germany) was added to the supernatant. The resulting plant extract mixture was incubated overnight at 4 °C on a rotary shaker (Kisker-Biotech, Steinfurt, Germany). To collect the Affinity matrix with HA beads the supernatant was centrifuged over TM spin columns for purification of the HA tagged proteins (Pierce / Thermo Scientific, Bonn, Germany) and the flow-through was discarded. After washing five times each with 1 ml of TBS buffer the proteins bound to anti-HA matrix were eluted by addition of 20 µl SDS-gel loading buffer with 100 mM DTT and were subsequently boiled for 5 min at 99 °C. The proteins were then separated by SDS-PAGE and HA-fusion proteins were detected by Western blot as described earlier.

4.6.11 *In planta* phosphorylation assay

The *in planta* phosphorylation assay was done to check the mechanistic basis of the See1-SGT1 interaction. The Zm-SGT1 in the presence and absence of See1 and also in addition to the earlier mentioned controls (as mentioned in the results section), were infiltrated by the *Agrobacterium* mediated transformation into 4 week-old *N. benthamiana* leaves as described earlier. Expression of the NbMEK₂ variants was induced with 30 µM dexamethasone (DEX) 40–48 hours later (Yang et al., 2001). Treated leaves were collected approximately 5 hours after dexamethasone infiltration. The DEX treated leaves are monitored by the activity of necrotization as the expression of MEK₂ kinase cause necrosis induction. Ground leaf material was thawed in 10 ml Ex-strep buffer (100 mM

Tris HCl pH 8.0; 5 mM EGTA; 5 mM EDTA; 150 mM NaCl; 10 mM DTT; 0.5 mM AEBSF; 5 µg/ml antipain; 5 µg/ml leupeptin; 50 mM NaF; 1 % (v/v), Phosphatase Inhibitor Cocktail 1 (Sigma-Aldrich); 0.5 % (v/v) Triton X-100; and 100 µg/ml avidin) as described previously (Witte et al., 2004). The slurry was centrifuged for 10 min at 4°C (15000 g) and the resultant supernatant was filtered through Miracloth and 0.5 ml StrepTactin Sepharose (IBA GmbH, Göttingen, Germany) was added. Binding was performed by incubation of this suspension on a rotator for 1 hour at 4 °C. The slurry was transferred into a Poly-Prep column (Bio-Rad) and the flow-through was discarded. The resin was washed twice with 10 ml W-buffer (100 mM Tris HCl pH 8.0; 150 mM NaCl; 1 mM EDTA). Subsequently, four times 250 µl E-buffer (100 mM Tris HCl pH 8.0; 150 mM NaCl; 1 mM EDTA; 2.5 mM desthiobiotin) was added to the column and eluates were collected. The samples were concentrated on a Microcon YM-10 (Millipore) for 30 min at 4 °C (13,000 g) to a volume of 20 µl and resolved by SDS-PAGE.

4.6.12 Mass spectrometry analysis

Gel bands containing the proteins of interest in the SDS gels were subjected to a standard proteomic procedure during which proteins were reduced with 100 mM DTT for 30 min at 56 °C, alkylated with iodoacetamide in darkness for 45 min at RT and digested overnight with sequencing grade modified trypsin (Promega Corporation, Madison, WI, USA). The resulting peptides were eluted from the gel with 0.1 % TFA and 2 % ACN and applied to the SwellGel Gallium-Chelated Discs (Thermo Fisher Scientific, Waltham, MA, USA). Phosphopeptide isolation was carried out according to the manufacturer's instructions and finally the phosphopeptide fraction was eluted from Ga (III) resin with 100 mM ammonium bicarbonate. Liquid chromatography (LC) and mass spectrometry (MS) analyses of peptides were carried out using a nano-acquity (Waters Corp., Milford, MA, USA) LC system coupled to an Orbitrap Velos (Thermo) mass spectrometer. Spectrometer parameters were as follows: capillary voltage, 2.5 kV; cone, 40 V; N₂ gas flow, 0; range, 300–2000 (*m/z*). The spectrometer was calibrated on a weekly basis with Calmix (caffeine, MRFA, Ultramark 1621). The sample was first loaded from the autosampler tray (cooled to 10 °C) to the pre-column (Symmetry C18, 180 µm × 20 mm, 5 µm; Waters) with a mobile phase of 100 % MilliQ H₂O acidified by 0.1% formic acid. The peptides were then transferred to a nano-UPLC column (BEH130 C18, 75 µm × 250 mm, 1.7 µm; Waters) by a gradient of 5–30 % acetonitrile, 0.1 % FA in 45 min. The column outlet was directly coupled to the ESI ion source of the Orbitrap Velos (Thermo Fisher Scientific) mass spectrometer working in the regime of data dependent MS to MS/MS switch. A blank run ensuring lack of cross contamination from previous samples preceded each analysis. After pre-processing of the raw data with Mascot Distiller software (version 2.1.1, Matrix

Science), output lists of precursor and product ions were compared to NCBI nr database using Mascot database search engine (v2.1, Matrix Science). Search parameters included semiTrypsin enzyme specificity, one missed cleavage site, Cys carbamidomethyl fixed modification and variable modifications including Met oxidation and phosphorylation of Ser, Thr or Tyr residues. Protein mass and taxonomy were unrestricted, peptide mass tolerance was 20 ppm and the MS/MS tolerance was 0.8 Da. Proteins containing peptides with Mascot cut-off scores >50, indicating identity or extensive homology ($p < 0.05$) of peptide, were considered positive identifications. The MS/MS spectra of phosphorylated peptides were curated manually.

4.7 Plant Methods

4.7.1 Maize varieties (*Zea mays* sp.)

For infection experiments for the purpose of quantification of *U. maydis* seedling infection (section 4.7.4) or microscopy (section 4.8), *Zea mays* cv. Early Golden Bantam (Old Seeds, Madison, WI, USA) were used. To perform the tassel infection, *Zea mays* cv. Gaspé Flint was used as this variety has an early floral switch in 15 days and are suitable for early meristematic tassel infections. In addition for the electron microscopy infections and immunoprecipitation of HA-tagged proteins from infected maize tissue (section 4.6.9), the corn variety Gaspé Flint was used. Throughout various experiments these two varieties of *Z. mays* have been used and they show similar infection symptoms which are verified by the infection of the two varieties independently.

4.7.2 Cultivation of *Z. mays*

All corn plants were cultivated in temperature controlled greenhouse, where the night phase lasted 20 °C and 60 % humidity 9h, the diurnal phase at 28 °C and 40 % humidity for 15 hours. Also included in the daytime phase was the 2.5 hours for the simulation of sunrise and 3.5 hours for the simulation of the sunset (ramping). During the day phase, the illumination intensity was at least 28,000 Lux and additional sunlight to 90,000 Lux. Four corn grains were sown per pot. Both the varieties were grown in Frühstorfer Pikiererde “T” type, soil and watered once a day. For the microarray experiment, the plants were grown in the walk-in phytochamber with the same conditions described above and one corn grain per pot was sowed to maintain uniformity of nutrient availability.

4.7.3 Infection of *Z. mays* with *U. maydis*

U. maydis strains that were used for infection of *Z. mays* were grown overnight in YEPS_{light} liquid medium at 28 °C with shaking at rpm until the OD₆₀₀ nm of 0.6–1.0 is reached. Subsequently, the cells were harvested by centrifugation (10 min at 2,400 g) and

resuspended in sterile water so that OD₆₀₀ nm of 1.0 is reached. For the purpose of microscopy or for immunoprecipitation of HA-tagged proteins from infected maize tissue (section 4.8 or 4.6.9), the inoculum was set to an OD₆₀₀ nm of 3 in sterile water with 0.1 % (v/v) Tween-20 and then infected. By default, syringe infections were made with 300–500 µl of the cell suspension into the interior of leaf whorl of 7-day-old corn plants for seedling infections. The injection site was chosen to be approximately 1 cm above the earth, which is about 2.5 to 3 cm above the basal plant meristem. Here, the leaf sheaths of the first and second leaf and the leaf blades of the third and fourth sheet were pierced by the syringe which later shows an infection mark after the symptom development.

Tassel infections were done after 15 days in the cv. Gaspé flint and after around 4 weeks in cv. Early Golden Bantam. The tassel infections were also performed using a syringe based method. The immature tassels location was identified without cutting the plant. Above the tassel which terminates the shoot, the leaf sheaths overlap, but there is no solid center and this region contains the inflorescence. Prior to injection, one or two plants were cut open with a sharp knife, to see the tassel wrapped in the leaf whorl. Based on this height, the tassel location was identified on all plants. The standard injection protocol involved 1 ml of the *U. maydis* culture injected all at once, taking care to penetrate only halfway across the plant diameter. This ensured the inoculum to the entire floral meristem. The inoculum seeps into the air space around the tassel. Disease symptoms in the tassels were scored 10 days after infection in cv. Gaspé Flint and after 14 days in cv. Early Golden Bantam.

4.7.4 Quantification of the *U. maydis* infection symptoms

For quantification of disease symptoms in seedlings, a classification scheme of symptoms was made according to the severity of symptoms in seven different categories 12 dpi, as previously described (Kämper et al., 2006). This scheme is shown in Table 9. By default, three independent infections, each with about 40 plants were performed for every experiment. To allow the quantitative evaluation of tassel infections comparable with that of seedling leaves, a new scoring scheme was developed. *U. maydis* symptoms formed in the tassel were classified into five categories, depending on symptom severity (Fig. 8A). The criteria for tassel scoring were based on both the area of the tassel converted to tumor as well as tumor size. In addition, developmental changes of infected tassels were assessed, including a growth arrest at the 1–3 cm stage, which was induced by $\Delta see1$ mutant as well as by SG200 infections (Fig. 8A). The categories of tassel symptom classification are also shown in Table 10. A minimum of 40 tassels were infected in independent triplicates in the mutant and wild-type. In both the seedling and tassel

disease ratings, the symptoms are represented by an average of the percentage of the total number of infected plants.

Tab. 9: Classification of symptoms of infected maize seedlings

Plant Symptoms	Description
No symptom	The plant shows no signs of infection
Chlorosis	The plant shows chlorotic discolouration of the infected leaves (third leaf and younger)
Small tumors	The largest tumors of the plant are <1.5 mm
Normal tumors	Tumors of the plant are 2–4 mm in diameter
Heavy Tumors	Very strong tumors with an associated curvature of the stem axis
Dead Plant	The plant is dead due to the infection with <i>U. maydis</i>

Tab. 10: Classification of symptoms of infected maize tassels

Tassel Symptom	Description
Tumors<50% of tassel, small	The part of the tassel is converted into small tumors in range of 2–4 mm
Tumors<50% of tassel, large	Less than half of the tassel is converted into large tumors >4 mm
Tumors>50% of tassel, small	The small tumors cover all over the entire tassel
Tumors>50% os tassel, large	The complete tassel is converted into heavy tumors by <i>U. maydis</i>
Tassel growth stunted	The tassel is arrested at the developmental timepoint at which it was infected and this 1–3 cm stunted tassel becomes tumoros.

4.7.5 Cultivation of *N. benthamiana*

Seeds of *N. benthamiana* plants (BN3) were seeded evenly on Frühstorfer Pikiererde of type "T" soil. After germination at around 4–7 days after sowing individual seedlings were transplanted into new pots. These individual seedlings were grown in phytochamber (Vötsch) under controlled environmental conditions (21 °C, 16 hours light, 8 hours dark), as described previously by Talarczyk et. al., 2002 and were used further after 2 weeks for infiltration experiments.

4.7.6 Infiltration of *N. benthamiana*

The cultivation of *A. tumefaciens* and the subsequent infiltration of *N. benthamiana* was performed as described previously according to a protocol of Sparkes et al., 2006. Infected leaves were harvested 3 days after infiltration for the respective planned experiment.

4.7.7 Transient expression in *Z. mays* via ballistic transformation

For transient protein expression in maize ballistic gene transfer method was implemented using the 1.6 μm gold particles (Bio-Rad, München, Germany). The 60 mg gold particles (Biorad, Germany) were resuspended in 100 % ethanol, vortexed (Vortex Genei 2, USA) for 9 min at maximum speed and pelleted (Pico 17 centrifuge, Thermo Scientific, Germany) at 13,300 rpm for 1 min. The supernatant was discarded and the gold microcarriers were washed twice with 1 ml of sterile dH_2O and resuspended in 250 μl of sterile 50 % glycerol, vortexed for 3 min at max speed and divided into 40 μl aliquots in 1.5 ml reaction tubes. After this the gold microcarrier aliquots were ready for labeling with DNA and were either used directly or frozen at -80°C for later use.

For labeling with DNA, 1 μg of plasmid DNA was added to the homogenized aliquot of 20 μl gold suspension. The tube was vortexed for 1 min at max speed. While vortexing 20 μl of 2.5 M calcium chloride solution was added and the tube was vortexed for 3 min at maximum speed. 10 μl of 0.1 M sterile spermidine solution was added and the tube was vortexed for 30 sec at maximum speed. 1 ml of 70 % ethanol was added and the tube was vortexed again for 30 sec at maximum speed. The tube was then left standstill to allow the gold microcarriers to settle down. The supernatant was removed and the pelleted gold microcarriers were washed with 100 % ethanol and were then finally pelleted. The supernatant was discarded and the DNA loaded gold microcarriers were resuspended in 40 μl of 100 % ethanol, which were ready for ballistic transformation of leaves.

Leaves of 10 days old maize seedlings were placed upside down on three layers of wet paper towels in a petri dish. The dish was placed onto the second level from the bottom inside the pDS/1000 HeTM Biolistic Particle Delivery System (Biorad, Hercules, USA). 20 μl of the DNA loaded gold microcarrier suspension were given onto the carrier disc and let dry for several min. The gene gun was assembled according to the manufacturer's instructions with a 900 psi rupture disc. A vacuum of upto 3.6 kPa was applied and immediately stopped. Pressure was given until the rupture disc broke. The vacuum was then immediately released. The bombarded leaves were kept at RT for 3 days in petri dish and expression and localization of the fusion protein was monitored using a confocal laser scanning microscope (TCS-SP5, Leica, Germany).

4.8 Staining, Microscopy and Image Processing

4.8.1 Confocal microscopy

All confocal analysis was performed on a TCS SP5 confocal laser scanning microscope (Leica, Bensheim, Germany). The laser channels used for fluorescence-microscopic analysis of excitation and detection wavelengths are summarized in Table 11. Control of the microscope and processing of the image data was performed by the software Leica Application Suite (LAS, Leica, Bensheim, Germany).

Tab. 11: Lasers used and the excitation and detection wavelength

Detection	Excitation Wavelength	Detection Wavelength	Laser type
Cell wall autofluorescence; Calcofluor White;	405 nm	435–480 nm	405 Diode
WGA-AF488; EdU Coupled to WGA AF488	488 nm	490–540 nm	Argon
Propidiumiodid; FM4-64	561 nm	570–640 nm	561 DPSS
mCherry	561nm	580–660nm	561 DPSS
Yellow Fluorescent Protein (YFP)	561nm	520–540nm	561 DPSS

4.8.2 Staining with Calcofluor white

To visualize the hyphae and appressoria of *U. maydis in planta* the leaf samples were harvested at specific time points after infection. For this, the third leaf was removed and cutted of about 2 cm length, 1 cm below the infection needle marks. The leaf fragment is stained in Calcofluor White (Fluorescent Brightener 28, Sigma-Aldrich, Deisenhofen, Germany) for about 30 sec. After washing with water, the middle lamella was dissected apart and the specimen was mounted on the microscope slide. The leaf fragments were analyzed by confocal microscopy.

Calcofluor-Stock Solution	10 mg/ml Fluorescent Brightener 28 in DMSO; Dark Storage, at -20 °C
Calcofluor-Staining Solution	1:100 dilution of the stock solution in 0.2 M Tris-HCl, pH 8.0; Storage at 4 °C

4.8.3 Staining with WGA-AF488 and propidium iodide

This staining method was implemented to track the phenotype of the mutant fungal hyphae during the process of colonization in infected plant tissue. Here, WGA-AF488 stains fungal structures, whereas propidium iodide stains plant cell walls. The harvested

maize leaves were placed in 100 % ethanol for 2–3 days to undergo bleaching and complete removal of chlorophyll. Subsequently, they were incubated for 4 hours in 10 % KOH at 85 °C. This step makes the tissue fleshy and transparent. The samples were washed at least 4–5 times in PBS (pH 7.4) for neutralization. More frequent washing with PBS is necessary to lower the pH near to neutral for the efficient WGA staining. The staining solution was vacuum infiltrated for 3–4 times each for 5 min at 250 mbar in a dessicator. After the stain infiltration, the leaf samples were transferred into PBS and stored in the dark at 4 °C until analysis by confocal microscopy.

WGA-AF488-Stock Solution	1 mg/ml in H ₂ O Storage at 4 °C
Propidium iodide-Stock Solution	10 mg/ml in PBS (pH 7.4) Storage in dark
PBS (pH 7.4)	1.5 mM KH ₂ PO ₄ 8 mM Na ₂ PO ₄ 2.7 mM KCl 137 mM NaCl in H ₂ O _{bid.}
Staining Solution	20 µg/ml Propidium iodide 10 µg/ml WGA-AF488 0.1% Tween 20 in PBS (pH 7.4)

4.8.4 Edu-WGA-AF488 based DNA synthesis assay

This assay was used for monitoring the DNA synthesis in the proliferating tumorous tissues of both seedling and tassels. The infections were done as previously mentioned in section 4.7.3. In seedlings, after 4 dpi the third infected leaf which is seen to induce first infection symptom was used for the EdU assay and incubated for 5 hours with 10 µM EdU (Invitrogen, Karlsruhe, Germany) in small chambers designed for labeling physiologically active leaves. In case of tassels at 3 dpi after infection, the immature mitotically active tassel was injected with 1 ml of 20 µM EdU with an 26-gauge hypodermic needle through the whorl of leaves surrounding the inflorescence apex and labeling was done for 5 hours to label the anther cells. After the labeling procedure the area in seedling, below the infection holes was detached and fixed in 100 % ethanol. For the tassel tissue, around 150 anthers from different parts of the tassel were dissected to ensure random sampling with equal probability of labeled anthers and fixed in ethanol. The EdU staining procedure

was done as describe previously by Kelliher and Walbot, 2011. The samples were washed once with fresh ethanol which was followed by washing the samples two times in PBS (pH 7.4) + 2 % BSA, then the samples were transferred to permeabilization solution (PBS + 1 % Triton X-100) at RT for 20 min with rocking. After permeabilization, samples were washed twice in PBS + 2 % BSA then directly incubated for 30 min at room temperature (RT) with EdU Click-IT cocktail for detection (Invitrogen) and 20 µg/ml PI (PI, Molecular Probes, Eugene) in addition, which was directly added to the solution. The additions for EdU detection solution was done as per the manufacturer's instruction. The samples were then washed twice in PBS (pH 7.4) +2 % BSA, transferred to PBS (pH 7.4), and kept at 4 °C in the dark for till imaging and analyzing by confocal microscope. Triton treatment results in a nuclear stain and is compatible with EdU co-staining. Moreover, it prevents the cell shrinkage and quick penetration of the fixer and allows better preservation of mitotic chromosomes (Kotogany et al., 2010).

4.8.5 Fluorescence microscopy and image processing

The cell morphological observations of *U. maydis* were performed predominantly on a light microscope (Axiophot, Zeiss) using Nomarski optics. 100-fold and Plan-Apochromat objective of 40 or 63 X (Zeiss) was used, with a 1.4 numerical aperture for DIC microscopy and fluorescence microscopy. Digital images of a high-resolution CCD camera (C4742, Hamamatsu) were processed with the programs MetaMorph (version 6.2.6) and Photoshop 5.5 (Adobe).

4.8.6 Transmission electron microscopy (TEM) with immunogold labeling

Preparation of samples for TEM and immunogold labeling was performed with a modified method as described previously by Heyneke et al., 2013. Small samples (about 1.5 mm²) from at least 12 different leaves from 2 dpi and 6 dpi were cut on a modeling wax plate in a drop of 2.5 % paraformaldehyde, 0.5 % glutaraldehyde in 0.06 M Sørensen phosphate buffer at pH 7.2. Samples were then fixed for 90 min at RT in the same fixing solution. For cytohistochemical investigations samples were rinsed in 0.06 M Sørensen phosphate buffer (pH 7.2) for 4 times 15 min each after fixation. They were then dehydrated in increasing concentrations of acetone (50 %, 70 %, and 90 %) at RT for 20 min at each step. Subsequently, specimens were gradually infiltrated with increasing concentrations of LR-White resin (30 %, 60 % and 100 %; London Resin Company Ltd., Berkshire, UK) mixed with acetone (90 %) for a minimum of 3 hours per step. Samples were finally embedded in pure, fresh LR-White resin and polymerized at 50 °C for 48 hours in small plastic containers under anaerobic conditions. Ultrathin sections (80 nm) were cut with a Reichert Ultracut S ultramicrotome (Leica Microsystems, Vienna, Austria).

Immunogold labeling of See1-3X HA was done with the same modified method according to Heyneke et al., 2013 with ultrathin sections on coated nickel grids with the automated immunogold labeling system Leica EM IGL (Leica, Microsystems, Vienna, Austria). The ideal dilutions and incubation times of the primary monoclonal anti HA antibody (produced in rabbit by Sigma, St Louis, MO, USA) and secondary antibodies (goat anti rabbit from British BioCell International, Cardiff, UK) were determined in preliminary studies by evaluating the labeling density after a series of labeling experiments. The final dilution of primary and secondary antibodies used in this study showed a minimum of background labeling outside the sample with a maximum of specific labeling in the sample. The sections were blocked for 20 min with 2 % bovine serum albumin (BSA, Sigma-Aldrich, St. Louis, MO, USA) in phosphate buffered saline (PBS, pH 7.2) and then treated with the primary antibodies against See1 3X-HA diluted 1:2000 in PBS containing 1 % BSA . After washing sections with PBS containing 1 % BSA 3 times for 5 min each, they were treated with a 10 nm gold-conjugated secondary antibodies (goat anti rabbit IgG) diluted 1:100 in PBS containing 1 % BSA for 90 min at RT. After a short wash in PBS (3 times for 5 min), and distilled water (2 times for 5 min) labeled grids were post-stained with uranyl-acetate (2 % dissolved in aqua bidest) for 15 s and then investigated with a Philips CM10 transmission electron microscope. Micrographs of randomly photographed immunogold labeled sections were digitized and gold particles were counted automatically using the software package Cell D with the particle analysis tool (Olympus, Life and Material Science Europa GmbH, Hamburg, Germany) in different visually identified and manually traced cell structures. The obtained data were statistically evaluated using Statistica (Stat-Soft Europe, Hamburg, Germany).

4.9 Bioinformatic methods

The cloning strategies and amino acid or nucleotide sequence comparisons was carried out with the program Clone Manager 9.0 which has been developed by the company Sci-Ed Software. The necessary sequences were identified using the National Center for Biotechnology Information (NCBI; www.ncbi.nlm.nih.gov/) and MIPS *U. maydis* Database (<http://mips.helmholtz-muenchen.de/genre/proj/ustilago/>). The nucleotide sequences and the similar protein were screened from the web pages of BLAST (Basic Local Alignment Search Tool; Altschul et al., 1990). Domain analyzes were performed using the SMART (Simple Modular Architecture Research Tool) program (<http://smart.embl-heidelberg>) and proteins were analyzed by the program SignalP 4.0 program (Nielsen et al., 1997; Bendtsen et al., 2004; www.cbs.dtu.dk/services/SignalP/) and TargetP (<http://www.cbs.dtu.dk/services/TargetP/>) for prediction of an N-terminal signal sequence. Analysis and

comparison of peptides obtained from the Mass Spectrometry was performed with the MASCOT Search Engine (Matrix Science, USA).

5 Bibliography

- Aarts, N., Metz, M., Holub, E., Staskawicz, B.J., Daniels, M.J. and Parker, J.E.** (1998). Different requirements for EDS1 and NDR1 by disease resistance genes define at least two R gene-mediated signaling pathways in Arabidopsis. *Proc. Natl. Acad. of Sci. USA* **95**: 10306-10311.
- Abramovitch, R.B. and Martin, G.B.** (2005). AvrPtoB: a bacterial type III effector that both elicits and suppresses programmed cell death associated with plant immunity. *FEMS microbiology letters* **245**: 1-8.
- Aichinger, C., Hansson, K., Eichhorn, H., Lessing, F., Mannhaupt, G., Mewes, W. and Kahmann, R.** (2003). Identification of plant-regulated genes in *Ustilago maydis* by enhancer-trapping mutagenesis. *Mol Genet Genomics* **270**: 303-314.
- Altschul, S.F., Gish, W., Miller, W., Myers, E.W. and Lipman, D.J.** (1990). Basic local alignment search tool. *J Mol Biol* **215**: 403-410.
- Austin, M.J., Muskett, P., Kahn, K., Feys, B.J., Jones, J.D. and Parker, J.E.** (2002). Regulatory role of SGT1 in early R gene-mediated plant defenses. *Science* **295**: 2077-2080.
- Ausubel, F.M.** (2005). Are innate immune signaling pathways in plants and animals conserved? *Nature immunology* **6**: 973-979.
- Ausubel, F.M., Brent, R., Kingston, R.E., Moore, D.D., Seidman, J.G., Smith, J.A. and Struhl, K.** (2002). Short protocols in molecular biology: a compendium of methods from current protocols in molecular biology. *Wiley*.
- Azevedo, C., Sadanandom, A., Kitagawa, K., Freialdenhoven, A., Shirasu, K. and Schulze-Lefert, P.** (2002). The RAR1 interactor SGT1, an essential component of R gene-triggered disease resistance. *Science* **295**: 2073-2076.
- Bai, C., Sen, P., Hofmann, K., Ma, L., Goebel, M., Harper, J.W. and Elledge, S.J.** (1996). SKP1 connects cell cycle regulators to the ubiquitin proteolysis machinery through a novel motif, the F box. *Cell*. **86**: 263-274.
- Bakkeren, G., Kamper, J. and Schirawski, J.** (2008). Sex in smut fungi: Structure, function and evolution of mating-type complexes. *Fungal Genet Biol* **45 Suppl 1**: S15-21.
- Bansal, P.K., Nourse, A., Abdulle, R. and Kitagawa, K.** (2009). Sgt1 Dimerization Is Required for Yeast Kinetochores Assembly. *J Biol Chem* **284**: 3586-3592.
- Banuett, F. and Herskowitz, I.** (1994). Morphological Transitions in the Life-Cycle of *Ustilago-Maydis* and Their Genetic-Control by the a-and-B-Loci. *Exp Mycol* **18**: 247-266.
- Banuett, F. and Herskowitz, I.** (1996). Discrete developmental stages during teliospore formation in the corn smut fungus, *Ustilago maydis*. *Development* **122**: 2965-2976.

- Bao, Z., Yang, H. and Hua, J.** (2013). Perturbation of cell cycle regulation triggers plant immune response via activation of disease resistance genes. *Proc. Natl. Acad. Sci. USA* **110**: 2407-2412
- Basse, C.W. and Steinberg, G.** (2004). *Ustilago maydis*, model system for analysis of the molecular basis of fungal pathogenicity. *Mol. Plant Pathol.* **5**: 83-92.
- Bauer, R., Begerow, D., Sampaio, J.P., Weiß, M. and Oberwinkler, F.** (2006). The simple-septate basidiomycetes: a synopsis. *Mycol. Progress* **5**: 41-66.
- Begerow, D., Stoll, M. and Bauer, R.** (2006). A phylogenetic hypothesis of Ustilaginomycotina based on multiple gene analyses and morphological data. *Mycologia* **98**: 906-916.
- Bendtsen, D.J., Nielsen, H., von Heijne, G. and Brunak, S.** (2004). Improved prediction of signal peptides: SignalP 3.0. *J Mol Biol* **340**: 783-795.
- Bhattacharjee, S., Stahelin, R.V., Speicher, K.D., Speicher, D.W. and Haldar, K.** (2012). Endoplasmic reticulum PI(3)P lipid binding targets malaria proteins to the host cell. *Cell* **148**: 201-212.
- Bhavsar, A.P., Brown, N.F., Stoepel, J., Wiermer, M., Martin, D.D., Hsu, K.J., Imami, K., Ross, C.J., Hayden, M.R., Foster, L.J., Li, X., Hieter, P. and Finlay, B.B.** (2013). The Salmonella type III effector SspH2 specifically exploits the NLR co-chaperone activity of SGT1 to subvert immunity. *PLoS Pathog.* **9**: e1003518.
- Birch, P.R., Rehmany, A.P., Pritchard, L., Kamoun, S. and Beynon, J.L.** (2006). Trafficking arms: oomycete effectors enter host plant cells. *Trends Microbiol* **14**: 8-11.
- Birch, P.R., Boevink, P.C., Gilroy, E.M., Hein, I., Pritchard, L. and Whisson, S.C.** (2008). Oomycete RXLR effectors: delivery, functional redundancy and durable disease resistance. *Curr Opin Plant Biol* **11**: 373-379.
- Bohlmann, R.** (1996). Isolierung und Charakterisierung von filamentspezifisch exprimierten Genen aus *Ustilago maydis*. Dissertation, Ludwig-Maximilians-Universität, München.
- Bolker, M., Urban, M. and Kahmann, R.** (1992). The a Mating Type Locus of *U. maydis* Specifies Cell Signaling Components. *Cell* **68**: 441-450.
- Boller, T. and Felix, G.** (2009). A Renaissance of Elicitors: Perception of Microbe-Associated Molecular Patterns and Danger Signals by Pattern-Recognition Receptors. *Annu Rev Plant Biol* **60**: 379-406.
- Boller, T. and He, S.Y.** (2009). Innate immunity in plants: an arms race between pattern recognition receptors in plants and effectors in microbial pathogens. *Science* **324**: 742-744.

- Bos, J.I., Armstrong, M.R., Gilroy, E.M., Boevink, P.C., Hein, I., Taylor, R.M., Zhendong, T., Engelhardt, S., Vetukuri, R.R., Harrower, B., Dixelius, C., Bryan, G., Sadanandom, A., Whisson, S.C., Kamoun, S. and Birch, P.R.** (2010). Phytophthora infestans effector AVR3a is essential for virulence and manipulates plant immunity by stabilizing host E3 ligase CMPG1. *Proc. Natl. Acad. Sci. USA* **107**: 9909-9914.
- Boter, M., Amigues, B., Peart, J., Breuer, C., Kadota, Y., Casais, C., Moore, G., Kleanthous, C., Ochsenbein, F., Shirasu, K. et al.** (2007). Structural and functional analysis of SGT1 reveals that its interaction with HSP90 is required for the accumulation of Rx, an R protein involved in plant immunity. *Plant Cell* **19**: 3791–3804.
- Bozkurt, T.O., Schornack, S., Banfield, M.J. and Kamoun, S.** (2012). Oomycetes, effectors, and all that jazz. *Curr Opin Plant Biol* **15**: 483-492.
- Bozkurt, T.O., Schornack, S., Win, J., Shindo, T., Ilyas, M., Oliva, R., Cano, L.M., Jones, A.M., Huitema, E., van der Hoorn, R.A. and Kamoun, S.** (2011). Phytophthora infestans effector AVRblb2 prevents secretion of a plant immune protease at the haustorial interface. *Proc. Natl. Acad. Sci. of the USA* **108**: 20832-20837.
- Brachmann, A., Weinzierl, G., Kamper, J. and Kahmann, R.** (2001). Identification of genes in the bW/bE regulatory cascade in *Ustilago maydis*. *Mol Microbiol* **42**: 1047-1063.
- Bradford, M.M.** (1976). A rapid and sensitive method for the quantitation of microgram quantities of protein utilizing the principle of protein-dye binding. *Anal Biochem* **72**: 248-254.
- Brefort, T., Doehlemann, G., Mendoza-Mendoza, A., Reissmann, S., Djamei, A. and Kahmann, R.** (2009). *Ustilago maydis* as a Pathogen. *Annu Rev Phytopathol* **47**: 423-445.
- Brefort, T., Tanaka, S., Neidig, N., Doehlemann, G., Vincon, V. and Kahmann, R.** (2014). Characterization of the Largest Effector Gene Cluster of *Ustilago maydis*. *Plos Pathog* **10**: e1003866.
- Broomfield, P.L.E. and Hargreaves, J.A.** (1992). A single amino-acid change in the iron-sulphur protein subunit of succinate dehydrogenase confers resistance to carboxin in *Ustilago maydis*. *Curr Genet* **22**: 117-121.
- Brukhin, V., Gheyselinck, J., Gagliardini, V., Genschik, P. and Grossniklaus, U.** (2005). The RPN1 subunit of the 26S proteasome in Arabidopsis is essential for embryogenesis. *Plant Cell* **17**: 2723-2737.

- Chandran, D., Inada, N., Hather, G., Kleindt, C.K. and Wildermuth, M.C.** (2010). Laser microdissection of Arabidopsis cells at the powdery mildew infection site reveals site-specific processes and regulators. *Proc. Natl. Acad. Sci. USA* **107**: 460-465.
- Chauhan, R.S., Farman, M.L., Zhang, H.B. and Leong, S.A.** (2002) Genetic and physical mapping of a rice blast resistance locus, Pi-CO39(t), that corresponds to the avirulence gene AVR1-CO39 of *Magnaporthe grisea*. *Mol. Genet. Genomics* **267**: 603–612.
- Chisholm, S.T., Coaker, G., Day, B. and Staskawicz, B.J.** (2006). Host-microbe interactions: Shaping the evolution of the plant immune response. *Cell* **124**: 803-814.
- Christensen, J.J.** (1963). Corn smut caused by *Ustilago maydis*. *An. Phytopathol. Soc. Monogr.* **2**: 1-41.
- Clayton, A. L., Rose, S., Barratt, M. J. and Mahadevan, L. C.** (2000). Phosphoacetylation of histone H3 on *c-fos*- and *c-jun*-associated nucleosomes upon gene activation. *The EMBO Journal* **19**: 3714–3726.
- Cohen, S.N., Chang, A.C.Y. and Hsu, L.** (1972). Nonchromosomal antibiotic resistance in bacteria: genetic transformation of *Escherichia coli* by R-factor DNA. *Proc. Natl. Acad. Sci.* **69**: 2110-2114.
- Conover, W.J.** (1999). *Practical Nonparametric Statistics*, 3rd ed. John Wiley and Sons, New York.
- Collier, S.M. and Moffett, P.** (2009). NB-LRRs work a "bait and switch" on pathogens. *Trends Plant Sci* **14**: 521-529.
- Cui, H., Wang, Y., Xue, L., Chu, J., Yan, C., Fu, J., Chen, M., Innes, R.W. and Zhou, J.M.** (2010). *Pseudomonas syringae* effector protein AvrB perturbs Arabidopsis hormone signaling by activating MAP kinase 4. *Cell Host Microbe* **7**: 164-175.
- Cuzick, A., Maguire, K. and Hammond-Kosack, K.E.** (2009). Lack of the plant signalling component SGT1b enhances disease resistance to *Fusarium culmorum* in Arabidopsis buds and flowers. *New Phytol.* **181**: 901–912.
- Dangl, J.L. and Jones, J.D.G.** (2001). Plant pathogens and integrated defence responses to infection. *Nature* **411**: 826-833.
- Dangl, J.L., Horvath, D.M. and Staskawicz, B.J.** (2013). Pivoting the Plant Immune System from Dissection to Deployment. *Science* **341**: 746-751.
- De Bary, A.** (1853). *Untersuchungen über die Brandpilze*, Berlin.
- de Jonge, R., van Esse, H.P., Kombrink, A., Shinya, T., Desaki, Y., Bours, R., van der Krol, S., Shibuya, N., Joosten, M.H. and Thomma, B.P.** (2010). Conserved fungal LysM effector Ecp6 prevents chitin-triggered immunity in plants. *Science* **329**: 953-955.

- De Pamphilis, M.L.** (2003). Eukaryotic DNA replication origins: reconciling disparate data. *Cell* **114**: 274–275.
- de Wit, P.J.G.M.** (2007). Visions & reflections (minireview) - How plants recognize pathogens and defend themselves. *Cell Mol Life Sci* **64**: 2726-2732.
- Dielen, A.S., Badaoui, S., Candresse, T. and German-Retana, S.** (2010). The ubiquitin/26S proteasome system in plant-pathogen interactions: a never-ending hide-and-seek game. *Mol. Plant Pathol.* **11**: 293-308.
- Djamei, A. and Kahmann, R.** (2012). *Ustilago maydis*: Dissecting the Molecular Interface between Pathogen and Plant. *Plos Pathog* **8**.
- Djamei, A., Schipper, K., Rabe, F., Ghosh, A., Vincon, V., Kahnt, J., Osorio, S., Tohge, T., Fernie, A.R., Feussner, I., Feussner, K., Meinicke, P., Stierhof, Y.D., Schwarz, H., Macek, B., Mann, M. and Kahmann, R.** (2011). Metabolic priming by a secreted fungal effector. *Nature* **478**: 395-398.
- Dodds, P.N. and Rathjen, J.P.** (2010). Plant immunity: towards an integrated view of plant-pathogen interactions. *Nat Rev Genet* **11**: 539-548.
- Doebley, J.** (1992). Mapping the Genes That Made Maize. *Trends Genet* **8**: 302-307.
- Doehlemann, G., Reissmann, S., Assmann, D., Fleckenstein, M. and Kahmann, R.** (2011). Two linked genes encoding a secreted effector and a membrane protein are essential for *Ustilago maydis*-induced tumour formation. *Mol Microbiol* **81**: 751-766.
- Doehlemann, G., Requena, N., Schaefer, P., Brunner, F., O'Connell, R. and Parker, J.E.** (2014). Reprogramming of plant cells by filamentous plant-colonizing microbes. *New Phytol.* doi: 10.1111/nph. 12938
- Doehlemann, G., Schirawski, J. and Kamper, J.** (2014). Functional genomics of smut fungi: From genome sequencing to protein function. *Adv. in Bot. Res.* **70**: 143-172.
- Doehlemann, G., Wahl, R., Vranes, M., de Vries, R.P., Kamper, J. and Kahmann, R.** (2008a). Establishment of compatibility in the *Ustilago maydis*/maize pathosystem. *J Plant Physiol* **165**: 29-40.
- Doehlemann, G., van der Linde, K., Assmann, D., Schwambach, D., Hof, A., Mohanty, A., Jackson, D. and Kahmann, R.** (2009). Pep1, a secreted effector protein of *Ustilago maydis*, is required for successful invasion of plant cells. *Plos Pathog* **5**: e1000290.
- Doehlemann, G., Wahl, R., Horst, R.J., Voll, L.M., Usadel, B., Poree, F., Stitt, M., Pons-Kuhnemann, J., Sonnewald, U., Kahmann, R. and Kamper, J.** (2008b). Reprogramming a maize plant: transcriptional and metabolic changes induced by the fungal biotroph *Ustilago maydis*. *Plant J.* **56**: 181-195.

- Dong, S., Yin, W., Kong, G., Yang, X., Qutob, D., Chen, Q., Kale, S.D., Sui, Y., Zhang, Z., Dou, D., Zheng, X., Gijzen, M., Tyler, B.M. and Wang, Y.** (2011). Phytophthora sojae avirulence effector Avr3b is a secreted NADH and ADP-ribose pyrophosphorylase that modulates plant immunity. *Plos Pathog* **7**: e1002353.
- Dou, D., Kale, S.D., Wang, X., Jiang, R.H., Bruce, N.A., Arredondo, F.D., Zhang, X. and Tyler, B.M.** (2008). RXLR-mediated entry of Phytophthora sojae effector Avr1b into soybean cells does not require pathogen-encoded machinery. *Plant Cell* **20**: 1930-1947.
- Dreher, K. and Callis, J.** (2007). Ubiquitin, hormones and biotic stress in plants. *Annals of botany* **99**: 787-822.
- Dubacq, C., Guerois, R., Courbeyrette, R., Kitagawa, K. and Mann, C.** (2002). Sgt1p contributes to cyclic AMP pathway activity and physically interacts with the adenyl cyclase Cyr1p/Cdc35p in budding yeast. *Eukaryot Cell* **1**: 568-582.
- El Oirdi, M. and Bouarab, K.** (2007). Plant signalling components EDS1 and SGT1 enhance disease caused by the necrotrophic pathogen *Botrytis cinerea*. *New Phytol.* **175**: 131–139.
- Ellis, J.G., Dodds, P.N. and Lawrence, G.J.** (2007). The role of secreted proteins in diseases of plants caused by rust, powdery mildew and smut fungi. *Curr Opin Microbiol* **10**: 326-331.
- Evert, R.F., Russin, W.A. and Bosabalidis, A.M.** (1996). Anatomical and ultrastructural changes associated with sink to source transition in developing maize leaves. *Int. J. Plant. Sci.* **157**: 247-261.
- Faulkner, C. and Robatzek, S.** (2012). Plants and pathogens: putting infection strategies and defence mechanisms on the map. *Curr Opin Plant Biol* **15**: 699-707.
- Feng, F. and Zhou, J.M.** (2012). Plant-bacterial pathogen interactions mediated by type III effectors. *Curr Opin Plant Biol* **15**: 469-476.
- Flor, H.H.** (1971). Current Status of Gene-for-Gene Concept. *Annu Rev Phytopathol* **9**: 275-296.
- Flowers, J.L. and Vaillancourt, L.J.** (2005). Parameters affecting the efficiency of Agrobacterium tumefaciens-mediated transformation of Colletotrichum graminicola. *Current Genetics* **48**: 380-388.
- Friesen, T.L., Faris, J.D., Solomon, P.S. and Oliver, R.P.** (2008). Host-specific toxins: effectors of necrotrophic pathogenicity. *Cell Microbiol* **10**: 1421-1428.
- Gao, L., Kelliher, T., Nguyen, L., and Walbot, V.** (2013). Ustilago maydis reprograms cell proliferation in maize anthers. *Plant J.* **75**: 903-914.

- Garcia-Ranea, J.A., Mirey, G., Camonis, J. and Valencia, A.** (2002). p23 and HSP20/alpha-crystallin proteins define a conserved sequence domain present in other eukaryotic protein families. *Febs Lett* **529**: 162-167.
- Gillissen, B., Bergemann, J., Sandmann, C., Schroeer, B., Bolker, M. and Kahmann, R.** (1992). A 2-Component Regulatory System for Self Non-Self Recognition in *Ustilago-Maydis*. *Cell* **68**: 647-657.
- Giraldo, M.C., Dagdas, Y.F., Gupta, Y.K., Mentlak, T.A., Yi, M., Martinez-Rocha, A.L., Saitoh, H., Terauchi, R., Talbot, N.J. and Valent, B.** (2013). Two distinct secretion systems facilitate tissue invasion by the rice blast fungus *Magnaporthe oryzae*. *Nat. Comm.* **4**: 1996.
- Godfrey, D., Bohlenius, H., Pedersen, C., Zhang, Z., Emmersen, J. and Thordal-Christensen, H.** (2010). Powdery mildew fungal effector candidates share N-terminal Y/F/WxC-motif. *BMC Genomics* **11**: 317.
- Gomez, S.K., Javot, H., Deewatthanawong, P., Torres-Jerez, I., Tang, Y., Blancaflor, E.B., Udvardi, M.K., and Harrison, M.J.** (2009). *Medicago truncatula* and *Glomus intraradices* gene expression in cortical cells harboring arbuscules in the arbuscular mycorrhizal symbiosis. *BMC plant biology* **9**: 10.
- Gonzalez, N., Vanhaeren, H. and Inze, D.** (2012). Leaf size control: complex coordination of cell division and expansion. *Trends Plant Sci.* **17**: 332-340.
- Gopalan, S., Bauer, D.W., Alfano, J.R., Loniello, A.O., He, S.Y. and Collmer, A.** (1996). Expression of the *Pseudomonas syringae* avirulence protein AvrB in plant cells alleviates its dependence on the hypersensitive response and pathogenicity (Hrp) secretion system in eliciting genotype-specific hypersensitive cell death. *Plant Cell* **8**: 1095-1105.
- Grant, S.G., Jessee, J., Bloom, F.R. and Hanahan, D.** (1990). Differential plasmid rescue from transgenic mouse DNAs into *Escherichia coli* methylation-restriction mutants. *Proc. Natl. Acad. Sci. USA* **87**: 4645-4649.
- Gray, W.M., Muskett, P.R., Chuang, H.W. and Parker, J.E.** (2003). Arabidopsis SGT1b is required for SCF(TIR1)-mediated auxin response. *Plant Cell* **15**: 1310-1319.
- Gurtley, L.R., Walters, R.A. and Tobey, R.A.** (1975). Sequential phosphorylation of histone subfractions in the Chinese hamster cell cycle. *J. Biol. Chem.* **250**: 3936-3944.
- Hahn, M. and Mendgen, K.** (2001). Signal and nutrient exchange at biotrophic plant-fungus interfaces. *Curr Opin Plant Biol* **4**: 322-327.
- Hann, D.R. and Rathjen, J.P.** (2007). Early events in the pathogenicity of *Pseudomonas syringae* on *Nicotiana benthamiana*. *Plant J.* **49**: 607-618.

- Hawes, M.C. and Smith, L.Y.** (1989). Requirement for Chemotaxis in Pathogenicity of *Agrobacterium-Tumefaciens* on Roots of Soil-Grown Pea-Plants. *J Bacteriol* **171**: 5668-5671.
- Hellens, R.P., Edwards, E.A., Leyland, N.R., Bean, S. and Mullineaux, P.M.** (2000). pGreen: a versatile and flexible binary Ti vector for *Agrobacterium*-mediated plant transformation. *Plant Mol. Biol.* **42**: 819-832.
- Hemetsberger, C.** (2012). Das Effektorprotein Pep1 und seine Rolle in der Biotrophie von Brandpilzen. *Dissertation*. Philipps-Universität Marburg.
- Hemetsberger, C., Herrberger, C., Zechmann, B., Hillmer, M. and Doehlemann, G.** (2012). The *Ustilago maydis* effector Pep1 suppresses plant immunity by inhibition of host peroxidase activity. *Plos Pathog* **8**: e1002684.
- Heyneke, E., Luschin-Ebengreuth, N., Krajcer, I., Wolking, V., Muller, M. and Zechmann, B.** (2013). Dynamic compartment specific changes in glutathione and ascorbate levels in *Arabidopsis* plants exposed to different light intensities. *BMC Plant Biol.* **13**: 104.
- Hof, A.** (2009). Identifizierung von Zelltod-supprimierenden Proteinen in *Ustilago maydis* und *Ustilago hordei*. *Masterarbeit*. Philipps-Universität Marburg.
- Hofmann, J., Wiczorek, K., Blochl, A. and Grundler, F.M.** (2007). Sucrose supply to nematode-induced syncytia depends on the apoplasmic and symplasmic pathways. *J. Exp. Bot.* **58**: 1591-1601.
- Hoffman, C.S. and Winston, F.** (1987). A ten-minute DNA preparation from yeast efficiently releases autonomous plasmids for transformation of *Escherichia coli*. *Gene* **57**: 267-272.
- Höfgen, R. and Willmitzer, L.** (1988). Storage of competent cells for *Agrobacterium* transformation. *Nucleic Acids Res* **16**:
- Hogenhout, S.A., Van der Hoorn, R.A.L., Terauchi, R. and Kamoun, S.** (2009). Emerging Concepts in Effector Biology of Plant-Associated Organisms. *Mol Plant Microbe In* **22**: 115-122.
- Holliday, R.** (2004). Early studies on recombination and DNA repair in *Ustilago maydis*. *DNA repair* **3**: 671-682.
- Horbach, R., Navarro-Quesada, A.R., Knogge, W. and Deising, H.B.** (2011). When and how to kill a plant cell: Infection strategies of plant pathogenic fungi. *J Plant Physiol* **168**: 51-62.
- Hoser, R., Zurczak, M., Lichocka, M., Zuzga, S., Dadlez, M., Samuel, M.A., Ellis, B.E., Stuttmann, J., Parker, J.E., Hennig, J. and Krzymowska, M.** (2013). Nucleocytoplasmic partitioning of tobacco N receptor is modulated by SGT1. *The New phytologist* **200**: 158-171.

- Houben A., Wako, T., Furushima-Shimogawara, R., Presting, G., Kunzel, G., Schubert, I. and Fukui, K.** (1999). The cell cycle dependent phosphorylation of histone H3 is correlated with the condensation of plant mitotic chromosomes. *Plant J.* **18**: 675-679.
- Ingold, C.T.** (1989). Basidium Development in Some Species of *Ustilago*. *Mycol Res* **93**: 405-412.
- Irieda, H., Maeda, H., Akiyama, K., Hagiwara, A., Saitoh, H., Uemura, A., Terauchi, R. and Takano, Y.** (2014). *Colletotrichum orbiculare* Secretes Virulence Effectors to a Biotrophic Interface at the Primary Hyphal Neck via Exocytosis Coupled with SEC22-Mediated Traffic. *Plant Cell* **26**: 2265-2281.
- Jelenska, J., van Hal, J.A. and Greenberg, J.T.** (2010). *Pseudomonas syringae* hijacks plant stress chaperone machinery for virulence. *Proc. Natl. Acad. Sci. USA* **107**: 13177-13182.
- Jia, Y., McAdams, S.A., Bryan, G.T., Hershey, H.P. and Valent, B.** (2000). Direct interaction of resistance gene and avirulence gene products confers rice blast resistance. *EMBO J* **19**: 4004-4014.
- Jiang, R.H., Tripathy, S., Govers, F. and Tyler, B.M.** (2008). RXLR effector reservoir in two *Phytophthora* species is dominated by a single rapidly evolving superfamily with more than 700 members. *Proc. Natl. Acad. Sci. USA* **105**: 4874-4879.
- Jones, J.D.G. and Dangl, J.L.** (2006). The plant immune system. *Nature* **444**: 323-329.
- Jurado, S., Diaz-Trivino, S., Abraham, Z., Manzano, C., Gutierrez, C. and del Pozo, C.** (2008). SKP2A, an F-box protein that regulates cell division, is degraded via the ubiquitin pathway. *Plant J.* **53**: 828-841.
- Kahmann, R., Steinberg, G., Basse, C., Feldbrügge, M. and Kämper, J.** (2000). *Ustilago maydis*, the causative agent of corn smut disease. *Fungal Pathology*. Kronstad, J.W. (ed.). Kluwer academic publishers. Dordrecht, The Netherlands: 347-371.
- Kamoun, S.** (2006). A catalogue of the effector secretome of plant pathogenic oomycetes. *Annu Rev Phytopathol* **44**: 41-60.
- Kamoun, S.** (2007). Groovy times: filamentous pathogen effectors revealed. *Curr Opin Plant Biol* **10**: 358-365.
- Kamper, J.** (2004). A PCR-based system for highly efficient generation of gene replacement mutants in *Ustilago maydis*. *Mol Genet Genomics* **271**: 103-110.
- Kamper, J., Reichmann, M., Romeis, T., Bolker, M. and Kahmann, R.** (1995). Multiallelic recognition: nonself-dependent dimerization of the bE and bW homeodomain proteins in *Ustilago maydis*. *Cell* **81**: 73-83.

- Kamper, J. et al.** (2006). Insights from the genome of the biotrophic fungal plant pathogen *Ustilago maydis*. *Nature* **444**: 97-101.
- Kankanala, P., Czymmek, K. and Valent, B.** (2007). Roles for rice membrane dynamics and plasmodesmata during biotrophic invasion by the blast fungus. *Plant Cell* **19**: 706-724.
- Kaszas, E. and Cande, W. Z.** (2000). Phosphorylation of histone H3 is correlated with changes in the maintenance of sister chromatid cohesion during meiosis in maize, rather than the condensation of chromatin. *J. Cell Sci* **113**: 3217-3226.
- Kay, S. and Bonas, U.** (2009). How *Xanthomonas* type III effectors manipulate the host plant. *Curr. Opin. Microbiol.* **12**: 37-43.
- Kazan, K. and Lyons, R.** (2014). Intervention of Phytohormone Pathways by Pathogen Effectors. *Plant Cell* **26**: 2285-2309.
- Kelliher, T. and Walbot, V.** (2011). Emergence and patterning of the five cell types of the *Zea mays* anther locule. *Dev. Biol.* **350**: 32-49.
- Kemen, E., Kemen, A.C., Rafiqi, M., Hempel, U., Mendgen, K., Hahn, M. and Voegelé, R.T.** (2005). Identification of a protein from rust fungi transferred from haustoria into infected plant cells. *Molecular plant-microbe interactions : Mol Plant Microbe In.* **18**: 1130-1139.
- Khang, C.H., Berruyer, R., Giraldo, M.C., Kankanala, P., Park, S.Y., Czymmek, K., Kang, S. and Valent, B.** (2010). Translocation of *Magnaporthe oryzae* effectors into rice cells and their subsequent cell-to-cell movement. *Plant Cell* **22**: 1388-1403.
- Kim, N.H., Kim, D.S., Chung, E.H. and Hwang, B.K.** (2014). Pepper suppressor of the G2 allele of *skp1* interacts with the receptor-like cytoplasmic kinase1 and type III effector *AvrBsT* and promotes the hypersensitive cell death response in a phosphorylation-dependent manner. *Plant Physiol.* **165**: 76-91.
- Kitagawa, K., Skowrya, D., Elledge, S.J., Harper, J.W. and Hieter, P.** (1999). SGT1 encodes an essential component of the yeast kinetochore assembly pathway and a novel subunit of the SCF ubiquitin ligase complex. *Mol Cell* **4**: 21-33.
- Kleemann, J., Rincon-Rivera, L.J., Takahara, H., Neumann, U., Ver Loren van Themaat, E., van der Does, H.C., Hacquard, S., Stuber, K., Will, I., Schmalenbach, W., Schmelzer, E. and O'Connell, R.J.** (2012). Sequential delivery of host-induced virulence effectors by appressoria and intracellular hyphae of the phytopathogen *Colletotrichum higginsianum*. *Plos Pathog* **8**: e1002643.
- Koeck, M., Hardham, A.R. and Dodds, P.N.** (2011). The role of effectors of biotrophic and hemibiotrophic fungi in infection. *Cell Microbiol* **13**: 1849-1857.

- Koncz, C. and Schell, J.** (1986). The promoter of TL-DNA gene 5 controls the tissue-specific expression of chimaeric genes carried by a novel type of *Agrobacterium* binary vector. *Mol Gen Genet.* **204**: 383-396.
- Kotogany, E., Dudits, D., Horvath, G.V. and Ayaydin, F.** (2010). A rapid and robust assay for detection of S-phase cell cycle progression in plant cells and tissues by using ethynyl deoxyuridine. *Plant Meth.* **6**: 5.
- Kunkel, B.N. and Brooks, D.M.** (2000) Cross talk between signaling pathways in pathogen defense *Curr Opin Plant Biol.* **5**: 325-331.
- Lahrman, U., Ding, Y., Banhara, A., Rath, M., Hajirezaei, M.R., Dohlemann, S., von Wiren, N., Parniske, M. and Zuccaro, A.** (2013). Host-related metabolic cues affect colonization strategies of a root endophyte. *Proc.Natl. Acad. Sci. USA* **110**: 13965-13970.
- Laemmli, U.K.** (1970). Cleavage of structural proteins during the assembly of the head of bacteriophage T4. *Nature* **227**: 680-685.
- Laurie, J.D., Ali, S., Linning, R., Mannhaupt, G., Wong, P., Guldener, U., Munsterkotter, M., Moore, R., Kahmann, R., Bakkeren, G. and Schirawski, J.** (2012). Genome comparison of barley and maize smut fungi reveals targeted loss of RNA silencing components and species-specific presence of transposable elements. *Plant Cell* **24**: 1733-1745.
- Li, P., Ponnala, L., Gandotra, N., Wang, L., Si, Y., Tausta, S.L., Kebrom, T.H., Provar, N., Patel, R., Myers, C.R., Reidel, E.J., Turgeon, R., Liu, P., Sun, Q., Nelson, T. and Brutnell, T.P.** (2010). The developmental dynamics of the maize leaf transcriptome. *Nature Genet.* **42**: 1060-1067.
- Liu, Y., Schiff, M., Serino, G., Deng, X.W. and Dinesh-Kumar, S.P.** (2002). Role of SCF ubiquitin-ligase and the COP9 signalosome in the N gene-mediated resistance response to Tobacco mosaic virus. *Plant Cell* **14**: 1483-1496.
- Lotze, M.T., Zeh, H.J., Rubartelli, A., Sparvero, L.J., Amoscato, A.A., Washburn, N.R., DeVera, M.E., Liang, X., Tor, M. and Billiar, T.** (2007). The grateful dead: damage-associated molecular pattern molecules and reduction/oxidation regulate immunity. *Immunol Rev* **220**: 60-81.
- Loubradou, G., Brachmann, A., Feldbrugge, M. and Kahmann, R.** (2001). A homologue of the transcriptional repressor Ssn6p antagonizes cAMP signalling in *Ustilago maydis*. *Mol Microbiol* **40**: 719-730.
- Luttrell, E.S.** (1981). Tissue Replacement Diseases Caused by Fungi. *Annu Rev Phytopathol* **19**: 373-389.

- Mahadevan L.C., Willis, A. C. and Barratt, M.J.** (1991). Rapid histone H3 phosphorylation in response to growth factors, phorbol esters, okadaic acid and protein synthesis inhibitors. *Cell* **65**: 775–783.
- Manning, V.A., Hamilton, S.M., Karplus, P.A. and Ciuffetti, L.M.** (2008). The Arg-Gly-Asp-containing, solvent-exposed loop of Ptr ToxA is required for internalization. *Molecular plant-microbe interactions : Mol. Plant Microbe Int.* **21**: 315-325.
- Marshall, R., Kombrink, A., Motteram, J., Loza-Reyes, E., Lucas, J., Hammond-Kosack, K.E., Thomma, B.P. and Rudd, J.J.** (2011). Analysis of two in planta expressed LysM effector homologs from the fungus *Mycosphaerella graminicola* reveals novel functional properties and varying contributions to virulence on wheat. *Plant Physiol* **156**: 756-769.
- Martinez-Espinoza, A.D., Garcia-Pedrajas, M.D. and Gold, S.E.** (2002). The Ustilaginales as plant pests and model systems. *Fungal Genet Biol* **35**: 1-20.
- Massonnet, C., Vile, D., Fabre, J., Hannah, M.A., Caldana, C., Lisec, J., Beemster, G.T., Meyer, R.C., Messerli, G., Gronlund, J. T., et al.** (2010). Probing the reproducibility of leaf growth and molecular phenotypes: a comparison of three *Arabidopsis* accessions cultivated in ten laboratories. *Plant Physiol.* **152**: 2142–2157
- Maunoury, N., Redondo-Nieto, M., Bourcy, M., Van de Velde, W., Alunni, B., Laporte, P., Durand, P., Agier, N., Marisa, L., Vaubert, D., Delacroix, H., Duc, G., Ratet, P., Aggerbeck, L., Kondorosi, E. and Mergaert, P.** (2010). Differentiation of symbiotic cells and endosymbionts in *Medicago truncatula* nodulation are coupled to two transcriptome-switches. *PloS one* **5**: e9519.
- Mendgen, K. and Hahn, M.** (2002). Plant infection and the establishment of fungal biotrophy. *Trends Plant Sci* **7**: 352-356.
- Mendoza-Mendoza, A., Berndt, P., Djamei, A., Weise, C., Linne, U., Marahiel, M., Vranes, M., Kamper, J. and Kahmann, R.** (2009). Physical-chemical plant-derived signals induce differentiation in *Ustilago maydis*. *Mol Microbiol* **71**: 895-911.
- Mentlak, T.A., Kombrink, A., Shinya, T., Ryder, L.S., Otomo, I., Saitoh, H., Terauchi, R., Nishizawa, Y., Shibuya, N., Thomma, B.P. and Talbot, N.J.** (2012). Effector-mediated suppression of chitin-triggered immunity by *magnaporthe oryzae* is necessary for rice blast disease. *Plant Cell* **24**: 322-335.
- Mims, C.W., Snetselaar, K.M. and Richardson, E.A.** (1992). Ultrastructure of the Leaf Stripe Smut Fungus *Ustilago-Striiformis* - Host-Pathogen Relationship and Teliospore Development. *Int J Plant Sci* **153**: 289-300.

- Montillet, J.L. and Hirt, H.** (2013). New checkpoints in stomatal defense. *Trends Plant Sci* **18**: 295-297.
- Mueller, A.N., Ziemann, S., Treitschke, S., Assmann, D. and Doehlemann, G.** (2013). Compatibility in the *Ustilago maydis*-maize interaction requires inhibition of host cysteine proteases by the fungal effector Pit2. *Plos Pathog* **9**: e1003177.
- Mueller, O., Kahmann, R., Aguilar, G., Trejo-Aguilar, B., Wu, A. and de Vries, R.P.** (2008). The secretome of the maize pathogen *Ustilago maydis*. *Fungal Genet Biol* **45 Suppl 1**: S63-70.
- Mukhtar, M.S., et al.** (2011). Independently evolved virulence effectors converge onto hubs in a plant immune system network. *Science* **333**: 596-601.
- Mullis, K., Faloona, F., Scharf, S., Saiki, R., Horn, G. and Erlich, H.** (1986). Specific enzymatic amplification of DNA in vitro: the polymerase chain reaction. *Cold Spring Harb Symp Quant Biol* **51 Pt 1**: 263-273.
- Munkvold, K.R. and Martin, G.B.** (2009). Advances in experimental methods for the elucidation of *Pseudomonas syringe* effector function with a focus on AvrPtoB. *Mol. Plant Pathol* **10**: 777-793.
- Muskett, P.R., Kahn, K., Austin, M.J., Moisan, L.J., Sadanandom, A., Shirasu, K., Jones, J.D. and Parker, J.E.** (2002). Arabidopsis RAR1 exerts rate-limiting control of R gene-mediated defenses against multiple pathogens. *Plant Cell* **14**: 979-992.
- Nielsen, H., Engelbrecht, J., Brunak, S. and Heijne, G.** (1997). Identification of prokaryotic and eukaryotic signal peptides and prediction of their cleavage sites. *Protein Eng* **10**: 1-6.
- Noel, L.D., Cagna, G., Stuttmann, J., Wirthmuller, L., Betsuyaku, S., Witte, C.P., Bhat, R., Pochon, N., Colby, T. and Parker, J.E.** (2007). Interaction between SGT1 and cytosolic/nuclear HSC70 chaperones regulates Arabidopsis immune responses. *Plant Cell* **19**: 4061-4076.
- Noir, S., Bömer, M., Takahashi, N., Ishida, T., Tsui, T.L., Balbi, V., Shanahan, H., Sugimoto, K. and Devoto, A.** (2013). Jasmonate controls leaf growth by repressing cell proliferation and the onset of endoreduplication while maintaining a potential stand-by mode. *Plant Physiol* **161**: 1930–1951.
- Nurnberger, T. and Brunner, F.** (2002). Innate immunity in plants and animals: emerging parallels between the recognition of general elicitors and pathogen-associated molecular patterns. *Curr Opin Plant Biol* **5**: 318-324.
- Oerke, E.C.** (2006). Crop losses to pests. *J Agr Sci* **144**: 31-43.
- Oerke, E.C. and Dehne, H.W.** (1997). Global crop production and the efficacy of crop protection - Current situation and future trends. *Eur J Plant Pathol* **103**: 203-215.

- Oparka, K.J., Prior, D.A., Santa Cruz, S., Padgett, H.S. and Beachy, R.N.** (1997). Gating of epidermal plasmodesmata is restricted to the leading edge of expanding infection sites of tobacco mosaic virus (TMV). *Plant J.* **12**: 781-789.
- Panstruga, R. and Dodds, P.N.** (2009). Terrific Protein Traffic: The Mystery of Effector Protein Delivery by Filamentous Plant Pathogens. *Science* **324**: 748-750.
- Park, C.H., Chen, S., Shirsekar, G., Zhou, B., Khang, C.H., Songkumarn, P., Afzal, A.J., Ning, Y., Wang, R., Bellizzi, M., Valent, B. and Wang, G.L.** (2012). The Magnaporthe oryzae effector AvrPiz-t targets the RING E3 ubiquitin ligase APIP6 to suppress pathogen-associated molecular pattern-triggered immunity in rice. *Plant Cell* **24**: 4748-4762.
- Parker, J.E., Holub, E.B., Frost, L.N., Falk, A., Gunn, N.D. and Daniels, M.J.** (1996). Characterization of eds1, a mutation in Arabidopsis suppressing resistance to Peronospora parasitica specified by several different RPP genes. *Plant Cell* **8**: 2033-2046.
- Peart, J.R., Lu, R., Sadanandom, A., Malcuit, I., Moffett, P., Brice, D.C., Schauser, L., Jaggard, D.A., Xiao, S., Coleman, M.J., Dow, M., Jones, J.D., Shirasu, K. and Baulcombe, D.C.** (2002). Ubiquitin ligase-associated protein SGT1 is required for host and nonhost disease resistance in plants. *Proc. Natl. Acad. Sci. USA* **99**: 10865-10869.
- Pfaffl, M.W., Horgan, G.W. and Dempfle, L.** (2002). Relative expression software tool (REST©) for group-wise comparison and statistical analysis of relative expression results in real-time PCR. *Nucleic Acids Research* **30**: 1–10.
- Prigent, C. and Dimitrov, S.** (2003). Phosphorylation of serine 10 in histone H3, what for? *J. Cell Sci.* **116**: 3677-3685.
- Poething, R.S. and Szymkowiak, E.J.** (1995). Clonal analysis of leaf development in maize. *Maydica* **40**: 67-76.
- Rafiqi, M., Ellis, J.G., Ludowici, V.A., Hardham, A.R. and Dodds, P.N.** (2012). Challenges and progress towards understanding the role of effectors in plant-fungal interactions. *Curr Opin Plant Biol* **15**: 477-482.
- Rafiqi, M., Gan, P.H., Ravensdale, M., Lawrence, G.J., Ellis, J.G., Jones, D.A., Hardham, A.R. and Dodds, P.N.** (2010). Internalization of flax rust avirulence proteins into flax and tobacco cells can occur in the absence of the pathogen. *Plant Cell* **22**: 2017-2032.
- Rooney, H.C., Van't Klooster, J.W., van der Hoorn, R.A., Joosten, M.H., Jones, J.D. and de Wit, P.J.** (2005). Cladosporium Avr2 inhibits tomato Rcr3 protease required for Cf-2-dependent disease resistance. *Science* **308**: 1783-1786.

- Salic, A. and Mitchison, T.J.** (2008). A chemical method for fast and sensitive detection of DNA synthesis in vivo. *Proc. Natl. Acad. Sci. USA* **105**: 2415-2420.
- Sambrook, J., Frisch, E.F. and Maniatis, T.** (1989). *Molecular Cloning: A laboratory manual*. Cold Spring Harbour, New York.
- Sanger, F., Nicklen, S. and Coulson, A.R.** (1977). DNA sequencing with chain-terminating inhibitors. *Proc. Natl. Acad. Sci. USA* **74**: 5463-5467.
- Schilling, L., Matei, A., Redkar, A., Walbot, V., and Doehlemann, G.** (2014). Virulence of the maize smut *Ustilago maydis* is shaped by organ-specific effectors. *Mol. Plant Pathol.* **15**: 780-789.
- Schirawski, J., Mannhaupt, G., Munch, K., Brefort, T., Schipper, K., Doehlemann, G., Di Stasio, M., Rossel, N., Mendoza-Mendoza, A., Pester, D., Muller, O., Winterberg, B., Meyer, E., Ghareeb, H., Wollenberg, T., Munsterkotter, M., Wong, P., Walter, M., Stukenbrock, E., Guldener, U. and Kahmann, R.** (2010). Pathogenicity determinants in smut fungi revealed by genome comparison. *Science* **330**: 1546-1548.
- Schreiner, P., Chen, X., Husnjak, K., Randles, L., Zhang, N., Elsasser, S., Finley, D., Dikic, I., Walters, K.J. and Groll, M.** (2008). Ubiquitin docking at the proteasome through a novel pleckstrin-homology domain interaction. *Nature* **453**: 548-552.
- Schulz, B., Banuett, F., Dahl, M., Schlesinger, R., Schafer, W., Martin, T., Herskowitz, I. and Kahmann, R.** (1990). The b-alleles of *U. maydis*, whose combinations program pathogenic development, code for polypeptides containing a homeodomain-related motif. *Cell* **60**: 295-306.
- Segonzac, C. and Zipfel, C.** (2011). Activation of plant pattern-recognition receptors by bacteria. *Curr. Opin. Microbiol.* **14**: 54-61.
- Shirasu, K.** (2009). The HSP90-SGT1 chaperone complex for NLR immune sensors. *Annu Rev Plant Biol* **60**: 139-164.
- Shurtleff, M.C.** (1980). *Compendium of Corn Diseases*, 2nd Ed. American Phytopathological Society, St Paul, MN.
- Skibbe, D.S., Doehlemann, G., Fernandes, J. and Walbot, V.** (2010). Maize tumors caused by *Ustilago maydis* require organ-specific genes in host and pathogen. *Science* **328**: 89-92.
- Snetselaar, K.M. and Mims, C.W.** (1994). Light and Electron-Microscopy of *Ustilago maydis* hyphae in maize. *Mycol Res* **98**: 347-355.
- Snetselaar, K.M., Bolker, M. and Kahmann, R.** (1996). *Ustilago maydis* mating hyphae orient their growth toward pheromone sources. *Fungal Genet Biol* **20**: 299-312.

- Song, J.Q., Durrant, W.E., Wang, S., Yan, S.P., Tan, E.H. and Dong, X.N.** (2011). DNA Repair Proteins Are Directly Involved in Regulation of Gene Expression during Plant Immune Response. *Cell Host Microbe* **9**: 115-124.
- Song, J., Win, J., Tian, M., Schornack, S., Kaschani, F., Ilyas, M., van der Hoorn, R.A. and Kamoun, S.** (2009). Apoplastic effectors secreted by two unrelated eukaryotic plant pathogens target the tomato defense protease Rcr3. *Proc. Natl. Acad. Sci. USA* **106**: 1654–1659.
- Southern, E.M.** (1975). Detection of specific sequences among DNA fragments separated by gel electrophoresis. *J Mol Biol* **98**: 503-517.
- Spanu, P.D. et al.** (2010). Genome expansion and gene loss in powdery mildew fungi reveal tradeoffs in extreme parasitism. *Science* **330**: 1543-1546.
- Sparkes, I.A., Runions, J., Kearns, A. and Hawes, C.** (2006). Rapid, transient expression of fluorescent fusion proteins in tobacco plants and generation of stably transformed plants. *Nat Protoc* **1**: 2019-2025.
- Stergiopoulos, I., and de Wit, P.J.** (2009). Fungal effector proteins. *Annu Rev Phytopathol* **47**: 233-263.
- Steinberg, G. and Perez-Martin, J.** (2008). *Ustilago maydis*, a new fungal model system for cell biology. *Trend Cell Biol* **18**: 61-67.
- Stone, S.L. and Callis, J.** (2007). Ubiquitin ligases mediate growth and development by promoting protein death. *Curr Opin Plant Biol* **10**: 624-632.
- Stotz, H.U., Mitrousis, G.K., de Wit, P.J.G.M. and Fitt, B.D.L.** (2014). Effector-triggered defence against apoplastic fungal pathogens. *Trends Plant Sci* **19**: 491-500.
- Sylvester, A.W., Cande, W.Z. and Freeling, M.** (1990). Division and differentiation during normal normal and liguleless-1 maize leaf development. *Development*, **110**: 985-1000.
- Takahashi, A., Casais, C., Ichimura, K. and Shirasu, K.** (2003). HSP90 interacts with RAR1 and SGT1 and is essential for RPS2-mediated disease resistance in *Arabidopsis*. *Proc. Natl. Acad. Sci. USA* **100**: 11777-11782.
- Takken, F.L. and Tameling, W.I.** (2009). To nibble at plant resistance proteins. *Science* **324**: 744-746.
- Takken, F.L.W., Albrecht, M. and Tameling, W.I.L.** (2006). Resistance proteins: molecular switches of plant defence. *Curr Opin Plant Biol* **9**: 383-390.
- Talarczyk, A., Krzymowska, M., Borucki, W. and Hennig, J.** (2002). Effect of yeast CTA1 gene expression on response of tobacco plants to tobacco mosaic virus infection. *Plant Physiol.* **129**: 1032-1044.

- Tanaka, S., Brefort, T., Neidig, N., Djamei, A., Kahnt, J., Vermerris, W., Koenig, S., Feussner, K., Feussner, I. and Kahmann, R.** (2014). A secreted *Ustilago maydis* effector promotes virulence by targeting anthocyanin biosynthesis in maize. *Elife* **3**: e01355.
- Tor, M., Gordon, P., Cuzick, A., Eulgem, T., Sinapidou, E., Mert-Turk, F., Can, C., Dangl, J.L. and Holub, E.B.** (2002). *Arabidopsis* SGT1b is required for defense signaling conferred by several downy mildew resistance genes. *Plant Cell* **14**: 993-1003.
- Tornero, P., Merritt, P., Sadanandom, A., Shirasu, K., Innes, R.W. and Dangl, J.L.** (2002). RAR1 and NDR1 contribute quantitatively to disease resistance in *Arabidopsis*, and their relative contributions are dependent on the R gene assayed. *Plant Cell* **14**: 1005-1015.
- Tsukuda, T., Carleton, S., Fotheringham, S. and Holloman, W.K.** (1988). Isolation and characterization of an autonomously replicating sequence from *Ustilago maydis*. *Mol. Cell. Biol.* **8**: 3703-3709.
- Tsukaya, H.** (2005). Leaf shape: genetic controls and environmental factors. *Int. J. Dev. Biol.* **49**: 547-555.
- Tyler, B.M., Kale, S.D., Wang, Q., Tao, K., Clark, H.R., Drews, K., Antignani, V., Rumore, A., Hayes, T., Plett, J.M., Fudal, I., Gu, B., Chen, Q., Affeldt, K.J., Berthier, E., Fischer, G.J., Dou, D., Shan, W., Keller, N.P., Martin, F., Rouxel, T. and Lawrence, C.B.** (2013). Microbe-independent entry of oomycete RxLR effectors and fungal RxLR-like effectors into plant and animal cells is specific and reproducible. *Molecular plant-microbe interactions : Mol. Plant Microbe Int.* **26**: 611-616.
- Valent, B. and Khang, C.H.** (2010). Recent advances in rice blast effector research. *Curr Opin Plant Biol* **13**: 434-441.
- Valverde, M.E., Paredeslopez, O., Pataky, J.K. and Guevaralara, F.** (1995). Huitlacoche (*Ustilago-Maydis*) as a Food Source - Biology, Composition, and Production. *Crit Rev Food Sci* **35**: 191-229.
- van den Burg, H.A., Spronk, C.A., Boeren, S., Kennedy, M.A., Vissers, J.P., Vuister, G.W., de Wit, P.J. and Vervoort, J.** (2004). Binding of the AVR4 elicitor of *Cladosporium fulvum* to chitotriose units is facilitated by positive allosteric protein-protein interactions: the chitin-binding site of AVR4 represents a novel binding site on the folding scaffold shared between the invertebrate and the plant chitin-binding domain. *J Biol Chem* **279**: 16786-16796.
- van der Hoorn, R.A.L., and Kamoun, S.** (2008). From Guard to Decoy: A new model for perception of plant pathogen effectors. *Plant Cell.* **20**: 2009-2017.

- van der Linde, K., Hemetsberger, C., Kastner, C., Kaschani, F., van der Hoorn, R.A., Kumlehn, J. and Doehlemann, G.** (2012). A maize cystatin suppresses host immunity by inhibiting apoplastic cysteine proteases. *Plant Cell* **24**: 1285-1300.
- van der Linde, K., Kastner, C., Kumlehn, J., Kahmann, R. and Doehlemann, G.** (2011). Systemic virus-induced gene silencing allows functional characterization of maize genes during biotrophic interaction with *Ustilago maydis*. *New Phytol* **189**: 471-483.
- van Hooser, A., Goodrich, D.W., Allis, C.D., Brinkley, B.R. and Mancini, M.A.** (1998). Histone H3 phosphorylation is required for the initiation, but not maintenance, of mammalian chromosome condensation. *J. Cell. Sci.* **111**: 3497-3506.
- Vanky, K.** (1987) *Illustrated Genera of Smut fungi: Cryptogamic studies, Vol I.* Gustav Fischer Verlag, New York.
- Ve, T., Williams, S.J., Catanzariti, A.M., Rafiqi, M., Rahman, M., Ellis, J.G., Hardham, A.R., Jones, D.A., Anderson, P.A., Dodds, P.N. and Kobe, B.** (2013). Structures of the flax-rust effector AvrM reveal insights into the molecular basis of plant-cell entry and effector-triggered immunity. *Proc. Natl. Acad. Sci. USA* **110**: 17594-17599.
- Wahl, R., Wippel, K., Goos, S., Kamper, J. and Sauer, N.** (2010). A novel high-affinity sucrose transporter is required for virulence of the plant pathogen *Ustilago maydis*. *PLoS Biology* **8**: e1000303.
- Walbot, V. and Skibbe, D.S.** (2010). Maize host requirements for *Ustilago maydis* tumor induction. *Sex Plant Reprod* **23**: 1-13.
- Wang, K., Uppalapati, S.R., Zhu, X., Dinesh-Kumar, S.P. and Mysore, K.S.** (2010). SGT1 positively regulates the process of plant cell death during both compatible and incompatible plant-pathogen interactions. *Mol. Plant Pathol.* **11**: 597-611.
- Wawra, S., Djamei, A., Albert, I., Nurnberger, T., Kahmann, R. and van West, P.** (2013). In vitro translocation experiments with RxLR-reporter fusion proteins of Avr1b from *Phytophthora sojae* and AVR3a from *Phytophthora infestans* fail to demonstrate specific autonomous uptake in plant and animal cells. *Mol. Plant Microbe Int.* **26**: 528-536.
- Whisson, S.C., Boevink, P.C., Moleleki, L., Avrova, A.O., Morales, J.G., Gilroy, E.M., Armstrong, M.R., Grouffaud, S., van West, P., Chapman, S., Hein, I., Toth, I.K., Pritchard, L. and Birch, P.R.** (2007). A translocation signal for delivery of oomycete effector proteins into host plant cells. *Nature* **450**: 115-118.
- White, D.G.** (1999). *Compendium of corn diseases*, 3rd edition. VII + 78 pp.

- Win, J., Morgan, W., Bos, J., Krasileva, KV., Cano, LM., et al.** (2007) Adaptive evolution has targeted the C-terminal domain of the RXLR effectors of plant pathogenic oomycetes. *Plant Cell* **19**: 2349–2369
- Witte, C.P., Noel, L.D., Gielbert, J., Parker, J.E. and Romeis, T.** (2004). Rapid one-step protein purification from plant material using the eight-amino acid StrepII epitope. *Plant Mol. Biol.* **55**: 135-147.
- Xiao, S., Calis, O., Patrick, E., Zhang, G., Charoenwattana, P., Muskett, P., Parker, J.E. and Turner, J.G.** (2005). The atypical resistance gene, RPW8, recruits components of basal defence for powdery mildew resistance in Arabidopsis. *Plant J.* **42**: 95-110.
- Yan, S., Wang, W., Marques, J., Mohan, R., Saleh, A., Durrant, W.E., Song, J. and Dong, X.** (2013). Salicylic acid activates DNA damage responses to potentiate plant immunity. *Mol Cell* **52**: 602-610.
- Yang, K.Y., Liu, Y. and Zhang, S.** (2001). Activation of a mitogen-activated protein kinase pathway is involved in disease resistance in tobacco. *Proc. Natl. Acad. Sci. USA* **98**: 741-746.
- Zambryski, P., and Crawford, K.** (2000). Plasmodesmata: gatekeepers for cell-to-cell transport of developmental signals in plants. *Ann. Rev. Cell and Dev. Biol.* **16**: 393-421.
- Zhang, S. and Liu, Y.** (2001). Activation of salicylic acid-induced protein kinase, a mitogen-activated protein kinase, induces multiple defense responses in tobacco. *Plant Cell* **13**: 1877-1889.
- Zipfel, C.** (2009). Early molecular events in PAMP-triggered immunity. *Curr Opin Plant Biol* **12**: 414-420.

Tab. 12: *U. maydis* strains used and generated in this study

Name	Genotype	Resistance ¹	Reference
SG200	a1mfa2bW2bE1	P	Kämper et al., 2006
SG200Δsee1	a1mfa bW2bE1 Δ <i>um02239</i> ::hph	P , H	Schilling et al., 2014
SG200Δsee1-see1	a1mfa2 bW2bE1 Δ <i>um02239</i> ::hph ip ^r [Psee1::see1]ip ^s	P , H , C	Schilling et al., 2014
SG200Δtin3	a1mfa bW2bE1 Δ <i>um10556</i> ::hph	P , H	Brefort et al., 2014
SG200AM1	a1 mfa2 bE1 bW2 ip ^r [Pum01779:egfp] ip ^s	P , H	Mendoza –Mendoza et al., 2008
SG200Δsee1-see1-mCherry	a1mfa2 bW2bE1 Δ <i>um02239</i> ::hph ip ^r [Psee1::see1:mcherry]ip ^s	P , H , C	This Study
SG200Δsee1AM1	a1 mfa2 bE1 bW2 Δ <i>um02239</i> ::egfp ip ^r [Pum01779:gfp] ip ^s	P , H , C	This Study
SG200Δsee1-Ppit2-see1	a1mfa2 bW2bE1 Δ <i>um02239</i> ::hph ip ^r [Ppit2::see1]ip ^s	P , H , C	This Study
SG200Δsee1-Ppit2-see1-mCherry	a1mfa2 bW2bE1 Δ <i>um02239</i> ::hph ip ^r [Ppit2::see1:mCherry]ip ^s	P , H , C	This Study
SG200-Ppit2-see1	a1mfa2 bW2bE1 ip ^r [Ppit2::see1]ip ^s	P , C	This Study
SG200-Ppit2-see1-mCherry	a1mfa2 bW2bE1 ip ^r [Ppit2::see1:mCherry]ip ^s	P , C	This Study
SG200Δsee1-Srsee1	a1mfa2 bW2bE1 Δ <i>um02239</i> ::hph ip ^r [PSrsee1::Srsee1]ip ^s	P , H , C	This Study
SG200Δsee1-Uhsee1	a1mfa2 bW2bE1 Δ <i>um02239</i> ::hph ip ^r [PUhsee1::Uhsee1]ip ^s	P , H , C	This Study
SG200Δsee1-Ppit2-Srsee1	a1mfa2 bW2bE1 Δ <i>um02239</i> ::hph ip ^r [Ppit2::Srsee1]ip ^s	P , H , C	This Study
SG200Δsee1-Psee1-SPsee1-see1-3XHA	a1mfa2 bW2bE1 Δ <i>um02239</i> ::hph ip ^r [Psee1:SPsee1:see1::3XHA]ip ^s	P , H , C	This Study
SG200-Psee1-SPsee1-mcherry-3XHA	a1mfa2 bW2bE1::hph ip ^r [Psee1:SPsee1:mcherry::3XHA]ip ^s	P , C	This Study
SG200-Psee1-GFP-3XHA	a1mfa2 bW2bE1 ::hph ip ^r [Psee1:GFP::3XHA]ip ^s	P , C	This Study
SG200Δsee1-Psee1-Srsee1	a1mfa2 bW2bE1 Δ <i>um02239</i> ::hph ip ^r [Psee1::Srsee1]ip ^s	P , H , C	This Study
SG200Δsee1-Psee1-Uhsee1	a1mfa2 bW2bE1 Δ <i>um02239</i> ::hph ip ^r [Psee1::Uhsee1]ip ^s	P , H , C	This Study

¹ Phleomycin (P), Hygromycin (H), Carboxin (C)

Tab. 13: Oligonucleotides used in this study

Serial Number	Label	Nucleotide Sequence (5' > 3')	Application
OAR01	See1_comp_Sbfl_Fw	GACCTGCAGGGTGTGCACGGTGCTACTG	Amplification of See1 from wildtype DNA for complementation of knockout
OAR02	See1_comp_NotI_Rv	GAGCGGCCGCCCACTCGTGA CTGCTAC	Amplification of See1 from wildtype DNA for complementation of knockout
OAR03	See1_mCherry-HindIII-Fw	GAAAGCTTGTGTGCACGGTGCTACTG	For localization of See1 with a fluorescence fusion protein with mCherry
OAR04	See1_mCherry-BamHI-Rv	CAGGATCCCGTCGTCGGCCCAAATTATAC	For localization of See1 with a fluorescence fusion protein with mCherry
OAR05	See1_qPCR_Fw	TCAGGTGCAAGGAGAAGG	For expression profile of See1 during tumor progression
OAR06	See1_qPCR_Rv	ACAGAATACTCCGCTTCCC	For expression profile of See1 during tumor progression
OAR07	Ppit2_See1_SacII_fw	ATACCGCGGATGCTCTTACCACCTTCGTTTC	For overexpression of See1 with pit2 promoter
OAR08	Ppit2_See1_mCherry_XbaI_Rv	CGCTCTAGATTACTTGTACAGCTCGTCCA	For overexpression of See1 fused to mCherry with pit2 promoter for localization
OAR11	Ppit2_See1_XbaI_Rv	CGCTCTAGATTACGTCGTCGGCCCAAATT	For overexpression of See1 with pit2 promoter
OAR12	Umsee1_SacI_Fw	GCGAGCTCATGCATCCTCTACAATCGTTTCG	For See1 expression in the E.coli expression vector pRSET-GST
OAR13	Umsee1_HindIII_Rv	CGCAAGCTTACGTCGTCGGCCCAAAATT	For See1 expression in the E.coli expression vector pRSET-GST
OAR20	SrSee1_comp_Sbfl_Fw	GACCTGCAGGTCTGAACGTACGTGGGAAAG	Complementation of the $\Delta see1$ knockout with the Srsee1 with <i>S. reilianum</i> promoter
OAR21	SrSee1_comp_NotI_Rv	GAGCGGCCGCTTCTCCAACCCACACAAT	Complementation of the $\Delta see1$ knockout with the Srsee1 with <i>S. reilianum</i> promoter
OAR26	PUmsee1_Sbfl_Fw	GCGCCTGCAGGCAGAATCCATGAAAAGTGG	For cloning of the Umsee1 promoter alone in vector p123.
OAR27	PUmsee1_NcoI_Rv	GACCATGGTTGCGAGCGAAGAAAGTAGAGG	For cloning of the Umsee1 promoter alone in vector p123
OAR28	Srsee1_NcoI_Fw	GACCATGGGATGCGCGCCTCTACACT	For Srsee1 cloning along with Umsee1 promoter for complementation of $\Delta see1$ knockout.
OAR29	Srsee1_NotI_Rv	TAGCGGCCGCTCTACGTGTACGAATCGC	For Srsee1 cloning along with Umsee1 promoter for complementation of $\Delta see1$ knockout.
OAR30	pGADT7_ColI_PCR_Fw	CGCGTTTGAATCACTAC	For yeast colony PCR in Y2H on flanking region of pGADT7
OAR31	pGADT7_ColI_PCR_Rv	GATGGTGCACGATGCAC	For yeast colony PCR in Y2H on flanking region of pGADT7
OAR32	pGBKT7_ColI_PCR_Rv	GCTGACTAGGGCACATCT	For yeast colony PCR in Y2H on flanking region of pGBKT7
OAR33	pGBKT7_ColI_PCR_Rv	CCGGAATTAGCTTGGCTG	For yeast colony PCR in Y2H on flanking region of pGBKT7

OAR38	UhSee1_comp_SbfI_Fw	GACCTGCAGGGAAAGGTCAAAGAGTCC	Complementation of the $\Delta see1$ knockout with the Uhsee1 with <i>U. hordei</i> promoter
OAR39	UhSee1_comp_NotI_Rv	GAGCGGCCGCGAAAGGGAAGAAGACA	Complementation of the $\Delta see1$ knockout with the Uhsee1 with <i>U. hordei</i> promoter
OAR40	Umsee1_Ndel_Fw	GCGCATATGCATCCTCTACAATCGTTTCG	For the amplification of Umsee1 without signal peptide for cloning in Y2H vectors and also for protein expression vector pET 15b
OAR41	Umsee1_BamHI_Rv	CGCGGATCCTTACGTCGTCGGCCCAATT	For the amplification of Umsee1 without signal peptide for cloning in Y2H vectors and also for protein expression vector pET 15b
OAR49	Umsee1_mCherry_SacI_Rv	CGGGAGCTCTTACTTGTACAGCTCGTCCA	Cloning of Umsee1 fused to mCherry in pGreen for transient expression of See1 in <i>Z. mays</i>
OAR50	Umsee1_mCherry_XbaI_Fw	CGCTCTAGAATGCATCCTCTACAATCGTTTCG	Cloning of Umsee1 fused to mCherry in pGreen for transient expression of See1 in <i>Z. mays</i>
OAR61	Uhsee1_Ndel_Fw	ATTCATATGCTCCCACCACGCCACGCTCG	For the amplification of Uhsee1 without signal peptide for cloning in Y2H vector pGBKT7
OAR62	Uhsee1_BamHI_Rv	AATAGGATCCTCAACCCCCTCTCCGCCTC	For the amplification of Uhsee1 without signal peptide for cloning in Y2H vector pGBKT7
OAR63	Srsee1_NdeI_Fw	ATACATATGCGACCCACCAACTCCGCG	For the amplification of Srsee1 without signal peptide for cloning in Y2H vector pGBKT7
OAR64	Srsee1_BamHI_Rv	AAGGATCCCTACGTGTACGAATCGCCCA	For the amplification of Srsee1 without signal peptide for cloning in Y2H vector pGBKT7
OAR65	ZmSGT1_EcoRI_Fw	CCGGAATTCATGGCCGCGTCGGATCTGGAGAG	For amplification of ZmSGT1 for cloning in the yeast expression vectors pB42AD and pGREG536 for the <i>sgt1</i> yeast complementation assay.
OAR66	ZmSGT1_Psi_Rv	CGCAAGCTTTTACGTCGTCGGCCCAATT	For amplification of ZmSGT1 for cloning in the yeast expression vectors pB42AD for the <i>sgt1</i> yeast complementation assay.
OAR67	ZmSGT1_Xho_Rv	GGCCTCGAGTCAAATTTCCCACTTCTTG	For amplification of ZmSGT1 for cloning in the yeast expression vectors pGREG536 for the <i>sgt1</i> yeast complementation assay.
OAR68	AtSGT1a_Ndel_Fw	GCCATATGATGGCGAAGGAGCTTGTGA	For the amplification of AtSGT1a for cloning in Y2H vectors
OAR69	AtSGT1a_NotI_Rv	GCGGCCGCTCAGATCTCCATTTCTTGA	For the amplification of AtSGT1a for cloning in Y2H vector pGBKT7
OAR70	AtSGT1a_Xho_Rv	GCCTCGAGTCAGATCTCCATTTCTTGA	For the amplification of AtSGT1a for cloning in Y2H vector pGADT7
OAR71	AtSGT1b_Ndel_Fw	GGCCATATGATGGCCAAGGAATTAGCAG	For the amplification of AtSGT1b for cloning in Y2H vectors
OAR72	AtSGT1b_NotI_Rv	TAGCGGCCGCTCAATACTCCCACTTCTTGA	For the amplification of AtSGT1b for cloning in Y2H vector pGBKT7
OAR73	AtSGT1b_EcoRI_Rv	GGGCGAATTCTCAATACTCCCACTTCTTGA	For the amplification of AtSGT1b for cloning in Y2H vector pGADT7

OAR76	ZmGAPDH_qPCR_Fw	CTTCGGCATTGTTGAGGGTTTG	For reference housekeeping gene in quantification of maize gene expression
OAR77	ZmGAPDH_qPCR_Rv	TCCTTGGCTGAGGGTCCGTC	For reference housekeeping gene in quantification of maize gene expression
OAR88	Umsee1_Rv	CGTCGTCGGCCCAAATTTAT	Amplification of Umsee1 for the pENTR-D-TOPO entry vector cloning without stop codon for in planta assays
OAR89	Umsee1_Fw	CACCATGCATCCTCTACAATCGTTTCG	Amplification of Umsee1 for the pENTR-D-TOPO entry vector cloning without the signal peptide
OAR92	Umsee1_Spel_Fw	GGCACTAGTATGCATCCTCTACAATCGTTTCG	Amplification of Umsee1 without signal peptide for cloning in pTA7001 DEX vector for in planta phosphorylation assay
OAR93	Umsee1_HA_XhoI_Rv	CTCGAGTTAAGCGTAATCTGGAACATCGTATGGGTACGTCGGCCCAAATTTAT	Amplification of Umsee1 fused to HA tag for cloning in pTA7001 DEX vector for in planta phosphorylation assay
OAR95	Umsee1_SbfI_Fw	GGCCTGCAGGGTGGAGTGGAAGCAAAAAT	Amplification of Umsee1 along with the promoter and signal peptide for TEM and immunogold labeling.
OAR96	Umsee1_3XHA_NotI_Rv	GCGGCCGCTTAAGCGTAATCTGGAAATCGTATGGGTAAAGCGTAATCTGGAACATCGTATGGGTACGTCGGCCCAAATTTAT	Amplification of Umsee1 as a fusion protein along with 3X HA for TEM and immunogold labeling.
OAR97	PUmsee1_SPsee1_NcoI_Rv	CCATGGAGCAGACACGTGGACAAGA	Amplification of Umsee1 promoter and signal peptide alone in p123 for secretory cherry control
OAR98	GFP_3XHA_NcoI_Fw	TACCATGGATGGTGAGCAAGGGCGAAGGA	Amplification of the GFP fused to 3X HA under the promoter Umsee1. Non-secretory control for TEM
OAR99	GFP_3XHA_NotI_Rv	GGGCGGCCGCTTAAGCGTAATCTGGAACATCGTATGGGTAAAGCGTAATCTGGAACATCGTATGGGTACTTGTACAGCTCGTCCATGC	Amplification of the GFP fused to 3X HA under the promoter Umsee1. Non-secretory control for TEM
OAR100	mCherry_3XHA_NcoI_Fw	CCATGGATGGTGAGCAAGGGCGAAGGA	Amplification of the mCherry fused to 3X HA under the promoter Umsee1 and signal peptide of See1. Secretory control for TEM
OAR101	mCherry_3XHA_NotI_Rv	GCGGCCGCTTAAGCGTAATCTGGAAATCGTATGGGTAAAGCGTAATCTGGAACATCGTATGGGTACTTGTACAGCTCGTCCATGC	Amplification of the mCherry fused to 3X HA under the promoter Umsee1 and signal peptide of See1. Secretory control for TEM
OAR110	ZmSGT1_Ndel_Fw	ATTCATATGGCCGCGTCGGATCTGGA	For the amplification of ZmSGT1 for cloning in protein expression vector pET 15b
OAR111	ZmSGT1_BamHI_Rv	GGCCGGATCCTCAAATTTCCCACTTCTTGA	For the amplification of ZmSGT1 for cloning in protein expression vector pET 15b
OAR116	Uhsee1_NcoI_Fw	CCATGGATGAAGCGCGTTCTAACTCTC	Amplification of Uhsee1 along with the native promoter of Umsee1
OAR117	Uhsee1_NotI_Rv	ATTGCGGCCGCTCAACCCCTCTC	Amplification of Uhsee1 along with the native promoter of Umsee1

		CGCCTCT	
OAR118	ZmCDC6_q RT_Fw	AAAGCGCGGTGGTGGATAGC	For expression profiling of the late G1 phase marker in wildtype and knockout mutant
OAR119	ZmCDC6_q RT_Rv	TGTTTCAGTTCGCCCAGGGTG	For expression profiling of the late G1 phase marker in wildtype and knockout mutant
OAR133	ZmSGT1_F w	CACCATGGCCGCGTCGGATCTGGA	Amplification of ZmSGT1 for the pENTR-D-TOPO entry vector cloning
OAR134	ZmSGT1_R v_without SC	AATTTCCCACTTCTTGAGCTCC	Amplification of ZmSGT1 for the pENTR-D-TOPO entry vector cloning without stop codon for C terminal fusion in destination vector
OAR135	ZmSGT1_R v_with SC	TCAAATTTCCCACTTCTTGA	Amplification of ZmSGT1 for the pENTR-D-TOPO entry vector cloning with stop codon for N terminal fusion in destination vector
OAR144	Umsee1_Fw	GGAAGAAGTCCTTCGATCAGGATAG ATCC	Additional amplification primer for the site directed mutagenesis without restriction enzyme
OAR145	pTA_seq_F w	GTTCAATTCATTTGGAGAGGACACG	For sequencing of the pTA7001 DEX inducible constructs
OAR146	pTA_seq_Rv	TGAAACTGATGCATTGAACTTGACG	For sequencing of the pTA7001 DEX inducible constructs
OAR154	ZmSGT1_F w	AGGAAGGTGGCTCCTACAAATGCCA TC	Additional amplification primer for the site directed mutagenesis of TPP without restriction enzyme
OAR155	ZmSGT1_T PP mut_Fw	GTCGCAAATATGGATAATGCAGCAG CAGTGGTAGAACCCCAAGC	Amplification for the insertion of mutation in the phosphorylation site TPP with amino acid AAA with mutagenesis kit
OAR216	Zm_Histone H3_qPCR_F w	ATCGCGCAGGACTTCAAGAC	For expression profiling of the DNA synthesis marker Histone H3 in wildtype and knockout mutant
OAR217	Zm_Histone H3_qPCR_R v	GGATGGCGCAGAGGTTAGTG	For expression profiling of the DNA synthesis marker Histone H3 in wildtype and knockout mutant
OAR220	Zm_LRR_qP CR_Fw	TGTGTACAGCTACGGCATTG	For expression profiling of the putative LRR receptor from maize in wildtype and knockout mutant
OAR221	Zm_LRR_qP CR_Rv	GTCTCCATGACCGTGTCTC	For expression profiling of the putative LRR receptor from maize in wildtype and knockout mutant
OAR224	Zm_CCR_q PCR_Fw	ACACCCACGAGATACTTACC	For expression profiling of the Cell division control protein 2 from maize in wildtype and knockout mutant
OAR225	Zm_CCR_q PCR_Rv	CCAACGGACCATATGTCAAC	For expression profiling of the Cell division control protein 2 from maize in wildtype and knockout mutant
OAR226	Zm_KRS_q PCR_Fw	TCCTGTCCGAGAACGAGTG	For expression profiling of the Cyclin dependent kinase regulatory subunit from maize in wildtype and knockout mutant
OAR227	Zm_KRS_q PCR_Rv	GGCGGAACAGCATGATGTG	For expression profiling of the Cyclin dependent kinase regulatory subunit from maize in wildtype and knockout mutant

OLS54	Umppi_qPCR_Fw	TCATCCCGGACTTCATGC	For reference housekeeping gene in quantification of <i>U. maydis</i> candidate gene expression
OLS55	Umppi_qPCR_Rv	TGCCCTCGTTCTCGATAG	For reference housekeeping gene in quantification of <i>U. maydis</i> candidate gene expression
OLS118	Umsee1_BamHI_Fw	GCGCGGATCCATGCATCCTCTACAA TCGTTTC	Amplification of Umsee1 for cloning in the pSPYNE vector for BiFC
OLS119	Umsee1_XhoI_Rv	GACTCGAGCGTCGTCGGCCCAAATT T	Amplification of Umsee1 for cloning in the pSPYNE vector for BiFC
OLS120	ZmSGT1_BamHI_Fw	GTATGGATCCATGGCCGCGTCGGAT CTG	Amplification of ZmSGT1 for cloning in the pSPYCE vector for BiFC
OLS121	ZmSGT1_XhoI_Rv	GCTCTCGAGGATTCCCTGAATGACTT TG	Amplification of ZmSGT1 for cloning in the pSPYCE vector for BiFC
OLS130	ZmSGT1_Ndel_Fw	GTATATACCCGGGAATGGAGTACCC ATACGAC	For the amplification of ZmSGT1 for cloning in Y2H vectors
OLS131	ZmSGT1_BamHI_Rv	GCGCGGATCCTCAAATTTCCCACTTC TTG	For the amplification of ZmSGT1 for cloning in Y2H vectors
OLS147	Umsee1_XbaI_Fw	GCCGGCTCTAGATGCATCCTCTACA ATCGTTTC	For amplification of Umsee1 fused to Myc tag in pGreen vector for in planta co-immunoprecipitation
OLS148	Umsee1_SacI_Rv	GGCCGCGAGCTCTTAAAGATCCTCC TCAGAAATCAACTTTTGCTCCGTCGT CGGCCCAAATTTATACTCTCC	For amplification of Umsee1 fused to Myc tag in pGreen vector for in planta co-immunoprecipitation
OLS149	ZmSGT1_XbaI_Fw	CATCTAGATGGCCGCGTCGGATCTG	For amplification of ZmSGT1 fused to HA tag in pGreen vector for in planta co-immunoprecipitation
OLS152	ZmSGT1_BamHI_Rv	CCGGCCGGCGGATCCTTAAGCGTAA TCTGGAACATCGTATGGGTAAATTTCC CACTTCTTGAG	For amplification of ZmSGT1 fused to HA tag in pGreen vector for in planta co-immunoprecipitation

Peptides detected from the *in planta* phosphorylation of *see1* effector

4471	855.4120	1708.8094	1708.8057	2.21	0	(130)	2.1e-08	1	U	R.LPAQVQGEGETTYDR.Q
4472	855.4120	1708.8095	1708.8057	2.24	0	(91)	0.00017	1	U	R.LPAQVQGEGETTYDR.Q
4473	855.4121	1708.8096	1708.8057	2.32	0	(120)	2e-07	1	U	R.LPAQVQGEGETTYDR.Q
4474	855.4121	1708.8097	1708.8057	2.35	0	(125)	6.4e-08	1	U	R.LPAQVQGEGETTYDR.Q
4475	855.4121	1708.8097	1708.8057	2.37	0	(122)	1.1e-07	1	U	R.LPAQVQGEGETTYDR.Q
4476	855.4121	1708.8097	1708.8057	2.37	0	(125)	6.1e-08	1	U	R.LPAQVQGEGETTYDR.Q
4477	855.4122	1708.8099	1708.8057	2.50	0	(138)	3.3e-09	1	U	R.LPAQVQGEGETTYDR.Q
4478	855.4122	1708.8099	1708.8057	2.50	0	(98)	3e-05	1	U	R.LPAQVQGEGETTYDR.Q
4479	855.4123	1708.8100	1708.8057	2.56	0	(108)	2.9e-06	1	U	R.LPAQVQGEGETTYDR.Q
4480	855.4123	1708.8101	1708.8057	2.56	0	(115)	6.2e-07	1	U	R.LPAQVQGEGETTYDR.Q
4481	855.4124	1708.8102	1708.8057	2.66	0	(124)	8.7e-08	1	U	R.LPAQVQGEGETTYDR.Q
4482	855.4125	1708.8104	1708.8057	2.75	0	(108)	3e-06	1	U	R.LPAQVQGEGETTYDR.Q
4483	855.4125	1708.8105	1708.8057	2.85	0	(121)	1.7e-07	1	U	R.LPAQVQGEGETTYDR.Q
4484	855.4125	1708.8105	1708.8057	2.85	0	(120)	2e-07	1	U	R.LPAQVQGEGETTYDR.Q
4485	855.4125	1708.8105	1708.8057	2.85	0	(113)	1e-06	1	U	R.LPAQVQGEGETTYDR.Q
4486	855.4126	1708.8106	1708.8057	2.87	0	(115)	6.2e-07	1	U	R.LPAQVQGEGETTYDR.Q
4487	855.4127	1708.8109	1708.8057	3.09	0	(122)	1.1e-07	1	U	R.LPAQVQGEGETTYDR.Q
4488	855.4132	1708.8118	1708.8057	3.58	0	(103)	1e-05	1	U	R.LPAQVQGEGETTYDR.Q
4489	855.4132	1708.8118	1708.8057	3.60	0	(125)	5.8e-08	1	U	R.LPAQVQGEGETTYDR.Q
4490	855.4132	1708.8119	1708.8057	3.66	0	(115)	6.6e-07	1	U	R.LPAQVQGEGETTYDR.Q
4491	855.4133	1708.8121	1708.8057	3.79	0	(87)	0.0004	1	U	R.LPAQVQGEGETTYDR.Q
4492	855.4134	1708.8122	1708.8057	3.82	0	(92)	0.00013	1	U	R.LPAQVQGEGETTYDR.Q
4493	855.4146	1708.8147	1708.8057	5.27	0	(98)	3.4e-05	1	U	R.LPAQVQGEGETTYDR.Q
4495	855.4162	1708.8179	1708.8057	7.15	0	(108)	2.9e-06	1	U	R.LPAQVQGEGETTYDR.Q
4988	911.4567	1820.8989	1820.8945	2.46	0	136	4.3e-09	1	U	E.IAQQAEISIELEFPR.V

Fig. 40: *In planta* phosphorylation of Um-See1. Peptide sequences of Um-See1 detected in the Mass spectrometry with no phosphorylation detected for any of the peptide observed indicating that See1 might be undergoing a posttranslational modification that is not detected by the mass spectrometry approach.

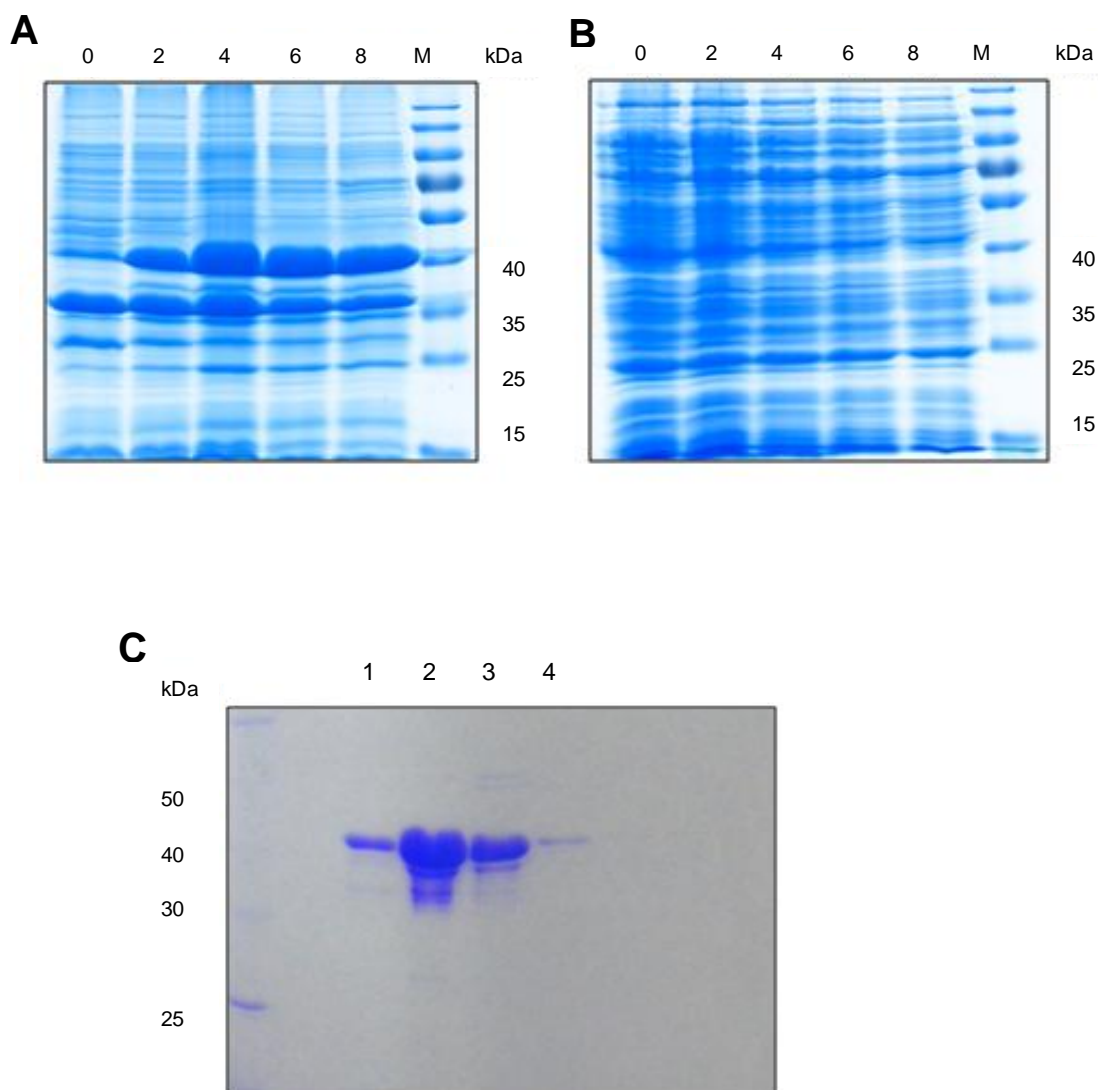
Protein Expression of See1 and SGT1 in *E. coli*

Fig. 41: Heterologous overexpression and purification of See1 and SGT1. (A) SDS-PAGE of test expression of See1 in the pellet fraction over consecutive timepoints from 0 hrs to 8 hrs. See1 was C-terminally fused to GST protein (37.5kDa) heterologously produced in *E. coli*. The size of the recombinant protein GST-See1 corresponds to 42.3kDa. (B) The supernatant fraction of the test expression gel of the GST-See1 where in only weak expression of the protein was detected from 0 hrs to 8 hrs timecourse. This expressed protein could not be purified in desired amounts. (C): Heterologous expression and purification of SGT1 of *Zea mays* (42.4kDa). SGT1 was charged with C-terminal His-tag and heterologously produced in *E. coli*. The soluble fraction was separated from the pellet fraction. The pellet fraction was denatured with the use of 6M guanidine-HCl, reconstituted by Ni-NTA, also under denaturing conditions, and finally purified. The purified protein from AKTA in several elution fractions have been shown on the gel representing the lanes 1 to 4.

Definition of own performance

The results presented in this work were carried out by me independently and without assistance other than that listed here. The design of experiments was done in collaboration with my supervisor Prof. Dr. Gunther Döhlemann. The other people participated in this study and their experimental contributions are mentioned below:

Ziba Ajami Rashidi

Generated the knockout mutant strain for *see1* effector deletion as a part of her Master thesis. All the knockout constructs SG200 Δ *see1* have been generated by her.

Dr. Christoph Hemetsberger

Helped with the initial microscopy of WGA-AF488 for the screening of the virulence defect in the SG200 Δ *see1* infected tissue. The images in Fig. 11 have been done in co-operation with him.

Lena Schilling

Did the experiments for confirmation of the See1-SGT1 interaction using the *in planta* co-immunoprecipitation and the bimolecular fluorescence complementation. The data represented in the Fig. 29 have been done by her.

Dr. Rafal Hoser

Helped to do the *in planta* phosphorylation experiments during a one months collaborative stay at IBB, Poland. The experiments mentioned in Fig. 32-33 have been done with his co-operation.

Dr. Magdalena Krzymowska

The design of the experiments for *in planta* phosphorylation of *see1* have been done with her expertise and in her group at Institute of Biochemistry and Biophysics, Warsaw, Poland.

Dr. Bernd Zechmann

Has made a contribution and collaboration for all the transmission electron microscopic investigations to show the localization of *see1* via immunogold labeling. The electron micrographs and quantification of the gold particles shown in Fig. 25 B and Fig. 26 have been done by him.

Marburg, November 2014

Acknowledgements

The present thesis holds the enriching experience of nearly last 4 years of study. These printed pages reflect the help I received from many inspiring and generous persons I met during this tenure. My thanks go to all those who contributed to this work. However, I would like to emphasize at this point some people whom I would like to sincerely acknowledge.

My thanks to my previous supervisors and guides Dr. Kanchan Gandhe, Dr. Ravindra Gandhe and Dr. Avinash Kamble, whose enthusiastic teaching in the subject developed my interest to this field of plant microbe interactions. My special thanks to Prof. Dr. Gunther Döhlemann whose support started long back in May 2011 through a telephonic interview accepting me as a PhD student. I am thankful to him for this exciting topic for my Doctoral work. I am grateful to have him as supervisor who gave me complete freedom to explore the subject on my own and also for the consistent support with many helpful ideas and guidance whenever I ran into an impasse.

I would also like to thank Prof. Dr. Alfred Batschauer, Prof. Dr. Regine Kahmann and Prof. Hans Ulrich Moesch for being members of 'Thesis Advisory Committee' and monitoring my work for last 3 years. Additionally I would like to thank Prof. Dr. Alfred Batschauer, Prof. Dr. Regine Kahmann and Prof. Dr. Uwe Maier for being into my examination committee.

My thanks to all collaborators on See1 Project who helped in several aspects of this Research. I would specially like to thank Dr. Bernd Zechmann for his willingness to collaborate, on the See1 project for electron microscopy work and for the fantastic electron micrographs and great explanation talks over telephone. Thanks to Dr. Magdalena Krzymowska and Dr. Rafal Hoser from IBB, Poland who helped me to get acquainted with the biochemical part of phosphorylation assays and also for smoothing my stay in Warsaw. Thanks to Prof. Virginia Walbot for active discussions during the manuscript preparation which were helpful in developing critical thinking.

I would sincerely like to thank Susanne Rommel, Simone Hain, Jens Hemer and Christian Bengelsdorff for all their help during the initial days after my arrival to settle in Marburg. It was their active support that created a homely atmosphere.

I would also like to thank all the current and former members of the AG Döhlemann who have made the lab atmosphere really enjoyable. Thanks of course to the members of the AGs Kahmann and Zuccaro, past and present, for many assistance, discussions and support. A special thanks goes to Ria, Anita and Stefan, facilitate the laboratory routine many times.

A big thank you to Alex and Lena, who also helped to balance the social life in Germany wherein I also became a good friend with them! Thanks to Alex Hof and Hannah Kleyer for their help in reading the thesis draft.

In my family, especially I would like to thank my parents and my sister, for their constant support and encouragement during my studies which really bought me at this stage. I am just everything because of them. The biggest thanks goes to my love Mugdha for always being as another part of my life during difficult and good times. Its because of her love and support I am able to finish this assignment in good time.

Last but not least I would like to acknowledge the German Academic Exchange Service (DAAD) and the COST FA 1208 STSM for providing me funding during various aspects of my PhD tenure which successfully completed the project.

Curriculum Vitae

Amey Redkar

born on 27. January 1986 in Belgaum, India

Education

University

6/2004– 06/2007

Bachelor of Science
From the University of Pune, India
Modern College of Arts, Science and Commerce
Ganeshkhind, Pune 53.
Maharashtra, India

7/2007 – 06/2009

Master of Science
From University of Pune, India
Specialization Cytogenetics and Plant Breeding
Department of Botany, University of Pune
Ganeshkhind, Pune 07
Maharashtra, India

Master Thesis:

In group of Asst. Prof. Dr. Avinash Kamble

Title: „ Study of defense responses in *Solanum lycopersicum*
L. against *Alternaria solani*”

07/2009 – 03/2011

DBT-Junior Research Fellow (JRF) in Interactive Research
School for Health Affairs (IRSHA)

In group of Associate Prof. Dr. Kanchanganga Gandhe

Title: „Identification of genes involved during disease
development by gall forming rust fungi in *Acacia*
eburnea and *Jasminum malbaricum*.

PROMOTION

from 10/2011

Doctoral studies at the Philipps-Universität Marburg;
in Max-Planck-Institute for Terrestrial Microbiology,
Department of Organismic Interactions

In the group of Prof. Dr. Gunther Döhlemann

Title: „Functional Characterization of an organ specific
effector See1 of *U. maydis*“

Member of the ‚*International Max Planck Research School*’
at the Max-Planck-Institute for Terrestrial Microbiology

